UNIVERSITA´ POLITECNICA DELLE MARCHE

DOCTORAL THESIS

Sulfur Metabolism in Microalgae

Tutor:

Prof. Mario Giordano

Co-tutors:

Prof. Arthur Grossman

PhD Candidate:

Hongmin LIN

Department of Life and Environmental Sciences - Di.S.V.A.

Ancona, 2018

To my study life.

Past present and

future.....

Abstract

Sulfur is a fundamental element for all living organisms. It is acquired as sulfate, which is also the most abundant S form in the ocean, and is assimilated as sulfide, which is fixed in the S-amino acid cysteine. Sulfate assimilation thus requires its reduction to sulfide. For sulfate to be reduced, it needs to be activated to Adenosine PhosphoSulfate (APS). This reaction is catalyzed by ATP-Sulfurylase, which in eukaryotic algae and oceanic cyanobacteria, differently from all other organisms are subject to redox regulation. The other steps of the sulfate assimilation pathways are believed not to differ in algae, as compared to embryophytes. The only other step on which the lack of information leaves crucial open questions is the synthesis of cysteine. Cysteine synthesis is catalyzed by two enzymes, Serine Acetyl Transferase (SAT) and O-Acetyl Serine (Thiol) Lyase (OAS-TL), which in embryophytes form a complex, the Cysteine Synthase Complex (CSC). My thesis will focus on these two steps, with special attention to cysteine synthesis.

With respect to ATP-sulfurylase, I have tried to assess if redox

regulation is mediated by the redox state of the plastoquinon pool of thylakoids. My results suggest that this is not the case. The in vivo blockage of PQ reduction through the use of DCMU, a specific inhibitor of electron transfer from QA to QB, did not affect ATP-S activity.

As for the enzymes of cysteine synthesis, my bioinformatic analysis showed that the phylogeny of SAT and OAS-TL are probably difficult to reconstruct due to the shuffling of these genes across groups with the possible contribution of horizontal gene transfer. By analyzing the protein sequences, I determined that the C-terminal domain of algal SAT, which is believed to be responsible for the interaction with OAS-TL, is very similar to that of embryophytes. This suggests that the interaction of SAT and OAS-TL occurs in algae as in embryophytes. However, the N-terminus of algal SAT, which is believed to be involved in the SAT/SAT interaction, is not equally conserved; therefore, differences in the assemblage of the CSC in algae are possible. In order to clarify this point, I purified OAS-TL from the freshwater cyanobacterium *Synechocystis* sp. PCC 6803, the green marine algae *Tetraselmis suecica* and *Dunaliella tertiolecta*, the green freshwater algae *Chlamydomonas reinhardtii*, the marine diatoms *Thalassiosira pseudonana* and

Phaeodactylum tricornutum, and from the marine dinoflagellate *Amphidinium klebsii*. These purified proteins showed some differences in mass, which was however always within the 35-44 kDa range. All the purified proteins were active, although specific activity differed among species. Interestingly, the activity, in most cases, was higher when the enzyme was more diluted; the enzyme is more active, as it also happens in embryophytes. For embryophytes, this has been interpreted as an indication that OAS-TL activity is modulated through protein-protein interaction. To verify the hypothesis that algae have CSC like embryophytes, I studied the ability of algae OAS-TL to form a complex with *Arabidopsis thaliana* SAT (overexpressed in *E. coli*). In all cases, a complex was formed, although the strength of the interaction between SAT and OAS-TL appeared to be different for different algal species. The presence of OAS-TL and SAT in the purified native complexes was confirmed by immunodetection of both proteins. The cysteine synthase complexes that were formed in these experiments were appreciably larger (approximately 600 kDa vs 320 kDa) than those of embryophytes. Further experiments will be required to ascertain the actual stoichiometry and structure of the algal CSC. However, based on the above observation, I

propose that algal CSC is composed by two SAT trimers, with an OAS-TL dimer bound to each SAT monomer. This configuration would give a mass of about 600 kDa, compatible with the results obtained in our CSCS purification experiments.

It is also noteworthy that the strength of the binding of algal OAS-TL to AtSAT5 was greater in green algae than in algae of the red lineage. This may be an indication of the fact that a greater proportion of OAS-TL is in the free form, in red-lineage algae, leading to a higher flux of S into cysteines. At this stage, this is only a hypothesis that requires further confirmation.

Keywords:

Sulfate, Cysteine, O-Acetyl Serine (Thiol) Lyase (OAS-TL), Cysteine Synthase Complex (CSC)

CONTENT

Abstract III
Keywords: VI
LIST OF FIGURES XI
LIST OF TABLES XV
1. Introduction 2
1.1. Impact of sulfur availability on algae ecology, evolution and radiation 2
1.2. Sulfur metabolism 3
1.2.1. Sulfate acquisition 3
1.2.2. Sulfate reduction 4
1.2.3. Cysteine synthesis 5
2. Hypotheses 11
3. Materials and methods 14
3.1. Bioinformatic methods 14
3.1.1. Protein sequences and phylogenetic trees 14
3.1.2. Predictions on the location of SAT and OAS-TL proteins 14
3.1.3. Analysis of SAT and OAS-TL algae sequences 15
3.2 Experimental organisms 16
3.2.1. *Synechocystis* sp. PCC 6803 16
3.2.2. *Chlamydomonas reinhardtii* 16
3.2.3. *Dunaliella tertiolecta* 17
3.2.4. *Tetraselmis suecica* 18
3.2. 5. *Thalassiosira pseudonana* 18
3.2.6. *Phaeodactylum tricornutum* 19
3.2.7. *Amphidinium klebsii* 20
3.3. Cultures 20
3.3.1. Culture conditions 20
3.3.1.1. *Synechocystis* sp. PCC 6803 21
3.3.1.2. Eukaryotic algae 21
3.3.2. Growth media. 21
3.3.2.1. BG-11 medium 21
3.3.2.2. TAP and TP medium 22
3.3.2.3. Artificial Multipurpose Complement for the Nutrition of Algae (AMCONA) 22
3.3.3. Determination of cell concentration 23
3.3.4. Growth rate determination 24
3.3.5. Biomass harvesting 25
3.4. Overexpression of AtSAT5 25
3.4.1. Primer design 25
3.4.2. AtSAT5 Colony transformation assessment in *E. coli* 26
3.4.3. Colony PCR 29
3.4.4. AtSAT5 overexpression 30
3.4.5. Extraction of AtSAT5 protein from *E. coli* 31

3.4.6. OAS-TL purification 32
3.4.7. Algal OAS-TL extraction 34
3.4.8. Determination of protein content 35
3.4.9. SDS-Polyacrylamide Gel Electrophoresis (SDS-PAGE) 36
3.4.10. Western Blots 39
3.5. OAS-TL activity measurements 41
3.6. Cysteine Synthase Complex purification 42
3.7. Determination of the impact of the plastoquinone redox state on ATPS activity 46
4. Results 51
4.1. Bioinformatics 51
4.1.1. Phylogeny of Serine Acetyltransferase 51
4.1.2. Phylogeny of O-Acetylserine (thiol) lyase 54
4.1.3. Observations on SAT and OAS-TL protein sequences 57
4.1.3.1. Number of cysteine residues in algae SAT sequences 57
4.1.3.2. Predicted location of SAT proteins 57
4.1.3.3. Number of cysteine residues in algal OAS-TL sequences 61
4.1.3.4. Predicted OAS-TL location 61
4.1.4. Comparison of SAT and OAS-TL sequences among algae and with *A. thaliana* sequences 66
4.1.4.1. Alignment of the SAT sequences of Cyanobacteria with *A. thaliana* SAT isoforms 66
4.1.4.2. Alignment of the SAT sequences of green algae with *A. thaliana* SAT isoforms 67
4.1.4.3. Alignment of the SAT sequences of red algae and red-lineage algae with *A. thaliana* SAT isoforms 68
4.1.4.4. Alignment of the OAS-TL sequence of Cyanobacteria with OAS-TL isoforms of *A. thaliana* 71
4.1.4.5. Alignment of the OAS-TL sequence of green algae with OAS-TL isoforms of *A. thaliana* 71
4.1.4.6. Alignment of the OAS-TL sequence of red algae and red-lineage algae with OAS-TL isoforms of *A. thaliana* 72
4.1.5. Main motives of SAT and OAS-TL algal sequences 76
4.1.5.1. SAT sequences main motives in algae 76
4.1.5.2. Main motives in algal OAS-TL sequences 81
4.2. OAS-TL from algae 90
4.2.1. OAS-TL purification 90
4.2.2. OAS-TL enzyme activity in crude extract 97
4.2.3. OAS-TL specific activityin different microalgae 107
4.2.4. Cysteine Synthase Complex (CSC) 108
4.3. In vivo redox regulation of ATP-S activity 115
5. Discussion 121
5.1. SAT and OAS-TL in algae 121
5.2. Cysteine Synthase Complex in algae 123
5.3. ATP-S redox regulation 126

6. References 129
7. Supplemental material 144
7.1. Growth curves 144
7.2. Correlation between relative mobility of protein with protein size 148
7.3. Comparision of algae SAT and OAS-TL with *A. thaliana* sequences 152
7.3.1. Alignment of the SAT sequences of Cyanobacteria with *A. thaliana* SAT isoforms 152
7.3.2. Alignment of the SAT sequences of green algae with *A. thaliana* SAT isoforms 155
7.3.3. Alignment of the SAT sequences of red algae and red-lineage algae with *A. thaliana* SAT isoforms 161
7.3.4. Alignment of the OAS-TL sequence of Cyanobacteria with *A. thaliana* OAS-TL isoforms 167
7.3.5. Alignment of the OAS-TL sequence of green algae with *A. thaliana* OAS-TL isoforms 172
7.3.6. Alignment of the OAS-TL sequence of red and red-lineage algae with *A. thaliana* OAS-TL isoforms 181
7.4. The amino acid code 193
ACKNOWLEDGEMENTS 195

LIST OF FIGURES

Fig. 1-1. Sulphate metabolism in algal cells.. 8
Fig. 3-1. *Synechocystis* sp. PCC 6803. 16
Fig. 3-2. *Chlamydomonas reinhardtii*. 17
Fig. 3-3. *Dunaliella tertiolecta*. 18
Fig. 3-4. *Tetraselmis suecica*. 18
Fig. 3-5. *Thalassiosira pseudonana*. 19
Fig. 3-6. *Phaeodactylum tricornutum*. 19
Fig. 3-7. *Amphidinum klebsii* 20
Fig. 3-8. AtSAT5-pET28^{a} construct map. 27
Fig. 3-9. Protein loading onto the affinity chromatography column. 33
Fig. 3-10. Procedure followed for affinity chromatography. 34
Fig. 3-11. Assembly of a western blot sandwich. 39
Fig. 3-12. Principle of operation of the Amersham ECL Western blotting detection reagent. 40
Fig. 3-13. Basic principles of size exclusion chromagraphy. 43
Fig. 3-14. Fast Protein Liquid Chromatography (FPLC). 44
Fig. 3-15. FPLC Protein standards for column calibration. 45
Fig. 3-16. FPLC column calibration curve. 45
Fig. 3-17. DCMU blocks the electron transfer from Q_A to Q_B. 47
Fig. 4-1. Serine Acetyltransferase phylogenetic tree. 53
Fig. 4-2. The O-Acetylserine (thiol) lyase phylogenetic tree. 56
Fig. 4-3. Alignment of the SAT protein of the freshwater cyanobacterium *Synechocystis* sp. PCC 6803 and the SAT protein of *A. thaliana*. 67
Fig. 4-4. Alignment of SAT protein of algae and *A. thaliana*. 80
Fig. 4-5. Alignment of OAS-TL of algae and *A. thaliana*. 87
Fig. 4-6. Elution pattern of OAS-TL protein from different algal species. 94
Fig. 4-7. Immunodetection of OAS-TL purified from *Synechocystis* sp. PCC 6803. 95
Fig. 4-8. Immunodetection of OAS-TL purified from *Chlamydomonas reinhardtii* grown in TAP medium. 95
Fig. 4-9. Immunodetection of OAS-TL purified from *Chlamydomonas reinhardtii* grown in TP medium. 95
Fig. 4-10. Immunodetection of OAS-TL purified from *Dunaliella tertiolecta*. 96
Fig. 4-11. Immunodetection of OAS-TL purified from *Tetraselmis suecica*. 96
Fig. 4-12. Immunodetection of OAS-TL purified from *Thalassiosira pseudonana*. 96
Fig. 4-13. Immunodetection of OAS-TL purified from *Phaeodactylum tricornutum*. 96
Fig. 4-14. Immunodetection of OAS-TL purified from *Amphidinium klebsii*. 97
Fig. 4-15. OAS-TL enzyme activity in crude extracts of different algae. 98
Fig. 4-16. OAS-TL activity per unit of protein in crude and diluted extracts of *Synechocystis* sp. PCC 6803. 99
Fig. 4-17. OAS-TL activity per unit of protein in crude and diluted extracts of *Chlamydomonas reinhardtii* cultured in TAP medium. 100

Fig. 4-18. OAS-TL activity per unit of protein in crude and diluted extracts of *Chlamydomonas reinhardtii* cultured in TP medium. 101
Fig. 4-19. OAS-TL activity per unit of protein in crude and diluted extracts of *Dunaliella tertiolecta*. 102
Fig. 4-20. OAS-TL activity per unit of protein in crude and diluted extracts of *Tetraselmis suecica*.....103
Fig. 4-21. OAS-TL activity per unit of protein in crude and diluted extracts of *Thalassiosira pseudonana*. 104
Fig. 4-22. OAS-TL activity per unit of protein in crude and diluted extracts of *Phaeodactylum tricornutum*.....105
Fig. 4-23. OAS-TL activity per unit of protein in crude and diluted extracts of *Amphidinium klebsii*. 106
Fig. 4-24. OAS-TL enzyme activity. 108
Fig. 4-25. FPLC chromatogram for OAS-TL from different algae complexed with SAT-5 from *A. thaliana*. 109
Fig. 4-26. Immunodetection of OAS-TL from *Synechocystis* sp. PCC 6803 after elution of the CSC with SAT-5 by FPLC. 110
Fig. 4-27. Immunodetection of OAS-TL from *Chlamydomonas reinhardtii* in TAP medium after elution of the CSC with SAT-5 by FPLC. 110
Fig. 4-28. Immunodetection of OAS-TL from *Dunaliella tertiolecta* after elution of the CSC with SAT-5 by FPLC. 111
Fig. 4-29. Immunodetection of OAS-TL from *Tetraselmis suecice* after elution of the CSC with SAT-5 by FPLC. 111
Fig. 4-30. Immunodetection of OAS-TL from *Thalassiosira pseudonana* after elution of the CSC with SAT-5 by FPLC. 112
Fig. 4-31. Immunodetection of OAS-TL from *Phaeodactylum tricornutum* after elution of the CSC with SAT-5 by FPLC. 112
Fig. 4-32. Immunodetection of OAS-TL from *Amphidinium klebsii* after elution of the CSC with SAT-5 by FPLC. 113
Fig. 4-33. Western blot using antibodies raised against SAT-5 from *A. thaliana*. 114
Fig. 4-34. Fv/Fm of *Thalassiosira pseudonana* incubated in the presence of 5 and 10 µM DCMU, for 0, 1, 3 and 6 hours.....115
Fig. 4-35. *Thalassiosira pseudonana* cell number during incubation with 10 µM DCMU. .116
Fig. 4-36. *Thalassiosira pseudonana* cell volume during incubation with 10 µM DCMU...116
Fig. 4-37. Comparison of ATPS assay blanks obtained with different procedures. The error bars show the standard deviations (n = 3). 117
Fig. 4-38. Comparison of ATPS activity in the presence and absence of DMSO. 118
Fig. 4-39. *Thalassiosira pseudonana* ATP-S activity in the presence or absence of 10 µM DCMU over a period of 6 hours. The error bars show the standard deviations (n = 3). 119
Fig. 5-1. Proposed structure of Algae Cysteine Synthase Complex. 126
Fig. 7-1. *Synechocystis* sp. PCC 6803 growth curve. 144
Fig. 7-2. Calibration curve to convert the OD of *Synechocystis* sp. PCC 6803 cultures to cell numbers. 144

Fig. 7-3. Growth curve of *Chlamydomonas reinhardtii* cultured in TAP medium.....145
Fig. 7-4. Growth curve of *Chlamydomonas reinhardtii* cultured in TP medium 145
Fig. 7-5. *Dunaliella tertiolecta* growth curve 146
Fig. 7-6. *Tetraselmis suecica* growth curve.....146
Fig. 7-7. *Thalassiosira pseudonana* growth curve. 147
Fig. 7-8. *Phaeodactylum tricornutum* growth curve. 147
Fig. 7-9. *Amphinidium klebsii* growth curve. 148
Fig. 7-10. Standard curve for the determination of protein size from the relative protein mobility in binding affinity test chromatography for *Synechocystis* sp.PCC 6803.....148
Fig. 7-11. Standard curve for the determination of protein size from relative protein mobility in binding affinity test chromatography for *Chlamydomonas reinhardtii*with TAP medium culture extract.....149
Fig. 7-12. Standard curve for the determination of protein size from the relative protein mobility in binding affinity test chromatography for *Chlamydomonas reinhardtii* with TP medium culture extract. 149
Fig. 7-13. Standard curve for the determination of protein size from the relative protein mobility in binding affinity test chromatography for *Tetraselmis suecica* extract. 150
Fig. 7-14. Standard curve for the determination of protein size from the relative protein mobility in binding affinity test chromatography for *Dunaelilla tertiolecta* extract.....150
Fig. 7-15. Standard curve for the determination of protein size from the relative protein mobility in binding affinity test chromatography for *Thalassiosira psedonana* extract. 151
Fig. 7-16. Standard curve for the determination of protein size the relative protein mobility in binding affinity test chromatography for *Phaedactylum tricornum* extract. 151
Fig. 7-17. Standard curve for the determination of protein size from the relative protein mobility in binding affinity test chromatography for *Amphidinium klebsii* extract. 152
Fig. 7-18. Alignment of *Synechocystis* sp. PCC 6803 SAT amino acid sequences with *A. thaliana*. 153
Fig. 7-19. Alignment of *Synechococcus* sp. WH 7803 SAT amino acid sequences with *A. thaliana.* 154
Fig. 7-20. Alignment of 1-*C. reinhardtii* SAT amino acid sequence with *A. thaliana* isoforms. 156
Fig. 7-21. Alignment of 2-*C. reinhardtii* SAT amino acid sequence with *A. thaliana* isoforms. 157
Fig. 7-22. Alignment of 1-*T. suecica* SAT amino acid sequence with *A. thaliana* isoforms. 158
Fig. 7-23. Alignment of 2-*T. suecica* SAT amino acid sequence with *A. thaliana* isoforms. 159
Fig. 7-24. Alignment of 3-*T. suecica* SAT amino acid sequence with *A. thaliana* isoforms. 160
Fig. 7-25. Alignment of 1-*C. merolae* SAT amino acid sequence with *A. thaliana* isoforms. 162
Fig. 7-26. Alignment of 2-*C. merolae* SAT amino acid sequence with *A. thaliana* isoforms. 163
Fig. 7-27. Alignment of *T. pseudonana* SAT amino acid sequence with *A. thaliana* isoforms. 164
Fig. 7-28. Alignment of *P. tricornutum* SAT amino acid sequence with *A. thaliana* isoforms.

.....165
Fig. 7-29. Alignment of *E. huxleyi* SAT amino acid sequence with *A. thaliana* isoforms. ...166
Fig. 7-30. Alignment of 1-*Synechocystis* sp. PCC 6803 OAS-TL amino acid with *A. thaliana* isoforms.....168
Fig. 7-31. Alignment of 2-*Synechocystis* sp. PCC 6803 OAS-TL amino acid with *A. thaliana* isoforms.....169
Fig. 7-32. Alignment of 1-*Synechococcus* sp. WH 7803 OAS-TL amino acid with *A. thaliana* isoforms.....170
Fig. 7-33. Alignment of 2-*Synechococcus* sp. WH 7803 OAS-TL amino acid with *A. thaliana* isoforms.....171
Fig. 7-34. Alignment of 1-*C. reinhardtii* OAS-TL amino acid with *A. thaliana* isoforms....173
Fig. 7-35. Alignment of 2-*C. reinhardtii* OAS-TL amino acid with *A. thaliana* isoforms....174
Fig. 7-36. Alignment of 3-*C. reinhardtii* OAS-TL amino acid with *A. thaliana* isoforms....175
Fig. 7-37. Alignment of 4-*C. reinhardtii* OAS-TL amino acid with *A. thaliana* isoforms....176
Fig. 7-38. Alignment of 1-*T. suecica* OAS-TL amino acid with *A. thaliana* isoforms. 177
Fig. 7-39. Alignment of 2-*T. suecica* OAS-TL amino acid with *A. thaliana* isoforms. 178
Fig. 7-40. Alignment of 3-*T. suecica* OAS-TL amino acid with *A. thaliana* isoforms. 179
Fig. 7-41. Alignment of 4-*T. suecica* OAS-TL amino acid with *A. thaliana* isoforms. 180
Fig. 7-42. Alignment of 1-*C. merolae* OAS-TL amino acid with *A. thaliana* isoforms.....182
Fig. 7-43. Alignment of 2-*C. merolae* OAS-TL amino acid with *A. thaliana* isoforms.....183
Fig. 7-44. Alignment of 1-*T. pseudonana* OAS-TL amino acid with *A. thaliana* isoforms. .184
Fig. 7-45. Alignment of 2-*T. pseudonana* OAS-TL amino acid with *A. thaliana* isoforms. .185
Fig. 7-46. Alignment of 1-*P. tricornutum* OAS-TL amino acid with *A. thaliana* isoforms. .186
Fig. 7- 47. Alignment of 2-*P. tricornutum* OAS-TL amino acid with *A. thaliana* isoforms. 187
Fig. 7-48. Alignment of *E. huxleyi* OAS-TL amino acid with *A. thaliana* isoforms.....188
Fig. 7-49. Alignment of 1-*A. klebsii* OAS-TL amino acid with *A. thaliana* isoforms.....189
Fig. 7-50. Alignment of 2-*A. klebsii* OAS-TL amino acid with *A. thaliana* isoforms.....190
Fig. 7-51. Alignment of 3-*A. klebsii* OAS-TL amino acid with *A. thaliana* isoforms.....191
Fig. 7-52. Alignment of 4-*A. klebsii* OAS-TL amino acid with *A. thaliana* isoforms.....192
Fig. 7-53. Amino acid code and relative character. 193

LIST OF TABLES

Table. 3-1. Primer for AtSAT5 amplification 26
Table. 3-2. Reagents for Peterson's protein assay 36
Table. 3-3. Recipe for the SDS-PAGE resolving gel buffer 38
Table. 3-4. Recipe for the SDS-PAGE Stacking gel buffer 38
Table. 3-5. Resolving gel (for 2 gels in the Protean minigel system) 38
Table. 3-6. Stacking gel (for 2 gels in the Protean minigel system). 38
Table. 3-7. Coomassie Staining solution 38
Table. 3-8. Coomassie Destaining solution 38
Table. 4-1. Number of Cysteines residues, sequence length and location of algae serine acetyltransferase (SAT) 59
Table. 4-2. O-acetylserine (thiol) lyase (OAS-TL) of algae with different taxonomy, ecology, and the location prediction 62
Table. 4-3. Comparasion of N'-terminus and C'-terminus sequences of algal SAT the corresponding regions as *A. thaliana* SAT isoforms 69
Table. 4-4. Identity and similarity of algal SAT protein sequence with *A. Thaliana* isoforms 70
Table. 4-5. Alignment of N'-terminus and C'-terminus sequences of algal OAS-TL corresponding regions in *A. thaliana* OAS-TL isoforms 74
Table. 4-6. Identity and Similarity of algae OAS-TL with reference species of *A. thaliana* isoforms 75
Table. 4-7. Main binding motives in OAS-TL sequences 88
Table. 4-8. Features of purified algae OAS-TL 91
Table. 4-9. Summary of OAS-TL activity in 100-fold diluted and undiluted crude extracts. 106

1. Introduction

1.1. Impact of sulfur availability on algae ecology, evolution and radiation

Photosynthetic organisms acquire the macronutrient sulfur (S) as sulfate (SO_4^{2-}), with the highest oxidation number of +6. Sulfur, however, is assimilated into organic matter (in cysteine) as sulfide (S^{-2}). Consequently, a conspicuous amount of reducing power is needed to support S assimilation. In embryophytes, this reducing power can derive from linear electron transport, from the pentose phosphate shunt or from the mitochondrial electron transfer chain (Schmidt, 1979). Sulfur assimilation in algae is believed to be more strictly dependent on photosynthesis (Schmidt, 1979).

On average, S is typically below 1 mM (sometimes, much below this value) in freshwater, but it is very abundant in the ocean (about 29 mmol L^{-1}). This makes S never limited in the ocean, although in oligotrophic freshwaters, there are indications that S-limitation may be possible (Giordano, 2005).

The concentration of S in the oceans has not always been so high (Ratti et al., 2011). Sulfate concentration was probably around 200 μmol L^{-1} when the first cyanobacteria appeared (Habicht et al., 2002), and raised to less than 5 mM in the Proterozoic Era and to 10-15 mM in the late Palaeozoic Era (Shen et al., 2002; Canfield, 2004; Kah et al., 2004). At the beginning of the Mesozoic, sulfate concentration increased stepwise to a concentration of 13-27 mM (Giordano & Prioretti, 2016.) In concomitance with the Mesozoic increase of oceanic S, phytoplankton composition changed and a domination shift from green algae to the red-lineage algae occurred (Giordano, 2005; Ratti et al., 2011; Knoll et al., 2017). It has been proposed that this shift in dominance was favored, although not fully determined, by the sulfate increase (Sulfate

Facilitation Hypothesis, Ratti et al., 2011; Prioretti et al., 2014).

It is still not clear if the influence of S on phytoplankton radiation was associated with differences in the S metabolism of red-lineage algae compared to green algae or if the increased S availability exerted an indirect effect on the success of some clades (Giordano & Prioretti, 2016); the indirect effect of S may have been associated to the higher S quotas of red lineage algae, which allocate a large portion of S to dimethylsulfoniopropionate (DMSP) (Ratti et al., 2011; Norici et al., 2005). The synthesis of DMSP may have been a response to ocean oxygenation, which led to a decrease of N availability: DMSP, under these circumstances, would have been a cheaper osmolyte than the N-containing glycine betaine (Andreae, 1986; Dacey et al., 1987; Turner & Beidel, 1988; Gröne & Kirst, 1992; Andreae & Meinrat, 1990; Liss et al., 1997; McNeil et al., 1999). DMSP, when a cell is lysed due to predation or other causes, is degraded by bacterial lyases (de Souza & Yoch, 1995a, b; Yoch et al., 1997) and marine algae DMSP lyases (Steinke et al., 1996; Steinke & Kirst, 1996; Stefels, 2000); the products of such degradation are DMS and acrylate, both capable of anti-grazing activity (Steinke et al., 2002a; Steinke et al., 2002b).

Thus, the increased grazing pressures exerted by some micrograzers (especially copepods) at the beginning of the Mesozoic era (see Giordano et al., 2018 for a discussion on this event) may have exerted a selective pressure in favor of those phytoplankton clades more capable of responding to the challenge, among these those groups with a higher S cell quota and thus a higher DMSP content (Prioretti & Giordano, 2016).

1.2. Sulfur metabolism

1.2.1. Sulfate acquisition

Three main types of sulfate transporters have been identified in algae. As described in Fig. 1-1. In the plasmalemma of eukaryotic algae, H^+/SO_4^{2-} (SULTR) and Na^+ /SO_4^{2-} (SLT) co-transporters have been identified; the expression of both types of transporters is induced by low sulfate availability. The proton gradients across the plasmalemma possibly energize, more or less directly, these transporters. In Cyanobacteria, sulfate transport is carried out by an ATP-binding-cassette (ABC) transporter, with a transmembrane channel constituted by the SulP and SulP2 proteins (SULP stands for sulfate permeases). A sulfate binding protein (Sbp) is linked to the Sup and SulP2 proteins, on the side of the protein emerging on the extracellular face of plasmalemma; ATP-binding proteins (Sabc) are instead present on the cytosolic portion of Sulp and Sulp2; the Sabc catalyzes the hydrolysis of ATP, which energizes the transport of sulfate (Melis & Chen, 2005). Interesting, a similar type of transporter is present on the inner chloroplast membrane of *Chlamydomonas reinhardtii* (Lindberg & Melis, 2008).

1.2.2. Sulfate reduction

In photosynthetic organisms, sulfate reduction occurs in the chloroplast. The only known exception is *Euglena gracilis*, which reduces sulfate in the mitochondrion (Takahashi et al., 2011). Sulfate reduction is a rather complicated process, due to the fact that the redox potential of the sulfate/sulfite pair is too negative (E_0' = -0.454) for the cell electron donors to provide the energy for this chemical transformation. For sulfate to be reduced to sulfite, it needs to be activated to adenosine 5′-phosphosulfate (APS. E_0' = -0.060) (Schmidt & Jager, 1992). This sulfate adenylation was catalyzed by the enzyme ATP sulfurylase (ATPS; EC 2.7.7.4). Algal ATPS differ from those of vascular plants (Prioretti et al., 2014). Among the most typical features of algal ATPS is the high number of cysteine residues. It has been shown that, in oceanic cyanobacteria and in eukaryotic algae, some of these cysteine residues are involved in

the redox regulation of ATPS (Giordano & Prioretti, 2016; Prioretti et al., 2016). The ATPS of dinoflagellates and freshwater and coastal cyanobacteria, instead, appears not to be subject to redox regulation (Giordano & Prioretti, 2016; Prioretti et al., 2016).

The APS generated in the reaction of ATPS is then reduced to sulfite with the intervention of APS reductase (APR; EC 1.8.4.9). In vascular plants, glutathione is used as the donor of reducing power in this reaction; no direct evidence on whether this is the case in algae exists. The sulfite generated in the reaction catalyzed by APR is further reduced to sulfide by a ferredoxin-dependent sulfite reductase (EC 1.8.7.1); 6 electrons are required for this reduction.

Instead of being used for the production of reduced S, APS can also initiate the sulfation pathway. In this case, APS is probably produced by different isoforms of ATPS from those used in the plastid for sulfate reduction, mostly located in the cytosol; unfortunately, not much is known on sulfation in algae and thus I can only provide limited and anecdotical information on this pathway. Sulfation, in vascular plants, requires that APS is further phosphorylated by APS kinase (APK; EC 2.7.1.25); 3´-phosphoadenosine 5´-phosphosulfate is thus produced PAPS; (Takahashi et al., 2011). PAPS is used by sulfotransferases (EC 2.8.2.24) to donate sulfate groups to all sorts of different molecules (Giordano & Prioretti, 2016). This is mostly done to increase the polar character of molecules and make them more soluble (Dahl et al., 2008).

1.2.3. Cysteine synthesis

Once sulfide is produced, it is assimilated into organic matter by the production of the S-amino acid cysteine. Cysteine synthesis requires two reactions. The first reaction is catalyzed by the enzyme serine acetyltransferase (SAT; EC 2.3.1.30), which produces

O-acetylserine (OAS) from serine and acetyl-CoA (Fig. 1-1,). O-acetylserine, together with sulfide, then acts as the substrate of OAS-(thiol) lyase (OAS-TL; EC 4.2.99.8), which catalyzes the synthesis of cysteine (Leustek et al., 2000; Kopriva, 2006). SAT and OAS-TL are regulated through the assemblage and disassemblage of a complex, the so called Cysteine Synthase Complex (CSC) (Bogdanova & Hell, 1997). The complex does not facilitate the reaction by substrate channeling, because the OAS-TL is not functional when complexed with SAT; the synthesis of cysteine is only accomplished by free OAS-TL (Droux et al., 1998; Wirtz et al., 2001).

In vascular plants, SAT is a hexamer of 29 kDa subunits. It is a member of the hexapeptide acyltransferase enzyme family (Olsen et al., 2004). The functional analysis of SAT domains, using the yeast two-hybrid system, showed that the N-terminal α-helical domain of SAT is involved in SAT/SAT interaction; the C-terminal domain, instead appears to be responsible for both enzymatic activity and SAT/OAS-TL interaction (Bogdanova & Hell, 1997). The idea of a bifunctional C-terminal SAT domain was further strengthened by the modelling of the C-terminus of plant SAT using bacterial acyltransferase structures as templates (Hell & Wirtz, 2008). The location of SAT is already known in different higher plants: *Arabidopsis* SAT isoform located in mitochondria (Roberts & Wray, 1996; Noji et al., 1998; Wirtz et al., 2001; Krueger et al., 2009), *Arabidopsis* SAT located in the plastid (Murillo et al., 1997; Noji et al., 1998; Krueger et al., 2009), *Arabidopsis* SAT located in the cytosol (Howarth et al., 1997; Noji et al., 1998; Howarth et al., 2003), *Citrullus vulgaris* (watermelon) SAT2 (Saito et al., 1995), spinach SATase *Allium tuberosum* ASAT5 (Urano et al., 2000), *Glycine max* cytosolic isoform SATase1 (Chronis & Krishnan, 2004), through the domain analised of *O. parapolymorpha* SAT (OpSat1p) and other fungal SATs the new research data revealed a mitochondrial targeting sequence (MTS) at the N-terminus and an α/β hydrolase one domain at the C-terminal region possessed in the fungal (Yeon et al., 2018).

O-acetylserine (thiol) lyase (EC 4.2.99.8) (OAS-TL) is also known as O-acetylserine sulfhydrylase or cysteine synthase (CSase) belongs to the family of β-replacement enzymes (Kopriva et al., 2008). OAS-TL, in embryophytes, is a homodimer with 35

kDa subunits (León et al., 1987). In higher plants and algae, isoforms of OAS-TL are located in the cytosol (Álvarez et al., 2010), mitochondria (Álvarez et al., 2012), and plastids (Heeg et al., 2008).

The structure of the first plant OAS-TL was recently resolved, demonstrating a high degree of conformational similarities between plant and enterobacterial OAS-TL (Bonner et al., 2005); such similarities allow plant and bacteria OAS-TL to form stable homodimers, with a molecular weight from 68 to 75 kDa. Crystallization of OAS-TL from bacteria showed that each OAS-TL subunit carries a tightly bound pyridoxal 5′-phosphate at the catalytic site (Hatzfeld et al., 2000). The conservation of the active site residues strongly supports the idea that the same prokaryotic and eukaryotic OAS-TLs share the same kinetic mechanism.

SAT and OAS-TL of bacteria and embryophytes form CSC of similar size (Becker et al., 1968; Kredich et al., 1969). By using size-exclusion chromatography, a total molecular weight of 309 kDa for the hetero-oligomeric CSC was determined from *Salmonella typhimurium* (Kredich et al., 1969); 160 kDa were attributed to two SAT trimer and 68 kDa were due to a OAS-TL dimer (Kredich & Becker, 1969). In *Arabidopsis thaliana*, the Cysteine Synthase Complex is formed when an excess of sulfide is present and is disassembled when OAS accumulates in the cell (Droux et al., 1998; Hell & Wirtz, 2011).

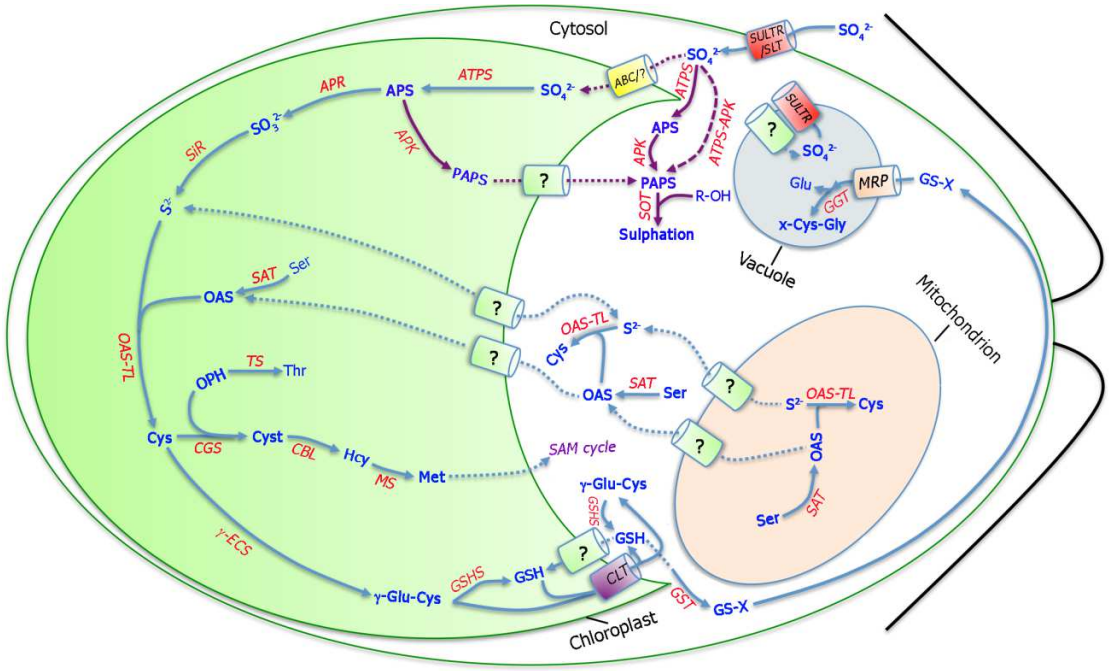

Fig. 1-1. Sulphate metabolism in algal cells.

An overall view of sulphur assimilation and of sulphation is depicted here (Giordano & Prioretti, 2016): the enzymes are indicated in red, metabolites in blue and transporters in black. The light blue lines indicate the reactions of the reductive sulphate assimilation pathway; the dark purple lines indicate reactions of the sulphation pathway; dashed lines indicate putative pathways for metabolite transport that are not been incon- trovertibly demonstrated. ABC ATP-binding cassette SO_4^{2-} transporter, APK APS kinase, APR APS reductase, APS adenosine 5′-phosphosulphate, ATPS ATP sulphurylase, CBL cystathionine β-lyase, CGS cystathionine γ-synthase, CLT thiol transporter (chloroquine resistance transporter-like transporter, Cys cysteine, Cyst cystathionine, γ-ECS γ-glutamylcysteine synthetase, GGT γ-glutamyltransferase, Glu glutamate, γ-Glu-Cys γ-glutamylcysteine, GSH glutathione, GSHS glutathione synthetase,

GST glutathione-S- transferase, GS-X glutathione conjugate, Hcy homocysteine, Met methionine, MRP multidrug resistance-associated protein, MS methionine synthase, OAS O-acetylserine, OAS-TL OAS (thiol) lyase, OPH O-phosphohomoserine, PAPS 3′-phosphoadenosine 5′-phosphosulphate, R-OH hydroxylated precursor, SAM S-adenosylmethionine, SAT serine acetyltrans- ferase, Ser serine, SiR sulphite reductase, SLT Na^{+}/SO_4^{2-} transporter, SOT sulphotransferase, SULTR H^{+}/SO_4^{2-} transporter, Thr threonine, TS threo- nine synthase, X-Cys-Gly cysteinylglycine conjugate.

2. Hypotheses

In this thesis, I focused on the first and on the last step of the S assimilation pathway.

The first step, the one catalyzed by ATPS, still requires to be elucidated with respect to the *invivo* mechanisms for redox regulation. By similarity with other enzymes (e.g. nitrate reductase; Giordano et al., 2005), I hypothesize that:

Hp 1: the perception of the availability of redox power for the initiation of sulfate assimilation is constituted by the redox state of the plastoquinone pool of the electron transfer chain in the chloroplast.

The reduction state of the plastoquinone pool is the indicator of the rate of electron transport and of the level of reduction of ferredoxin, which possibly is the main donor of electrons for sulfate assimilation. It would, therefore, be a good sensor for the overall availability of electrons available for the reduction of sulfate to sulfide. If such a regulation mechanisms exists, this would represent a major difference with respect to embryophytes: in embryophytes, the main control step of sulfate reduction is at APR reduction (Takahashi et al. 2011); if ATPS activity is finely regulated *in vivo* via the redox state of the plastoquinone pool, this would move the first control step of the pathway already at sulfate activation. This is intriguing because it would suggest that a greater control on energy investment exists on S assimilation in algae, which would not commit to the use of ATP for sulfate activation, unless sufficient redox power for the completion of the pathway is available.

The last step of S assimilation is that of cysteine synthesis. In the absence of any

data on SAT and OAS-TL from algae, it is not possible to generalize the regulatory mechanism proposed for embryophytes to all photosynthetic organisms. I thus intended to verify whether a CSC is involved in cysteine synthesis in algae and test the following hypothesis:

HP 2: Cysteine synthesis of algae works through the constitution of a CSC.

3. Materials and methods

3.1. Bioinformatic methods

3.1.1. Protein sequences and phylogenetic trees

All protein sequences were obtained from the NCBI Protein Database (http://www.ncbi.nlm.nih.gov/protein/), both by looking for the SAT and OAS-TL sequences of specific organisms and by using BLASTP (protein-Basic Local Alignment Search Tool) (Altschul et al., 1990; Goujon et al., 2010; Sievers et al., 2011). The phylogenetic analysis was conducted using the MEGA 5.0 software (Tamura et al., 2011). The Maximum Likely hood method was used for the construction of phylogenetic trees (Saitou & Nei, 1987; Sanderson & Driskell, 2003). The bootstrap values (Fron et al., 1996) shown on the tree branches represented the confidence level of clades, i.e. the number of reiterations (out of 100) of data analysis that gives the same branch (Karlin & Altschul, 1990). The evolutionary distance between branches (corresponding to the branch length) was computed using the Poisson correction method (Zuckerkandl & Pauling, 1965) and expressed in terms of the number of amino acid substitutions per site. All positions containing gaps and missing data were eliminated.

3.1.2. Predictions on the location of SAT and OAS-TL proteins

Prediction of sub-cellular localization of proteins was performed with the Target P 1.1

online software (http://www.cbs.dtu.dk/services/TargetP/), as described in Emanuelsson and coauthors, 2007. Also, the on line software identified the sequences signal peptides and prediction of their cleavage sites (Nielsen et al., 1997).

The http://mobyle.pasteur.fr/cgi-bin/portal.py#jobs::boxshade online software was used to acquire the bioinformatic about the proteins and then to identify protein homogeneity predicting evolutionary relationship among different species (Koonin & Galperin, 2003).

3.1.3. Analysis of SAT and OAS-TL algae sequences

Fig. 4-4 and Fig. 4-5 showed the degree of SAT and OAS-TL conserved area in different species, respectively. Multiple sequence alignment was done with the T-Coffee on line software (http://tcoffee.crg.cat/apps/tcoffee/do:regular) (Notredame et al., 2000; Felix et al., 2005; Moretti et al., 2011; Weimbs & Santa, 2012). Representation of the alignment was done using the Boxshade program (http://www.ch.embnet.org/software/BOX_form.html). In the Boxshade figures, for clarity, only some species were shown for each algal clade.

Pairwise Sequence Alignment through the on line software (https://www.ebi.ac.uk/Tools/psa/emboss_matcher/) EMBOSS Matcher identifies local similarities between two sequences using a rigorous algorithm based on the LALIGN application (Koonin, & Galperin, 2003; Kleckner et al., 2016).

3.2 Experimental organisms

3.2.1. *Synechocystis* sp. PCC 6803

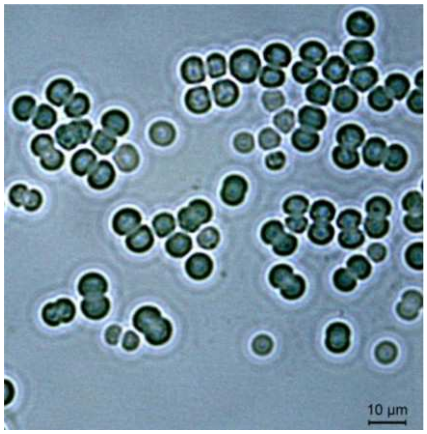

Fig. 3-1. *Synechocystis* sp. PCC 6803.

The cyanobacterium *Synechocystis* (phylum Cyanobacteria, order *Chroococcales*) (Fig. 3-1) (Selim et al., 2018) is a freshwater organism with cells of about 2 µm in diameter, and coccoid in shape. The cells blue-green color is mainly due to phycocyanin, abundant in the antenna complex of photosystem II (PSII). In this thesis I used strain PCC 6803, which is the first photoautotrophic organism whose genome was fully sequenced (Nakamura et al., 1998); the size of *Synechocystis* PCC 6803 genome is 3.57 Mbp. The ease with which this organism can be cultivated and genetically manipulated (Kufryk et al., 2002) made it a model for the study of physiology and genetics of photosynthetic organisms.

3.2.2. *Chlamydomonas reinhardtii*

The *Chlamydomonas reinhardtii* (phylum Chlorophyta, class Chlorophyceae, order *Volvocales*) (Fig. 3-2) is a ubiquitous freshwater green algae, with ovoid, biflagellate cells of about 10 µm in diameter (Harris et al., 2009). Its mitochondrial (15.8 Kbps;

Trans & Land, 1988; Rochaix, 1995), plastidial (203.4 Kbps; Maul et al., 2002) and nuclear (121 Mbps; Merchant et al., 2010) genomes have been sequenced and a large collection of mutants is available.

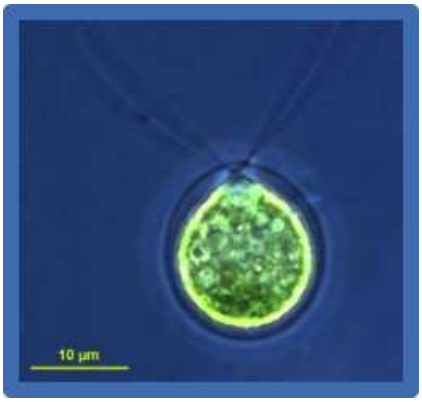

Fig. 3-2. *Chlamydomonas reinhardtii.*

3.2.3. *Dunaliella tertiolecta*

Unicellular green algae *Dunaliella* belong to the Chlorophytes (Oren-shamir et al., 1990; Oren, 2005). The algae were first described (Dunal, 1838), but it was not until 1905 that the name *Dunaliella* was given by Teodoresco (1905). *Dunaliella tertiolecta* (phylum Chlorophyta, class Chlorophyceae, order *Volvocales*) (Fig. 3-3) (Mesquita et al., 2013) is a marine green flagellate with a cell size of 10−12 µm. This genus is characterized by the absence of a rigid polysaccharide wall (Gibbs & Duffus, 1976), instead, cells are covered by the amorphous mucilaginous layer of variable thickness called a glycocalyx. *Dunaliella* cells are motile with two equally long flagella. In 2017 (Yao et al., 2017), RNA-Seq technology data were *de novo* assembled and annotated, 17,845 protein-coding transcripts resulted in *Dunaliella tertiolecta* (~95% completeness).

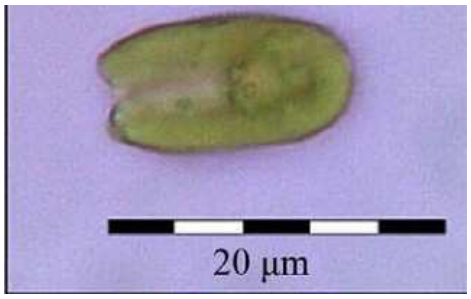

Fig. 3-3. *Dunaliella tertiolecta.*

3.2.4. *Tetraselmis suecica*

Tetraselmis suecica Strain 1878 (phylum Chlorophyta, class Chlorodendrophyceae, order *Chlorodendrales*) (Fig. 3-4) (Mesquita et al., 2013) is a green marine flagellate alga. It is often classified in the informal group of Chlorella pyrenoidosa prasinophytes, some members of which belong to the basal Chlorophyta. A transcriptome was produced by M. Giordano and C. Delwiche (unpublished).

Fig. 3-4. *Tetraselmis suecica.*

(Photo by David Patterson and Bob Andersen via Encyclopedia of Life).

3.2. 5. *Thalassiosira pseudonana*

Thalassiosira pseudonana Cleve 1873 (phylum Heterokonta, class

Coscinodiscusphyceae, order *Thalassiosirales*) (Fig. 3-5). *Thalassiosira pseudonana* is a small centric diatom with an average cell diameter of 2-15 μm. This diatom is found both as a single cell or chain colony of up to 6 cells. It is especially abundant in coastal waters. Its genome has been sequenced (Armbrust et al., 2004).

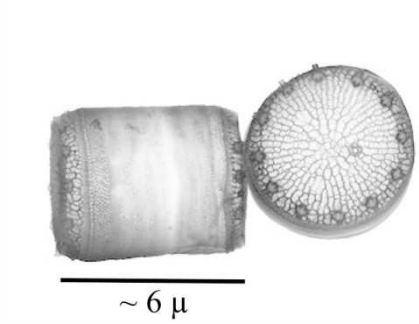

Fig. 3-5. *Thalassiosira pseudonana.*

(SEM Photo by N. Kröger, Alfred Wegener Institute, Germany).

3.2.6. *Phaeodactylum tricornutum*

Phaeodactylum tricornutum Bohlin 1897 (phylum Heterokonta, class Bacillariophyceae, order Naviculales) (Fig. 3-6) (Miyahara et al., 2014) is a pennate marine diatom, with little silicified cells (Lewin et al., 1958), and four morphotypes: oval, fusiform, triradiate and cruciform, the latter being rarely reported (He et al., 2014). *P. tricornutum* genome has been sequenced (Daboussi et al., 2014).

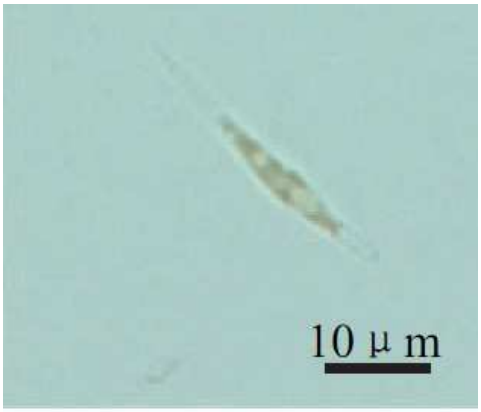

Fig. 3-6. *Phaeodactylum tricornutum.*

3.2.7. *Amphidinium klebsii*

The dinoflagellate group encompasses a variety of morphologically very dissimilar organisms. It includes marine and freshwater species; autotrophic, mixotrophic, and heterotrophic modes of nutrition; pelagic and benthic forms. *Amphidinium klebsii* (phylum Miozoa, Class Dinoflagellata, order *Gymnodiniaceae*) (Fig. 3-7) is a common dinoflagellate in temperate and tropical marine waters. The cell diameter is around 10-15 µm. A transcriptome was produced by M. Giordano and C. Delwiche (unpublished).

Fig. 3-7. *Amphidinum klebsii.*

(photo by Jacob Larsen).

3.3. Cultures

3.3.1. Culture conditions

Prior to any experiment/measurement, algae were allowed to acclimate to their

culture conditions for at least 4 generations.

3.3.1.1. *Synechocystis* sp. PCC 6803

Synechocystis sp. PCC 6803 was cultured in batch, in 250 mL Erlenmeyer flasks containing 150 mL of algal suspension. Only for protein purification, for all species, larger (4 L) vessels were used. The growth temperature was 20 ± 0.5 ℃. Cultures were illuminated continuously with PAR (340-700 nm) light at an irradiance of 50 µmol photons m^{-2} $s^{-}1$. The irradiance was measured with a quantometer (LI-250 Light Meter; LI-COR, Inc.). Cultures were bubbled with filter-sterilized air. As for all species, experiments were conducted on exponentially growing cells.

3.3.1.2. Eukaryotic algae

All eukaryotic species were cultured in the same conditions used for *Synechocystis*, except for the irradiance, which was 120 µmol photons m^{-2} s^{-1} (PAR).

3.3.2. Growth media.

3.3.2.1. BG-11 medium

For *Synechocystis* PCC 6803, BG-11 medium (Stanier et al., 1971) was used. BG-11 medium contained: $NaNO_3$ (17.65 mmol L^{-1}), K_2HPO_4 (0.23 mmol L^{-1}), $MgSO_4 \cdot 7H_2O$ (0.304 mmol L^{-1}), $CaCl_2$ (0.245 mmol L^{-1}), citric acid (0.031 mmol L^{-1}), Ammonium Ferric Citrate (6 mg L^{-1}), $EDTANa_2 \cdot 2H_2O$ (0.0027 mmol L^{-1}), Na_2CO_3

(0.0189 mmol L^{-1}), and trace metals. The trace metal solution had the following composition: H_3BO_3 (0.0463 mmol L^{-1}), $MnCl_2•4H_2O$ (0.0091 mmol L^{-1}), $ZnSO_4•7H_2O$ (0.00077 mmol L^{-1}), $Na_2MoO_4•2H_2O$ (0.0016 mmol L^{-1}), $CuSO_4•5H_2O$ (0.00032 mmol L^{-1}), $Co(Cl)_2•6H_2O$ (0.000172 mmol L^{-1}), Tris-HCl pH 7.6 (10 mmol L^{-1}); 0.5 ml of this trace metal solution was used in 1 L of BG-11.

3.3.2.2. TAP and TP medium

Chlamydomonas reinhardtii was cultured in either Tris-Acetate-Phosphate (TAP) medium or Tris-Phosphate (TP) minimal medium (Gorman & Levine, 1965). TAP medium contained: Trizma base (17.67 mmol L^{-1}), NH_4Cl (7.48 mmol L^{-1}), $CaCl_2$ (0.45 mmol L^{-1}), $MgSO_4•7H_2O$ (0.41 mmol L^{-1}), Na_2EDTA (0.13 mmol L^{-1}), $FeSO_4•7H_2O$ (0.018 mmol L^{-1}), $ZnSO_4•7H_2O$ (0.077 mmol L^{-1}), H_3BO_3 (0.18 mmol L^{-1}), $MnCl_2•4H_2O$ (0.026 mmol L^{-1}), $MnCl_2•4H_2O$ (8.04 mmol L^{-1}), $CuSO_4•5H_2O$ (0.0064 mmol L^{-1}), $Na_2MoO_4•2H_2O$ (0.0032 mmol L^{-1}), $CoCl•6H_2O$ (0.012 mmol L^{-1}), potassium phosphate buffer (1 mmol L^{-1}), pH 7.2; 0.1% (v/v) glacial acetic acid was added to the medium to adjust the pH to 7.2, after the medium was autoclaved. TP medium had the same composition as TAP, with the exception of the acetic acid, which was omitted; the pH of TP medium was adjusted with HCl, after the medium was autoclaved, to obtain a final pH of 7.2.

3.3.2.3. Artificial Multipurpose Complement for the Nutrition of Algae (AMCONA)

All other species were cultured in AMCONA medium (Fanesi et al., 2014). The composition of this medium was as follows: NaCl (363 mmol L^{-1}), Na_2SO_4 (8.04

mmol L^{-1}), KCl (8.04 mmol L^{-1}), $NaHCO_3$ (2.07 mmol L^{-1}), KBr (725 µmol L^{-1}), H_3BO_3 (372 µmol L^{-1}), NaF (65.7 µmol L^{-1}), $MgCl_2 \cdot 6H_2O$ (41.2 mmol L^{-1}), $CaCl_2 \cdot 2H_2O$ (9.14 mmol L^{-1}), $SrCl_2 \cdot 6H_2O$ (82 µmol L^{-1}), $NaNO_3$ (549 µmol L^{-1}), $NaH_2PO_4 \cdot H_2O$ (21 µmol L^{-1}), $NaSiO_3 \cdot 9H_2O$ (205 µmol L^{-1}), $CuSO_4 \cdot 5H_2O$ (40 nmol L^{-1}), Tris-HCl, Ph 8.0 (10 mmol L^{-1}), $FeCl_3 \cdot 6H_2O$ (6.56 mmol L^{-1}), $Na_2EDTA \cdot 2H_2O$ (6.56 mmol L^{-1}), $ZnSO_4 \cdot 7H_2O$ (254 µmol L^{-1}), $CoSO_4 \cdot 7H_2O$ (5.69 µmol L^{-1}), $MnSO_4 \cdot 4H_2O$ (6.1 µmol L^{-1}), $Na_2MoO_4 \cdot 2H_2O$ (6.1 µmol L^{-1}), Na_2SeO_3 (1 µmol L^{-1}), $NiCl_2 \cdot 6H_2O$ (6.3 µmol L^{-1}), $Na_2EDTA \cdot 2H_2O$ (8.29 mmol L^{-1}), Thiamine-HCl (297 µmol L^{-1}), Biotin (4.09 µmol L^{-1}), B12 (1.47 µmol L^{-1}).

3.3.3. Determination of cell concentration

Since the cyanobacteria *Synechocystis* sp. PCC 6803 cell size is too small to be easily counted with an optical microscope and also counts with an automatic cell counter are not fully reliable, because cells are undistinguishable from debris and occasional bacteria, cell concentration of *Synechocystis* was routinely measured as optical density at 750 nm with a Beckman DU 640 Spectrophotometer (Beckman Coulter) (Zerulla & Ludt, 2016). At 750 nm, photosynthetic pigments do not significantly absorb light (Rabinowitch & Govindjee, 1969; Govindjee, 2004). In order to convert optical density to cell number, a calibration curve was made with samples containing serially diluted subsamples of a concentrated culture of *Synechocystis* sp. PCC 6803 of known cell concentration. The cell concentration of the reference *Synechocystis* sp PCC 6803 culture was determined by counts under a microscope (Zeiss Axioskop, Germany) applying the following equation:

Cell concentration (cell ml^{-1}) = [N×S1/ S2]/ V1

Where S1 is the slide area (mm^2); V1 is the sample volume (ml); S2 is 5 times the field area at a 400x magnification (mm^2); N is the total cell number counted in 5 field areas.

Freshly made, 0.2 µm filtered cell free BG-11 medium was used as the blank.

Slide area (mm^2) was 24×40, the field area was 400 mm^2.

To determine cell concentration of all the others experimental algae, cells were counted with an automatic cell counter CASY TT (Roche Innovatis, Mannheim, Germany). An aliquot of 100 µl of culture was diluted in 10 ml of CASYton, an electrolyte solution specifically developed by the counter manufacturer. The sample was sucked into the counter through a measuring capillary (60 µm pore size), at a constant flow rate. Then a pulsed low voltage (1 MHz) was applied between two platinum electrodes; the electrolyte provided the background electrical resistance. When a cell intersected the electric field in the capillary, the cell acted as an insulator and increased resistance between the electrodes. The number of cells was determined from the number of events of current disturbance. The duration of this change in conductivity is proportional to the size of cells (corresponding to the volume of electrolytes displaced by cells). This allowed the determination of a cell volume. Since dead cells are partially empty, they exert a lower resistance to the current and can therefore be discriminated from live cells. Cell concentration was determined twice or thrice per day and used to construct growth curved.

3.3.4. Growth rate determination

The specific growth rate, µ, was calculated from the equation below (Maqsood, 1974):

$$\mu = \frac{\mathrm{lnX1} - \mathrm{LnX2}}{\mathrm{t(day)}}$$

Where X_1 is the cell number at time 1 and X_2 is cell number at time 2. Both time points were chosen to be in the exponential growth phase; t is the time expressed in days.

3.3.5. Biomass harvesting

For all measurements/experiments, algae acclimated to the growth conditions were collected by centrifugation using are refrigerated centrifuge (Beckman, California, USA) equipped with a JA-10 rotor (Beckman, California, USA). The algal suspension was centrifuged at 5000 g, for 10 min, at 4 ℃. The pellet was collected and frozen -80 ℃ until used.

3.4. Overexpression of AtSAT5

In order to purify OAS-TL, *Arabidopsis thaliana* SAT5 (AtSAT5 or SAT-5) was used as the ligand in the affinity column. This protein was modified by a histidine tag, in view of its utilization as a ligand in affinity chromatography. It was then overexpressed in *E. coli*, after transfection of the bacterium with the plasmid pET28a, into which the AtSAT5 gene had been inserted (Fig. 3-8). The plasmid containing the His-Tagged AtSAT5 was kindly donated by Prof. Ruediger Hell, Heidelberg University.

The amount of plasmid was determined by reading the DNA concentration in MilliQ water using a NANODROP 1000 spectrophotometer V3.8 (Thermofisher, Massachusetts, USA). The concentration used for the transformation was 20 ng/µl.

3.4.1. Primer design

In order to verify that the gene of interest was in the plasmid and then in the transformed cells, primers specific for AtSAT5 (Gene ID: 835778, SAT 5: AT5G56760) (Tabata et al., 2000) were designed with the Prim Primer, 5.0 software. Their sequences were shown in Table. 3-1. the gene regions that these primers amplified were located at the beginning, middle and end of the AtSAT5 DNA sequence.

Table. 3-1. Primer for AtSAT5 amplification

Gene Name	Length	Primer sequence
AtSAT5-1	187 bp	FW: AAACAGCGGTGATTGGGAAC; RV: ATCAGCACAACAGAACCAGC
AtSAT5-2	307 bp	FW: CAGAAGCAGCGTCAGC; RV: TCACGAACACGAGCAG
AtSAT5-3	285 bp	FW: TCCGATGAAGCAGAAG; RV: GGTGGCGTTACGAAGAG
AtSAT5-4	322 bp	FW: ACAATCACGGAAGCCATTAGCAT; RV: GTCAATCAGCACAACAGAACCAG
Vector		FW: (T7) TAATACGACTCACTATAG; RV: (T7 terminator) GCTAGTTATTGCTCAGCGG

FW = forward primer, RV = reverse primer. T7 = T7 RNA Polymerase.

3.4.2. AtSAT5 Colony transformation assessment in *E. coli*

The pET28a plasmid (Wirtz, 2004) (Fig. 3-8) was used for the insertion of the AtSAT5 gene into *E. coli*. This plasmid was donated by Prof. Ruediger Hell, Heidelberg University.

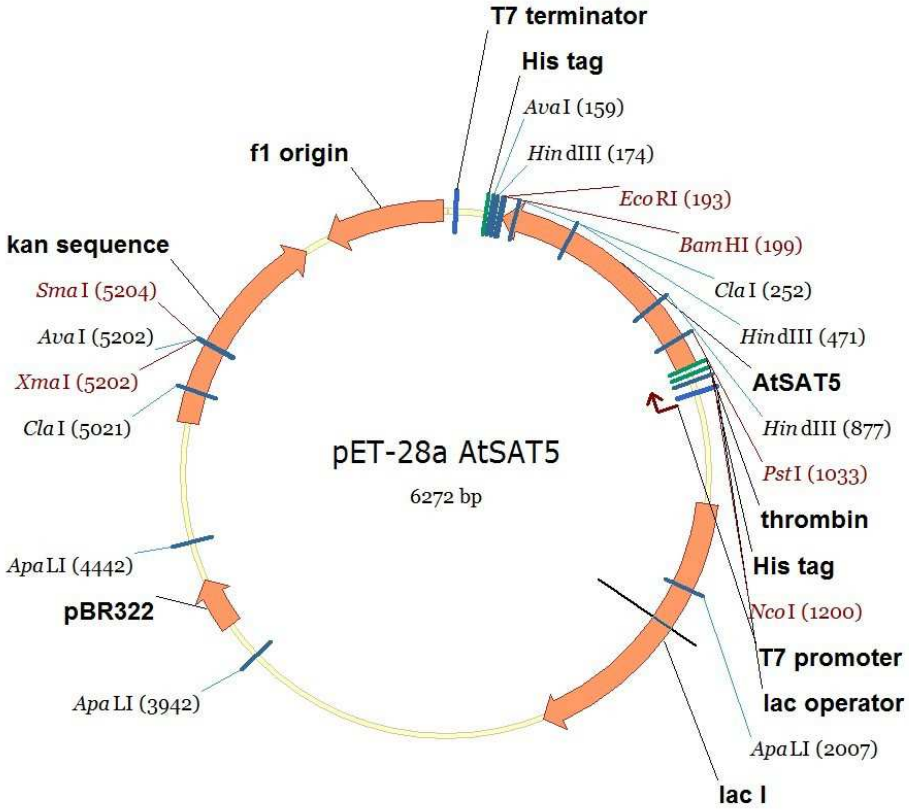

Fig. 3-8. AtSAT5-pET28[a] construct map.

Cloning was conducted using *E.coli* DH10 competent cells, according to the protocol shown below:

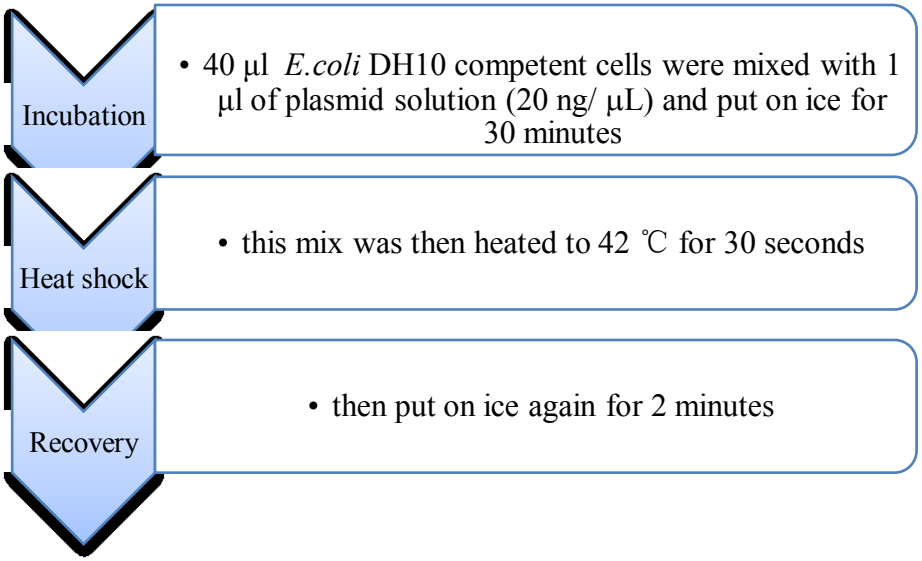

Subsequently, 950 µl of Super Optimal Broth with Catabolite (SOC) medium

(Sambrook & Russell, 2001) were added to the *E. coli*/plasmid mix and incubated at 37℃, for 1 hour, in an incubator (SSI5 SHEL LAB Floor Model Shaking Incubator, 5 Cu.Ft.), under continuous shaking at 250 rpm. The SOC medium included the following components: 2% Tryptone, 0.5% Yeast extract, 10 mM NaCl, 2.5 mM KCl, 20 mM $MgSO_4$, 10 mM MgCl, 20 mM glucose.

After incubation, 50 µl of transformed *E. coli* were loaded onto a Lysogeny Broch (LB) agar plate, which contained the antibiotic kanamycin. Additional 250 µl of *E. coli* culture were loaded on another LB agar plate with kanamycin. The LB plates contained 1% Tryptone, 0.5% Yeast extract, 1% NaCl, 1.5% agar. The plates were incubated overnight at 37 ℃. The following day, if colonies appeared, they were transferred with a sterilized toothpick into a 2 ml sterile Eppendorf tube containing 1ml of 2×TY (1.6% Tryptone, 1% Yeast extract, 0.5% NaCl) medium with Kanamycin. The Eppendorf tube was whirly mixed for 10 minutes; then the toothpick was removed. The Eppendorf tube was put in an incubator (SSI5 SHEL LAB Floor Model Shaking Incubator, 5 Cu.Ft.) at 37 ℃, under shaking at 700 rpm, for 3 hours. The *E.coli* DH10 transformed culture was then resuspended 1:1 in a 40% Glycerol solution. This “cloning stock” was stored at -80 ℃.

3.4.3. Colony PCR

Polymerase Chain Reaction (PCR) was carried out using the Invitrogen^{TM}Platinum^{TM}SuperFi^{TM} PCR Master Mix Kit (Invitrogen, Massachusetts, USA). This kit was designed to work at room temperature. It was a hot-start kit and it was suited for cloning.

The reaction mix had this composition:

3 µl of nuclease-free water

12.5 µl of 2×Platinum^{TM}SuperFi^{TM} PCR Master Mix

1.25 µl of 10 µM forward primer

1.25 µl of 10 µM reverse primer

2 µl of Template DNA

5 µl of 5×SuperFi^{TM} GC Enhancer

The following PCR protocol was applied:

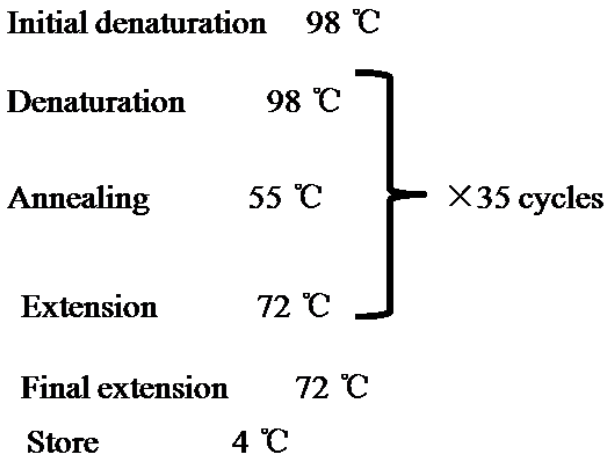

Agarose gels (2%) were used to assess the size of the PCR products. The DNA Ladder with a range 200-300 bp was produced. The gels were run at 100 V for 30

minutes. Then a picture was taken with a Bio-Rad Gel System (Biorad, California, USA).

3.4.4. AtSAT5 overexpression

As expression vector, *E.coli* BL-21(DE3) plysS was used. These cells were kindly provided by Dr. Tiziana Cacciamani, MaSByc, DISVA, Università Politecnica delle Marche. BL-21(DE3) pLysS is a chemically competent *E. coli* strain. The BL-21(DE3) pLysS strain allowed inducible protein expression from the gene of interest, under the control of the lac UV5 promoter, via the T7 RNA polymerase. The pLysS plasmid also contained the T7 lysozyme gene (lysozyme had the function of repressing low-level transcription prior to induction), a chloramphenicol resistance gene and a p15A replication origin which was compatible with those found in pBR322 and pUC derived plasmids.

This competent strain could be made permeable to exogenous DNA through the following procedure:

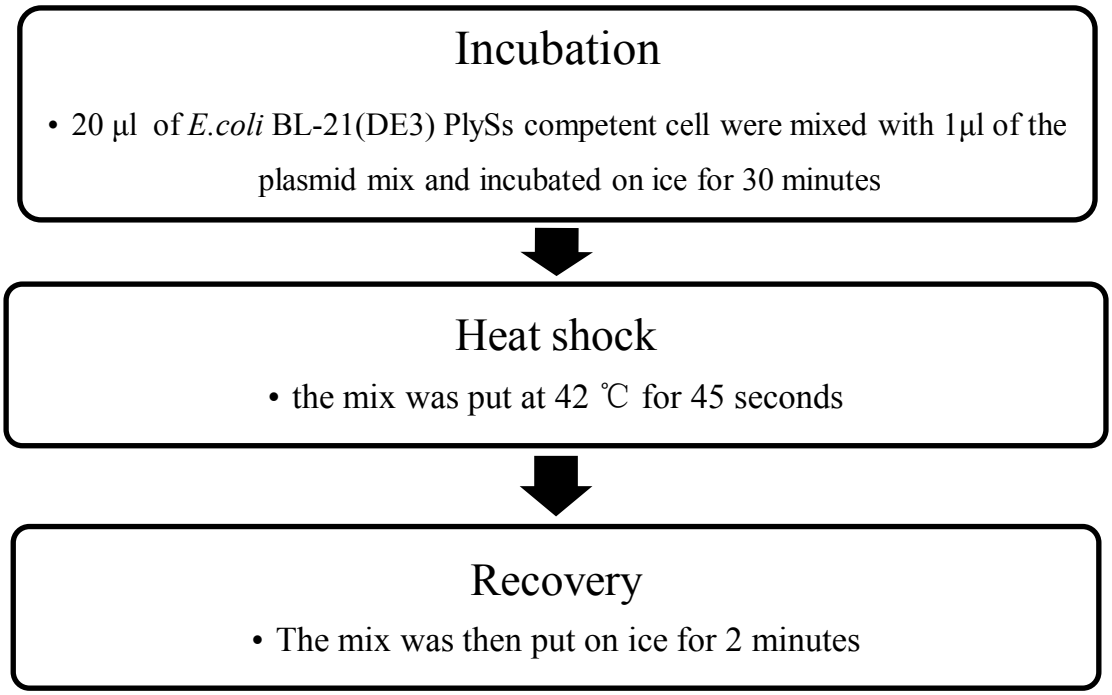

Subsequently, 90 µl of SOC medium was added to the mix. This suspension was incubated for 1 hour at 37 ℃, under continuous shaking at 600 rpm. Then, 600 µl of 2×TY medium containing kanamycin and chloramphenicol, were added. A further incubation at 37 ℃ and 400 rpm was conducted overnight. The next morning, 40 µl of the culture incubated overnight was added to an Eppendorf tube containing 2×TY medium and kanamycin and chloramphenicol. These cultures were allowed to grow to an optical density (600 nm) of 1. At that point, 100 µl of 100 mM isopropyl-1-thio-β-D-galactopyranoside (IPTG) was added to induce the expression of AtSAT5 protein. The incubation at 37 ℃ and 400 rpm was continued for 4 hours. The suspension was then centrifuged at 4500 g, 4 ℃, for 10 min; the pellet, containing the *E. coli* cells overexpressing AtSAT5, was collected and stored at -80 °C.

The production of the AtSAT5 containing *E. coli* was scaled up by New Brunswick™ Innova® 44/44R Shaker, setting the shaking speed at 250 RPM and a temperature of 37°C. When the OD_{600} reached 0.6-0.8, 250 µl of 1 M IPTG were added into the culture (250 ml) for inducing the protein SAT5 expression. The incubation at 37 ℃ and 400 rpm was continued for 4 hours. The suspension was then centrifuged at 4500 g, 4 ℃, for 10 min; the pellet, containing the *E. coli* cells overexpressing AtSAT5, was collected and stored at -80 °C, these pellets were used for the followed purification experiment.

3.4.5. Extraction of AtSAT5 protein from *E. coli*

The *E. coli* cells were resuspended in 10 ml of binding buffer (buffer B: 20 mM Imidazole, 50 mM Tris (pH 8.0) and 250 mM NaCl), then used for the affinity (binding) chromatography. To protect the proteins, buffer B was added containing 10

µl of 500 mM phenylmethylsulfonyl fluoride (PMSF) protease inhibitor (VWR, USA). The PMSF stock solution was prepared in ethanol, filtered through 0.2 µm filter (sterilized, USA) and kept at -20 °C till used. Cells in buffer B were sonicated on ice using a SONICS Vibra-Cell™ (SONICS & MATERIALS INC, Newton, CT, USA), with an energy of 60% amplitude for 5 minutes, with 5 seconds bursts and 10 seconds intervals. The slurry was spun down at 12000 g, for 10 min, at 4 °C, in a J2-MC Beckman centrifuge equipped with a JA-20 rotor (Beckman, California, USA). The supernatant was filtrated through a 0.45 µm membrane filter (VWR, Pennylvania, USA), and then again through a 0.2 µm filter (VWR, Pennsylvania, USA) (Fig. 3-9). Then, 10 µl of 500 mM PMSF was added to the filtered crude extract and the samples were stored at -20 °C, until they were used.

3.4.6. OAS-TL purification

The purification of OAS-TL was carried out by affinity chromatography, using the protein overexpressed in *E. coli* as the ligand. A 1 ml HiTrap^{TM} Chelating Column (GE Healthcare, Buckinghamshire, UK) was used (Fig. 3-9). Prior to its utilization, the column was washed with MilliQ water for 5 min, at a flow rate of 1 ml/min (which was maintained for all the following steps). The column was then loaded with 50 mM $NiCl_2$, for 5 min. Subsequently, the column was equilibrated with the binding buffer (buffer B: 20 mM Imidazole, 50 mM Tris (pH 8.0), and 250 mM NaCl), for 10 min.

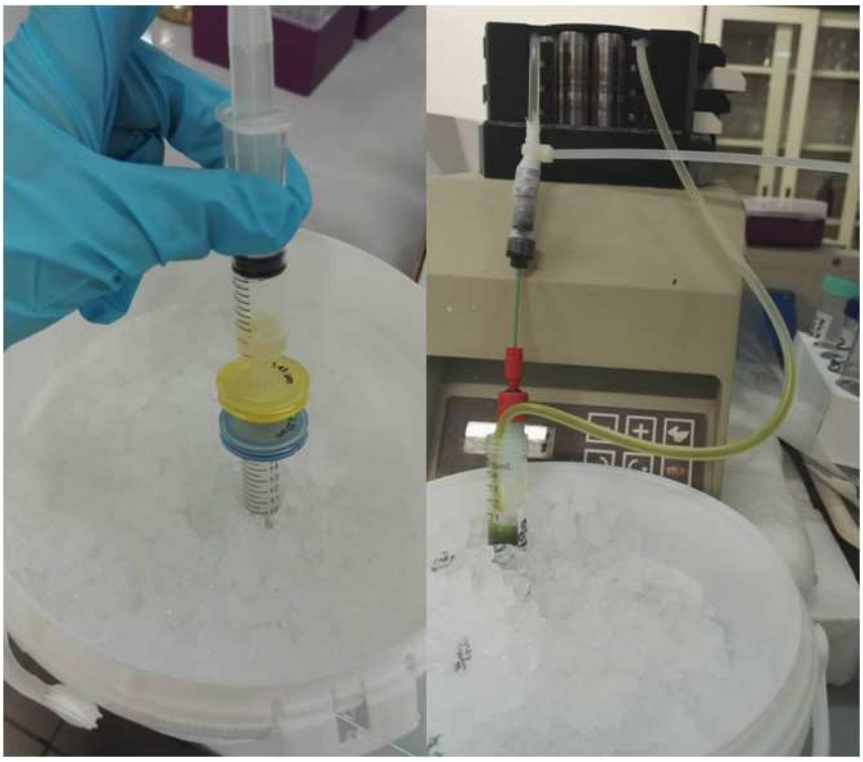

Fig. 3-9. Protein loading onto the affinity chromatography column.

The His-tagged AtSAT5 was then loaded onto the column. The loading lasted 1.5 hour. The column was conditioned with washing buffer (Washing buffer: 80 mM Imidazol, 50 mM Tris (pH 8.0), and 250 mM NaCl). Subsequently, the column was washed for 5 minutes with the same buffer (Washing buffer) used for conditioning. Finally, a volume of 5 ml washing buffer containing 10 mM O-Acetylserine was added; this step was applied to remove any residual bacterial OAS-TL. The column was finally washed for 5 minutes with the same washing buffer and the algal extract was loaded.

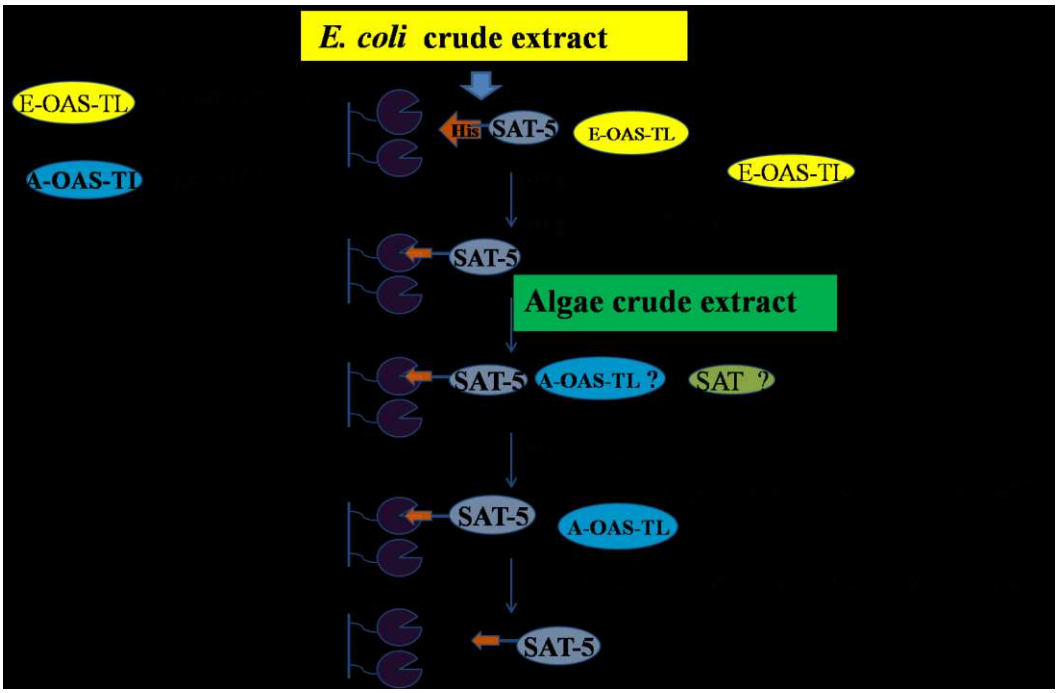

Fig. 3-10. Procedure followed for affinity chromatography.

3.4.7. Algal OAS-TL extraction

Algae in mid-exponential growth phase were used for the extraction of OAS-TL. Cells were harvested by centrifugation in a J2-MC Beckman centrifuge with a JA-10 rotor (Beckman, California, USA), at 5000 g, 4 °C, for 10 minutes. The pellet was stored at -80 °C until it could be processed further.

When needed, the pellets were resuspended in 10 ml of buffer B additioned with 50 mM PMSF, 0.001 mM $MgCl_2$, 0.1% Triton-100 (v/v), and 1% Glycerol (v/v) and subject to sonication, centrifugation, and filtration as described above for the extraction of AtSAT5 from *E. coli.*

About 10 ml of crude extract were then loaded onto the column, with a flow rate of 1ml/min. The extract was allowed to circulate through the columns for 1.5 hours (Fig. 3-10). The column was then washed for 10 minutes with 10 mL buffer W, which contained 80 mM Imidazole, 50 mM Tris (pH 8.0), and 250 mM NaCl; this was done to wash out unbound proteins. The column was then washed for 5 min with 5 ml of

Buffer W added with 10 mM OAS; this step was necessary to displace the protein OAS-TL bound to the affinity ligand. The eluted solution was collected in 10 fractions of 500 µl each. A further 5 min wash with Buffer W followed. Finally, the His-tagged AtSAT5 protein was eluted with 5 ml Buffer E, which contained 400 mM Imidazole, 50 mM Tris (pH 8.0), and 250 mM NaCl.

3.4.8. Determination of protein content

Proteins were determined according to the method by Peterson (1977), a modification of Lowry's method (Lowry et al., 1951). The denaturing power of SDS in combination with NaOH allowed the complete disruption of membranes. To 480 µl of a solution containing 1% SDS and 0.1 M NaOH, a volume of 20 µl of sample was added, followed by 500 µl of reagent A (Table. 3-2); the solution was let sit for 10 min. Reagent A was a mixture of copper and Na-K tartrate: the former specifically binds to proteins in an alkaline environment; the tartrate was used to stabilize the Cu ions (Lowry et al., 1951). Subsequently, 250 µl of solution B (Table. 3-2) were added. Solution B contained the Folin & Ciocalteu's phenol reagent (Sigma-Aldrich) and carried out the oxidation of the Cu-protein complexes; this gave, almost instantaneously, a blue color to the protein solution (Lowry et al., 1951). The samples were incubated for about 30 minutes at room temperature to allow a complete development of the blue color. Finally, the absorbance was measured at 750 nm in a Beckman DU 640 Spectrophotometer (Beckman Coulter, California, USA).

Protein concentration was calculated by interpolating the samples' absorbances into a calibration curve constructed with known quantities of bovine serum albumin (BSA). The BSA standards were prepared as the samples. Standard curves were made for all the buffers employed in the various purification steps, to take into account possible interferences by all buffer components.

Table. 3-2. Reagents for Peterson's protein assay

Reagents	Stock solution
Solubilizing solution	1% SDS, 0.1 M NaOH
	a: CTC (CopperTartrate/Carbonate)
	0.1% $CuSO_4$ 5 H_2O
	0.2% NaKTartrate 4 H_2O
Reagent A (v/v) (a: b: c: d = 1: 1: 1: 1)	10% Na_2CO_3
	b: 10% SDS
	c: 0.8 M NaOH
	d: MilliQH_2O
Reagent B (v/v) (d: e = 5: 1)	e: Folin-Ciocalteu reagent (1 Folin-Ciocalteu :5 MilliQ H_2O)

3.4.9. SDS-Polyacrylamide Gel Electrophoresis (SDS-PAGE)

OAS-TL purity was assessed through SDS-Polyacrylamide Gel Electrophoresis (SDS-PAGE). Proteins were denatured by mixing the samples with 4 volumes of 5X Laemmli Sample Buffer containing 10% (w/v) SDS, 20% (v/v) Glycerol, 100 mM Tris pH 7, 0.1% (w/v) Bromophenol blue, 25% (v/v) β-Mercaptoethanol (Laemmli, 1970). The mixture was quickly whirly mixed for 1 min, then incubated for 10 minutes at 95.5 °C, transferred on ice for 2 minutes and finally centrifuged at 12,000 g at room temperature. Samples were then loaded on a 12% polyacrylamide gel. Resolving gel and stacking gel buffers were prepared as described in Table. 3-3 and 3-4. First, an appropriate volume (Table. 3-5) of resolving gel was loaded into the electrophoresis sandwich; a thin layer of isopropanol was deposited on its surface to ensure that the surface was flat and horizontal. After the gel polymerized, isopropanol was removed with the syringe. The stacking gel was then added (Table. 3-6). After polymerization, the gel sandwich was placed in an electrophoresis chamber (Bio-Rad Laboratories Inc., California, USA). The running buffer contained 25 mM Tris-HCl pH 8.3, 192 mM glycine and 0.1% (W/V) SDS. The electrophoresis was performed at 80 V for 30 min (or until samples ran through the stacking gel) and at 120 V for

additional 120 min or until bromophenol blue ran out of the gel. Protein pre-stained molecular weight markers (10-180 kDa, Abcam, Cambridge, UK) were used to identify the mass of the proteins in the samples.

Protein bands were visualized by Coomassie Staining (Table. 3-7). The Coomassie Staining was stopped when the first protein bands became visible, by washing the gel three times with tap water. The Coomassie destaining solution was then added to the stained gel (Table. 3-8).

Table. 3-3. Recipe for the SDS-PAGE resolving gel buffer

1 x Resolving Gel Buffer	Final concentration	For 100 ml
Tris pH 8.8	1.5 M	18.18 g
SDS	0.4% (w/v)	0.4 g

Table. 3-4. Recipe for the SDS-PAGE Stacking gel buffer

1 x Stacking Gel Buffer	Final concentration	Add to 100 ml
Tris pH 6.8	0.5 M	6.06 g
SDS	0.4 % (w/v)	0.4 g
Add few grains of bromphenol blue		

Table. 3-5. Resolving gel (for 2 gels in the Protean minigel system)

Resolving Gel	H_2O	Resolving Gel Buffer	Acrylamide solution, 30% (w/v)	10% APS	TEMED
12%	4.73 ml	3.3 ml	5.37 ml	90 µl	16 µl

Table. 3-6. Stacking gel (for 2 gels in the Protean minigel system)

Stacking Gel	H_2O	Stacking gel buffer	Acrylamide solution, 30% (w/v)	10% APS	TEMED
4%	2.61 ml	0.72 ml	1.13 ml	45 µl	9 µl

Table. 3-7. Coomassie Staining solution

	Final concentration	Add to 1 L
Methanol	50% (v/v)	500 ml
Acetic acid	1% (v/v)	10 ml
Coomassie Brilliant Bleu R-250 (more sensitive)	0.1% (w/v)	0.1 g

Table. 3-8. Coomassie Destaining solution

Coomassie Destaining Solution recipe	Final concentration	Add to 1 L
Ethanol	20% (v/v)	200 ml
Acetic acid	10% (v/v)	100 ml

3.4.10. Western Blots

The transfer of protein from the gel to a 0.45 µm PVDF membrane (Amersham, GE Healthcare, Buckinghamshire, UK) for immune detection was carried out in a wet system (Bio-RAD, California, USA). The transfer sandwich was assembled as shown in Fig. 3-11. The PVDF membrane was activated by soaking in methanol before the blotting sandwich was assembled. Subsequently, the blotting sandwich was put in the transfer chamber (Biorad, California, USA). The transfer was conducted at 350 mA for 1 hour, at 4 °C.

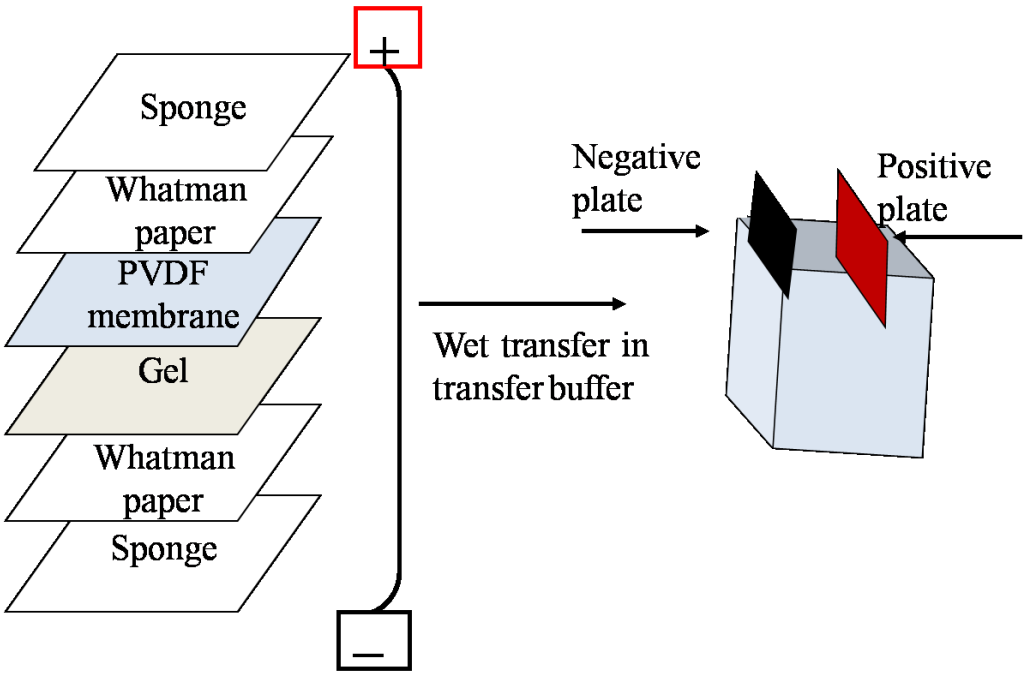

Fig. 3-11. Assembly of a western blot sandwich.

This scheme was modified from Mahmood, 2012.

The membrane was blocked by soaking for 1 hour in a blocking solution containing 5% (w/v) BSA, 0.5% (v/v) Tween 20 in TBS (20 mM Tris, pH7.6, 0.137 M NaCl) while slowly shaking at room temperature. After blocking, the membrane was washed with

0.5% TBS-T three times, for 5 min each time. As primary antibody, OAS-TL-A antibodies (from rabbit) were used. The membrane was incubated overnight in TBS-T buffer, containing 0.05% (v/v) Tween-20, 0.5% (w/v) BSA and the primary antibody (OAS-TL A as 1:5000 dilution), at 4 °C. It was then washed 3 times, for 5 min each time, with 1x TBS-T. Then the secondary antibody (goat anti-rabbit Horse Radish Peroxidase (HRP), HRP-conjugate (Pierce), Abcam, Cambridge, UK) was added in a 1:10000 dilution. The membrane was incubated for 1 hour in TBS-T buffer containing 0.05% (v/v) Tween-20, 0.5% (w/v) BSA and the secondary antibody. It was then washed 3 times for 5 min with TBS-T buffer (TBS-T contained 0.05% (v/v) Tween-20).

An identical procedure was used for the immunodetection of SAT5. The primary antibody in this case had a 1:5000 dilution.

Immunodetection was carried out with Amersham™ ECL™ start Western blotting detection reagent (Amersham, GE Healthcare, Buckinghamshire, UK). The basic principle of operation of this detection kit was shown in Fig. 3-12.

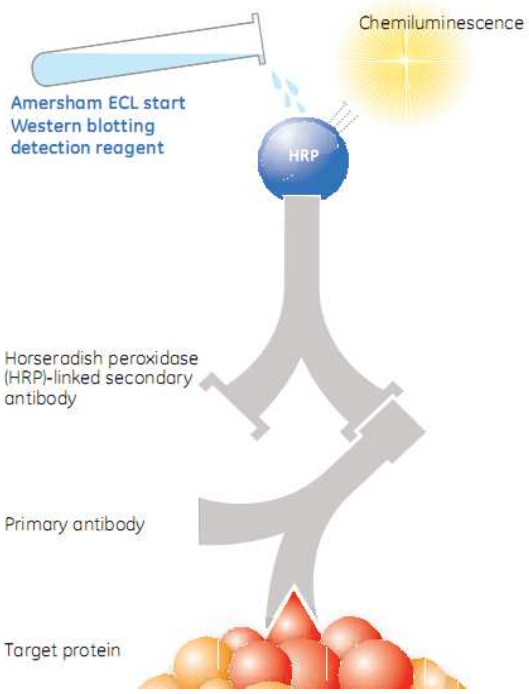

Fig. 3-12. Principle of operation of the Amersham ECL Western blotting detection reagent.

After the addition of 1 ml luminol peroxide detection reagent on the membrane, the HRP enzyme catalyzes the oxidation of luminol, which generates the emission of photons at a wave number of 428 nm.

After the membrane was wetted with 1 ml of ECL reagent, the membrane was wrapped in the transparent plastic film and incubated in the dark for 5 min. The excess of working solution was then removed with a pipette, and the membrane was transferred in a light-tight photographic cassette and fixed into position with tape. A photographic film was located on the membranes and the cassette was closed. All these operations were conducted in a dark room. The film was exposed to the membranes for several seconds to minutes, depending on signal strength. The film was then developed with ChemiDoc^{TM} XRS+ imaging system (BIO-RAD, California, USA).

The Molecular weight of proteins was determined by comparing the position of protein bands of unknown mass with prestained marker proteins of known molecular weight (Garfin, 1990). A standard curve was prepared by measuring the Retention Factor (R_f) of prestained marker protein bands. The sample R_f was interpolated Log(Mr) vs R_f standard curve to estimate the molecular weight of the protein of interest (Garfin, 1990; Lord, 2003).

3.5. OAS-TL activity measurements

OAS-TL uses sulfide and O-acetylserine (OAS) as substrates (Kredich, 1966). OAS is generated from the reaction between serine and acetyl coenzyme A catalyzed by SAT (Kredich, 1966; Hell et al., 2002; Droux, 2004). The measurement of OAS-TL activity was based on the spectrophotometric determination of cysteine production. In fact, what was measured was the change of absorbance consequent to the reaction

ofthe cysteine produced by OAS-TL with ninhydrin (cat. 485-47-2, Sigma-Aldrich, MO, USA). Ninhydrin reacted with the primary amino group of cysteine. As a product, Ruhemanns purple was formed, which absorbed at 560 nm (Gaitonde, 1967). O-acetylserine (thiol) lyase activity was measured as described in (Rolland et al., 1996; Droux et al., 1998) the reaction mix contained 50 mM Hepes-KOH, pH 7.5, 5 mM Na_2S, 10 mM O-Acetyl serine (OAS), 5 mM DTT, 10 µl of crude extract or purified OAS-TL protein, in a total volume of 100 µl. The reaction mixture was incubated, in the absence of sulfide, for 5 min, at 25 °C. The reaction was initiated by the addition of Na_2S; the reaction was allowed to run for 10 min at 25 °C and was stopped by the addition of 50 µl of 20% trichloroacetic acid (TCA). In the blank, TCA was added before Na_2S. Samples and blank, after completion of the reaction, were centrifuged (Microfuge* 20, Beckman Coulter, California, USA) at room temperature, at 13,000 rpm, for 5 min. The supernatant was then added to a 0.07 M Ninhydrin solution, which was composed of 12 M HCl and 100% acetic acid in a 1:3 (v/v) ratio, incubated at 95.5 °C for 10 min and cooled down for 1-2 min on ice. A volume of 550 µl of 100% ethanol was added to the mixture and the absorbance at 560 nm was measured in a glass cuvette. OAS-TL activity was expressed as g cysteine $\cdot g^{-1}$ protein $\cdot min^{-1}$; the amount of cysteine produced was derived from the equivalence: 1 unit of Absorbance at 560 nm = 36.6 nmol cysteine (Wirtz & Droux, 2004).

3.6. Cysteine Synthase Complex purification

Purification of CSCs from all the experimental species was conducted by Fast Protein Liquid Chromatography (FPLC) (ÄKTA pure system GE Healthcare, Buckinghamshire, UK), using a size exclusion column. The basic principle of size exclusion chromatography is depicted in Fig. 3-13. Gel filtration does not rely on the chemical interaction of the protein with the mobile phase; rather it is based on the

effective molecular radius of the protein, which, for most typical globular proteins, relates to mass.

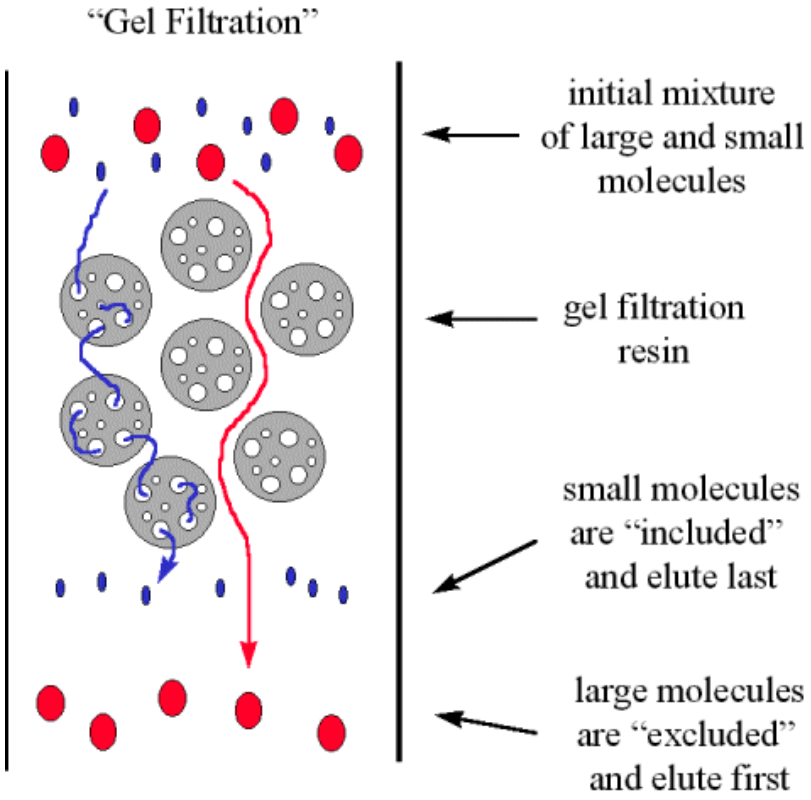

Fig. 3-13. Basic principles of size exclusion chromagraphy.

(http://www.mikeblaber.org/oldwine/bch5425/lect31/lect31.htm) (BCH5425 Molecular Biology and Biotechnology Spring 1998 Dr. Michael Blaber)

The running buffer contained 20 mM Tris-HCl and 150 mM NaCl; the pH was adjusted to 7.5. The column used for this analysis was a Superdex 200 5/150 GL (GE Healthcare, Buckinghamshire, UK), with 3 ml of bed volume, with a protein separation size range from 10 to 600 kDa. The choice was based on what known for *A. thaliana* CSC having a mass of about 320 kDa (Wirtz et al., 2010). The flow rate of the mobile phase was set at 0.1 ml/ min, and fraction collection was such that each fraction contained 0.1 ml of elution buffer.

The previous algal OAS-TL purified samples (section 3.4.7) were centrifuged for 10 min at 10000 g, at room temperature. The supernatant containing OAS-TL (100 µl)

was mixed with AtSAT 5 according to the concentration ratio 2 dimer (OAS-TL) to 1 hexamer (AtSAT 5) (Wirtz et al., 2010) and then it was loaded onto the FPLC column with a syringe, as shown in Fig. 3-14. The fractions were collected with Fraction collector F9-R (GE Healthcare, Buckinghamshire, UK).

Fig. 3-14. Fast Protein Liquid Chromatography (FPLC).

(ÄKTA pure system, GE Healthcare, Buckinghamhire, UK).

A LMW Gel Filtration Calibration Kit (Cat. No. 17-0442-01, Amersham, Buckinghamshire, UK) was used to calibrate the column (Fig. 3-15 and Fig. 3-16); a regression curve was generated, which was used to calculate the molecular weight of the proteins in the eluate. The following protein standards were contained in the LMW Kit: 1. Ferritin (440 kDa) 0.4 mg/ml; 2. Aldolase (158 kDa) 4 mg/ml; 3. Ovalbumin (43 kDa) 4 mg/ml; 4. Ribonuclease A (13.7 kDa) 3 mg/mL. The average elution volume was corrected by the total bed column volume and the void volume (Kav). Kav was calculated with the following equation:

$$\text{Kav protein} = \frac{\text{Elution volume protein} - \text{Void volume}}{\text{Column Bed volume} - \text{Void volume}}$$

The Column Void Volume was measured with a blue dextran solution (2000 kDa). Proteins were detected at 280 nm, using the UV detector of the ÄKTA pure system (GE Healthcare, Buckinghamshire, UK).

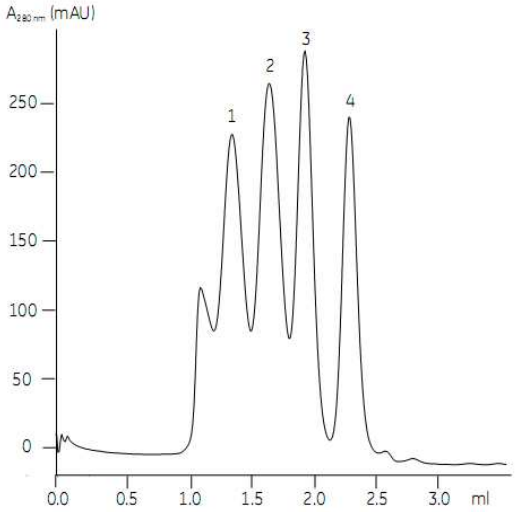

Fig. 3-15. FPLC Protein standards for column calibration.

1, Ferritin (440 kDa) 0.4 mg/ml; 2, Aldolase (158 kDa) 4 mg/ml; 3, Ovalbumin (43 kDa) 4 mg/ml; 4, Ribonuclease A (13.7 kDa) 3 mg/ml; See text for details.

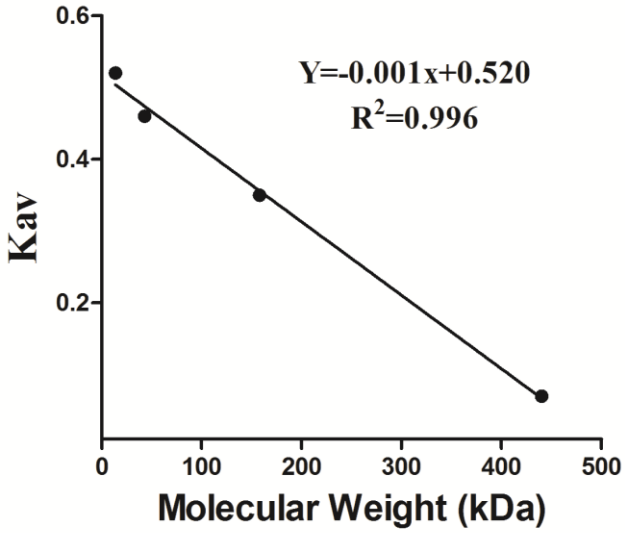

Fig. 3-16. FPLC column calibration curve.

Each dot represents a standard; from left to right: Ribonuclease A (13.7 kDa); Ovalbumin (43 kDa); Aldolase (158 kDa); Ferritin (440 kDa). The average elution volume corrected by the

total bed column volume and the void volume (Kav) is shown on the Y-axis, as a function of the protein mass in kDaltons (on the X-axis).

The Protein fractions were then subject to SDS-PAGE, according to the protocol described in (3.4.9.) paragraph 1. The proteins were transferred onto a PVDF membrane and identified by immunodetection (see section 3.4.10).
Before loading the sample, the column was equilibrated with running buffer; 5 column volumes (CV) of running buffer were used.

3.7. Determination of the impact of the plastoquinone redox state on ATPS activity

In order to assess whether ATPS redox regulation (Prioretti et al., 2016) is mediated by the redox state of the plastoquinone pool, *Thalassiosira pseuodonana* cultures were treated with 3-(3′ 4′-dichlorophenyl)-1, 1-dimethylurea (DCMU), which specifically and effectively inhibits Q_B reduction at PSII (Fig. 3-17). DCMU was dissolved in 100% DMSO to obtain a stock concentration of 20 mM. An amount of DCMU stock equivalent to 0.5‰ of the total culture volume was added, so that the final DCMU concentration in the culture was 10 µM.

T. pseudonana was chosen as the experimental organism because its ATPS is likely to be redox-regulated (Prioretti et al., 2016). To control cultures, 0.5‰ (v/v) DMSO was added.

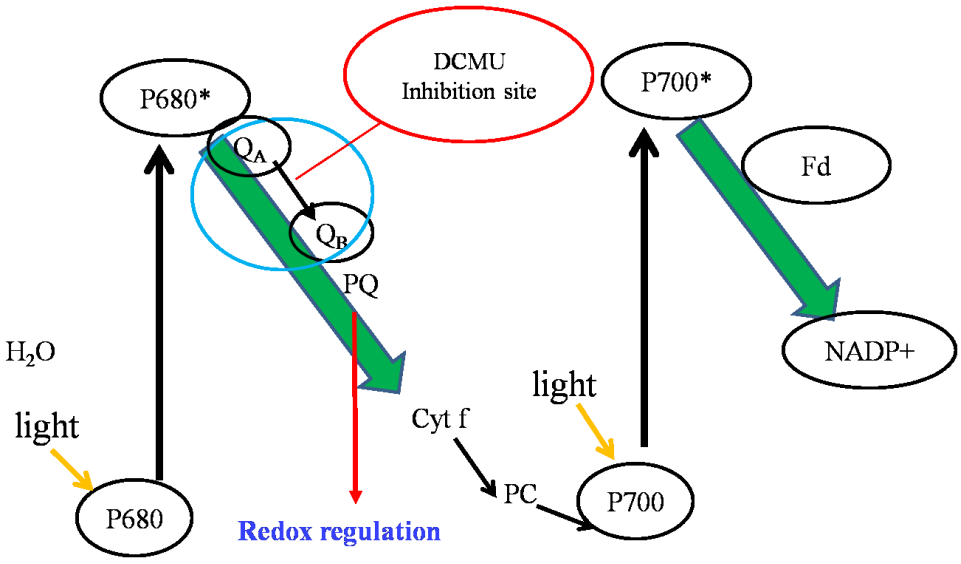

Fig. 3-17. DCMU blocks the electron transfer from Q_A to Q_B.

The ATPS enzyme activity was measured after 0, 1, 3 and 6 hours from the addition of the inhibitor (or just the solvent for the controls). The concentration of DCMU that consistently stopped PSII electron transfer rate, as determined with a Dual-PAM-100 fluorimeter (Heinz Walz GmbH, Effeltrich Germany), was used in the experiment.

Cells were collected by centrifugation at 3500 g for 10 minutes. The pellet was washed three times with a 0.5 mM NaCl solution and then resuspended in 800 µl of an extraction medium containing: 50 mM Tris-HCl (pH 8), 1 mM EDTA, 10 mM $MgCl_2$ (Giordano et al., 2000). The resuspended pellet was frozen by the addition of liquid N_2 and, while frozen, it was homogenized with a ceramic mortar and pestle. The slurry was transferred into a 1.5 ml plastic tube to which Triton X-100 (0.1% v/v) and glycerol (10% v/v) were added to a final volume of 1 ml. Samples were then kept on ice for 30 minutes to allow the Triton to completely solubilize the proteins. Subsequently, the slurry was centrifuged for 15 minutes at 12000 g, at 4 °C. The supernatant was collected and stored at -20 °C until used. The protein concentration in the crude extract was determined by the Peterson's method (Peterson, 1977).

ATP sulfurylase (ATPS) activity was measured spectrophotometrically at 25 °C, according to Burnell (1984). The reaction mixture contained: APS (1 mM), Sodium

diphosphate tetrabasic (PPi, 1 mM), $MgCl_2$ (5 mM), glucose (5 mM), Nicotinamide adenine dinucleotide phosphate (NADP, 300 µM), hexokinase and glucose-6-P dehydrogenase from baker's yeast (5 units, H8629 Sigma-Aldrich), Tris-HCl pH 8 (50 mM). The volume of crude extract added to the assay mixture was 40 µl for a final volume in the cuvette of 0.5 ml.

Since it is difficult to determine ATPS activity in the forward direction, the reverse reaction was used. The ATPS reaction was coupled with the reactions catalyzed by hexokinase and glucose-6-P dehydrogenase; the adenosine 5-phosphosulfate (APS)-depending reduction of NADP to NADPH was measured as the change in absorbance at 340 nm.

1) $APS + PPi \xrightarrow{ATPS} ATP + SO_4^{2-}$

2) $Glucose + ATP \xrightarrow{Hexokinase} Glucose\text{-}6\text{-}P + ADP$

3) $Glucose\text{-}6\text{-}P + NADP \xrightarrow{Glucose\ -6-p\ dehydrogenase} 6\text{-}phosphogluconate + NADPH$

The rate of NADPH production was recorded for 10 minutes at 340 nm, using a Beckman DU 640 Spectrophotometer (Beckman Coulter). The values of absorbance were converted to enzyme activity using the Lambert-Beer law:

$$\text{Enzyme activity } (\mu mol\ min^{-1}\ ml^{-1}) = \left[\frac{\Delta A340\ nm}{\varepsilon NADH \cdot d}\right] \cdot \left[\frac{Vtot}{V\ sample}\right]$$

Where: ΔA340 nm is the rate of NADPH production per minute measured at 340 nm; εNADH (6.22 $mM^{-1}\ cm^{-1}$) is the extinction coefficient of NADPH at 340 nm; d (1 cm) is the optical path length; V_{tot} (500 µl) is the total volume in the reaction vessel; V_{sample} (40 µl) is the volume of crude extract used for the assay. The activity of the enzyme per unit of protein was calculated by dividing the results of the above equation (with units of nmol $min^{-1}\ ml^{-1}$) by the concentration of protein in the sample (mg ml^{-1}); the final results thus had units of µmol NADH min^{-1} (mg protein)$^{-1}$.

Three different types of blanks were tested: 1) using boiled crude extract, 2) assaying

the crude extract without APS, 3) assaying the complete mixture without enzyme extract. All three types of blanks gave very similar results; for the experiments, blanks were prepared without APS in the assay mixture.

4. Results

4.1. Bioinformatics

4.1.1. Phylogeny of Serine Acetyltransferase

The phylogenetic tree of SAT showed two main branches (Fig. 4-1).

1) The first branch showed two main sub-branches. The first one (from the top) comprise sequences from early-diverging chlorophytes, such as the prasinophyte *Tetraselmis suecica*, core-Chlorophyceae belonging to Trebuxiophyceae and Chlorophyceae (Leliaert et al., 2003) and embryophytes (i.e. *Arabidopsis thaliana* and *Glycine max*). The first sub-branch could be divided into two further groups, only the first one of which included embryophyte sequences.
The second sub-branch was constituted by red algae and algae of the red lineage (diatoms and brown algae), but it also includes sequences from the marine cyanobacterium *Lyngbya confervoides.*

2) The second branch of the SAT tree was more heterogeneous; it could be separated into two sub-branches. The first sub-branch from the top included sequences from terrestrial and oceanic cyanobacteria (*Scytonema millei* VB511283, *Prochlorococcus* sp. Scb245), green algae (*Ostreoccus tauri* and *Micromonrias* sp.) cryptophytes (*Guillardia theta*), prymnesiophytes (*Emiliania huxleyi* and *Chrysochromulina* sp.), brown algae such as *Ectocarpus siliquosus* (also present in the first branch), and the diatom *Thalassiosira pseudonana* (also in the first branch).
The second sub-branch contained sequences from mamiellophyceae green algae (*Micromonas* sp*., Bathyococcus prasinos* and *Ostreococcus tauri*), which constituted

a compact group somewhat distant from the heterokonts *Aureococcus anophagefferens* (Pekagophyceae) and *Ectocarpus siliquosus* (Phaeophyceae) and even more distant from the diatom *Thalassiosira oceanica*.

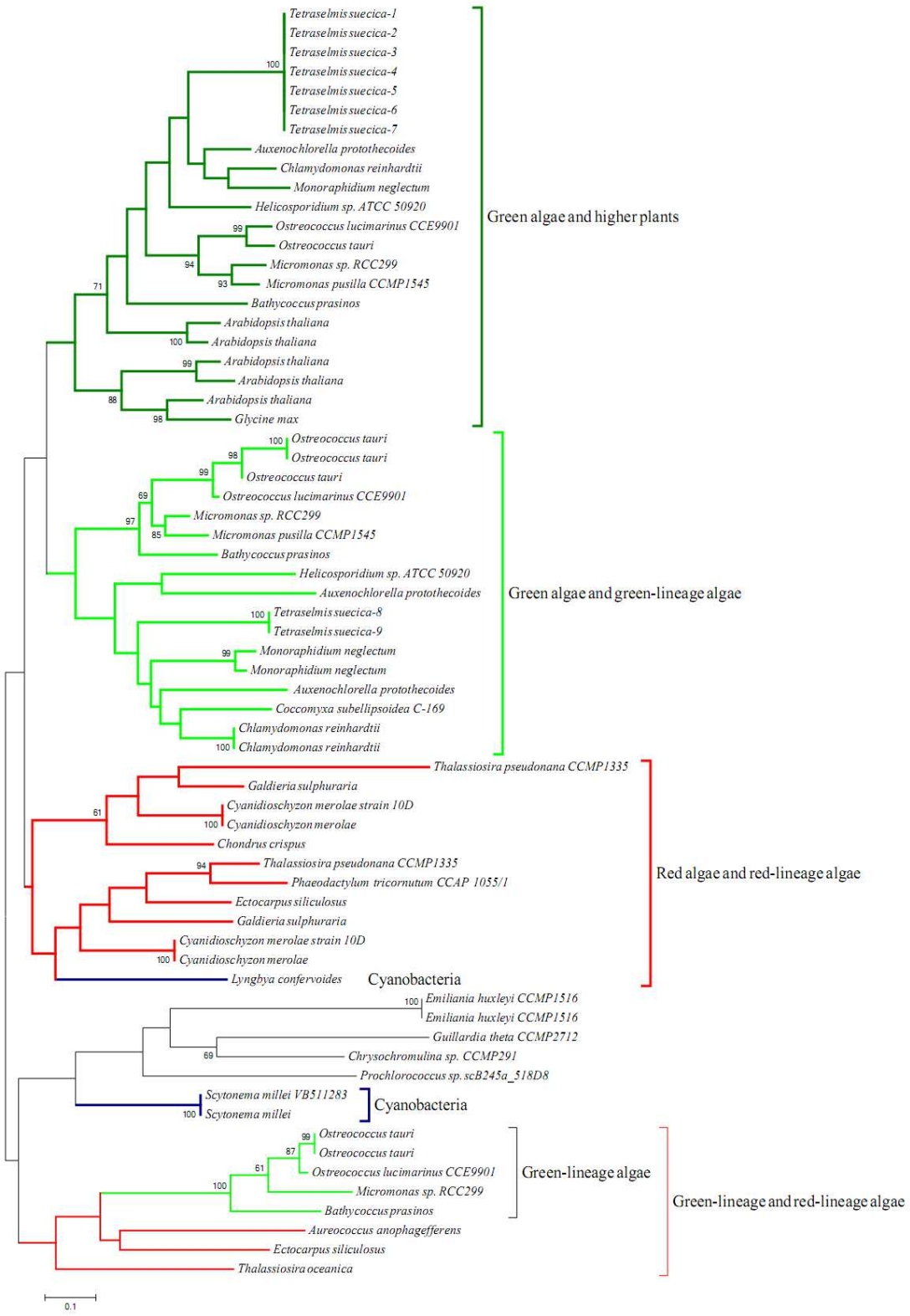

Fig. 4-1. Serine Acetyltransferase phylogenetic tree.

Dark green lines indicated green algae and higher plant; light green lines indicated green algae; red lines indicated lineage algae; blue lines indicated Cyanobacteria.

4.1.2. Phylogeny of O-Acetylserine (thiol) lyase

O-Acetylserine (thiol) lyases phylogenetic tree showed two main branches (Fig. 4-2).

1) In the first branch, *Bacillus cereus* sequence constituted a sister clade of a more composite group that included most of the species used to build the tree (Fig. 4-2).
In this group, two sub-branches could be identified: the branch in the lower position included dinoflagellates, diatoms, and prymnesiophytes; the green freshwater algae *Monoraphidium neglectum* constituted a sister group to these species.

In the other sub-branch, several groups could be distinguished: all cyanobacteria sequences grouped together. Another group was represented by sequences from green algae (the freshwater species *Chlamydomonas reinhardtii*, the marine species *Coccomyxa subellipsoidea* C-169, *Ostreococcus tauri*, *Ostreococcu slucimarinus* CCE9901, *Tetraselmis* sp. GSL018, *Coccomyxa subellipsoidea* C-169 and *Tetralsemis suecica*) and several sequences from the embryophyte *Arabidopsis thaliana* (due to the presence of different isoforms, in this organism). A third group was given by sequences from red algae and algae of the red lineage (*Porphyrapurpurea*, *Chondrus crispus, Galdieria sulphuraria, Cyanidioschyzon merolae* strain 10D), with the green mixotrophc algae *Auxenochlorella protothecoides* as the only intruder.

2) The second branch was formed by species belonging to heterogenous taxa: the freshwater green algae *Auxenochlorella protothecoides*, *Chlamydomonas reinhardtii*, *Monoraphidium neglectum*, the marine green algae *Tetraselmis suecica, Bathycoccus prasinos* and *Nannochloropsis gaditana*, the dinoflagellate *Amphidinium klebsii*, the diatom *Phaeodactylum tricornutum*, the red algae *Cyanidioschyzon merolae,* thebrown algae *Ectocarpus siliculosus,* the amoeba *Dictyostelium discoideum*, the protozoan *Thecamonas trahens*, the ascomycete *Aspergillus fumigates*. No obvious

connection could be found between the position of the OAS-TL sequences in this branch and the known phylogeny of the organisms, suggesting a shuffling of genes through horizontal gene transfer.

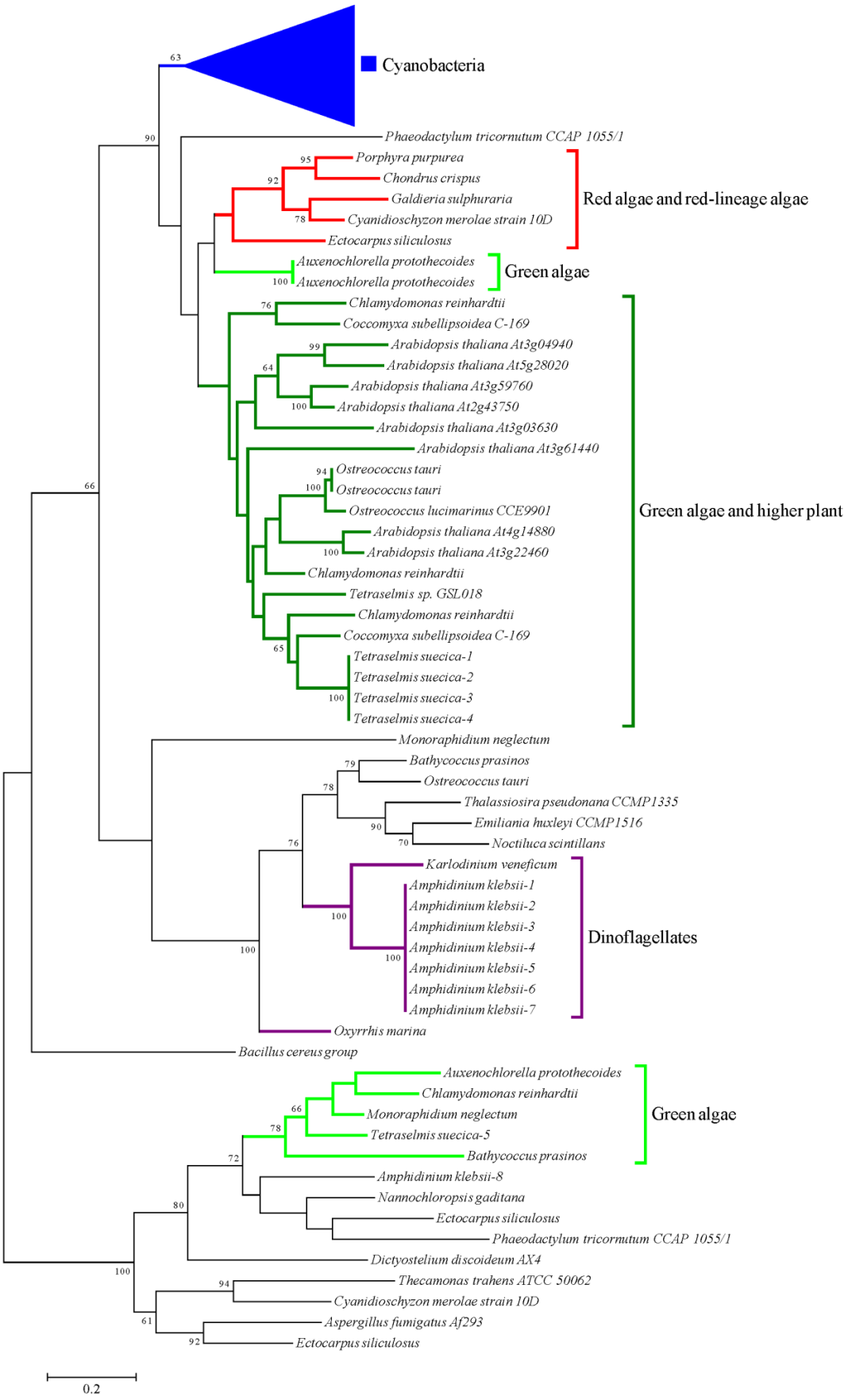

Fig. 4-2. The O-Acetylserine (thiol) lyase phylogenetic tree.

The dark green lines indicated green algae and higher plant; light green lines indicated green algae; red lines indicated red lineage algae; purple lines indicated dinoflagellates; the blue triangle indicated Cyanobacteria. The species of cyanobacteria included in this analysis were shown in the Table. 4-2.

4.1.3. Observations on SAT and OAS-TL protein sequences

4.1.3.1. Number of cysteine residues in algae SAT sequences

The number of cysteines represents an indication of the presence of potential disulfide bonds in the protein and of possible sites for redox regulation. For this reason, I verified whether a trend could be identified with respect to the number of cysteine residues (Table. 4-1). In Cyanobacteria, terrestrial, marine and freshwater species contained more or less similar numbers of Cys residues. In Chlorophyta, the SAT sequences from freshwater species had more Cys residues (typically 8 or 9) than marine species (5 to 7 residues). Somewhat interestingly, species able to grow both in freshwaters and marine environments (e.g. *Monoraphidium neglectum*) had the lowest number of cysteine residues (2 or 3) in their SAT sequences. In the red algae and in their descendants, the number of Cys residues was in the most case between 4 and 6. Only sequences from *Emiliania* (7 and 11), *Cyanidioschizon* (9) and some sequence from *Thalassiosira* (7 and 8) contained higher numbers of Cys.

4.1.3.2. Predicted location of SAT proteins

As shown in Table. 4-1, Cyanobacteria, being prokaryotes, did not have organellar localization of proteins (Table. 4-1). The SAT sequences of Cyanobacteria were between 238 and 272 amino acids (aa)-long. In Chlorophyta, SAT protein contained

229-480 aa and its location was in the chloroplasts or in mitochondria, depending on the species. In the case of *Tetraselmis suecica*, it was not possible to obtain a reliable location for SAT. The haptophyte *Emiliania huxley* SAT protein sequence was 344 to 656 aa-long; all two *Emiliania huxleyi* CCMP 1516 sequences appeared to be located in the mitochondrion. In Rhodophyta, SAT protein was from 323 to 406 aa. In Heterokontophyta, the amino acid number varied greatly, from 183 to 603 aa. Prediction software was unable to identify the location of heterokonts SAT.

Table. 4-1. Number of Cysteines residues, sequence length and location of algae serine acetyltransferase (SAT)

Phylum	Name	Environment	Total CYS number	Len	cTP	mTP	SP	other	Loc	RC	TPlen
Cyanobacteria	*Lyngbia sp.*	M	5	272	-	-	-	-	-	-	-
	Scytonema millei	T	4	269	-	-	-	-	-	-	-
	Scytonema millei VB511283	T	4	264	-	-	-	-	-	-	-
	Synechocystis sp. PCC 6803	F	3	249	-	-	-	-	-	-	-
	Synechococcus sp. PCC 7803	M	3	247	-	-	-	-	-	-	-
	Prochlorococcus sp. scB245a_518D8	M	3	238	-	-	-	-	-	-	-
Chlorophyta	*Auxenochlorella protothecoides*	F	7	271	0.077	0.522	0.076	0.039	M	3	38
	Auxenochlorella protothecoides	F	3	355	0.243	0.199	0.018	0.064	_	4	38
	Bathycoccus prasinos	M	5	370	0.803	0.097	0.028	0.207	C	3	9
	Bathycoccus prasinos	M	7	286	0.098	0.191	0.032	0.886	_	2	9
	Chlamydomonas reinhardtii	F	8	392	0.915	0.202	0.002	0.044	C	2	26
	Chlamydomonas reinhardtii	F	8	480	0.810	0.503	0.006	0.009	C	4	26
	Chrysochromulina sp.CCMP 291	M/F	3	416	0.240	0.213	0.061	0.087	C	5	26
	Coccomyxa subellipsoidea C169	F	8	296	0.023	0.419	0.022	0.772	_	4	-
	Helicosporidium sp. ATCC 50920	T	5	309	0.643	0.136	0.017	0.210	C	3	17
	Helicosporidium sp. ATCC 50920	T	6	307	0.061	0.076	0.019	0.877	_	1	17
	Micromona spusilla CCMP 1545	M	4	350	0.341	0.480	0.012	0.098	M	5	117
	Micromona spusilla CCMP 1545	M	2	306	0.103	0.144	0.046	0.860	_	2	117
	Micromonas sp. RCC 299	M	1	258	0.069	0.054	0.438	0.721	_	4	117
	Micromonas sp. RCC 299	M	3	363	0.846	0.236	0.006	0.039	C	2	117
	Micromonas sp. RCC 299	M	5	276	0.107	0.109	0.027	0.858	_	2	117
	Monoraphidium neglectum	F	2	318	0.025	0.456	0.120	0.327	M	5	11
	Monoraphidium neglectum	F	3	471	0.261	0.082	0.163	0.676	_	3	11
	Ostreococcus lucimarinus CCE 9901	M	2	374	0.842	0.257	0.005	0.033	C	3	18
	Ostreococcus lucimarinus CCE 9901	M	3	270	0.112	0.315	0.066	0.668	_	4	18
	Ostreococcus lucimarinus CCE 9901	M	5	265	0.154	0.120	0.032	0.827	_	2	18
	Ostreococcus tauri	M	5	284	0.045	0.473	0.014	0.105	M	5	18
	Ostreococcus tauri	M	6	436	0.702	0.235	0.014	0.105	C	3	18
	Tetraselmis suecica-1	M	6	308	0.121	0.225	0.083	0.597	_	4	-

	Tetraselmis suecica-2	M	5	303	0.097	0.148	0.060	0.798	_	2	-
	Tetraselmis suecica-3	M	5	251	0.069	0.161	0.133	0.614	_	3	-
	Tetraselmis suecica-4	M	5	234	0.058	0.276	0.093	0.739	_	3	-
	Tetraselmis suecica-5	M	5	250	0.058	0.276	0.093	0.739	_	3	-
	Tetraselmis suecica-6	M	5	229	0.012	0.090	0.680	0.700	_	5	-
	Tetraselmis suecica-7	M	4	258	0.058	0.276	0.093	0.739	_	3	-
	Tetraselmis suecica-8	M	7	283	0.106	0.440	0.012	0.582	_	5	-
Rhodophyta	*Chondrus crispus*	M	5	380	0.492	0.177	0.016	0.019	C	4	26
	Cyanidioschyzon meroiae 10D	M	4	402	0.565	0.881	0.001	0.022	M	4	38
	Cyanidios chyzon meroiae	M	9	406	0.751	0.616	0.003	0.030	C	5	38
	Galdieria sulphuraria	M	3	323	0.104	0.082	0.148	0.909	_	2	62
	Galdieria sulphuraria	M	6	344	0.667	0.327	0.019	0.089	C	4	62
Haptophyta	*Emiliania huxleyi CCMP 1516*	M	11	656	0.030	0.843	0.014	0.218	M	2	117
	Emiliania huxleyi CCMP 1516	M	7	344	0.291	0.863	0.008	0.010	M	3	117
Heterokontophyta	*Ectocarpus siliculosus*	M	5	479	0.539	0.083	0.049	0.549	_	5	-
	Ectocarpus siliculosus	M	6	333	0.317	0.130	0.036	0.715	_	4	-
	Thalassiosira oceanic THAOC 04795	M	7	554	0.017	0.673	0.011	0.737	_	5	26
	Thalassiosira pseudonana CCMP 1335	M	4	234	0.034	0.113	0.170	0.887	_	2	26
	Thalassiosira pseudonana CCMP 1335	M	8	603	0.020	0.025	0.821	0.079	S	2	26
	Phaeodactylum tricornutum CCAP 1055/1	M	4	539	0.042	0.325	0.353	0.075	S	5	18

The column “Environment” indicates whether the species is marine (M), freshwater (F) or terrestrial (T). The column “Number of Cys” refers to the number of cysteine residues in the sequence; Len, sequence length; cTP, chloroplast transit peptide; mTP, mitochondrial targeting peptide; SP, secretory pathway signal peptide; C, Chloroplast; M, Mitochondrial; RC, reliability class ranging area, from (1 to 5); Tplen, predicted presequence length. If the sequence contained a chloroplast or mitochondrion transit peptides, cTP or mTP score was assigned; if the sequence contained a secretory pathway signal peptide, a SP score was assigned; for any other location an “other” score was assigned. The reliability class RC ranged from (1 to 5), with the higher number indicating a more robust prediction. RC was measured calculating the difference between the highest and the second highest output scores: reliability was 1 when the difference was > 0.800; reliability was 2 when the difference was between 0.600 and 0.800; a reliability score of 3 indicates that the difference was between 0.400 and 0.600; a reliability of 4 was attributed when the difference was between 0.200 and 0.400; a reliability of 5 corresponds to a difference between the two highest scores < 0.200. The cleavage site was predicted and the presequence length (TPlen) reported.

4.1.3.3. Number of cysteine residues in algal OAS-TL sequences

As shown in Table. 4-2. all Cyanobacteria, both marine and freshwater species, showed less than 3 cysteine residues in their OAS-TL sequences; some sequences contained no Cys residues at all. The cysteine number in the OAS-TL sequences of Chlorophyta was extremely variable: with no obvious difference between marine and freshwater species. Rhodophyta and their descendants of the red lineage contained an extremely variable number of cysteines. This heterogeneity may reflect the presence of different isoforms. A finer phylogenetic analysis and possibly more sequences (at least for certain groups) were required to ascertain whether the different number of cysteine is associated with different origins of the proteins.

4.1.3.4. Predicted OAS-TL location

As shown in Table. 4-2, Cyanobacteria, being prokaryotes, did not have organellar localization of proteins (Table. 4-2). Cyanobacteria OAS-TL sequence length was between 307 and 336 aa. In Chlorophyta the protein length was between 307 and 491 aa; the predicted location was more often in mitochondria than in chloroplasts, some sequences could not be located in any particular compartment. In Dinophyta the sequences ranged from 331 to 388 aa; the predicted location was mostly in chloroplasts. In *Emiliania huxleyi* CCMP 1516 the sequence length was 382 aa and it was predicted to be located in mitochondria; Rhodophyta showed the OAS-TL length ranging from 326 to 390 aa, located both in chloroplasts and mitochondria. In Heterokontophyta, the sequences were 342-428 aa long.

Table. 4-2. O-acetylserine (thiol) lyase (OAS-TL) of algae with different taxonomy, ecology, and the location prediction

Phylum	Name	Environment	Total CYS number	Len	cTP	mTP	SP	other	Loc	RC	TPlen
Cyanobacteria	*Acaryochloris marina*	M	3	336							
	Anabaena 90	F	2	313							
	Anabaena 90	F	0	320							
	Anabaena variabilis ATCC 29413	M	2	320							
	Anabaena sp. Wa102	F	2	320							
	Bacilluscereus group	M	1	307							
	Calothrix sp. 336/3	F	2	313							
	Calothrix sp. PCC 7507	F	1	320							
	Chlorogloeopsis fritschii	M	2	320							
	Cyanobacterium PCC 7702	M	2	320							
	Cylindrospermopsis raciborskii	F	2	314							
	Cylindrospermum stagnale	F	2	322							
	Thermosynechococcus sp. NK55a	M	2	321							
	Dactylococcopsis salina	F	3	317							
	Dolichospermum circinale	F	1	313							
	Fischerella	F	2	311							
	Fischerella muscicola	F	0	320							
	Fischerella muscicola	F	2	319							
	Fischerella sp.JSC-11	F	3	344							
	Fischerella sp. PCC 9605	F	2	320							
	Fischerella sp. PCC 9431	F	0	320							
	Fischerella sp.PCC 9339	F	0	313							
	Halothece sp. PCC 7418	M	3	322							
	Hapalosiphon sp. MRB220	F	0	320							
	Hassalliabyssoidea VB512170	M	0	319							
	Mastigocladopsis repens	F	2	320							
	Mastigocladus laminosus	F	0	320							
	Microchaete sp. PCC 7126	F	1	320							
	Microcoleus vaginatus	F	1	326							
	Microcystis panniformis	F	2	319							
	Myxosarcina sp. GI1	F	1	321							
	Nodulariaspumigena	F	0	320							
	Nostocpunctiforme	F/M	0	320							
	Nostoc sp. PCC 7107	F/M	0	315							
	Nostoc sp. PCC 7120	F/M	1	320							
	Nostoc sp. PCC 7120	F/M	2	319							
	Nostoc sp. PCC 7524	F/M	1	320							
	Oscillatorianigroviridis sp. PCC 7112	F	1	326							
	Planktothrix agardhii	F	2	311							

	Planktothrix agardhii NIVA-CYA 126/8	F	2	311							
	Planktothrix	F	2	319							
	Pleurocapsa sp. PCC 7319	F	1	332							
	Pseudanabaena sp. PCC 6802	M/F	1	320							
	Raphidiopsis brookii	F	2	314							
	Rivularia sp. PCC 7116	F	3	320							
	Scytonema hofmanni	F	0	320							
	Scytonema hofmanni UTEX B 1581	F	1	319							
	Scytonema millei	M	0	320							
	Scytonema millei	M	1	320							
	Scytonema tolypothrichoides	F	1	317							
	Stigonematales	F	2	319							
	Synechococcus sp. CC9605	M	4	322							
	Synechococcus JA-3-3Ab	F	1	326							
	Synechococcus sp. PCC 6312	F	2	320							
	Synechococcus sp. PCC 7335	F	3	346							
	Synechococcus sp. PCC 7336	F	1	320							
	Synechococcus sp. WH 8109	M	4	322							
	Synechocystis sp. PCC 6714	F	2	312							
	Synechocystis sp. PCC 6803	F	0	331							
	Thecamonastrahens ATCC_50062	M	5	385							
	Thermosynechococcus sp. NK55a	M	2	321							
	Tolypothrix bouteillei	M	2	320							
	Tolypothrix campylonemoides VB511288	M	2	320							
	Tolypothrix sp. PCC 7601	F	2	320							
	Trichormus azollae	F	2	320							
	Xenococcus sp.PCC7305	M	2	321							
Chlorophyta	*Auxenochlorella protothecoides*	M	1	352	0.034	0.037	0.760	0.057	S	2	26
	Auxenochlorella protothecoides	M	5	361	0.308	0.067	0.038	0.644	_	4	26
	Bathycoccus prasinos	F	10	384	0.495	0.175	0.034	0.236	C	4	13
	Bathycoccus prasinos	F	8	491	0.067	0.064	0.235	0.444	_	4	-
	Chlamydomonas reinhardtii	F	7	359	0.052	0.863	0.029	0.064	M	2	11
	Chlamydomonas reinhardtii	F	6	414	0.885	0.100	0.003	0.070	C	2	53
	Chlamydomonas reinhardtii	F	8	382	0.016	0.293	0.612	0.018	S	4	26
	Chlamydomonas reinhardtii	F	6	387	0.136	0.890	0.036	0.072	M	2	33
	Chlorella variabilis	F	0	328	0.085	0.115	0.035	0.860	_	2	-
	Coccomyxa subellipsoidea C-169	F	4	405	0.534	0.335	0.006	0.102	C	5	60
	Coccomyxa subellipsoidea C-169	F	1	378	0.081	0.167	0.111	0.587	_	3	60
	Monoraphidium neglectum	F	5	406	0.077	0.171	0.283	0.069	S	5	23
	Monoraphidium neglectum	M	7	440	0.414	0.794	0.003	0.015	M	4	7

	Nannochloropsis gaditana	M	9	420	0.081	0.210	0.058	0.209	M	5	43
	Ostreococcus lucimarinus CCE9901	F	3	305	0.028	0.141	0.222	0.818	_	3	-
	Ostreococcus tauri	F	4	440	0.156	0.281	0.011	0.510	_	4	-
	Ostreococcus tauri	F	5	345	0.150	0.675	0.039	0.033	M	3	9
	Tetraselmis sp. GSL0	M	11	428	0.319	0.393	0.002	0.044	M	5	17
	Tetraselmis suecica-1	M	3	314	0.121	0.064	0.180	0.715	_	3	-
	Tetraselmis suecica-2	M	3	315	0.137	0.069	0.147	0.762	_	2	-
	Tetraselmis suecicia-3	M	2	297	0.036	0.415	0.145	0.391	M	5	21
	Tetraselmis suecicia-4	M	6	345	0.239	0.517	0.023	0.119	M	4	26
	Tetraselmis suecicia-5	M	3	333	0.121	0.064	0.180	0.715	_	3	-
Dinophyta	*Amphidinium klebsii*-1	M	3	347	0.019	0.196	0.053	0.950	_	2	-
	Amphidinium klebsii-2	M	3	331	0.018	0.058	0.125	0.948	_	1	-
	Amphidinium klebsii-3	M	3	342	0.018	058	0.125	0.948	_	1	-
	Amphidinium klebsii-4	M	3	329	0.184	0.207	0.051	0.266	_	5	-
	Amphidinium klebsii-5	M	3	334	0.018	0.058	0.125	0.948	_	1	–
	Amphidinium klebsii-6	M	3	356	0.018	0.356	0.045	0.878	_	3	-
	Amphidinium klebsii-7	M	3	355	0.016	0.403	0.043	0.893	_	3	
	Amphidinium klebsii-8	M	7	343	0.025	0.037	0.129	0.936	_	1	-
	Karlodinium veneficum	M	4	357	0.838	0.198	0.036	0.058	C	2	46
	Karlodinium veneficum	M	4	388	0.432	0.305	0.074	0.346	C	5	34
	Noctiluca scintillan	M	8	356	0.022	0.716	0.022	0.531	M	5	12
	Oxyrrhis marina	M	4	385	0.860	0.279	0.037	0.037	C	3	5
Rhodophyta	*Chondrus crispus*	M	6	326	0.238	0.094	0.111	0.486	_	4	-
	Cyanidioschyzon meroiae 10D	M	7	390	0.541	0.432	0.031	0.139	C	5	20
	Cyanidioschyzon meroiae	M	4	389	0.837	0.037	0.023	0.025	C	2	20
	Galdieria sulphuraria	M	9	385	0.211	0.402	0.042	0.186	M	5	43
Haptophyta	*Emiliania huxleyi* CCMP 1516	M	9	382	0.035	0.806	0.014	0.069	M	2	17
Heterokontophyta	*Ectocarpus siliculosus*	M	6	345	0.196	0.035	0.116	0.751	_	3	-
	Ectocarpus siliculosus	M	13	422	0.014	0.064	0.576	0.010	S	3	26
	Ectocarpus siliculosus	M	8	354	0.646	0.087	0.285	0.156	C	4	10
	Phaeodactylum tricornutum CCAP 1055/1	M	3	342	0.052	0.427	0.014	0.575	_	5	-
	Phaeodactylum tricornutum CCAP 1055/1	M	6	356	0.265	0.060	0.107	0.450	_	5	-
	Thalassiosira pseudonana CCMP 1335	M	6	355	0.160	0.211	0.052	0.589	_	4	-

The column “Environment” indicates whether the species is marine (M), freshwater (F) or terrestrial (T). The column “Number of Cys” refers to the number of cysteine residues in the sequence; Len, sequence length; cTP, chloroplast transit peptide; mTP, mitochondrial targeting peptide; SP, secretory pathway signal peptide; C, Chloroplast; M, Mitochondrial; RC, reliability class ranging area, from (1 to 5); Tplen, predictedpresequence length. If the sequence contained a chloroplast or mitochlondrion transit peptides, cTP or mTP score was assigned; if the sequence contained a secretory pathway signal peptide, a SP score was assigned; for any other location an “other” score was assigned. The reliability class RC ranged from (1 to 5), with the higher number indicating a

more robust prediction. RC was measured calculating the difference between the highest and the second highest output scores: reliability was 1 when the difference was > 0.800; reliability was 2 when the difference was between 0.600 and 0.800; a reliability score of 3 indicates that the difference was between 0.400 and 0.600; a reliability of 4 was attributed when the difference was between 0.200 and 0.400; a reliability of 5 corresponds to a difference between the two highest scores < 0.200. The cleavage site was predicted and the presequence length (TPlen) reported.

4.1.4. Comparison of SAT and OAS-TL sequences among algae and with *A. thaliana* sequences

4.1.4.1. Alignment of the SAT sequences of Cyanobacteria with *A. thaliana* SAT isoforms

The alignment of the SAT sequence of freshwater cyanobacteriums *Synechocystis* sp. PCC 6803 and the marine cyanobacterium *Synechococcus* sp. WH 7803 with the SAT sequences of the higher plant model organism *A. thaliana* (Mayer et al., 1999; Lin et al., 1999; Rhee et al., 2000; Theologis et al., 2000) was performed in order to observe the homology. The Table. 4-3 showed the details of this analysis. *A. thaliana* SAT sequences carried an amino-terminal extension (112-192 aa) that was not present in the cyanobacterial sequence. *Synechocystis* sp. PCC 6803 SAT contained a C-terminus extension that ranged 1-27 aa. The alignment of *Synechocystis* sp. PCC 6803 SAT protein with one of the *A. thaliana* SAT protein is shown in Fig. 4-3. When hypothetical deletions are omitted, a 168 amino acid-long region with the identity of 42.2% (70 identical amino acids) could be found. If the 32 additional equivalent amino acids were included in the identity analysis (i.e. equivalent amino acids are considered equal), the homology was 61.4%. The amino acid alignment with the other four *A. thaliana* SAT isoforms showed 41.3%, 42.4%, 44.6%, 46.7% identity, respectively (Table. 4-4). If the additional equivalent amino acids were included, the homology was (Table. 4-4) 61%, 60.3%, 63.6%, 63.5%. *A. thaliana* SAT sequences had an amino-terminal extension (112-192 aa) which was not present in the *Synechococcus* sp. WH 7803 sequence. *Synechococcus* sp. WH 7803 had a C-terminus extension of 2-29 amino acid residues. The identity of *Synechococcus* sp. WH 7803 SAT amino acid sequence to the five SAT isoforms of *A. thaliana*, ranged between 40.1% and 47.9%; if the equivalent amino acids were included, the

homology range was 56.3-64.2% (See supplementary data for details). The alignments of all other algae species were shown in Table. 4-4.

```
SAT1-A.thalia    143 SSIRLDVQAFKDRDPACLSYSSAILHLKGYLALQAYRVAHKLWKQGRKLL    192
                     :|:..|.:...:||||..:::...:....|..||..:|.:|:|:..|....
Synechocystis      3 NSLIADFRIIFERDPAARNWLEVLFCYPGLQALLIHRFSHRLYTLGLPFF     52

SAT1-A.thalia    193 ALALQSRVSEVFGIDIHPAARIGKGILLDHGTGVVIGETAVIGDRVSILH    242
                     ...:........||:|||.|:|||:|.:|||.||||||||::||...|..
Synechocystis     53 PRLMSHLARFFTGIEIHPGAQIGQGVFIDHGMGVVIGETAIVGDYSLIYQ    102

SAT1-A.thalia    243 GVTLGGTGKETGDRHPNIGDGALLGACVTILGNIKIGAGAMVAAGSLVLK    292
                     ||||||||||:|.|||.:|:..::||...:||||.||....:.|||:||:
Synechocystis    103 GVTLGGTGKESGKRHPTLGENVVVGAGAKVLGNIAIGDNVRIGAGSVVLR    152

SAT1-A.thalia    293 DVPSHSMVAGNPAKLI    308
                     |||:...|.|.|.:::
Synechocystis    153 DVPADFTVVGVPGRMV    168
```

Fig. 4-3. Alignment of the SAT protein of the freshwater cyanobacterium *Synechocystis* sp. PCC 6803 and the SAT protein of *A. thaliana*.

Identical amino acids are marked with a vertical line; equivalent amino acids are marked with a semicolon; positions with lower identity are identified by a point.

4.1.4.2. Alignment of the SAT sequences of green algae with *A. thaliana* SAT isoforms

Two of the *A. thaliana* SAT sequences (SAT-1, SAT-3) had an amino-terminal extension which was not present in *C. reinhardtii* SAT1. The alignment data indicated that *C. reinhardtii* SAT1 and SAT2 had an N-terminal extension (2-95 aa) that was not present in the other three *A. Thaliana* sequences. *C. reinhardtii* SAT sequences also showed a C-terminus extension of 4-117 amino acid residues. The identity of the two *C. reinhardtii* SAT sequences to the five SAT isoforms of *A. thaliana*, ranged between 50.2% and 59.1%; if the equivalent amino acids were included, the homology increased to 71.7-78.7%. Only one of the three SAT sequences of *T. suecica* carried an amino-terminal extension (around 20 aa), which was not present in one of *A. thaliana* SAT sequences. Also, the *T. suecica* SAT sequence showed a shorter C-terminus than *A. thaliana* (Table. 4-3). The identity of the three *T. suecica* SATs to the five SAT

isoforms of *A. thaliana*, ranged between 48.6% and 62.7%; it increased to 67.9-76.3% if the equivalent aa were considered identical (Table. 4-4), (See supplementary data for details).

4.1.4.3. Alignment of the SAT sequences of red algae and red-lineage algae with *A. thaliana* SAT isoforms

A. thaliana SAT sequences carried an N-terminus extension (45-83 aa) (Table. 4-3) that was not present in the *C. merolae* strain 10D. *C. merolae* strain 10D showed a 4-30 aa C-terminus extension. The identity of *C.merolae* strain 10D SAT sequences to the five SAT isoforms of *A. thaliana* ranged between 45.3% and 57.0% (65.8%-74.3%. with equivalent amino acids). *T. pseudonana* CCMP 1335 SAT had an N-terminal extension (199-295 aa), which was not present in three out of five *A. thaliana* SAT sequences. *T. pseudonana* CCMP 1335 also had a C-terminal extension.

The identity of *T. pseudonana* CCMP 1335 SAT with *A. thaliana* isoforms ranged between 46.7% and 52.1% (70.9%-74.2%. with equivalent amino acids). The SAT sequence of the diatom *P. tricornutum* CCAP 1055/1 carried N-terminus (164-231 aa) and C-terminus (16-127 aa) extension compared to *A. thaliana* sequences (Table. 4-3). The identity of the *P. tricornutum* CCAP 1055/1 SAT with the five *A. thaliana* isoforms ranged between 26.3% and 50.8% (41.9%-72.6% with equivalent amino acids) (Table. 4-4). *A. thaliana* SAT sequences carried N-terminus (13-18 aa) and C-terminus (21-26 aa) extensions that were not present in the *E. huxleyi* CCMP 1516 sequence (Table. 4-3). The identity of *E. huxleyi* CCMP 1516 SAT to the five *A. thaliana* sequences ranged between 44.1% and 47.7% (58.8%-61.1% with the equivalent amino acids) (Table. 4-4), (See supplementary data for details).

Table. 4-3. Comparasion of N'-terminus and C'-terminus sequences of algal SAT the corresponding regions as *A. thaliana* SAT isoforms

	SAT1-*A. thaliana*		SAT2-*A. thaliana*		SAT3-*A. thaliana*		SAT4-*A. thaliana*		SAT5-*A. thaliana*	
	N'-terminal	C'-terminal	N'-terminal	C'-terminal	N'-terminal	C'-terminal	N'-terminal	C'-terminal	N'-terminal	C'-terminal
Synechocystis sp. PCC 6803	-140	+6	-103	+1	-192	+27	-115	+27	-112	+27
Synechococcus sp. WH 7803	-140	+17	-103	+12	-192	+29	-116	+29	-112	+29
1-C. reinhardtii	-6	-17	+86	-22	-34	+4	+20	+4	+42	+4
2-C. reinhardtii	+2	+95	+64	+90	-11	+117	+22	+117	+41	+117
1-T. suecica	-14	-21	+17	-26	-75	0	-15	0	-6	0
2-T. suecica	-17	-32	+20	-37	-74	-11	-15	-11	-5	-11
3-T. suecica	-68	-35	-31	-40	-120	-14	-14	-14	-40	-14
1-C. merolae strain 10D	+46	+4	+83	-3	0	+30	+45	+30	+70	+30
2-C. merolae strain 10D	+40	+16	+77	+11	0	+22	+39	+22	+69	+22
T. pseudonana CCMP 1335	+263	-17	+295	-26	+199	+5	+263	+5	+278	+5
1-P. tricornutum CCAP 1055/1	+208	-16	+240	-21	+164	+8	+228	+8	+228	+8
2-P. tricornutum CCAP 1055/1	+205	-122	+243	-127	+168	-107	+231	-106	+231	-107
E. huxleyi CCMP 1516	+14	-21	+18	-26	-45	0	+13	0	+18	0

In this table, the positive numbers indicate the numbers of additional residues in algae sequences when aligned with their counterparts, the negative numbers indicate the number of residues missing in algae sequences when aligned with *A. thaliana* sequences.

Table. 4-4. Identity and Similarity of algal SAT protein sequence with *A. Thaliana* isoforms

	SAT1-*A. thaliana*		SAT2-*A. thaliana*		SAT3-*A. thaliana*		SAT4-*A. thaliana*		SAT5-*A. thaliana*	
	Identity	Similarity	Identity	Similarity	Identity	Similarity	Identity	Similarity	Identity	Similarity
Synechocystis sp. PCC 6803	42.2 %	61.4 %	41.3 %	61.0 %	42.4 %	60.3 %	44.6 %	63.6 %	46.7 %	63.5 %
Synechococcus sp. WH 7803	42.8 %	62.0 %	42.8 %	62.0 %	40.1 %	56.3 %	46.4 %	60.8 %	47.9 %	64.2 %
1-*C. reinhardtii*	55.1 %	76.7 %	55.3 %	75.1 %	50.2 %	71.7 %	51.9 %	72.2 %	54.4 %	73.0 %
2-*C. reinhardtii*	62.2 %	78.7 %	59.8 %	75.0 %	55.7 %	73.4 %	55.3 %	74.7 %	59.1 %	78.5 %
1-*T. suecica*	48.6 %	72.1 %	49.8 %	70.1 %	49.8 %	69.0 %	48.3 %	68.5 %	54.6 %	75.0 %
2-*T. suecica*	62.7 %	76.3 %	60.7 %	73.8 %	53.6 %	67.9 %	55.0 %	70.8 %	55.4 %	73.8 %
3-*T. suecica*	62.7 %	76.3 %	60.7 %	73.8 %	53.6 %	67.9 %	55.0 %	70.8 %	55.4 %	73.8 %
1-*C. merolae strain* 10D	51.8 %	68.2 %	50.6 %	67.5 %	49.4 %	72.0 %	45.3 %	65.8 %	54.0 %	70.5 %
2-*C. merolae strain* 10D	54.8 %	74.3 %	57.0 %	72.6 %	52.2 %	69.8 %	47.7 %	67.0 %	53.7 %	68.2 %
T. pseudonana CCMP 1335	52.1 %	71.8 %	52.1 %	71.4 %	46.7 %	74.2 %	47.7 %	73.2 %	50.6 %	70.9 %
1-*P. tricornutum* CCAP 1055/1	50.4 %	70.5 %	50.8 %	70.5 %	45.7 %	70.2 %	47.7 %	72.6 %	50.8 %	68.4 %
2-*P. tricornutum* CCAP 1055/1	26.3 %	52.6 %	29.7 %	45.9 %	28.0 %	48.0 %	36.0 %	44.0 %	29.0 %	41.9 %
E. huxleyi CCMP 1516	47.1 %	59.3 %	47.7 %	59.9 %	44.1 %	58.8 %	45.6 %	61.1 %	45.9 %	59.7 %

4.1.4.4. Alignment of the OAS-TL sequence of Cyanobacteria with OAS-TL isoforms of *A. thaliana*

A. thaliana contains four major OAS-TL isoforms (A, B, C, C1), (García et al., 2014). The sequences of these enzymes carried N-terminus (2-110 aa) and C-terminus (1-13 aa) extensions (Table. 4-5) that were not present in the cyanobacterial sequences. The identity of the two OAS-TL sequences of *Synechosystis* sp. PCC 6803 to the four OAS-TL isoforms of *A. thaliana* ranged between 34.0% and 61.1% (52.3%-78.5%, with equivalent amino acids) (Table. 4-6). Also the OAS-TL sequence of the marine cyanobacterium *Synechococcus* sp. WH 7803 differed at the N-terminus, in positions 1-110, relative to *A. thaliana* OAS-TL sequences (Table. 4-5). In contrast, *Arabidopsis* and *Synechococcus* had C-terminus domains of similar length. The identity of the two OAS-TL sequences of *Synechococcus* sp. WH 7803 to the four OAS-TL isoforms of *A. thaliana* ranged between 48.5% and 57.6% (66.3%-74.8%, if the equivalent amino acids were considered) (Table. 4-6), (See supplementary data for details).

4.1.4.5. Alignment of the OAS-TL sequence of green algae with OAS-TL isoforms of *A. thaliana*

When the three OAS-TL sequences of the green algae *C. reinhardtii* were compared to *A. thaliana* isoforms, it was observed that one of the *C. reinhardtii* OAS-TL sequences contained an N-terminal extension (36-72 aa) that was not present in *A. thaliana*-A. On the other hand, *A. thaliana* OAS-TL (B, C, C1) sequences carried an N-terminal extension (2-80 aa) that was mostly not present in *C. reinhardtii* OAS-TL sequences. *C. reinhardtii* had a C-terminus extension (2-20 aa) that was not observed

in *Arabidopsis* (Table. 4-5). The identity between *C. reinhardtii* and *A. thaliana* OAS-TL was between 29.7% and 74.1% (Table. 4-6) (50.0%-83.5% including the equivalent amino acids) (Table. 4-6), (See supplementary data for details).

A. thaliana OAS-TL sequences carried an N-terminal extension (5-113 aa) (Table. 4-5), which was not present in *Tetraselmis suecica* sequence. *A. thaliana* OAS-TL sequences carried a C-terminal extension (4-22 aa) that was partially 3 aa present in only one of the *Tetraselmis suecica* OAS-TL isoforms (Table. 4-5). The amino acid identity between *Tetraselmis suecica* and *A. thaliana* OAS-TL ranged between 28.9% and 66.6% (48.2%-80.4% with the equivalent amino acids) (Table. 4-6), (See supplementary data for details).

4.1.4.6. Alignment of the OAS-TL sequence of red algae and red-lineage algae with OAS-TL isoforms of *A. thaliana*

The *C. merolae* strain 10D OAS-TL sequences, when compared to OAS-TL-A of *A. thaliana* had an additional sequence (44-62 aa) at the N-terminus (Table. 4-5). When *C. merolae* OAS-TL sequences were aligned with the other *A. thaliana* OAS-TL sequences, the embryophytes sequences had an extension at the N-terminus (1-42 aa). *C. merolae* sequences also contained a C-terminal extension (3-28 aa) as compared to *A. thaliana* sequences (Table. 4-5). The identity between *C. merolae* OAS-TL and those of *A. thaliana* ranged between 34.7% and 64.2% (54.5%-80.4% with the equivalent aminoacids) (Table. 4-6), (See supplementary data for details).

T. pseudonana CCMP 1335 alignment with AtOAS-TL-A showed additional amino acids (10 aa and 42 aa) in the diatom at the N-terminus. In all other cases, *A. thaliana* OAS-TL had an amino-terminal extension (5-113 aa) (Table. 4-5). One of *T. pseudonana* OAS-TL contained additional aa at the C-terminus (8-11 aa) (Table. 4-5), while the other sequences showed a 1-18 aa C-terminal extension in *A. thaliana*

OAS-TL. The amino acid identity of *T. pseudonana* CCMP 1335 to *A. thaliana* isoforms varied between 33.7% and 63.0% (53.5%-77.4% with the equivalent amino acids) (Table. 4-6), (See supplementary data for details).

P. tricornutum 1055/1 sequences missed a section at the N-terminus that was present in *A. thaliana* (1-106 aa), while the C-terminus between these two species more or less similar (Table. 4-5). The identity of *P. tricornutum* and *A. thaliana* OAS-TL was between 36.2% and 50.8% (52.4%-79.7% if equivalent amino acids were considered identical) (Table. 4-6), (See supplementary data for details).

In *E. huxleyi* CCMP 1516 OAS-TL there was a 22 aa extension at the N-terminus compared to OAS-TL-A. While, the other three OAS-TL sequences of *A. thaliana*, which, in turn had amino acids at the N-terminus (27-79 aa) that were mostly not present in *E. huxleyi* enzyme (Table. 4-5). At the C-terminus, *E. huxleyi* contained a 25 aa amino acid extension, as compared to *A. thaliana* (Table. 4-5). The OAS-TL amino acid identity between *E. huxleyi* CCMP 1516 and *A. thaliana* ranged between 38.1% and 43.0% (53.5%-57.3% if equivalent amino acids were counted) (Table. 4-6), (See supplementary data for details).

When the OAS-TL sequences of *A. thaliana* were compared with those of the dinoflagellate *Amphidinium klebsii*, the embryophyte was found to have an N-terminal extension (4-112 aa) (Table. 4-5). In contrast, the C-terminus showed additional amino acids (1-3 aa; 1-16 aa, depending on isoforms) in *A. klebsii* sequence (Table. 4-5). The OAS-TL amino acid identity between *A. klebsii* and *A. thaliana* was between 32.3% and 39.5% (50.5%-56.8 considering equivalent aa as identical) (Table. 4-6), (See supplementary data for details).

Table. 4-5. Alignment of N'-terminus and C'-terminus sequences of algal OAS-TL corresponding regions in *A. thaliana* OAS-TL isoforms

	A-*A. thaliana*		B-*A. thaliana*		C-*A. thaliana*		C1-*A. thaliana*	
	N'-terminal	C'-terminal	N'-terminal	C'-terminal	N'-terminal	C'-terminal	N'-terminal	C'-terminal
1-*Synechocystis* sp. PCC 6803	+17	-10	-53	-10	-91	-13	-38	-12
2-*Synechocystis* sp. PCC 6803	-2	-1	-72	-1	-110	-4	-46	-3
1-*Synechococcus* sp. WH 7803	-2	0	-72	0	-110	-3	-46	-2
2-*Synechococcus* sp. WH 7803	-1	+1	-71	+1	-101	-2	-45	-1
1-*C. reinhardtii*	+72	+2	-8	+20	-41	+17	+2	+18
2-*C. reinhardtii*	+36	+9	-17	+9	-50	+6	-7	+7
3-*C. reinhardtii*	+50	+15	-10	+15	-43	+12	0	-7
4-*C. reinhardtii*	+35	+2	-51	+2	-89	-1	-19	0
1-*T. suecica*	-5	-8	-75	-8	-113	-11	-49	-10
2-*T. suecica*	+9	-4	-61	-4	-101	-7	-37	-6
3-*T. suecica*	-2	-4	-72	-22	-110	-21	-46	-20
4-*T. suecica*	-10	+3	-80	+3	-118	0	-54	1
1-*C. merolae strain* 10D	+62	+3	-1	+3	-34	0	-11	+1
2-*C. merolae strain* 10D	+44	+21	-9	+21	-42	+11	-4	+28
1-*T. pseudonana* CCMP 1335	+10	+11	-63	+11	-101	+8	-39	+9
2-*T. pseudonana* CCMP 1335	+42	-1	-6	-1	-39	-4	-2	-3
3-*T. pseudonana* CCMP 1335	-5	-15	-72	-15	-113	-18	-49	-7
1-*P. tricornutum* CCAP 1055/1	+2	-1	-68	-1	-106	-4	-43	-3
2-*P. tricornutum* CCAP 1055/1	+10	+3	-60	+3	-98	0	-37	+1
E. huxleyi CCMP 1516	+22	+24	-42	+26	-79	+26	-27	+23
1-*A. klebsii*	-4	+3	-72	+3	-112	0	-48	+1
2-*A. klebsii*	-7	-14	-75	-14	-115	-17	-51	-16
3-*A. klebsii*	+5	+3	-115	+3	-103	0	-39	+1
4-*A. klebsii*	0	+1	-51	+1	-108	-2	-44	-1

In this table, the positive numbers indicate the numbers of additional residues in algae sequences when aligned with their counterparts, the negative numbers indicate the number of residues missing in algae sequences when aligned with *A. thaliana* sequences.

Table. 4-6. Identity and Similarity of algae OAS-TL with reference species of *A. thaliana* isoforms

	A-*A. thaliana*		B-*A. thaliana*		C-*A. thaliana*		C1-*A. thaliana*	
	Identity	Similarity	Identity	Similarity	Identity	Similarity	Identity	Similarity
1-*Synechocystis* sp. PCC 6803	60.6 %	76.5 %	61.1 %	78.5 %	60.6 %	76.6 %	53.6 %	71.2 %
2-*Synechocystis* sp. PCC 6803	37.7 %	53.7 %	36.8 %	52.3 %	38.0 %	53.0 %	34.0 %	52.3 %
1-*Synechococcus* sp. WH 7803	55.2 %	71.9 %	55.2 %	73.7 %	56.5 %	74.4 %	48.5 %	68.3 %
2-*Synechococcus* sp. WH 7803	57.3 %	72.9 %	57.6 %	74.8 %	55.7 %	74.5 %	50.6 %	66.3 %
1-*C. reinhardtii*	64.6 %	80.0 %	64.4 %	82.8 %	65.0 %	83.2 %	57.9 %	76.5 %
2-*C. reinhardtii*	34.2 %	51.7 %	29.7 %	50.0 %	33.2 %	51.2 %	33.0 %	50.3 %
3-*C. reinhardtii*	66.7 %	83.5 %	65.6 %	79.8 %	68.4 %	82.2 %	56.9 %	74.5 %
4-*C. reinhardtii*	74.1 %	86.1 %	69.5 %	84.9 %	73.4 %	86.7 %	61.6 %	77.1 %
1-*T. suecica*	35.7 %	57.2 %	33.0 %	55.9 %	34.3 %	56.9 %	34.9 %	53.7 %
2-*T. suecica*	66.2 %	79.0 %	66.6 %	80.4%	64.2 %	78.6 %	59.0 %	74.3 %
3-*T. suecica*	34.1 %	54.0 %	32.7 %	54.0%	31.6 %	48.4 %	28.9 %	48.2 %
4-*T. suecica*	46.0 %	61.5 %	44.3 %	60.6%	45.4 %	61.4 %	42.8 %	55.9 %
1-*C. merolae strain* 10D	64.2 %	80.4 %	59.5 %	77.2 %	61.9 %	78.3 %	54.8 %	70.1 %
2-*C. merolae strain* 10D	35.8 %	52.8 %	35.2 %	52.8 %	38.1 %	55.0 %	34.7 %	54.5 %
3-*C. merolae strain* 10D	43.9 %	57.5 %	41.4 %	57.2 %	41.1 %	58.9 %	38.5 %	54.7 %
1-*T. pseudonana* CCMP 1335	40.6 %	56.6 %	39.7 %	57.6 %	40.4 %	58.7 %	37.7 %	55.6 %
2-*T. pseudonana* CCMP 1335	61.9 %	75.0 %	63.0 %	77.4 %	62.4 %	77.4 %	54.5 %	71.3 %
3-*T. pseudonana* CCMP 1335	37.6 %	54.0 %	35.5 %	57.0 %	36.6 %	57.0 %	33.7 %	53.5 %
1-*P. tricornutum* CCAP 1055/1	51.0 %	67.5 %	47.5 %	65.6 %	49.3 %	65.9 %	42.0 %	61.6 %
2-*P. tricornutum* CCAP 1055/1	43.5 %	58.7 %	40.4 %	57.4 %	42.0 %	57.1 %	36.2 %	52.4 %
3-*P. tricornutum* CCAP 1055/1	61.7 %	75.7 %	63.2 %	78.9 %	64.7 %	79.7 %	54.6 %	72.2 %
E. huxleyi CCMP 1516	43.0 %	57.3 %	40.2 %	57.1 %	39.8 %	56.0 %	38.1 %	53.5 %
1-*A. klebsii*	39.5 %	56.8 %	38.5 %	57.4 %	38.2 %	58.0 %	36.1 %	53.4 %
2-*A. klebsii*	37.4 %	56.3 %	37.0 %	53.8 %	35.9 %	54.9 %	35.7 %	55.1 %
3-*A. klebsii*	38.8 %	54.7 %	37.3 %	53.7 %	36.3 %	53.1 %	32.4 %	48.3 %
4-*A. klebsii*	36.6 %	53.9 %	36.5 %	54.0 %	36.4 %	53.5 %	32.3 %	50.5 %

4.1.5. Main motives of SAT and OAS-TL algal sequences

4.1.5.1. SAT sequences main motives in algae

The SAT protein, apparently, share with the embryophyte enzyme a C-terminal hexapeptide-repeat domain. This domain is common in a number of acyltransferases and is believed to be involved both in catalysis and hetero-oligomerization (i.e. formation of the Cysteine Synthase Complex) (Yeon et al., 2018). Our sequences alignment revealed a partial but long consensus sequence, with the following interesting features: i) a peculiar six-residue periodicity can be found in the consensus region; ii) each of the six hexapeptide units starts with isoleucine (I), leucine (L) or valine (V); iii) in four of the units, the second residue is glycine (G) and the fifth residue isalanine (A) or valine (V).

Fig. 4-4 showed the alignment of algal SATs and the five *Arabidopsis thaliana* SAT isoforms. The alignment revealed the similarity in the structures of algal and embryophyte enzymes. The six-residue periodical amino acid sequence of algae SAT was (-I/V/L)-G-XXXX-(I/V/L)-, thus very similar in structure to that of *Arabidopsis thaliana* (Vuorio et al., 1991; Vuorioa & Taina, 1994; Bogdanova & Hell, 1997; Pye, et al., 2004). In 1997, Bogdanova and Hell proved through truncated proteins experiments that the C-terminus of SAT was necessary for the interaction with OAS-TL. Also, this domain appeared to be associated with the putative transferase activity (Bogdanova & Hell, 1997). The hexapeptide domain was also found to be responsible for the formation of β-turns (Vuorio, 1991). In agreement with Bogdanva and Hell (1997) and based on the structural similarity suggested by the sequence alignments, it seems logical to assume that the catalytically functional domain of algae SATs is the central part of the sequence, where the region with the highest similarity to the *Arabidopsis thaliana* proteins was.

```
SAT1-A.thaliana    1 ------------------------------------------------------------
SAT2-A.thaliana    1 ------------------------------------------------------------
SAT3-A.thaliana    1 ------------------------------------------------------------
SAT4-A.thaliana    1 ------------------------------------------------------------
SAT5-A.thaliana    1 ------------------------------------------------------------
Synechocystis      1 ------------------------------------------------------------
Synechococcus      1 ------------------------------------------------------------
1-C.reinhardtii    1 ------------------------------------------------------------
2-C.reinhardtii    1 ------------------M-------------------------------------------
1-T.suecica        1 ------------------------------------------------------------
2-T.suecica        1 ------------------------------------------------------------
3-T.suecica        1 ------------------------------------------------------------
1-C.merolae        1 ------------------------------------------------------------
2-C.merolae        1 ------------------------------------------------------------
T.pseudonana       1 MDNTKKYLQAVLLTAPMLMALAFTPSISTVMSVHQYSSNQCDGFLPPSRARIRHYSSPRQ
1-P.tricornutum    1 -----MVAWLVLLTLSSLELVNGWIHQCTVMSLYIRR---------PTVSASLAFS----
2-P.tricornutum    1 ------------------------------------------------------------
E.huxleyi          1 ------------------------------------------------------------
consensus          1

SAT1-A.thaliana    1 ----------------------------------------------------------MA
SAT2-A.thaliana    1 ------------------------------------------------------------
SAT3-A.thaliana    1 ----------------------------------------------------------ML
SAT4-A.thaliana    1 ------------------------------------------------------------
SAT5-A.thaliana    1 ----------------------------------------------------------M
Synechocystis      1 ------------------------------------------------------------
Synechococcus      1 ------------------------------------------------------------
1-C.reinhardtii    1 ----------------------------------------------------------M
2-C.reinhardtii    2 ----------------------------------------------------------SF
1-T.suecica        1 ------------------------------------------------------------
2-T.suecica        1 ------------------------------------------------------------
3-T.suecica        1 ------------------------------------------------------------
1-C.merolae        1 ----------------------------------------------------------MF
2-C.merolae        1 ----------------------------------------------------------MF
T.pseudonana      61 RCCYQPTLLHHYKSSDDSHKNSTTPSTWQSSLKDLVSQIDSKPSTDDEQPQSRMDLVPQI
1-P.tricornutum   43 ----------HVTTHLDEHDH--------------------------------------EF
2-P.tricornutum    1 ----------------------------------------------------------MD
E.huxleyi          1 ------------------------------------------------------------
consensus         61

SAT1-A.thaliana    3 CING----------------ENRDFSSSS---SLSSLP-------MIVS----------
SAT2-A.thaliana    1 ------------------------------------------------------------
SAT3-A.thaliana    3 PVTS----------------RRHFTMSLYMLRSSSPHINHH--------S---------
SAT4-A.thaliana    1 ------------------------------------------------------------
SAT5-A.thaliana    2 PP----------------AGELRHQSPS----KEK-----------------------
Synechocystis      1 ------------------------------------------------------------
Synechococcus      1 ------------------------------------------------------------
1-C.reinhardtii    2 RSVFS-----D-------TCSAAPSTSRP----HAVSVIPSRPRRYA-GGRT--------
2-C.reinhardtii    4 PCLG----------------SKHALSGAS---SRAQQS-------VVA-----------
1-T.suecica        1 --ES----------------LEWVKDAIP-------------------------------
2-T.suecica        1 ------------------------------------------------------------
3-T.suecica        1 TWASP-----D-------KAGNLPAYSNG----RPVTVLPR------------------
1-C.merolae        3 SCLTS--V----------AQGNGRLQRTS----KQVPLVARRERRHRLAVRT--------
2-C.merolae        3 ATTG----------------RLYQTLRVHPSHRALQSVRKRVR-----SR---------
T.pseudonana     121 DAKSSQEDQEHRRPKYQLGLGKNRPLKSS----NASMSTADVDVQSKQPDSSPSENKDES
1-P.tricornutum   56 GANRTLETSTG-TTRYDLGIGKNAPLGSA----SNTTIPAMLAGPSDPNVPTPVATESTQ
2-P.tricornutum    3 DSGQ----------------TYTYLNYPLENGQVLAEAQLRYQTYG-Q--L--------
E.huxleyi          1 --ML--------------RFSRR--TPLP----AARRACS--------------------
consensus        121

SAT1-A.thaliana   26 ----------------------RNFSA-------R-DDGETGDEFPFERIFP--------
SAT2-A.thaliana    1 ---------------------------------------MNGDELPFESGFE--------
SAT3-A.thaliana   29 -------------------FLLPSFVSSKFKHHTL-SP-----PPSPPP----PPPMAA-
SAT4-A.thaliana    1 ------------------------------------------------------MAT-
SAT5-A.thaliana   17 ----------------------LSSV-------T-QS-----DEAE----A--A--SA-
Synechocystis      1 ------------------------------------------------------------
Synechococcus      1 ------------------------------------------------------------
1-C.reinhardtii   37 ------------------LGGHTLLSS-------R-NV-----GSVAVNTMARDRLSAQ-
2-C.reinhardtii   26 ----------------------RVWFA-------RGGSGRRCSPVLASNTEPASSKPSKA
1-T.suecica       12 ----------------------AYLTS-------R-SECSN-----------------FD
2-T.suecica        1 ------------------------------------------------------------
3-T.suecica       26 -------------------GNDNMFSS---------------------------------
1-C.merolae       39 --------------------LRPALESS-------L-SR-----FTEQ----E--QAFPT-
2-C.merolae       32 -------------------GQCPLRSARLQHVRGH-GR-----SSNDGV----SEARDS-
T.pseudonana     177 DV---ASAPFQYWNAPQPVAKPITPQH-------L-NK-----TSRQRYDMGMGKHAPL-
1-P.tricornutum  111 SVPFSAASRGENWVALDPVHKPSTPAS-------R-TR-----HSPHPVSEQTAKPVNG-
2-P.tricornutum   35 --------------------NETRDNVMV--------VC-----HALT------GNASLH-
E.huxleyi         19 ----------------------LRLRR---------CI--SSTSSLQTTI----------
consensus        181
```

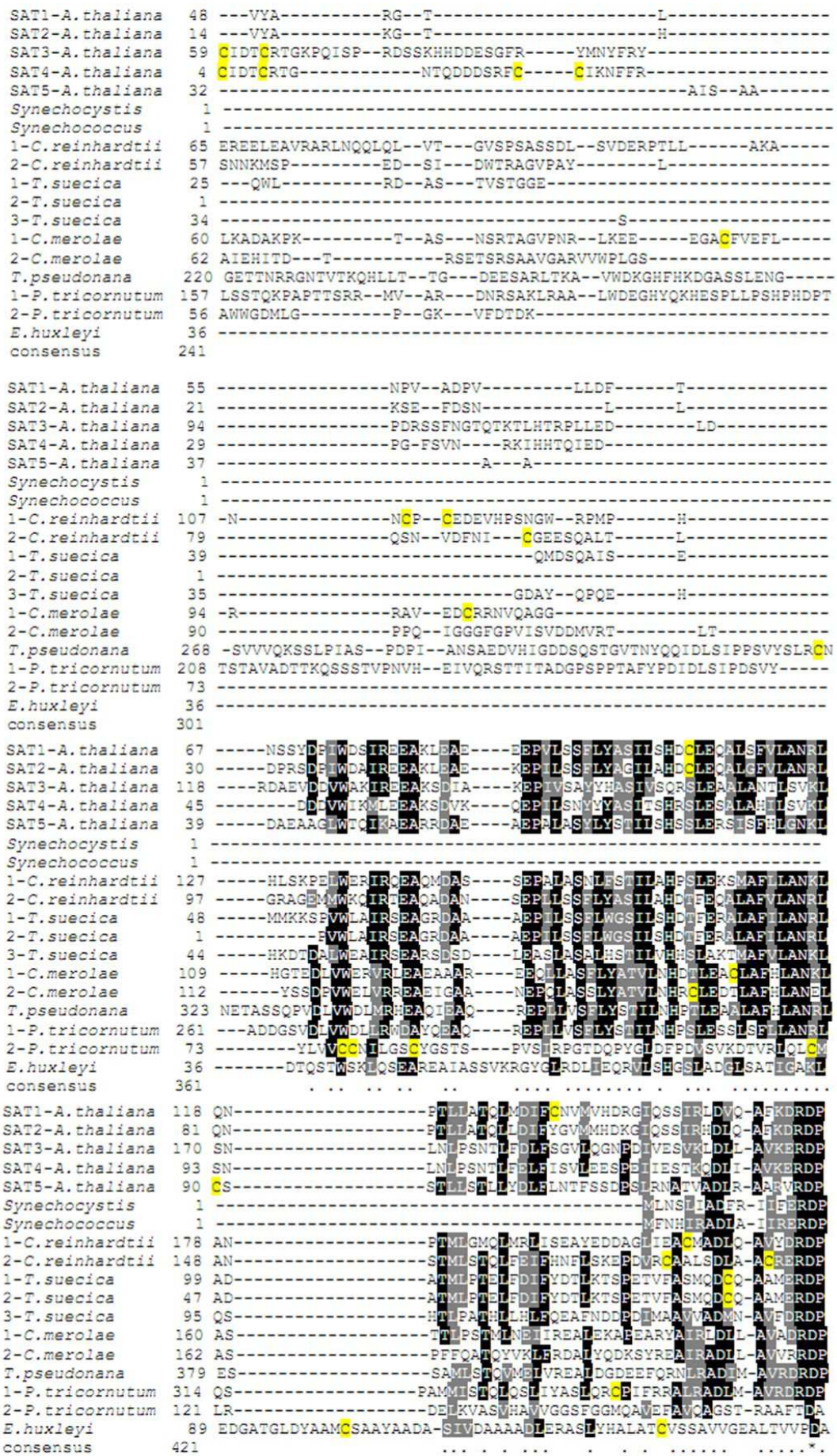

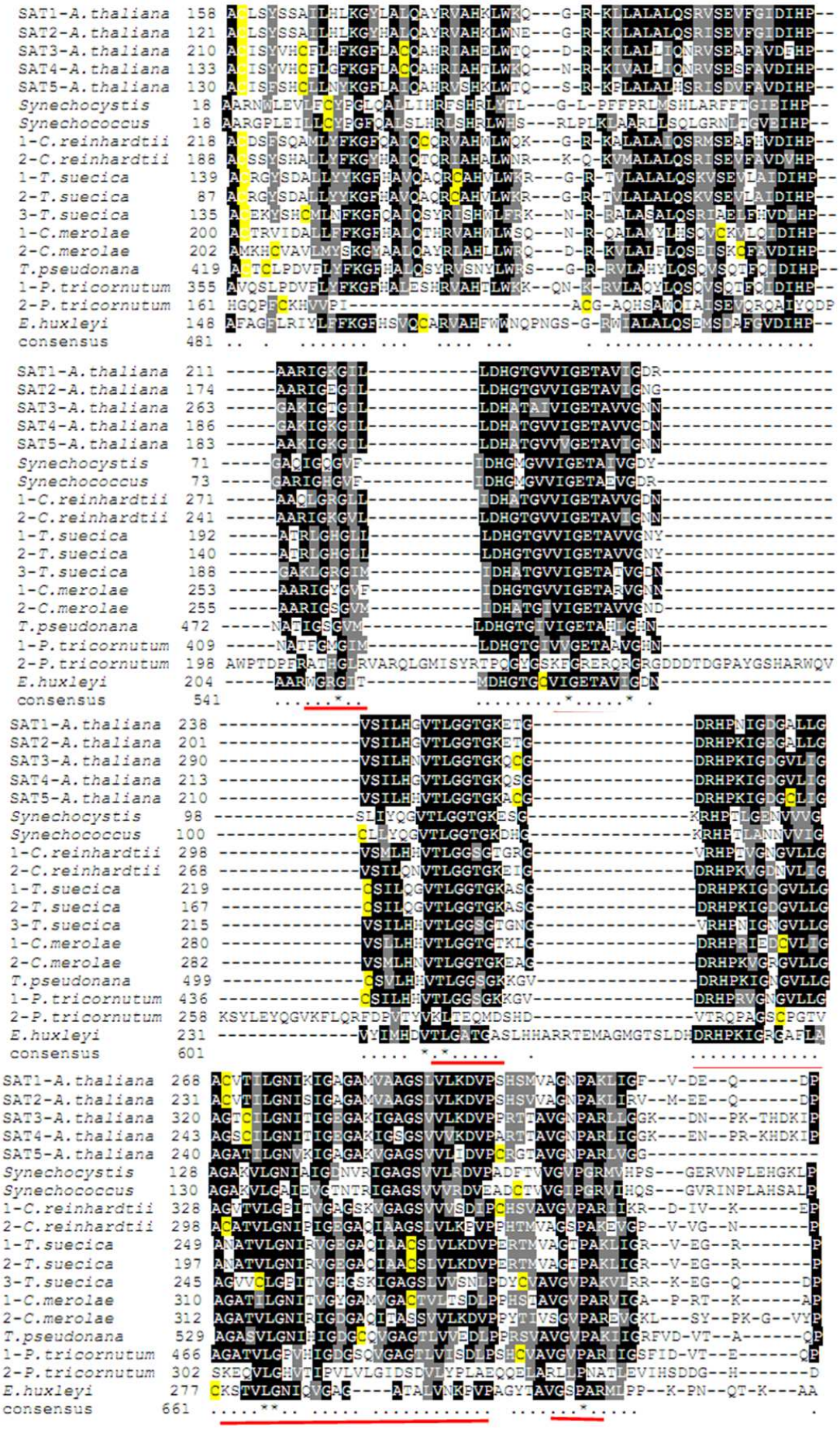

Fig. 4-4. Alignment of SAT protein of algae and *A. thaliana*.

The Cysteine residues are highlighted in yellow. Conserved amino acid was shown with dark (absolutely conserved) and grey (highly conserved residues) background. In the consensus line, asterisks indicate highly conserved amino acid. The hexapeptide motif (I/V/L)-G-XXXX-(I/V/L) is underlined in red.

The alignment sequences: SAT1 At2g17642, SAT2 At4g35642; SAT3 At5g56760; SAT4

At3g13110 SAT5 At1g55920; *Synechocystis* sp. PCC 6803 WP_010872790.1; *Synechococcus* sp. WH 7803 WP_011932076.1; 1-*C. reinhardtii* gi|159480774|; 2-*C. reinhardtii* gi|159484729|; *1-C. merolae* strain 10D gi|544212076|; 2-*C. merolae* strain 10D gi|544209228|; *T. pseudonana* CCMP1335 gi|224009682|; 1-*P. tricornutum* gi|224009682|; CCAP 1055/1; 2-*P. tricornutum* CCAP 1055/1 gi|219129378|; *E. huxleyi* CCMP1516 gi|551593375|; 1, 2, 3-*T. suecica* sequences were obtained through the transcriptom.

4.1.5.2. Main motives in algal OAS-TL sequences

In *A. thaliana* OAS-TL as Table. 4-7 showed, there are seven different interaction areas (Bonner et al., 2005). The OAS-TL sequences amino acid alignment data were shown in Fig. 4-5. The functional residue K (lysine, see supplementary materials for the one letter code for amino acids) was involved in the formation of the Schiff base with pyridoxal 5'-phosphate (PLP) and is absolutely conserved in all sequences. Also, the other aa residues in the K area were relatively conserved among all the species. Other portions of the protein are involved in PLP interaction (Bonner et al., 2005); they were separated into three different units: the first unit was formed by a single, highly conserved amino acid, H; the second unit was formed by five highly conserved residues, GTGGT; the last one was formed by a single amino acid, S, which was absolutely conserved. As shown in the Table. 4-7, these structures were pretty much conserved in all algal species. Only in the green algae *T. suecica*, the first unit, H, was substituted with a polar amino acid Y; in the second unit (GTGGT) the first polar amino acid, G, was substituted with the polar amino acid S.

The residues involved in substrates interaction (Bonner et al., 2005) were separated in two different units: the first one was formed by -TSGNT- (five highly conserved residues); the second unit was formed by a single amino acid -Q- which showed an absolutely conserved character. Table. 4-7 showed that, in the first unit involved in the interaction with the substrate, two residues were not highly conserved; they were i)

the second amino acid in the sequence, a -S- residue, which was a polar amino acid, and was substituted with A or -S, with the exception of the marine species *T. suecica*, in which the same position was occupied by the non-polar amino acid -V; ii) the fourth polar residues, N, which was always substituted by another polar amino acid, -S-.

The residues involved in SAT/OAS-TL interaction site were associated with a six amino acid unit, KPGPHK (Bonner et al., 2005). In algae, the first polar amino acid, K, and the last two amino acids, HK, of this motif were often substituted. In one of the sequences of the freshwater cyanobacterium *Synechocysis* sp. PCC 6803, the last two basic amino acid H and K, were substituted with the polar residues S and the non-polar I. In the OAS-TL of the marine cyanobacterium *Synechococcus* sp. WH 7803, one of the sequences showed the presence of a non-polar V in the place of the first basic amino acid K, and the terminal K was substituted by the basic amino acid R.

In *C. reinhardtii*, in one case both the first and the last K were substituted by polar residues (A and Q, respectively); in another isoform, the first K was substituted by the polar residue N, but the non-polar amino acid I, was found in the place of the terminal K.

As shown in Table. 4-7, in *T. suecica* OAS-TL, nearly all residues of the -KPGPHK- domain were substituted. In *T. suecica* OAS-TL 2-4, the first K was substituted by polar amino acids (Q in the 2 and 4 isoforms and N in isoform 3); In *T. suecica* OAS-TL 1, 3 and 4, the last two basic amino acids of the unit were substituted by YQ, TI and T, respectively.

In the OAS-TL of the red algae *C. merolae*, the first K was substituted by another basic amino acid, R. In the last two positions of the motif, the polar amino acid S and the non-polar amino acid I, where found instead of P and H.

In the diatom *T. pseudonana* CCMP 1335 OAS-TL 1 and 2, the first basic amino acid

of the motif was substituted by the polar amino acid A; in the isoform 3, it was substituted by the polar amino acid H. In the *T. pseudonana* isoform 1 and 3, the last two amino acids were substituted by a non-polar P, a polar T or non-polar F residues.

In *P. tricornutum* CCAP 1055/1 in one case the first basic amino acid K was substituted by a non-polar P residue.

In the OAS-TL of the dinoflagellate *A. klebsii,* in the six amino acid motif, nearly all residues were substituted. In the isoforms 1, 3 the K in the first position in the motif was substituted by a polar A, in the isoform 4 by a non-polar amino L. In *A. klebsii* isoforms 1, 2 and 4, the last two residues were substituted by P, TI and A, respectively.

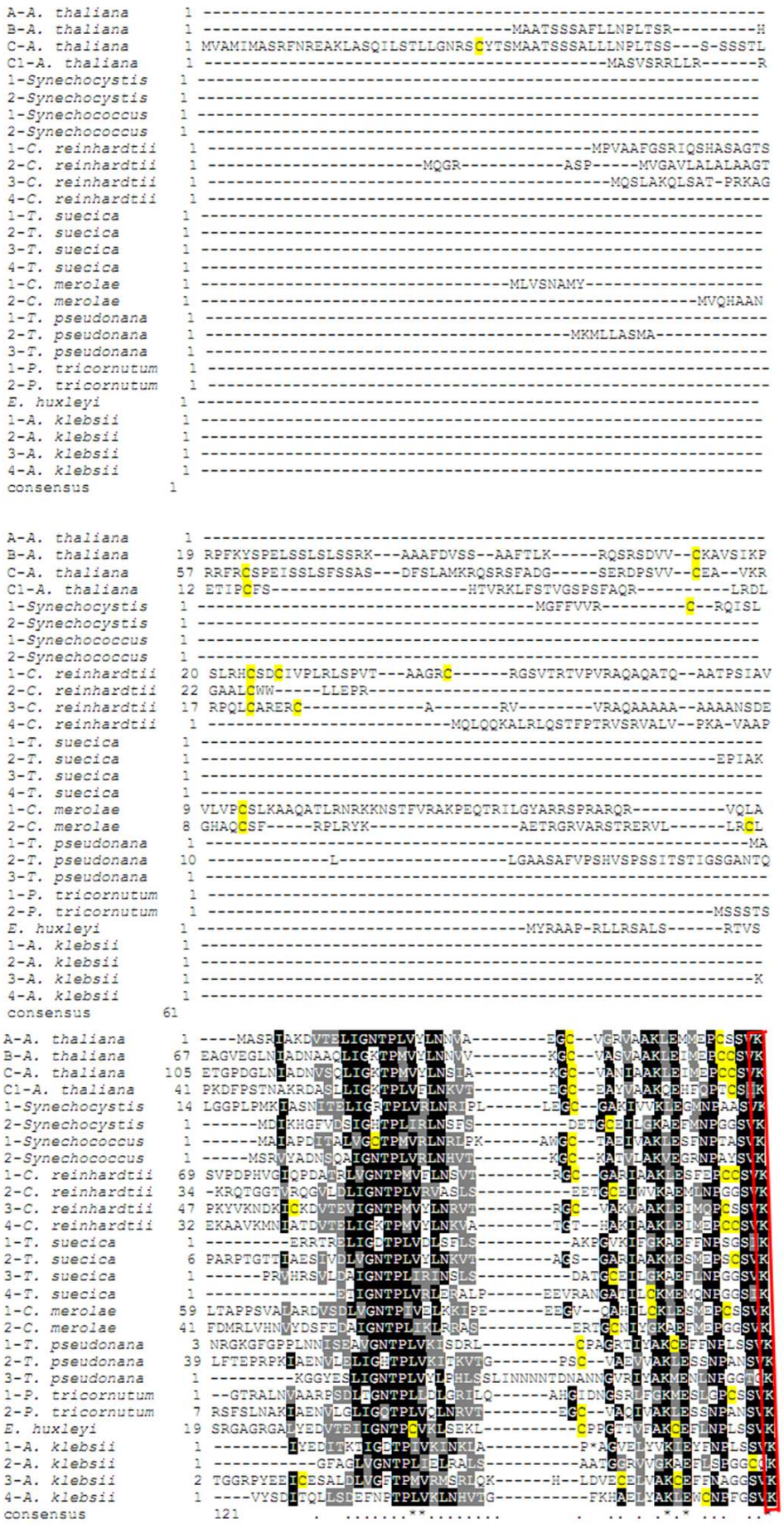

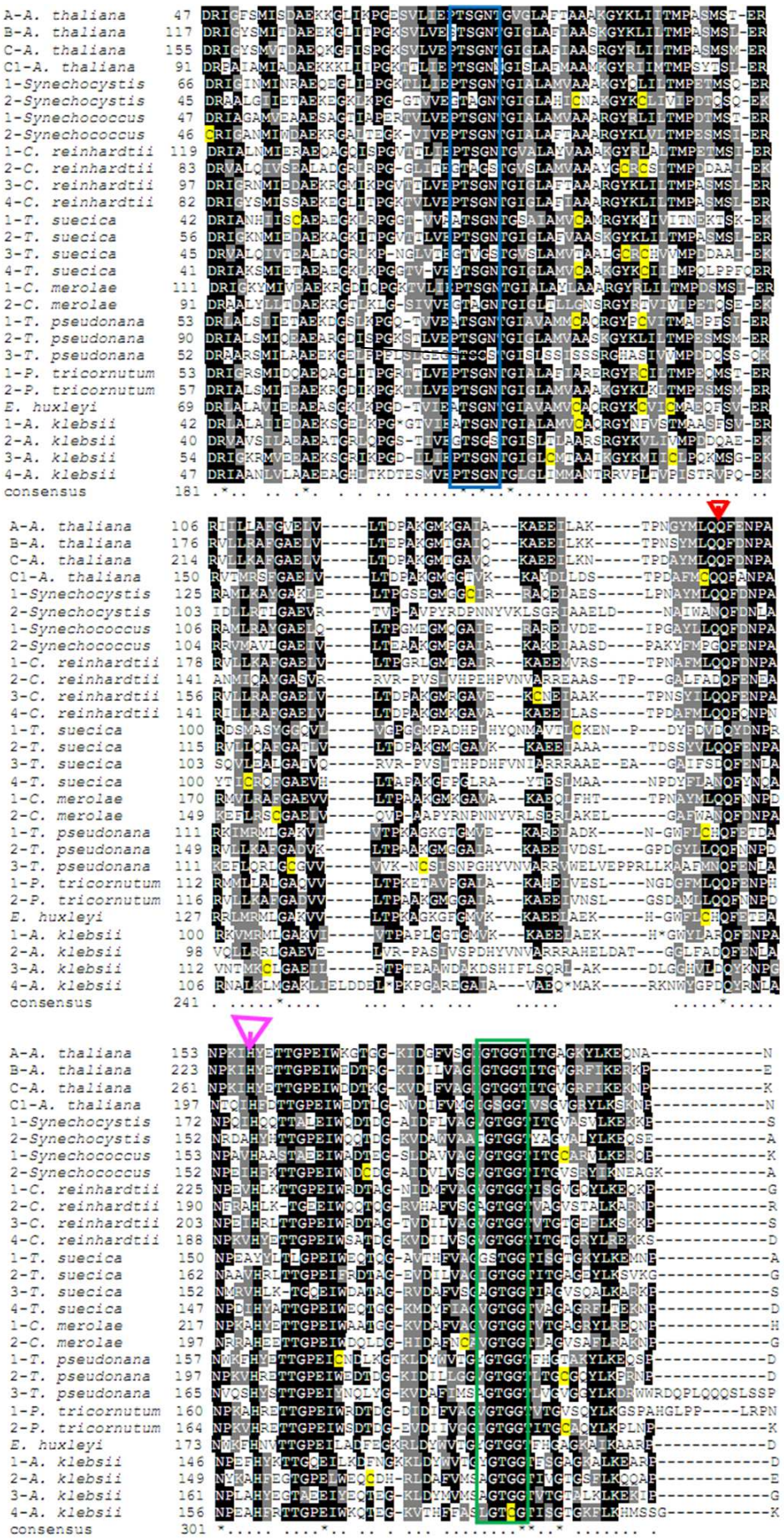

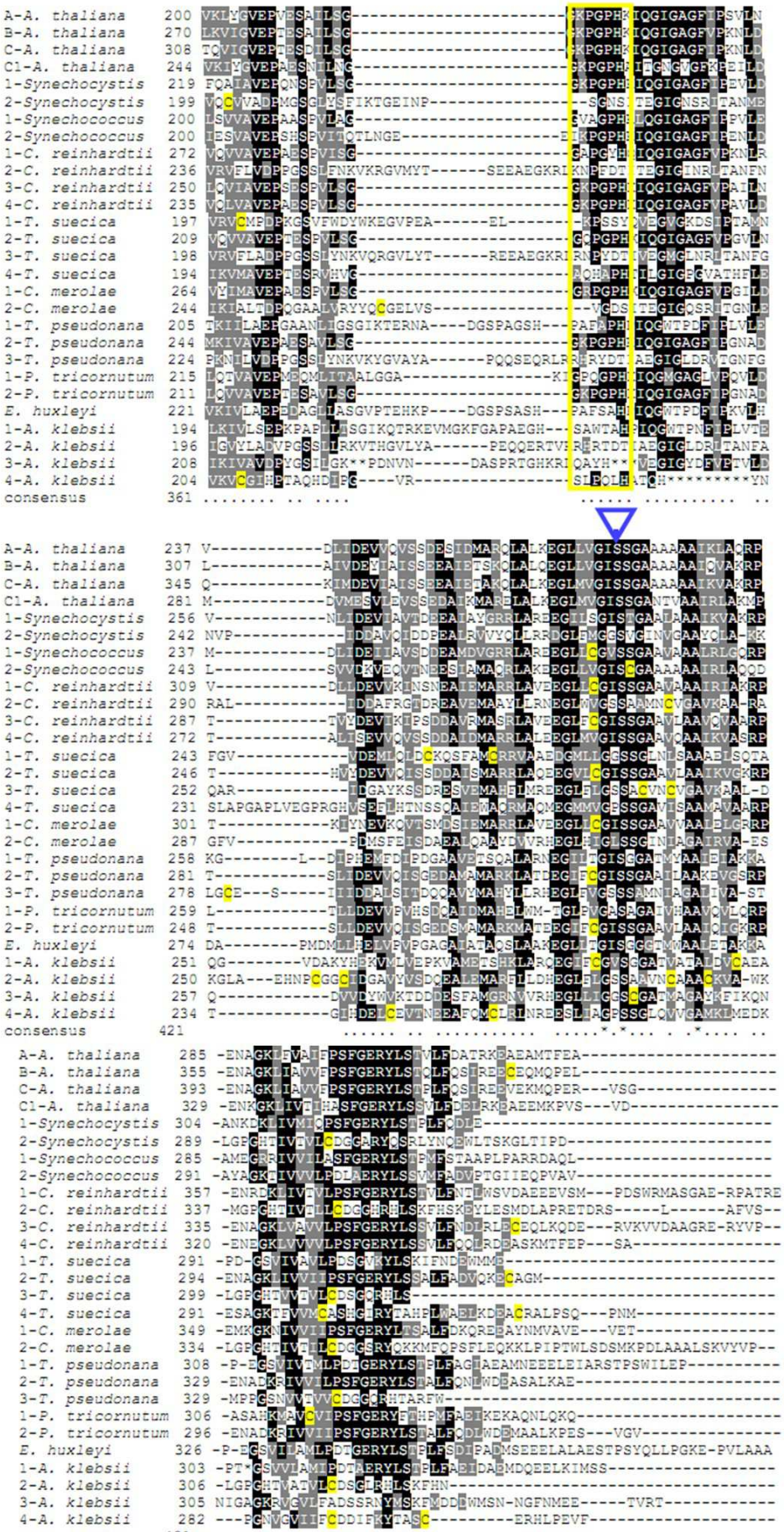

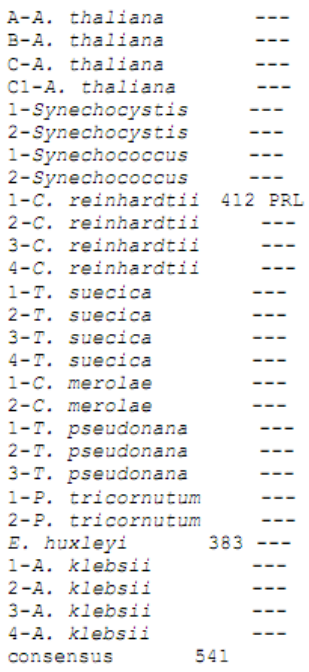

Fig. 4-5. Alignment of OAS-TL of algae and *A. thaliana*.

The red rectangle identifies the PLP binding site, with the functional lysine involved in the formation of the Schiff base; the purple triangle, the green rectangle, and the blue triangle indicated the other motif involved in PLP interaction; the blue rectangle and the red triangle indicate the residues involved in substrate interaction; the yellow rectangle indicated the SAT/OAS-TL interaction site. The Cysteine residues are highlighted in yellow. Absolutely conserved amino acids are shown with dark background, highly conserved residues with grey background. At the consensus line, asterisks indicate highly conserved aminoacids.

The alignment sequences: A-At4g14880; B-At2g43750; C-AT3G59760; C1-At3g61440; 1-*Synechocystis* sp. PCC 6803 BAA17450.1; 2-*Synechocystis* sp. PCC 6803 BAA16664.1; 1-*Synechococcus* sp. WH 7803 WP_011934122.1; 2-*Synechococcus* sp. WH 7803 WP_011932497.1; 1-*C. reinhardtii* XP_001696139.1; 2-*C. reinhardtii* XP_001701454.1; 3-*C. reinhardtii* XP_001703301.1; 4-*C. reinhardtii* XP_001691935.1; *1-C. merolae* strain 10D XP_005539314.1; 2-*C. merolae* strain 10D XP_005536023.1; 1-*T. pseudonana* CCMP 1335 XP_002286122.1; 2-*T. pseudonana* CCMP 1335 XP_002286707.1; 3-*T. pseudonana* XP_002287864.1; 1-*P. tricornutum* CCAP 1055/1 XP_002177040.1; CCAP 1055/1; 2-*P. tricornutum* CCAP 1055/1 XP_002180648.1; *E. huxleyi* CCMP 1516 gi|485641205|; 1, 2, 3, 4-*T. suecica*; 1, 2, 3, 4-*A. klebsii* these sequences were obtained through the transcriptom.

Table. 4-7. Main binding motives in OAS-TL sequences (from the N'-terminal to C'-terminal)

	PLP binding site	Residues binding with substrate		Residues binding with PLP		OAS-TL/SAT interaction site	Residues binding with PLP
	-K-	-TSGNT-	-Q-	-H-	-GTGGT-	-KPGPHK-	-S-
A-*A.thaliana*	-K-(46)	-TSGNT-(74-78)	-Q-(147)	-H-(157)	-GTGGT-(181-185)	-KPGPHK-(217-222)	-S-(269)
B-*A.thaliana*	-K-(116)	-TSGNT-(144-148)	-Q-(207)	-H-(217)	-GTGGT-(251-255)	-KPGPHK-(287-292)	-S-(239)
C-*A.thaliana*	-K-(154)	-TSGNT-(182-186)	-Q-(255)	-H-(265)	-GTGGT-(289-293)	-KPGPHK-(325-330)	-S-(377)
C1-*A.thaliana*	-K-(90)	-TSGNM-(118-122)	-Q-(191)	-H-(201)	-GSGGT-(225-229)	-KPGPHA-(261-266)	-S-(313)
1-*Synechocystis* sp. PCC 6803	-K-(65)	-TSGNT-(93-97)	-Q-(166)	-H-(176)	-GTGGT-(200-204)	-KPGPHK-(236-241)	-S-(288)
2-*Synechocystis* sp. PCC 6803	-K-(44)	-TAGNT-(71-75)	-Q-(146)	-H-(156)	-GTGGT-(180-184)	---SGNSI-(233-236)	-S-(274)
1-*Synechococcus* sp. WH 7803	-K-(46)	-TSGNT-(74-78)	-Q-(147)	-H-(157)	-GTGGT-(181-185)	-VAGPHR-(217-222)	-S-(269)
2-*Synechococcus* sp. WH 7803	-K-(45)	-TSGNT-(72-76)	-Q-(145)	-H-(155)	-GTGGT-(180-184)	-KPGPHK-(223-228)	-S-(275)
1-*C.reinhardtii*	-K-(118)	-TSGNT-(145-150)	-Q-(219)	-H-(229)	-GTGGT-(253-257)	-APGYHQ-(289-294)	-S-(341)
2-*C.reinhardtii*	-K-(82)	-TAGST-(109-113)	-Q-(184)	-H-(194)	-GTGGT-(217-221)	-NPFDTI-(269-274)	-S-(322)
3-*C.reinhardtii*	-K-(96)	-TSGNT-(124-128)	-Q-(197)	-H-(207)	-GTGGT-(231-235)	-KPGPHK-(270-275)	-S-(319)
4-*C.reinhardtii*	-K-(81)	-TSGNT-(109-113)	-Q-(182)	-H-(192)	-GTGGT-(216-221)	-KPGPHK-(252-257)	-S-(304)
1-*T.suecica*	-K-(41)	-TSGNT-(68-72)	-Q-(144)	-Y-(154)	-STGGT-(178-182)	-KPSSYQ-(221-226)	-S-(375)
2-*T.suecica*	-K-(55)	-TSGNT-(83-87)	-Q-(176)	-H-(186)	-GTGGT-(190-194)	-QPGPHK-(226-231)	-S-(278)
3-*T.suecica*	-K-(44)	-TVGST-(71-75)	-Q-(146)	-H-(156)	-GTGGT-(179-183)	-NPYDTI-(240-245)	-S-(284)
4-*T.suecica*	-K-(40)	-TSGNT-(67-71)	-Q-(149)	-H-(159)	-GTGGT-(175-179)	-QHAPHT-(210-215)	-S-(275)
1-*C.merolae strain* 10D	-K-(110)	-TSGNT-(138-142)	-Q-(211)	-H-(221)	-GTGGT-(245-249)	-RPGPHK-(281-286)	-S-(333)
2-*C.merolae strain* 10D	-K-(90)	-TAGNT-(117-171)	-Q-(191)	-H-(201)	-GTGGT-(225-229)	-IVGDSI-(268-271)	-S-(319)
1-*T.pseudonana* CCMP 1335	-K-(52)	-TSGNT-(79-83)	-Q-(152)	-H-(162)	-GTGGT-(185-189)	-AFAPHP-(237-242)	-S-(292)
2-*T.pseudonana* CCMP 1335	-K-(89)	-TSGNT-(117-121)	-Q-(191)	-H-(201)	-GTGGT-(225-229)	-KPGPHK-(261-266)	-S-(313)
3-*T.pseudonana* CCMP 1335	-K-(51)	-TSGST-(78-82)	-Q-(259)	-H-(169)	-GTGGT-(193-197)	-HRYDTF-(257-262)	-S-(314)
1-*P.tricornutum* CCAP 1055/1	-K-(52)	-TSGNT-(80-84)	-Q-(153)	-H-(163)	-GTGGT-(188-192)	-PQGPHK-(238-243)	-S-(290)
2-*P.tricornutum* CCAP 1055/1	-K-(56)	-TSGNT-(84-88)	-Q-(158)	-H-(168)	-GTGGT-(192-196)	-KPGPHK-(228-232)	-S-(280)
E.huxleyi CCMP 1516	-K-(68)	-TSGNT-(95-99)	-Q-(167)	-H-(177)	-GTGGT-(202-205)	-AFSAHP-(253-258)	-S-(320)
1-*A.klebsii*	-K-(42)	-TSGNT-(69-74)	-Q-(140)	-H-(150)	-GTGGT-(175-179)	-AWTAHP-(230-235)	-S-(287)
2-*A.klebsii*	-K-(39)	-TSGNT-(66-70)	-Q-(141)	-H-(151)	-GTGGT-(177-181)	-HRYDTI-(229-233)	-S-(291)
3-*A.klebsii*	-K-(53)	-TSGNT-(80-84)	-Q-(155)	-H-(165)	-GTGGT-(189-193)	-AYH----(239-241)	-S-(289)
4-*A.klebsii*	-K-(46)	-TSGNT-(74-78)	-Q-(150)	-H-(160)	-GTGGT-(184-188)	-LPQLHA-(222-227)	-S-(266)

Highlighted residues are those that are substituted in the sequence of a given species; the number inside parenthess indicate the position of the amino acids in the sequences.

4.2. OAS-TL from algae

4.2.1. OAS-TL purification

The elution patterns of OAS-TL showed differences among the experimental species (Fig. 4-6). The western blot analysis of the various fractions evidenced the presence of proteins of different sizes cross-reacting with OAS-TL antibody (Table. 4-8).

Table. 4-8. Features of purified algae OAS-TL

Species	PCP (Elution Volume of protein peak)	Immunoblot positive (+) or negative (-)	OAS-TL protein band number	OAS-TL size (kDa)
Synechocystis sp. PCC 6803	1 and 3 ml	(-) and (+)	2	33, 39
Chlamydomonas reinhardtii-TAP	3.5 ml	(+)	2	37, 40
Chlamydomonas reinhardtii-TP	3 ml	(+)	3	34, 44, 49
Dunaliella tertiolecta	2 and 3.5 ml	(-) and (+)	2	36, 38
Tetraselmis suecica	0.5 and 3 ml	(-) and (+)	2	33, 41
Thalassiosira pseudonana	2 and 3 ml	(-) and (+)	2	36, 37
Phaeodactylum tricornutum	3.5 ml	(+)	1	36
Amphidinium klebsii	2.5 ml	(+)	2	35, 39

Note: PCP, protein peak in terms of elution volume (ml) used as cross-reaction with the OAS-TL-A antibody present (+) or absence(-).

In *Synechocystis* sp. PCC 6803 (Fig. 4-6 A), a protein concentration peak appeared already after 1 ml of elution buffer passed through the column. The proteins of this peak (fraction E2), however, did not cross-react with OAS-TL antibody (Fig. 4-7). The main elution peak for *Synechocystis* sp. PCC 6803 was eluted after 3 mL of elution buffer (Fig. 4-6 A). The fractions corresponding with this following peak (fractions E6, 7, 8, 9, Fig. 4-7) were recognized by OAS-L antibody. Two proteins were detected in the western blot and had a mass of around 35 kDa (Fig. 4-7). Mobility analysis (supplemental data), indicated that these bands had sizes of 33 kDa and 39 kDa.

When *Chlamydomonas reinhardtii* was grown in TAP medium, the elution pattern only showed one protein concentration peak after 3.5 ml elution (Fig. 4-6 B). The collected fractions (E7, 8, 9, 10, Fig. 4-8) showed two signals with masses of 37 kDa and 40 kDa (Fig. 4-8). When *C. reinhardtii* was cultured in TP medium, the main elution peak appeared after 3 ml of elution buffer (Fig. 4-6 C). The western blot of the proteins in the peak fraction (E6) and in the following fractions (E7, 8, 9, Fig. 4-9) showed three bands of 34 kDa, 44 kDa and 49 kDa (Fig. 4-9).

The affinity chromatography of *Dunaliella tertiolecta* extract had a rather flat protein concentration profile, with two peaks of similar protein content after 2 and 3.5 ml elution (Fig. 4-6 D). The western blot of the protein sample obtained after 2 ml elution (E4, Fig. 4-10) showed no immunoreaction while it showed a strong band of 36 kDa and another band of 38 kDa in the fractions (E6, 7, 8, 9, Fig. 4-10) belonging to the 3.5 ml elution peak (Fig 4-6 D).

Tetraselmis suecica affinity chromatography afforded a peak at 0.5 ml and another at 3 ml (Fig. 4-6 E). Again, the earlier peak (E1 fraction) did not show any immunoreaction with OAS-TL antibodies (Fig. 4-11). The later peak consisting in fractions E5, 6, 7, 8, instead, showed a dense band of 41 kDa and a fainter one of 33 kDa (Fig.4-11).

Thalassiosira pseudonana showed an elution peak at 1 ml and a major one at 3 ml (Fig. 4-6 F). The first peak (E2 fraction) did not give a signal in the western blot. The

fractions obtained from the peak at 3 ml, instead, showed a band of 36 kDa (E7, Fig. 4-7) and of 37 kDa (E5, 6, 8, Fig. 4-12).

For *Phaeodactylum tricornutum*, one elution peak of protein concentration was observed after 3.5 ml (Fig. 4-6 G) of elution buffer. The mass of the OAS-TL contained in this peak was 36 kDa (E7, 8, 9, 10 fractions, Fig. 4-13).

OAS-TL of *Amphidinium klebsii* was eluted after 2.5 ml elution buffer (Fig. 4-6 H). A band of 35 kDa was visible in the immunoreaction (E5, 6, 7, 8 fractions, Fig. 4-14); only in the fraction E5 an additional band of 39 kDa was visible (Fig. 4-14).

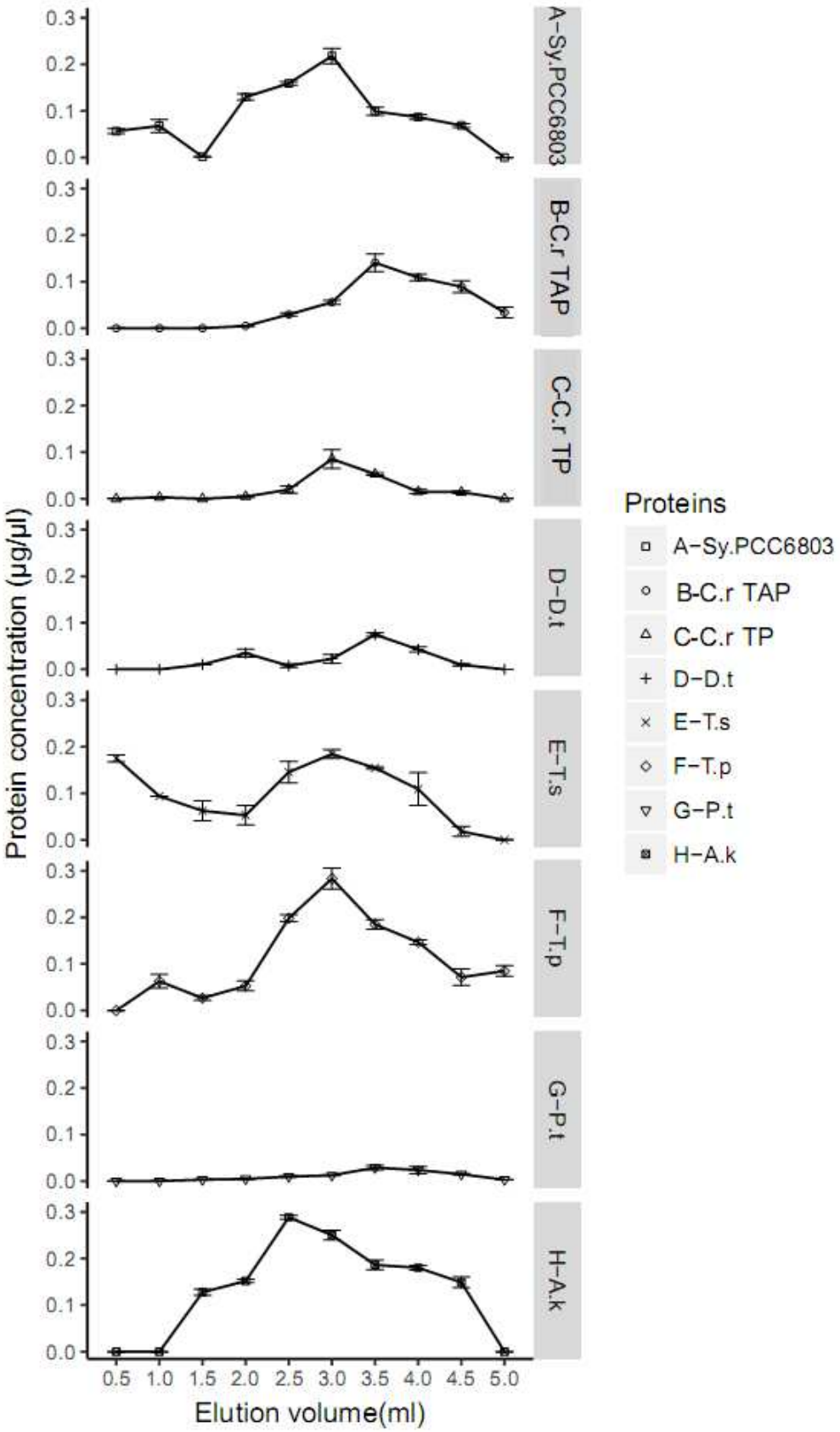

Fig. 4-6. Elution pattern of OAS-TL protein from different algal species.

From the top to the bottom different curve the algal species: A-Sy. PCC 6803: *Synechocystis* sp. PCC 6803; B-C.r-TAP: *Chlamydomonas reinhardtii* with TAP medium; C-C.r-TP:

Chlamydomonas reinhardtii with TP medium; D-D.t: *Dunaliella tertiolecta*; E-T.s: *Tetraselmis suecica*; F-T.p: *Thalassiosira pseudonana*; G-P.t: *Phaeodactylum tricornutum*; H-A.k: *Amphidinium klebsii*. There were three replicates the data was Mean ± SD.

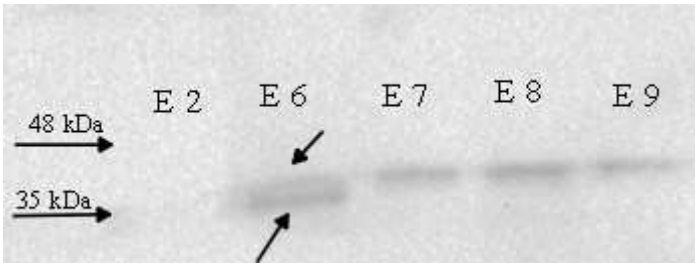

Fig. 4-7. Immunodetection of OAS-TL purified from *Synechocystis* sp. PCC 6803.

The amount of protein loaded on the gel were fraction E2 = 1.36 µg; E7 = 2.25 µg; E8 = 0.58 µg; E9 = 0.58 µg; E10 = 0.36 µg.

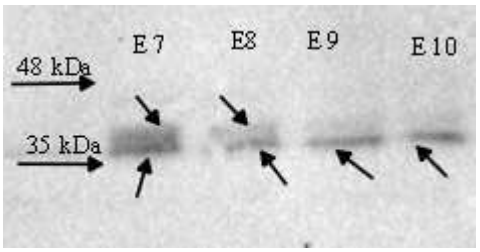

Fig. 4-8. Immunodetection of OAS-TL purified from *Chlamydomonas reinhardtii* grown in TAP medium.

The amount of protein loaded on the gel were fraction E7 = 0.62 µg; E8 = 0.45 µg; E9 = 0.29 µg; E10 = 0.26 µg.

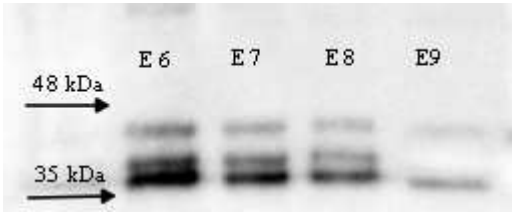

Fig. 4-9. Immunodetection of OAS-TL purified from *Chlamydomonas reinhardtii* grown in TP medium.

The amount of protein loaded on the gel were fraction E7 = 0.24 µg; E8 = 0.58 µg; E9 = 0.31 µg; E10 = 0.12 µg.

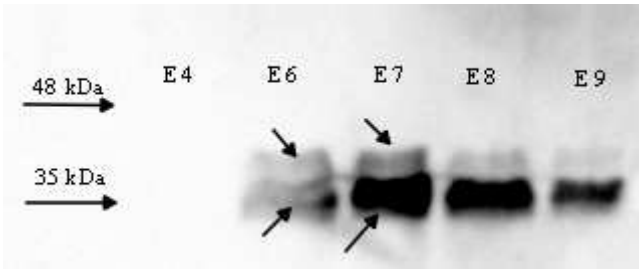

Fig. 4-10. Immunodetection of OAS-TL purified from *Dunaliella tertiolecta*.

The amount of protein loaded on the gel were fraction E4 = 0.49 µg; E6 = 0.12 µg; E7 = 0.48 µg; E8 = 0.35 µg; E9 = 0.21 µg.

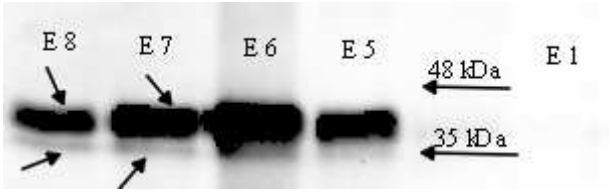

Fig. 4-11. Immunodetection of OAS-TL purified from *Tetraselmis suecica.*

The amount of protein loaded on the gel were fraction E1 = 1.35 µg; E5 = 1.50 µg; E6 = 1.75 µg; E7 = 1.31 µg; E8 = 0.92 µg.

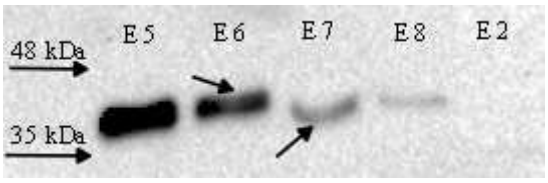

Fig. 4-12. Immunodetection of OAS-TL purified from *Thalassiosira pseudonana.*

The amount of protein loaded on the gel were fraction E2 =1.01 µg; E5 = 1.43 µg; E6 = 1.33 µg; E7 = 1.01 µg; E8 = 0.52 µg.

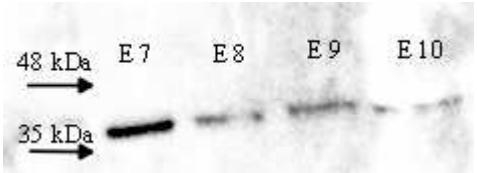

Fig. 4-13. Immunodetection of OAS-TL purified from *Phaeodactylum tricornutum.*

The amount of protein loaded on the gel were fraction E7 = 0.47 µg; E8 = 0.15 µg; E9 = 0.13 µg; E10 = 0.01 µg.

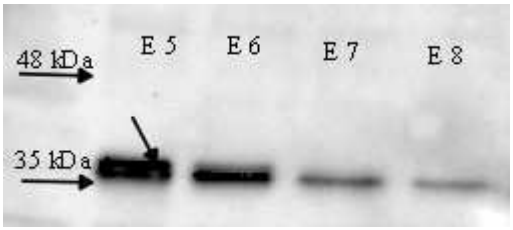

Fig. 4-14. Immunodetection of OAS-TL purified from *Amphidinium klebsii.*

The amount of protein loaded on the gel were fraction E5 = 0.87 µg; E6 = 0.32 µg; E7 = 0.31 µg; E8 = 0.22 µg.

4.2.2. OAS-TL enzyme activity in crude extracts

The activity of OAS-TL was present in the crude extracts of all tested algal species. Most of the species had similar OAS-TL enzyme activity on a protein basis except for *Tetraselmis suecica* (especially) and *Thalassiosira pseudonana,* which showed appreciably higher activities (Fig. 4-15, Table. 4-9).

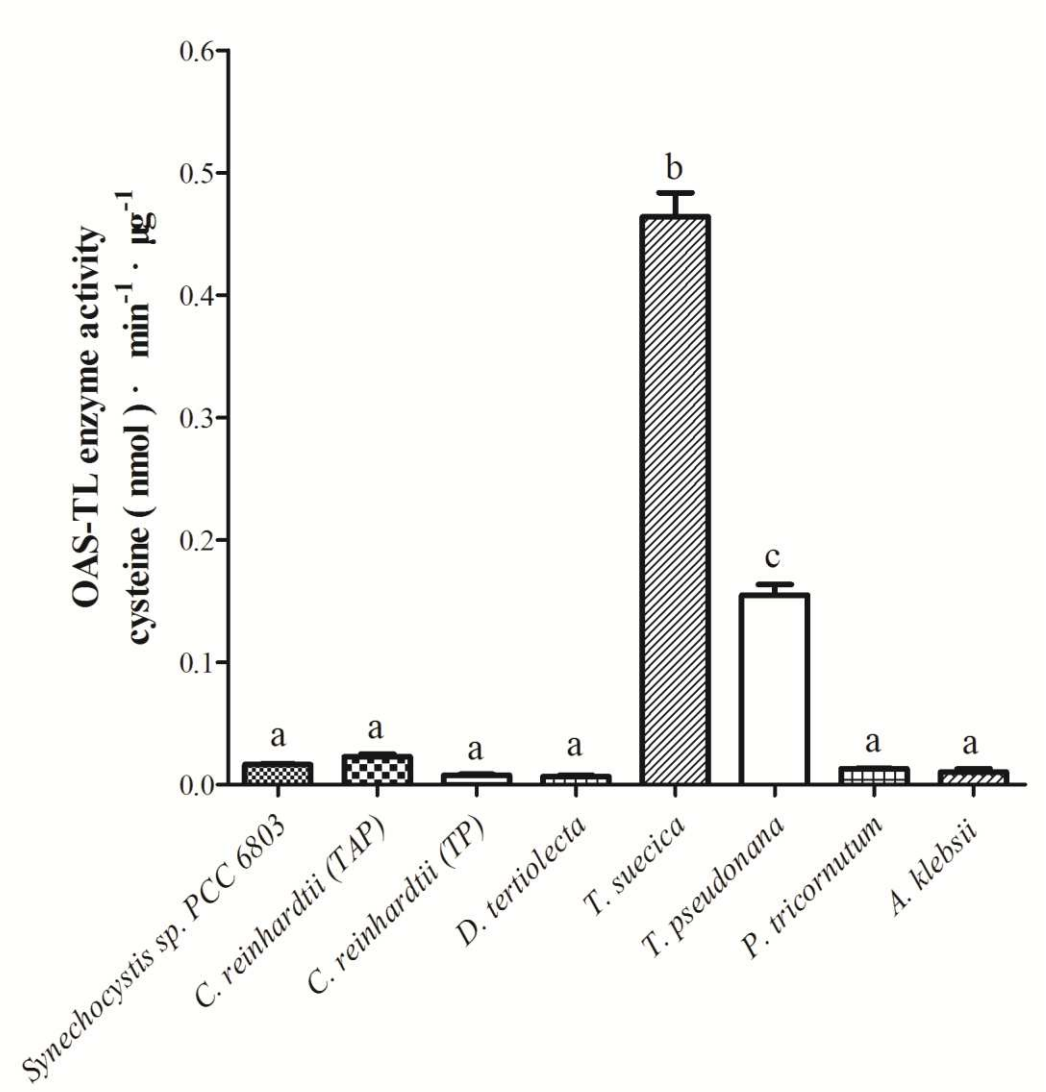

Fig. 4-15. OAS-TL enzyme activity in crude extracts of different algae.

Different letters show statistically different means ($P < 0.05$). The error bars represent the standard deviations ($n = 3$).

In *Synechocystis* sp. PCC 6803, the OAS-TL activity per μg of protein in the crude extract decreased appreciably if the crude extract was diluted 100 times (Fig. 4-16, Table. 4-9).

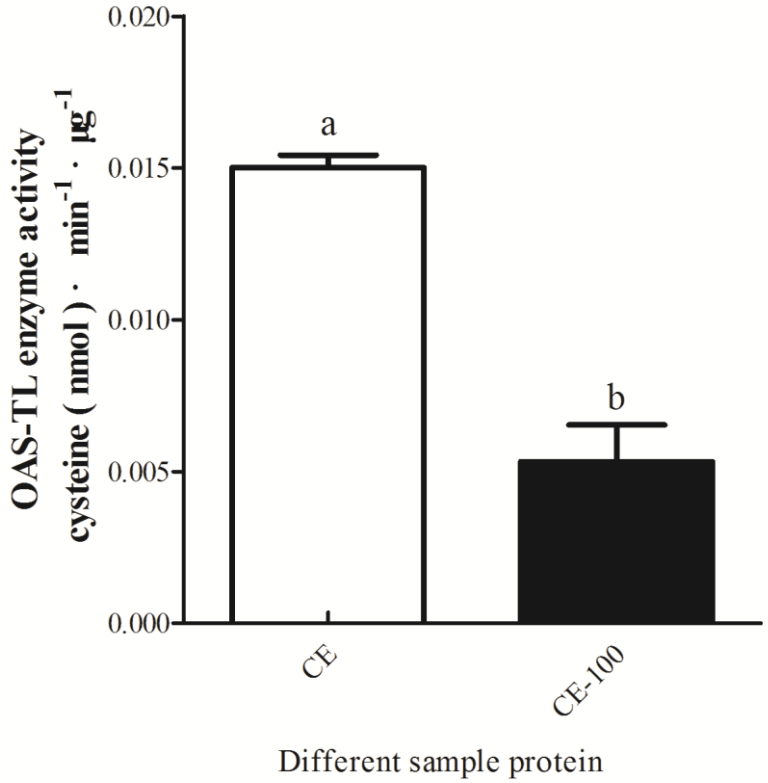

Fig. 4-16. OAS-TL activity per unit of protein in crude and diluted extracts of *Synechocystis* sp. PCC 6803.

CE is the activity of the crude extract obtained according to the extraction protocol. CE-100 is the activity in the crude extract with a 100-fold dilution. Different letters show statistically different means ($P < 0.05$). The error bars show the standard deviations ($n = 3$).

In the green algae *Chlamydomonas reinhardtii* cultured in TAP medium, the OAS-TL activity of the 100-fold diluted sample was similar to the activity in the undiluted extract (Fig. 4-17, Table. 4-9).

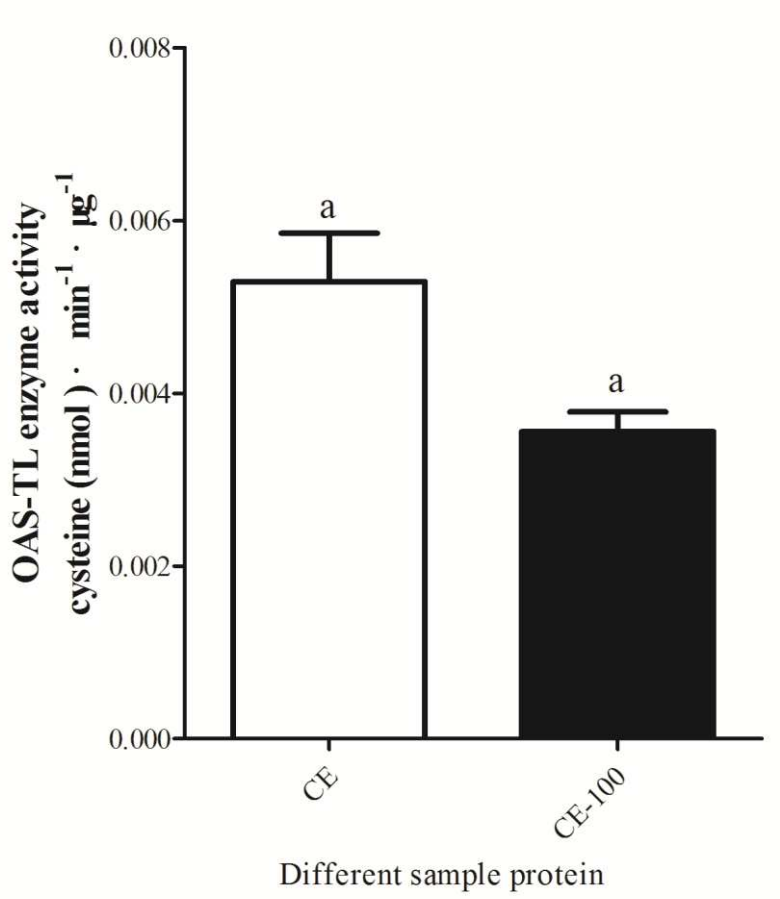

Fig. 4-17. OAS-TL activity per unit of protein in crude and diluted extracts of *Chlamydomonas reinhardtii* cultured in TAP medium.

CE is the activity of the crude extract obtained according to the extraction protocol. CE-100 is the activity in the crude extract with a 100-fold dilution. Different letters show statistically different means ($P < 0.05$). The error bars show the standard deviations ($n = 3$).

When *Chlamydomonas reinhardtii* was cultured in TP medium, OAS-TL activity per unit of protein was about 6.5 higher in diluted extracts (Fig. 4-18, Table. 4-9).

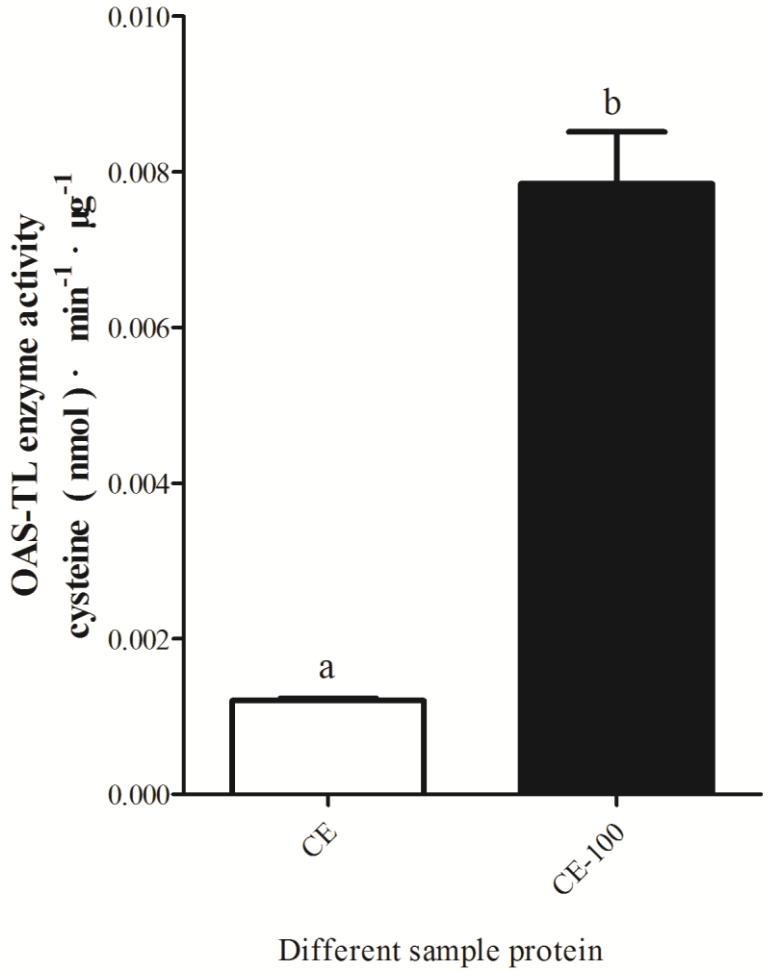

Fig. 4-18. OAS-TL activity per unit of protein in crude and diluted extracts of *Chlamydomonas reinhardtii* cultured in TP medium.

CE is the activity of the crude extract obtained according to the extraction protocol. CE-100 is the activity in the crude extract with a 100-fold dilution. Different letters show statistically different means ($P < 0.05$). The error bars show the standard deviations ($n = 3$).

In *Dunaliella tertiolecta,* OAS-TL activity of the 100-fold diluted sample was similar to that in the undiluted crude extract (Fig. 4-19, Table. 4-9).

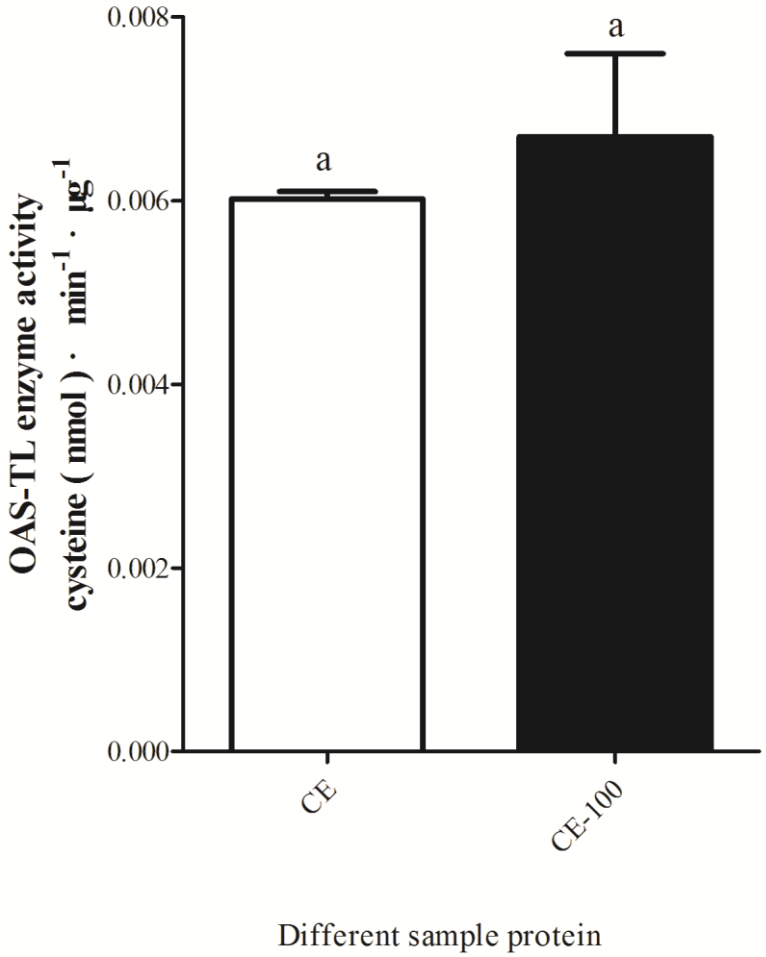

Fig. 4-19. OAS-TL activity per unit of protein in crudeand diluted extracts of *Dunaliella tertiolecta.*

CE is the activity of the crude extract obtained according to the extraction protocol. CE-100 is the activity in the crude extract with a 100-fold dilution. Different letters show statistically different means ($P < 0.05$). The error bars show the standard deviations ($n = 3$).

In *Tetraselmis suecica,* OAS-TL enzyme activity of the 100 times diluted sample was 1.6 times higher (Fig. 4-20, Table. 4-9).

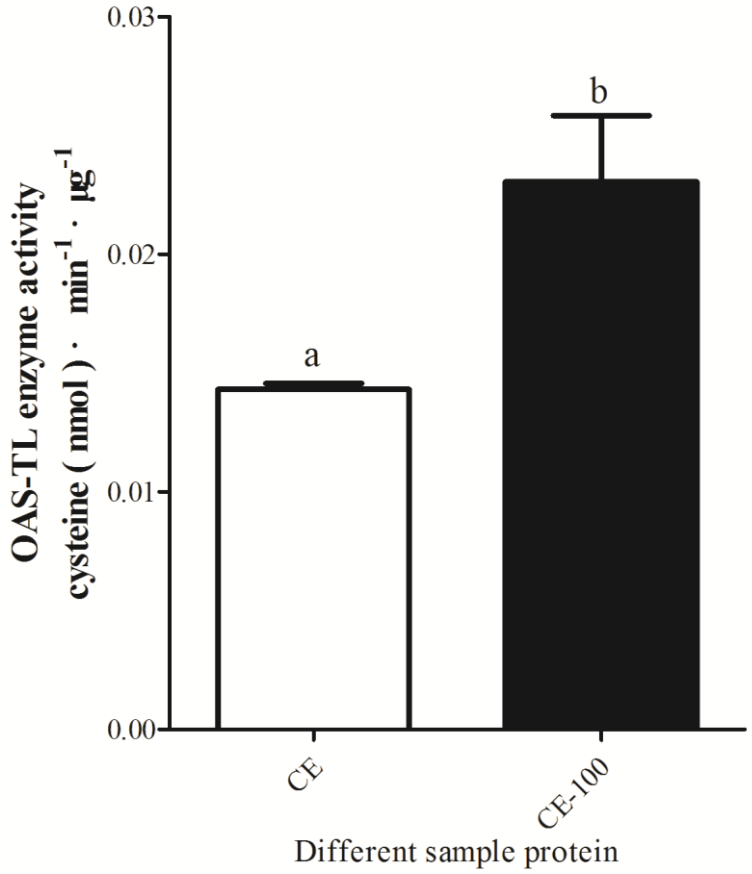

Fig. 4-20. OAS-TL activity per unit of protein in crude and diluted extracts of *Tetraselmis suecica*.

CE is the activity of the crude extract obtained according to the extraction protocol. CE-100 is the activity in the crude extract with a 100-fold dilution. Different letters show statistically different means ($P < 0.05$). The error bars show the standard deviations ($n = 3$).

In *Thalassiosira pseudonana*, OAS-TL enzyme activity of the 100 times diluted sample was 11.4 times higher compared to the undiluted extract (Fig. 4-21, Table. 4-9).

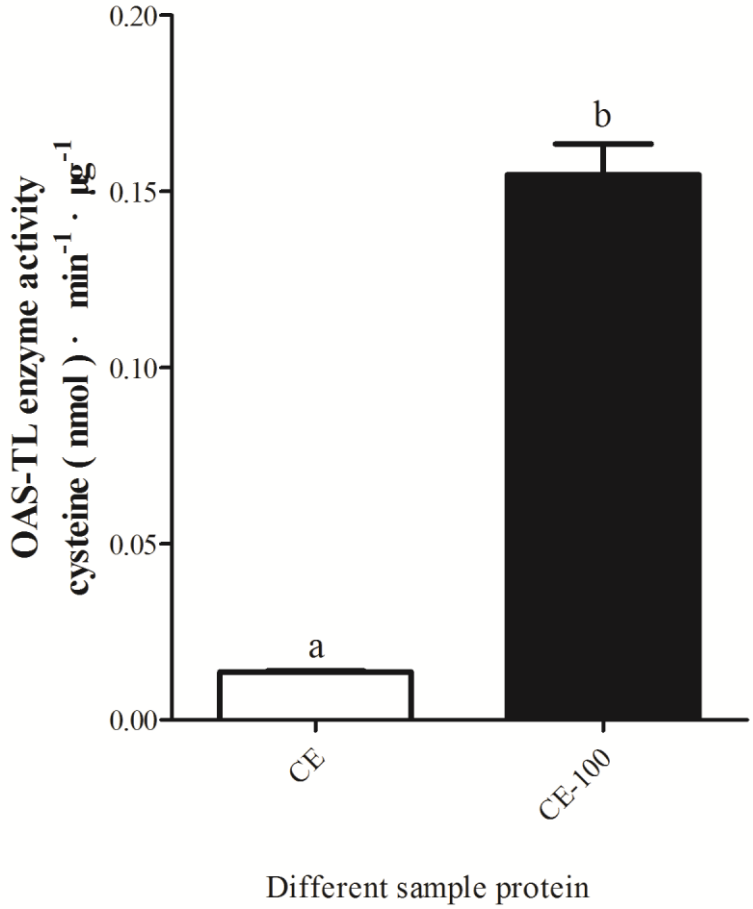

Fig. 4-21. OAS-TL activity per unit of protein in crude and diluted extracts of *Thalassiosira pseudonana.*

CE is the activity of the crude extract obtained according to the extraction protocol. CE-100 is the activity in the crude extract with a 100-fold dilution. Different letters show statistically different means ($P < 0.05$). The error bars show the standard deviations ($n = 3$).

In *Phaeodactylum tricornutum*, OAS-TL enzyme activity of the 100 times diluted extract was 3.3 times higher than the activity in the undiluted extract (Fig. 4-22, Table. 4-9).

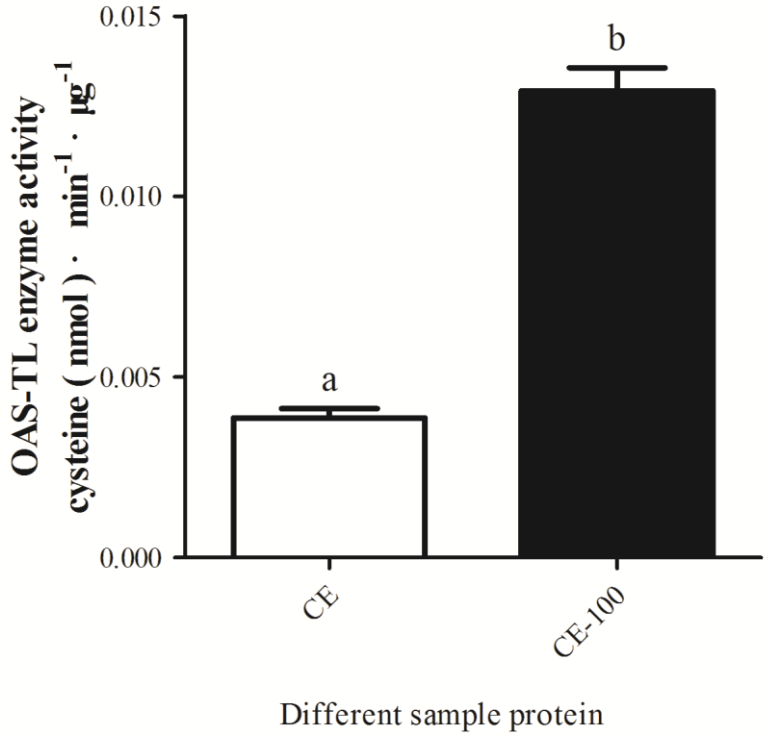

Fig. 4-22. OAS-TL activity per unit of protein in crude and diluted extracts of *Phaeodactylum tricornutum.*

CE is the activity of the crude extract obtained according to the extraction protocol. CE-100 is the activity in the crude extract with a 100-fold dilution. Different letters show statistically different means ($P < 0.05$). The error bars show the standard deviations ($n = 3$).

In *Amphidinium klebsii*, the OAS-TL activity of the 100 times diluted sample was 1.6 times higher than the activity in the undiluted extract (Fig. 4-23, Table. 4-9).

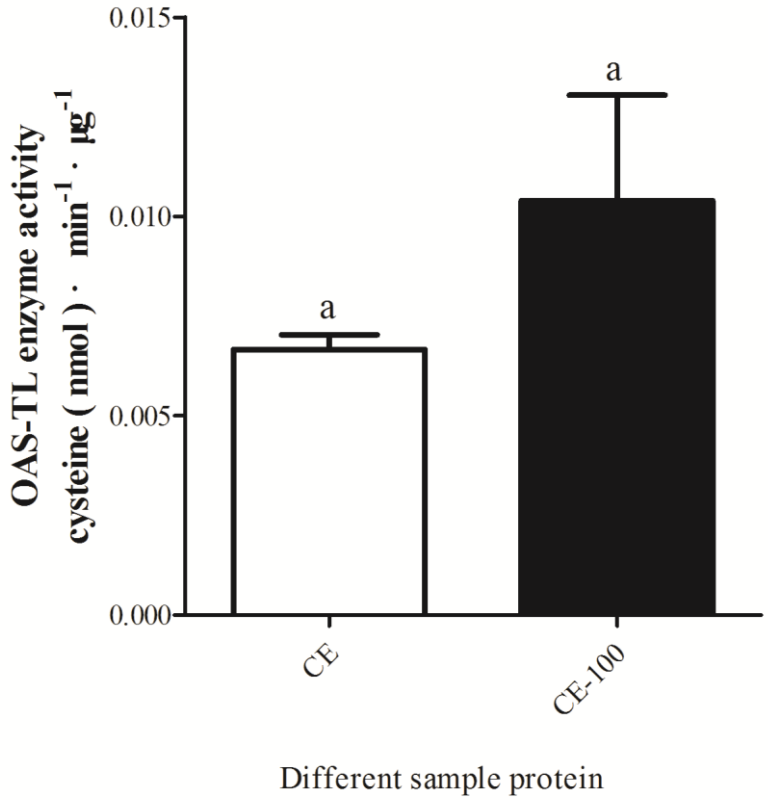

Fig. 4-23. OAS-TL activity per unit of protein in crudeand diluted extracts of *Amphidinium klebsii.*

CE is the activity of the crude extract obtained according to the extraction protocol. CE-100 is the activity in the crude extract with a 100-fold dilution. Different letters show statistically different means ($P < 0.05$). The error bars show the standard deviations ($n = 3$).

Table. 4-9. Summary of OAS-TL activity in 100-fold diluted and undiluted crude extracts.

Species name	OAS-TL enzyme activity (Mean ±SD) nmol cysteine · min^{-1} · ng^{-1}	
	CE	CE-100
Synechocystis sp. PCC 6803	15 (0.4)	5.0 (1.2)
Chlamydomonas reinhardtii TAP	5.3 (0.6)	3.6 (0.2)
Chlamydomonas reinhardtii TP	1.2 (0.0)	8.0 (0.7)
Dunaliella tertiolecta	6.0 (0.0)	7.0 (0.9)
Tetraselmis suecica	14.3 (0.3)	23.0 (2.8)
Thalassiosira pseudonana	13.6 (0.4)	155 (8.8)
Phaeodactylum triconutum	3.9 (0.3)	12.9 (0.6)
Amphidinium klebsii	6.7 (0.4)	10.4 (2.7)

CE: crude extract; CE-100: 100 fold diluted crude extract.The results are shown as mean ± SD (n=3).

4.2.3. OAS-TL specific activity in different microalgae

OAS-TL specific activity from the various experimental organisms was determined after purification (Fig. 4-24). The SDS-PAGEs (not shown) suggest that the purified fractions contained negligible amounts of contaminants proteins. The pure OAS-TL of the green freshwater species *Chlamydomonas reinhardtii* cultured in TP medium, and of the green marine species *Dunaliella tertiolecta* and *Tetraselmis suecica*, and especially of the marine diatom *Thalassiosira pseudonana* showed higher specific activities than the other species (Fig. 4-24). It is noteworthy that *C. reinhardtii* OAS-TL specific activity was strongly affected by the growth medium (Fig. 4-24).

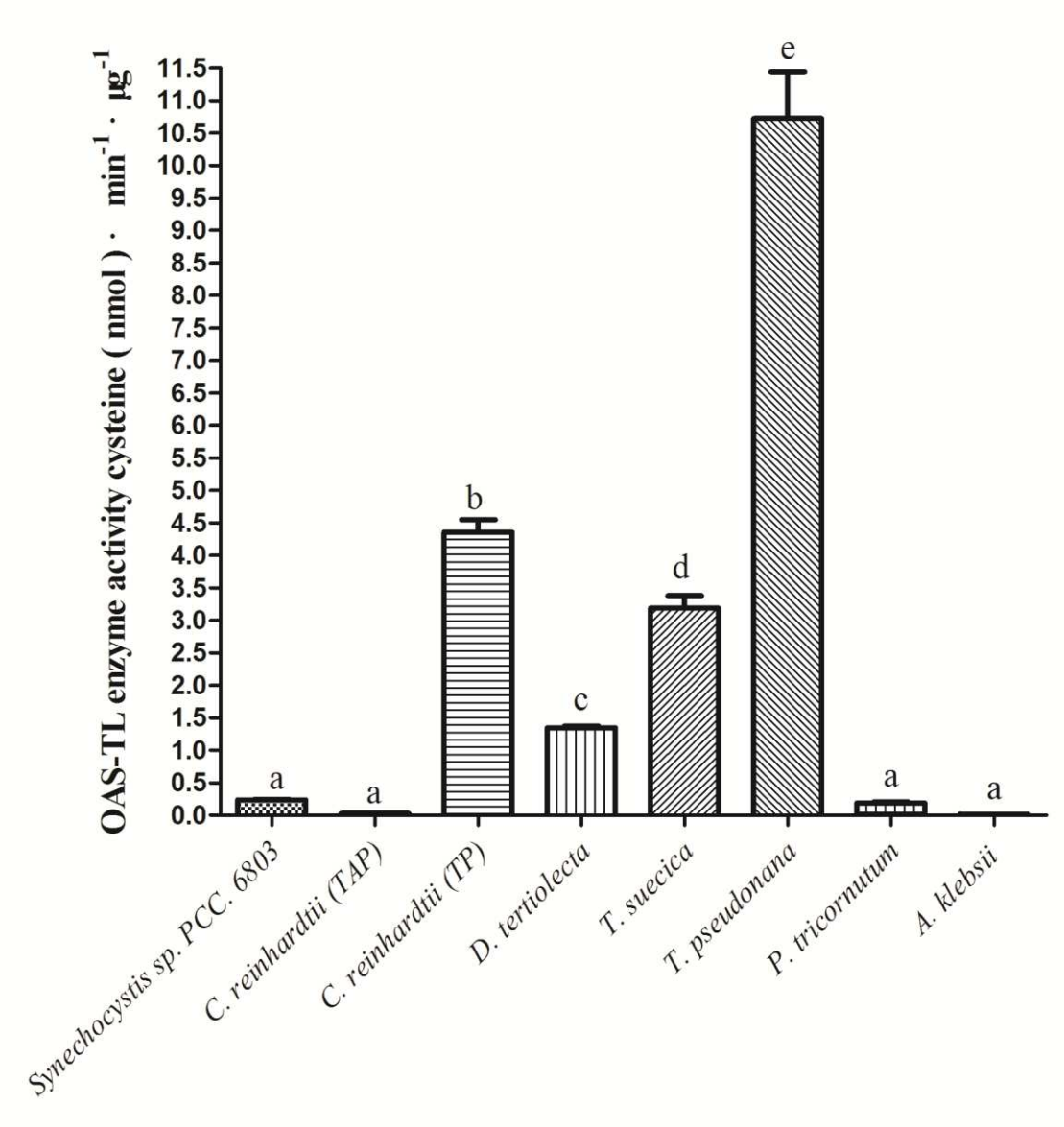

Fig. 4-24. OAS-TL enzyme activity.

Different letters show statistically different means ($P < 0.05$). The error bars show the standard deviations ($n = 3$).

4.2.4. Cysteine Synthase Complex (CSC)

For all species tested, when purified OAS-TL was mixed with *A. thaliana* SAT5 and subject to size exclusion chromatography, a complex of more than 600 kDa was eluted (Fig. 4-25).

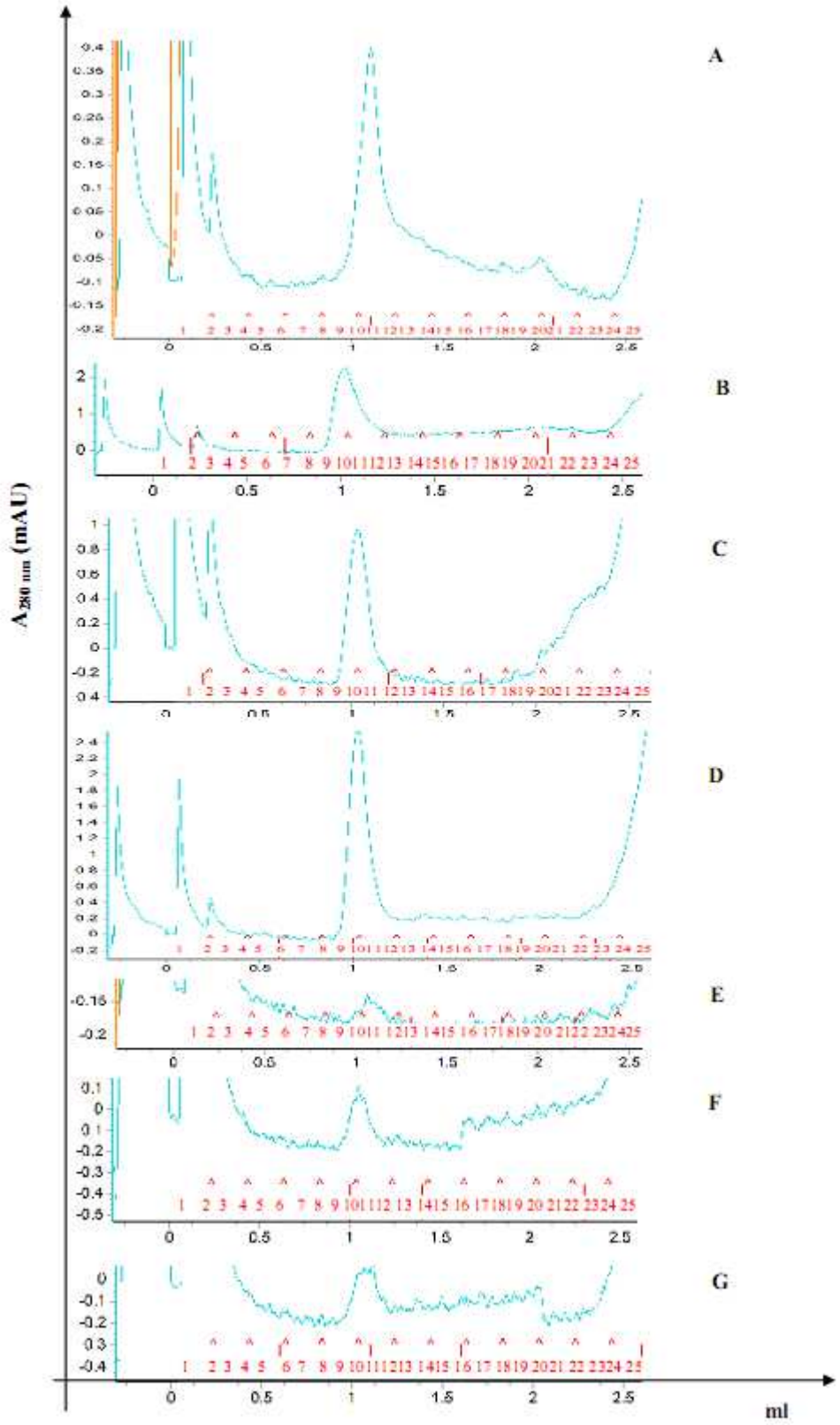

Fig. 4-25. FPLC chromatogram for OAS-TL from different algae complexed with SAT-5 from *A. thaliana*.

A: *Synechocystis* sp. PCC 6803; B: *Chlamydomonas reinhardtii*-TAP; C: *Dunaliella tertiolecta*; D: *Tetraselmis suecica*; E: *Thalassiosira pseudonana*; F: *Phaeodactylum*

tricornutum; G: *Amphidinium klebsii*. Red numbers represent fraction numbers in parallel with black numbers representing elution volume (ml).

In *Synechocystis*, fraction 12 (E-12) showed cross-reaction with OAS-TL antibody (Fig. 4-25 A, Fig. 4-26). The size of the protein band involved in the complex formation was 39 kDa as the size of bigger protein band found in the purification (Fig. 4-7). The same fraction also gave an immunological reaction with SAT-5 antibody (35 kDa), as shown in (Fig. 4-33 A, lane 5).

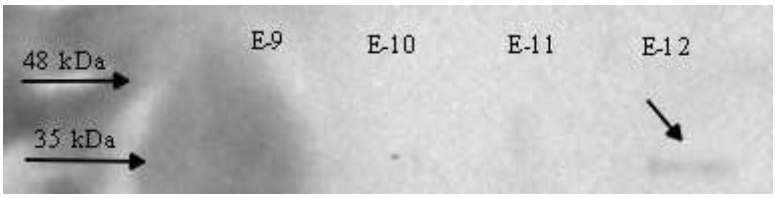

Fig. 4-26. Immunodetection of OAS-TL from *Synechocystis* sp. PCC 6803 after elution of the CSC with SAT-5 by FPLC.

E-9, E-10, E-11 and E-12 were different fractions of the FPLC separation.

The CSC of *C. reinhardtii* cultured in TAP medium was eluted in fractions E10 to E12 (Fig. 4-25 B). Both OAS-TL (Fig. 4-27) and SAT-5 immunoreactions (Fig. 4-33 B, lane 3) were present.

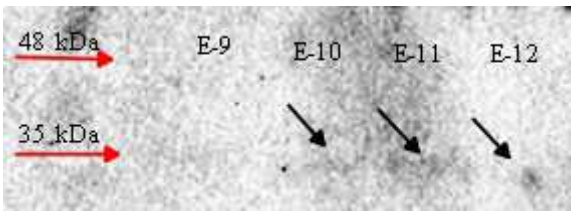

Fig. 4-27. Immunodetection of OAS-TL from *Chlamydomonas reinhardtii* in TAP medium after elution of the CSC with SAT-5 by FPLC.

E-9, E-10, E-11, E-12 were different fraction of the FPLC separation.

In *Dunaliella tertiolecta*, CSC was eluted in fractions E-10 to E-11 (Fig. 4-25 C), as confirmed by western blot analysis (Fig. 4-28 and 4-33 C). Two OAS-TL bands were present in the complex and

their sizes were consistent with the purified OAS-TL bands (Fig. 4-10).

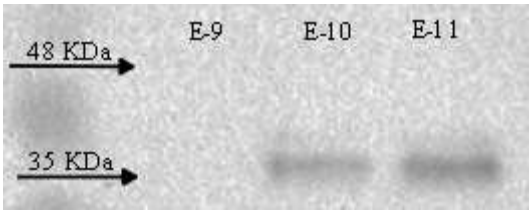

Fig. 4-28. Immunodetection of OAS-TL from *Dunaliella tertiolecta* after elution of the CSC with SAT-5 by FPLC.

E-9, E-10, E-11 were different fraction of the FPLC separation.

The CSC of *Tetraselmis suecica* was eluted in fractions E-9, 10, 11 (Fig. 4-31 D) as confirmed by the results of western blots with OAS-TL (Fig. 4-29) and SAT5 (Fig. 4-33 A, lanes 8 and 9). The OAS-TL of *T. suecica* CSC had a size of 41 kDa (Fig. 4-11), as the size of the strongest band in the western of the purified protein.

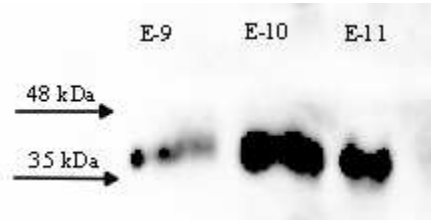

Fig. 4-29. Immunodetection of OAS-TL from *Tetraselmis suecice* after elution of the CSC with SAT-5 by FPLC.

E-9, E-10, E-11 were different fraction of the FPLC separation.

The CSC of the diatom *Thalassiosira pseudonana* was eluted in E-10, where also crossreaction with OAS-TL (Fig. 4-30) and SAT-5 (Fig. 4-33 C, lanes 5 and 6) antibodies was observed. The OAS-TL in the complex had a size of 36 kDa.

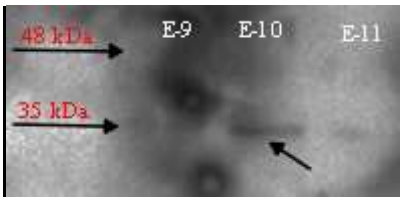

Fig. 4-30. Immunodetection of OAS-TL from *Thalassiosira pseudonana* after elution of the CSC with SAT-5 by FPLC.

E-9, E-10, E-11 were different fractions of the FPLC separation.

The CSC from *Phaeodactylum tricornutum* was eluted in fractions E-9 to E-11 (Fig. 4-25 F); the presence of the complex in these fractions was confirmed by the western blot analyses (Fig. 4-31, Fig. 4-33 C, lanes 2, 3 and 4). The OAS-TL signal in the complex corresponded to a protein of 36 kDa as shown also in the purified sample (Fig. 4-13).

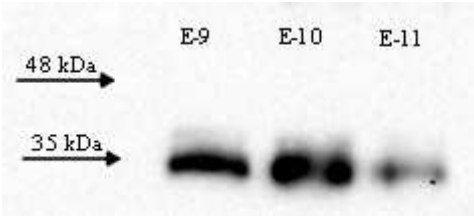

Fig. 4-31. Immunodetection of OAS-TL from *Phaeodactylum tricornutum* after elution of the CSC with SAT-5 by FPLC.

E-9, E-10, E-11 were different fractions of the FPLC separation.

In the dinoflagellate *Amphidinium klebsii*, the CSC appeared in fractions E-9 and E-10. In the same fractions, a band of 35 kDa cross reacted with OAS-TL antibody (Fig. 4-32) and a band cross reacting with SAT5 antibodies (Fig. 4-33 A, lanes 2, 3 and 4) was observed.

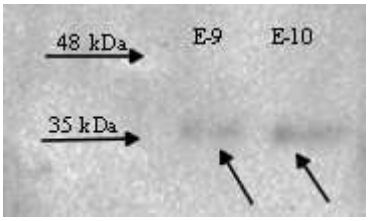

Fig. 4-32. Immunodetection of OAS-TL from *Amphidinium klebsii* after elution of the CSC with SAT-5 by FPLC.

E-9 and E-10 were different fractions of the FPLC separation.

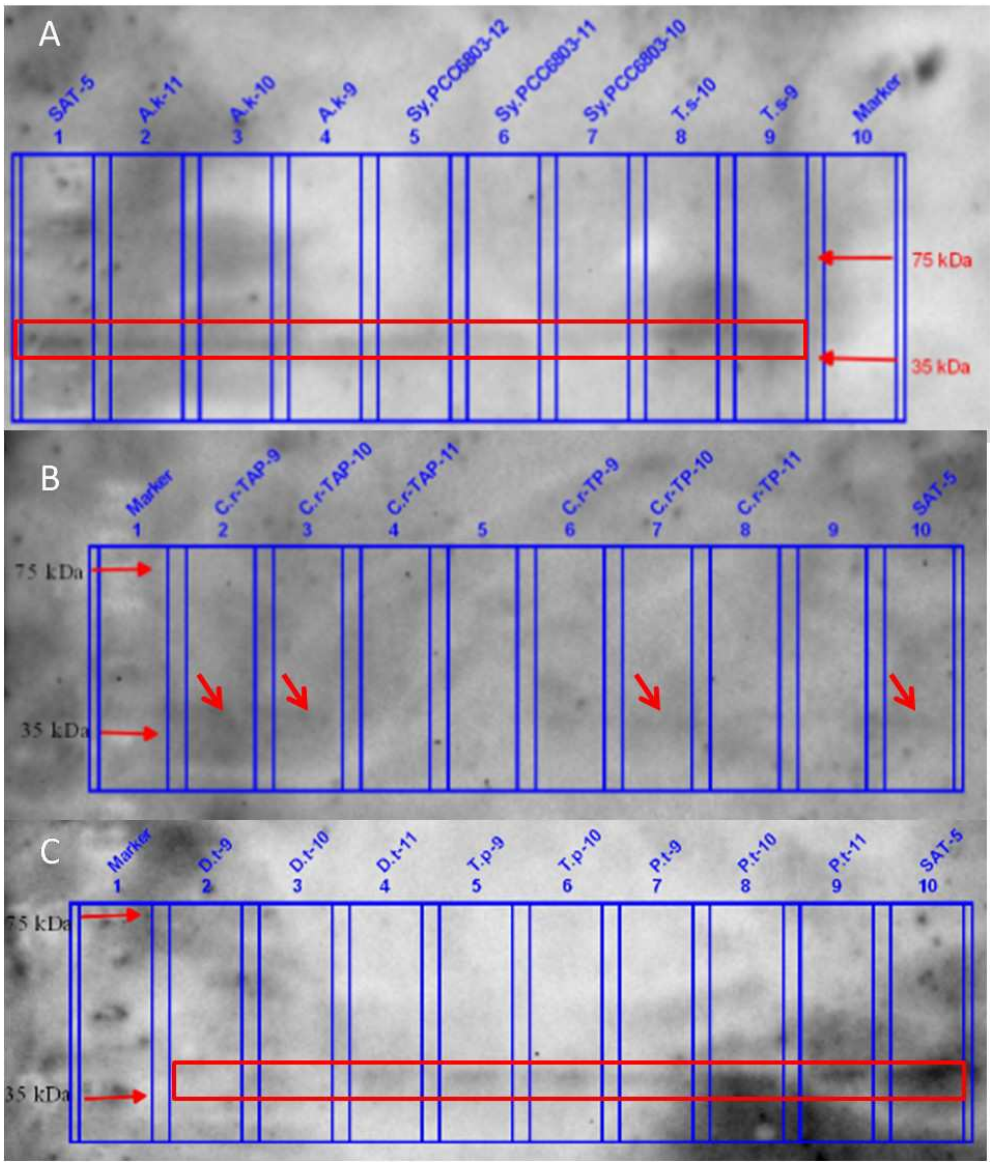

Fig. 4-33. Western blot using antibodies rose against SAT-5 from *A. thaliana.*

The samples corresponding to the peaks obtained by size exclusion chromatography for which a positive reaction with the antibody for OAS-TL was observed. Note: Marker, the protein ladder (10-180 kDa); A) from left to the right lane 1: SAT-5; lanes 2 to 4: *Amphidinium klebsii* (fractions 9-11); lanes 5 to 7: *Synechocystis sp*. PCC 6803 (fractions 10-12); lanes 8 to 9: *Tetraselmis suecica* (fractions 9-10); lane 10: Marker. B) From left to the right lane 1: Marker; lanes 2 to 4: TAP medium grown *Chlamydomonas reinhardtii* (fractions 9-11); lanes 6 to 8: TP medium grown *Chlamydomonas reinhardtii* (fractions 9-11); lane 10: SAT-5. C) From left to the right lane 1: Marker; lanes 2 to 4: *Dunaliella tertiolecta* (fractions 9-11); lanes 5 to 6: *Thalassiosira pseudonana* (fractions 9-11); lanes 7-9: *Phaeodactylum tricornutum* (fractions 9-11); lane 10: SAT-5. All the detected AtSAT-5 was showed in the red frame (A and C) and by red arrows (B).

4.3. In vivo redox regulation of ATP-S activity

Thalassiosira pseudonana, whose ATPS is believed to be redox regulated, was used for these experiments. DCMU interrupted electron transfer almost immediately at a concentration of 5 µM (data not shown). The quantum yield of PSII was determined as Fv/Fm and its response to 0, 5 and 10 µM DCMU was shown in Fig. 4-34. Already after 1 hour, DCMU at both 5 µM and 10 µM caused Fv/Fm to significantly decrease, as compared to the 0 DCMU controls ($P < 0.001$). This trend was accentuated after 3 and 6 hours. The concentration of 10 µM DCMU was chosen for the experiments.

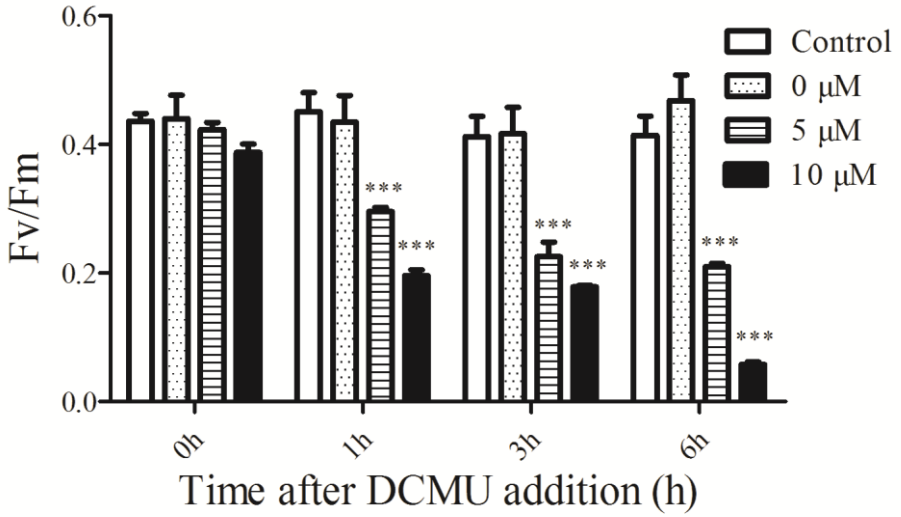

Fig. 4-34. Fv/Fm of *Thalassiosira pseudonana* incubated in the presence of 5 and 10 µM DCMU, for 0, 1, 3 and 6 hours.

The error bars represented the standard deviations (n = 3); asterisks indicated the significance of mean differences (* = $p < 0.05$; ** = $p < 0.01$; *** = $p < 0.001$).

DCMU (10 µM) had no impact on cell number and cell volume, in the course of the experiments. In the presence of 10 µM, no significant difference in cell number and cell volume was observed (Fig. 4-35 and Fig. 4-36, respectively).

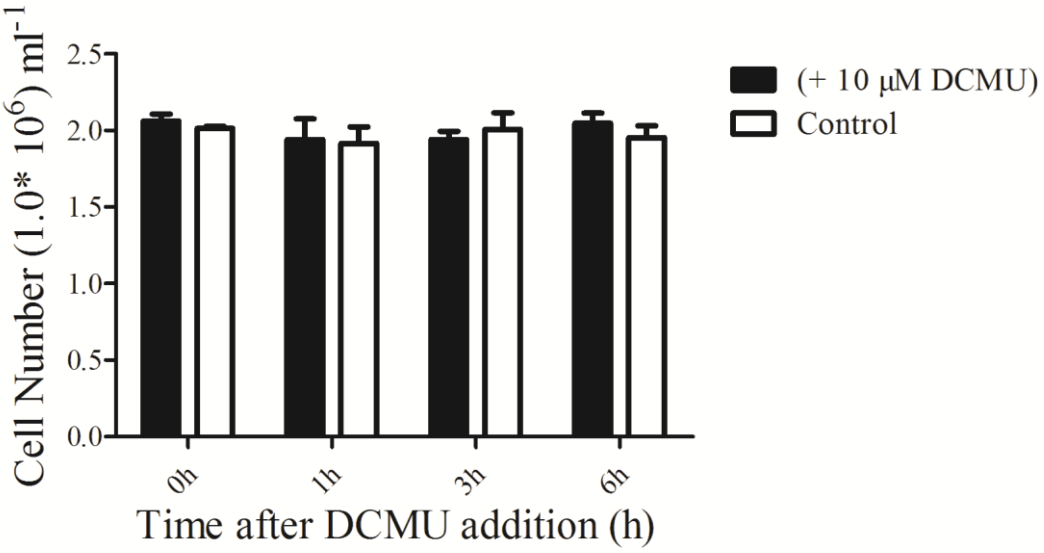

Fig. 4-35. *Thalassiosira pseudonana* cell number during incubation with 10 µM DCMU.

The error bars represented the standard deviations (n = 3). Means were not significantly different.

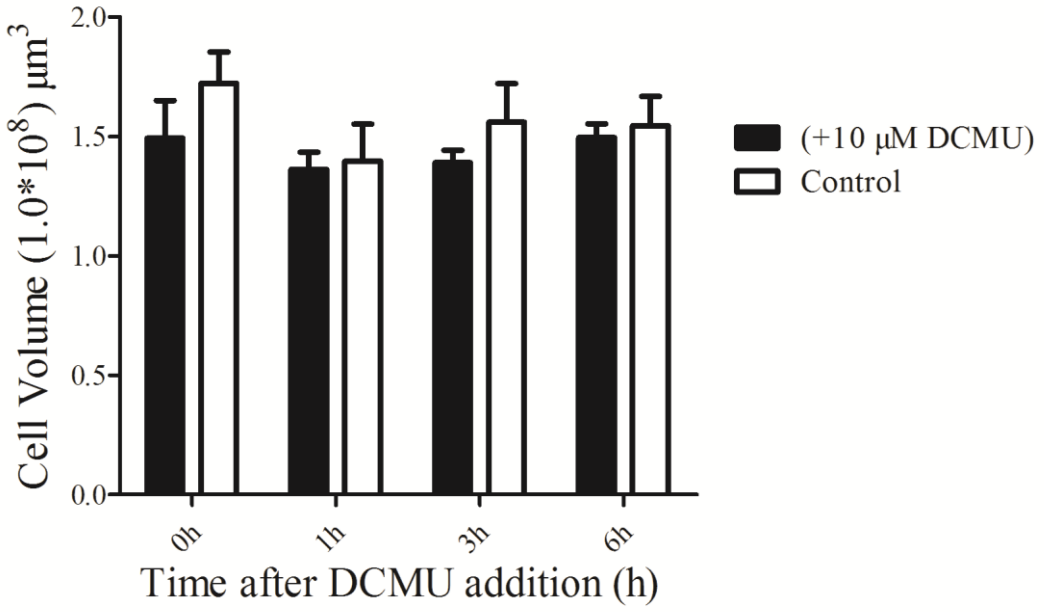

Fig. 4-36. *Thalassiosira pseudonana* cell volume during incubation with 10 µM DCMU.

The error bars represented the standard deviations (n = 3). Means were not significantly different.

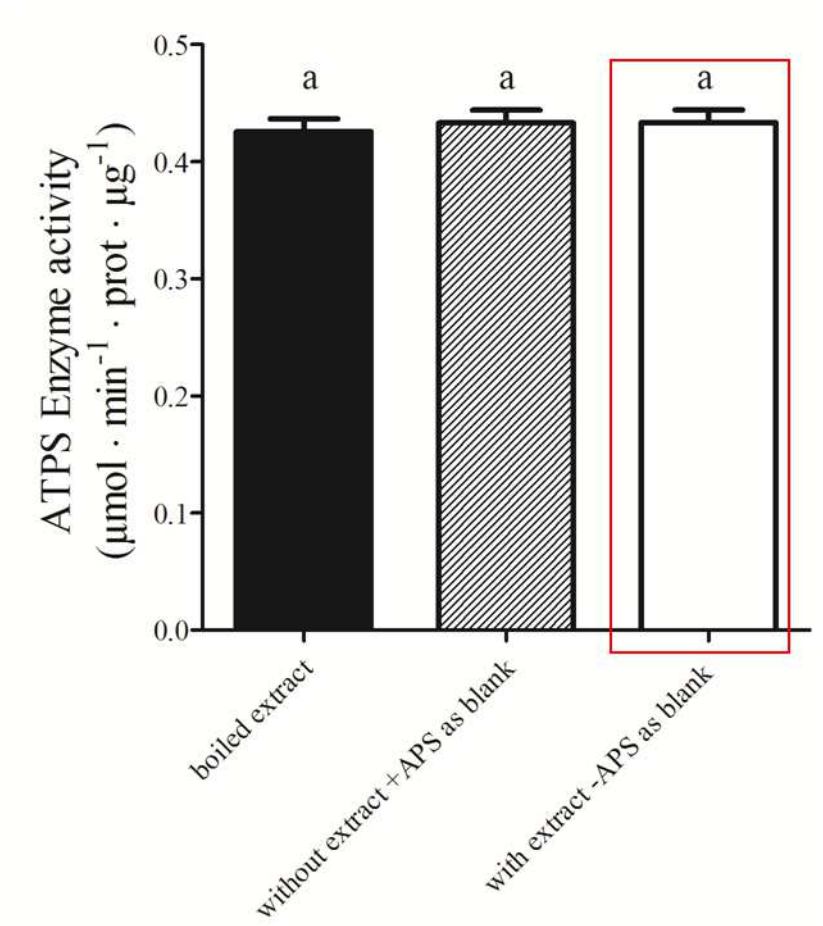

Fig. 4-37. Comparison of ATPS assay blanks obtained with different procedures. The error bars show the standard deviations (n = 3).

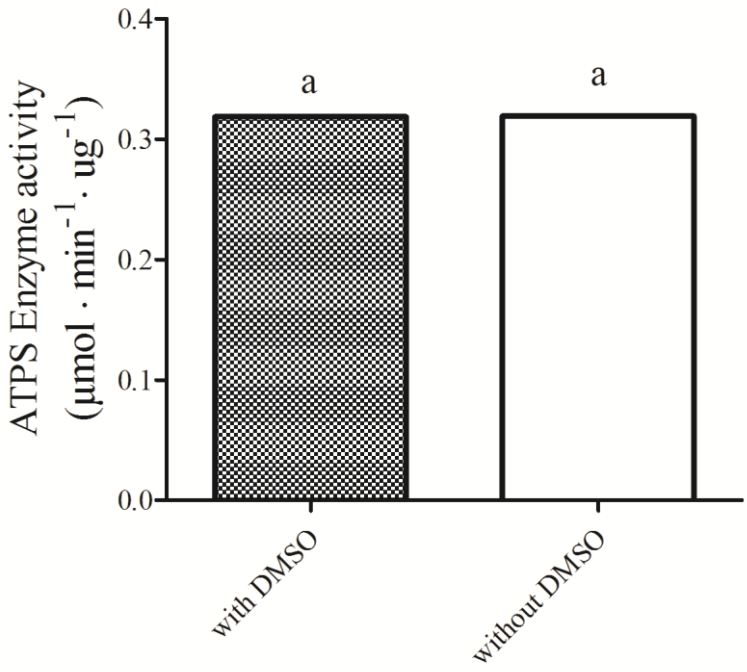

Fig. 4-38. Comparison of ATPS activity in the presence and absence of DMSO.

The error bars show the standard deviations (n = 3).

The ATP sulfurylase (ATP-S) enzyme activity was not affected by the incubation of the algae in the presence of DCMU (Fig. 4-39). Even though the activity changed over time, there was no statistically significant difference between the DCMU treated samples and the control samples.

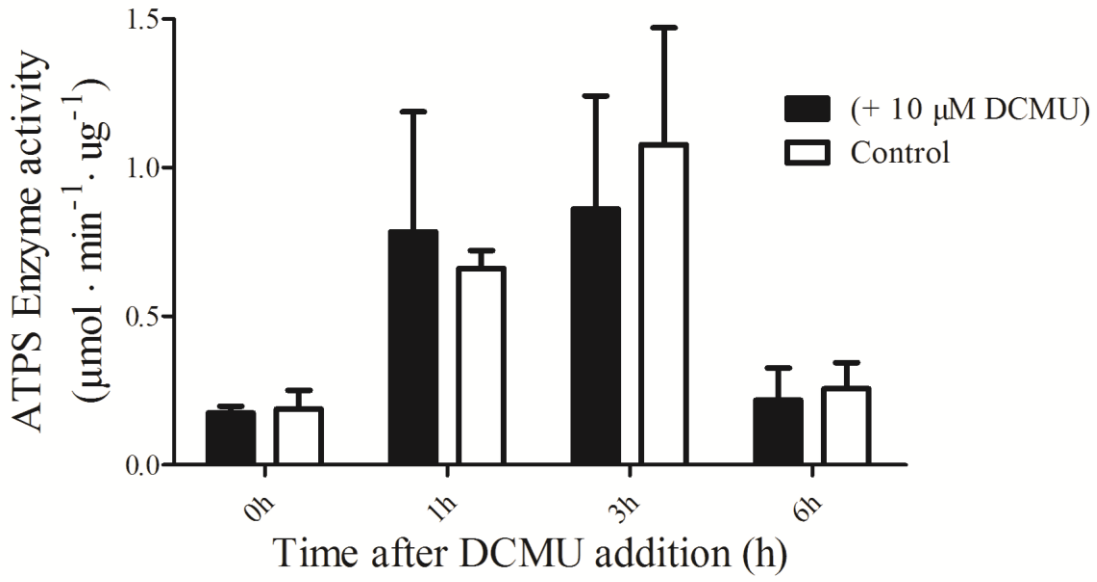

Fig. 4-39. *Thalassiosira pseudonana* ATP-S activity in the presence orabsence of 10 µM DCMU over a period of 6 hours.The error bars show the standard deviations (n = 3).

5. Discussion

5.1. SAT and OAS-TL in algae

The SAT protein tree indicates that phylogenetic difference exists between the protein in green algae and vascular plants and sequences obtained from species of the red-lineages (with rare exceptions). Interestingly, cyanobacterial SAT appears to be more closely related to that of red algae. It is hard to interpret this observation. It may simply due to the fact that extant cyanobacteria have acquired their current S assimilation complement secondarily, together with red lineage algae. The similarity between cyanobacteria and red lineage algae SATs also brings to mind the fact that cyanobacteria retained their prominence in post-Mesozoic oceans, together with red lineage algae, whereas green algae declined to a great extent. SAT phylogeny may thus be connected with the Sulfate Assimilation Hypothesis (Ratti et al., 2011), which suggests that sulfate availability in global oceans may have affected algae radiation. How SAT would affect phytoplankton radiation however, cannot be resolved with the data at hand and requires further investigations. The role of SAT in cysteine synthesis may speculatively suggest that a different control/regulation of cysteine synthesis may have repercussions on thiol metabolism and redox power management in the cell (Dickinson & Forman, 2002; Dietz & Hell, 2015).

It is also noteworthy that the C-terminus of algal SATs is rather similar to that of embryophytes with *Arabidopsis* sequence (Fig. 4-4). Thus the C-portion of algae SAT probably has a similar organization to that of *Arabidopsis* (Wirtz et al., 2001), *E.coli* (Pye et al., 2004) and *Haemophilus influenza Rd* (Gorman & Shapiro, 2004), whose SAT monomers contain a carboxyl-terminal left-handed β–helix (Gorman & Shapiro, 2004; Pye et al., 2004). The sequences alignments indicate that the C-terminal region of SATs is highly conserved in algae and other organisms and, based on the work

done on *E. coli* by Pye et al. (2004), it is likely to be responsible for the hetero-oligomerization with OAS-TL. The C-terminal domain is also where the catalytic site is located (Bogdanova & Hell, 1997). The idea of a bifunctional C-terminal SAT domain (involved in catalysis and oligomerization) was further strengthened by the modelling of the C-terminus of plant SAT using bacterial acyltransferase structures as template (Vuorio et al., 1991; Vaara, 1992): the C-terminus of SAT encompasses two sections, a left-handed parallel β- helix (LβH) domain, which carries the catalytically active site, and a C-terminal tail that could not be modelled due to low homology to the acyltransferases (Wirtz et al., 2001). Given the fact that the C-terminus domain aminoacid sequence of algae is very similar to that of empryophytes, it may operate as in embryophytes.

The SAT–SAT interaction domain is instead located at the N-terminal α-helical domain (Bogdanova & Hell, 1997). Here, homology between algae and vascular plants sequences are smaller and this may indicate possible differences in the size of the Cysteine Synthase Complex in algae and plants (see Fig. 5-1).

One thing seems to differentiate red lineage algae from green algae and their descendants: the number of cysteine residues, which are more numerous in the red lineage (especially in haptophyte). In ATPS, the number of cysteines was found to be related to redox regulation (Prioretti et al., 2016). At this stage, my data do not allow to verify if redox regulation exists in SAT and whether such regulation exists only in the SATs with more cysteine residues. In embryophytes, SAT does not appear to be redox-regulated; this is, of course, no proof that this is also the case in algae, as the work on ATPS demonstrates (Prioretti et al., 2014).

OAS-TL bioinformatic data showed a rather unclear phylogeny, possibly representing a higher variety of isoforms and a higher degree of gene exchanges, as compared to SAT. Overall the OAS-TL of algae showed a highly conserved C-terminal region. The OAS-TL protein size of algae is in the range 35-44 kDa, not too different from the enzymes of embryohytes (Table. 4-8; in *A. thaliana* OAS-TL has a mass of 33-37 kDa). The immunoreactions suggest that different sizes may be present in green algae,

although further analyses are required to confirm this. Interestingly, OAS-TL activity (as sulfide production) is higher when the enzyme is assayed in diluted crude extracts. This, in the literature (Bogdanova & Hell, 1997; Wirtz et al., 2001) is interpreted as an indication that the enzyme operates when not complexed. This is certainly a very indirect evidence, but support the idea that OAS-TL is regulated in plants as in embryophytes (Takahashi et al., 2011).

5.2. Cysteine Synthase Complex in algae

The main objective of my thesis was to verify whether algae form Cysteine Synthase Complexes, like vascular plants (Saito et al., 1995; Droux et al., 1998; Wirtz et al., 2001, 2010) and bacteria (Kredich & Tomkins, 1966). As reported above, the features of algae OAS-TL and SAT are suggestive that these proteins have structures similarity with the corresponding embryophyte proteins that make them capable of interacting in a Cysteine Synthase Complex. Both algae SAT and OAS-TL appeared to be located in both the chloroplast and mitochondrion. Other isoforms are possibly located in the cytosol. The algal distribution of the enzyme is thus similar to that of embryohpytes, in general terms. In embryophyte, mitochondria seems the main location of OAS production, whereas cysteine is mostly produced in the cytosol (Takahashi et al., 2011). In the chloroplast, cysteine synthesis is limited by the low OAS availability and the role of this organelle in sulfur metabolism is mostly that of producing sulfide. A similar situation is thought to occur in algae.

I observed that the OAS-TL of the green algae *Chlamydomonas reinhardtii*, *Dunaliella tertiolecta* and *Tetraselmis suecica* bound to the AtSAT5 affinity column much more strongly than the OAS-TL from the diatoms *Thalassiosira pseudonana* and *Phaeodactylum tricornutum* and from the dinoflagellate *Amphidinum klebsii*. If with some degree of approximation, I consider the elution time of OAS-TL from AtSAT5 affinity column as an indication of the strength of the interaction of the proteins in the complex, this may be an indication of a lower propension of algae of

the red lineage to form CSC complex. In embryophytes, OAS-TL only catalyzes cysteine production when it is free, whereas the complex is conducive to the synthesis of OAS. Therefore, the presumed lower tendency of red-lineage OAS-TL to bind SAT may reflect the higher tendency of red lineage algae to allocate C to cysteine, as compared to green algae. This may be linked to the appreciably higher DMSP concentration in red lineage algae than in green algae (Giordano et, al., 2008), which requires a higher flux of S through cysteine and then methionine (Giordano & Prioretti, 2016). If this will be confirmed by *ad hoc* measurements, it would provide further mechanistic support to the Sulfur Facilitation Hypothesis (Ratti et al., 2011): the different organization of red algae CSC may funnel more S into DMSP. This would lead to the higher S quotas of these cells and may consequently lead to the competitive advantage afforded by the anti-grazing power of the DMSP cleavage products (Norici et al., 2005).

In *A. thaliana*, *E. coli* and *S. typhimurium*, the Cystein Synthase Complex is composed of a hexamer of SAT and two dimers of OAS-TL (Wirtz et al., 2004). My experiments results, which were consisted with the reported data (Salbitani et al., 2014) provide proof-of-concept for the biochemical analysis of the cysteine synthase complex in different microalgal species. Subsequently, my experiments in size exclusion chromatography seem to suggest that the algal complexes (although with *A. thaliana* SAT) are always larger than the mass of 320 kDa reported by Wirtz et al, (2004) for the embryophytes complex. More recently, it has been suggested that each hexamer of SAT may bind up to six dimers of OAS-TL, one for each C-terminal domain of the protein (Pye et al., 2004). Based on the estimated mass of the eluted native complex, I propose that the stoichiometry of the algae Cysteine Synthase Complex is different from that in embryophytes: the algal CSC may be made of two SAT trimer connected 'head to head' form one hexamer, with one OAS-TL dimer bound to each SAT C-terminus (Fig. 5-1 A); this gives a total mass of about 600 kDa, compatible with the size of the complex eluted from the size exclusion column. Alternatively, given that the sequence difference at the N-terminus would lead to

believe that differences between algae and plant CSC are more likely to reside in the SAT-SAT interactions, I proposed a 6 SAT (2 SAT trimers): 12 OAS-TL (6 OAS-TL dimers) stoichiometry.

In *E. coli* and possibly in *Arabidopsis*, the Cysteine Synthase Complex appears to be composed of a SAT homohexamer and two OAS-TL dimmers (Fig. 5-1 Panel B). The SAT hexamer is constituted by two trimers arranged head-to-head with the C-terminal tails of each trimer at opposite ends of the hexamer (Kumaran et al., 2009). The interaction between SAT and OAS-TL occurs through portions of SAT C-terminus, with allegedly a crucial involvement of a hexapeptide with the sequence (I/V/L)-G-XXXX-(I/V/L) (Bogdanova & Hell., 1997; Wirtz et al., 2001). This general hexapeptide is present also in algae (Fig. 4-4). On the OAS-TL side, binding with SAT takes place through a KPGPHK sequence at the C-terminus. In algae the first and last two amino acids of this sequence are often substituted (Table. 4-7). As most proteins consist of multiple domains, and domains determine the function and evolutionary relationships of proteins, it is important to understand the principles of domain combinations and interactions (Vogel et al., 2004).

The purification of the algal CSC showed that the complex was much larger in algae than in plants (Fig. 4-25), with an approximate mass of 600 kDa (Fig. 4-26 to Fig. 4-32). On the basis of the information provided by Birke et al., 2015 and Yi et al., 2013, on the size difference between algal and *Arabidopsis* CSC complex, and on the variations in both SAT and of OAS-TL sequences involved in the interaction between these two proteins in algae, I propose that the algal CSC contains two SAT trimers, as in vascular plant, but each SAT protein binds one OAS-TL dimer through its C-terminus. The proposed structure of the algal CSC is shown in Fig. 5-1 Panel A.

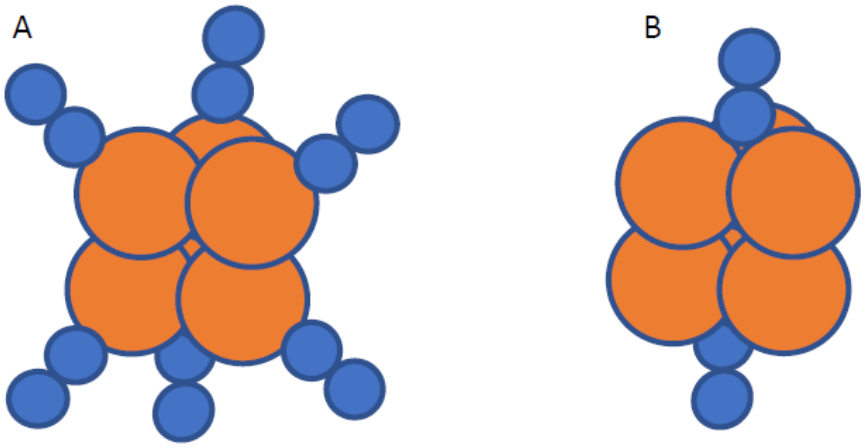

Fig. 5-1. Proposed structure of Algae Cysteine Synthase Complex.

Panel A shows the proposed structural organization of the

Cysteine Synthase Complex of algae (A) in comparison to that of vascular plants (B).

5.3. ATP-S redox regulation

The regulatory process that I envisage for the redox-regulated ATP-S assumed that the perception of the redox state of the cell was mediated by the plastoquinone pool of the photosynthetic electron transfer chain. This hypothesis was based on the fact that other redox-regulated processes involving early stages in nutrient assimilation pathway adopt this mode of regulation. For instance, *Chlamydomonas reinhardtii* nitrate reductase expression and activity are controlled by the redox state of the plastoquinone pool (Giordano et al., 2007). I, therefore, attempted to verify whether blocking plastoquinone reduction by using Dichloromethyl Urea (DCMU) I could modulate ATP-S activity.

The results of my experiments did not show any impact of plastoquinone oxidation on ATP-S activity. The interpretation of these results is difficult. Unfortinately, the limited time at my disposal made it impossible to go deeper in the matter. It is possible that the redox state of the plastoquinone pool only operates in the activation

direction, but not in the deactivation direction. In the case of nitrate reductase, it was observed that the expression of nitrate reductase gene could be effectively blockade blocked by the oxidation of the plastoquinone pool, but the opposite result was not obtained by the over reduction of the pool. It may also be that, as for instance in the case of some diatom carbonic anhydrase (Kikutani et al., 2012), redox regulation is exerted through thioredoxin, thus using the electrons most likely donated from ferredoxin. Unfortunately, I must leave this question open for future studies.

6. References

Álvarez, C., Calo, L., Romero, L. C., García, I., & Cecilia, G. (2010). An O-Acetylserine(thiol)lyase Homolog with L-Cysteine Desulfhydrase Activity Regulates Cysteine Homeostasis in *Arabidopsis*. *Plant physiology, 152,* 656–669. https://doi.org/10.1104/pp.109.147975.

Álvarez, C., García, I., Moreno, I., Pérez-pérez, M. E., Crespo, J. L., Romero, L. C., & Gotor, C. (2012). Cysteine-Generated Sulfide in the Cytosol Negatively Regulates Autophagy and Modulates the Transcriptional Profile in *Arabidopsis*. *The Plant Cell,* 1–15. https://doi.org/10.1105/tpc.112.105403.

Altschul, S. F., Madden, T. L., Schäffer, A. A., Zhang, Jinghui., Zhang, Zheng., Miller, Webb., & Lipman, D. J. (1997). Gapped BLAST and PSI-BLAST: a new generation of protein database search programs *Nucleic Acids Research, 25 (17)*, 3389-3402. https://doi.org/10.1093/nar/25.17.3389.

Altschul, S. F., Gish, W., Miller, W., Myers, E. W., & Lipman, D. J. (1990). Basic Local Alignment Search Tool. *Journal of Molecular Biology, 215 (3)*, 403-410.

Andreae, M.O. (1986) The Ocean as a Source of Atmospheric Sulfur Compounds. In: Buat-Ménard P. (eds.), The Role of Air-Sea Exchange in Geochemical Cycling. NATO ASI Series (*Series C: Mathematical and Physical Sciences*), vol 185. Springer, Dordrecht, p: 331-362. https://doi.org/10.1007/978-94-009-4738-2_14.

Andreae, Meinrat O. (1990). Ocean-atmosphere interactions in the global biogeochemical sulfur cycle *. *Marine Chemistry*, *30*, 1–29.

Armbrust, E. V., Berges, J. A., Bowler, C., Green, B. R., Martinez, D., Putnam, N. H., … & Rokhsar, D. S. (2004). The Genome of the Diatom *Thalassiosira pseudonona*: Ecology, Evolution, and Metabolsim. *Science (New York, N.Y.)*, *306* (October), 79–85.

Becker, A., Kredich, N. M., & Tomkins, G. M. (1968). The Purification and Characterization of O-Acetylserine from *Salmonella typhimurium* *. *Journal of biological chemistry 244 (9)*, 2418-2427.

Birke, H., Hildebrandt, T. M., Wirtz, M., & Hell, R. (2015). Sulfide detoxification in plant mitochondria. *Methods in Enzymology*, *555*, 271–286. https://doi.org/10.1016/bs.mie.2014.11.027.

Bogdanova, N., & Hell, R. (1997). Cysteine synthesis in plants : protein-protein interactions of serine acetyltransferase from *Arabidopsis thaliana*. *The Plant Journal, 11 (2)*, 251–262.

Bonner, E. R., Cahoon, R. E., Knapke, S. M., & Jez, J. M. (2005). Molecular basis of

cysteine biosynthesis in plants: Structural and functional analysis of O-acetylserine sulfhydrylase from *Arabidopsis thaliana*. *Journal of Biological Chemistry*, *280 (46)*, 38803–38813. https://doi.org/10.1074/jbc.M505313200.

Borowitzka, M. A. (2016) Systematics, taxonomy and species names: do they matter? In: Borowitzka, M. A., Beardall, J., Raven, J. A. (eds.), The physiology of microalgae. *Springer, Dordrecht,* p: 655–681. https://doi.org/10.1007/978-3-319-24945-2.

Bromke, M. A., Hoefgen, R. (2013). Phylogenetic aspects of the sulfate assimilation genes from *Thalassiosira pseudonana*. *Amino Acids* 44:1253–1265. https://doi.org/10.1007/s00726-013-1462-8.

Burnell, J. N. (1984). Sulfate assimilation in C4. plants. *Plant Physiology* 75, 873–875. https://doi.org/10.1104/pp.75.3.873.

Calo, L., Romero, L. C., & Garcı, I. (2010). An O-Acetylserine (thiol) lyase Homolog with L-Cysteine Desulfhydrase Activity Regulates Cysteine Homeostasis. *Plant Physiology*, *152* (February), 656–669. https://doi.org/10.1104/pp.109.147975.

Campanini, B., Speroni, F., Salsi, E., Cook, P.F., Roderick, S.L., Huang, B., Bettati, S., & Mozzarelli, A. (2005). Interaction of serine acetyl-transferase with O-acetylserine sulfhydrylase active site: evidence from fluorescence spectroscopy. *Protein Science. 14*, 2115-2124.

Canfield, D. E., Thamdrup, B., & Fleischer, S. (1998). Isotope fractionation and sulfur metabolism by pure and enrichment cultures of elemental sulfur-disproportionating bacteria. *Limnology and Oceanography, 43 (2),* 253-264.

Canfield, D. E. (2004). THE EVOLUTION OF THE EARTH SURFACE SULFUR RESERVOIR. *American Journal of Science*, *304* (December), 839–861.

Cabello-yeves, Pedro. J., Haro-moreno, Jose. M., & Coleman, Maureen. (2017). Novel *Synechococcus* Genomes Reconstructed from Freshwater Reservoirs. *Frontiers in Microbiology, 8,* 1-13. https://doi.org/10.3389/fmicb.2017.01151.

Chronis, D., & Krishnan, Æ. H. B. (2004). Sulfur assimilation in soybean (*Glycine max* [L.] Merr .): molecular cloning and characterization of a cytosolic isoform of serine acetyltransferase. *Palnta*, 417–426. https://doi.org/10.1007/s00425-003-1123-3.

Daboussi, F., Leduc, S., Maréchal, A., Dubois, G., Guyot, V., Perez-Michaut, C., … & Duchateau, P. (2014). Genome engineering empowers the diatom *Phaeodactylum tricornutum* for biotechnology. *Nature Communications*, *5* (May), 1–7. https://doi.org/10.1038/ncomms4831.

Dacey, J. W. H., King, G. M., & Wakeham, S. G. (1987). Factors controlling emission of dimethylsulphide from salt marshes. *Nature 330,* 643–645. https://doi.org/10.1038/330643a0.

Dahl, C., Hell, R., Leustek, T., & Knaff, D. (2008). Sulfur Metabolism in

Phototrophic Organisms. In: Rüdiger Hell, Christiane Dahl, Thomas Leustek. (eds.), *Sulfur Metabolism in Phototrophic Organisms*, p: 1–14. https://doi.org/10.1007/978-1-4020-6863-8_1.

de Souza, M. P. & Yoch, D. C. (1995a). Comparative physiol- ogy of dimethyl sulphide production by dimethylsulfoniopropionate lyase in *Pseudomonas doudoroffii* and *Alcaligenes* sp. strain M3A. *Appl Environ Microbiol 61 (11)*: 3986–3991.

de Souza, M. P. & Yoch, D. C. (1995b). Purification and characterization of dimethylsulfoniopropionate lyase from an Alcaligenes-like dimethyl sulphide-producing marine isolate. *Appl Environ Microbiol 61 (1)*, 21–26.

Dickinson, D. A., & Forman, H. J. (2002). Cellular glutathione and thiols metabolism. *Biochemical and Pharmacology*, *64 (2002)*, 1019-1026.

Dietz, K. (2015). Thiol switches in redox regulation of chloroplasts : balancing redox state , metabolism and oxidative stress. *The Journal of Biological Chemistry*,*396* (5), 483–494. https://doi.org/10.1515/hsz-2014-0281.

Droux, M., Ruffet, M. L., Douce, R., & Job, D. (1998). Interactions between serine acetyltransferase and O-acetylserine (thiol) lyase in higher plants-structural and kinetic properties of the free and bound enzymes. *European Journal of Biochemistry / FEBS*, *255 (1)*, 235–45. https://doi.org/10.1046/j.1432-1327.1998.2550235.x.

Droux, Michel. (2004). Sulfur assimilation and the role of sulfur in plant metabolism: A survey. *Photosynthesis Research, 79 (3)*, 331-348, https://doi.org/10.1023/B:PRES.0000017196.95499.11.

Emanuelsson, O., Brunak, S., von Heijne, G., & Nielsen, H. (2007). Locating proteins in the cell using TargetP, SignalP and related tools. *Nature Protocols*, *2 (4)*, 953–971. https://doi.org/10.1038/nprot.2007.131.

Fabregas, J., Herrero, C., Cabezas, B., & Abalde, J. (1986). Biomass production and biochemical composition in mass cultures of the marine microalga *Isochrysis galbana* Parke at varying nutrient concentrations. *Aquaculture*, *53 (2)*, 101–113. https://doi.org/10.1016/0044-8486(86)90280-2.

Fanesi, A., Raven, J. A., & Giordano, M. (2014). Growth rate affects the responses of the green alga Tetraselmis suecica to external perturbations. *Plant, Cell and Environment*, *37 (2)*, 512–519. https://doi.org/10.1111/pce.12176.

Felix Autenrieth., Barry Isralewitz., Zaida Luthey-Schulten., Anurag Sethi., Taras Pogorelov. (2005). Bioinformatics and Sequence Alignment. June 2005.

Fron, B. R. E., Alloran, E. L. H., & Olmes, S. U. H. (1996). Bootstrap confidence levels for phylogenetic trees. *Proc. Natl. Acad. Sci. USA*, *93 (14)*, 7085–7090.

Gaitonde, M. K. (1967). A spectrophotometric method for the direct determination of cysteine in the presence of other naturally occurring amino acids. *The Biochemical Journal*, *104 (2)*, 627–633.

Garfin, D. E. (1990). One-Dimensional Gel Electrophoresis. *Methods in Enzymology*, *182 (9)*, 497–513. https://doi.org/10.1016/S0076-6879(09)63029-9.

Gibbs, N., Duffus, C. M., (1976). Natural Protoplast *Dunaliella* as a source of protein. *Applied and environment microbiology*, *31 (4)*, 602–604.

Giordano, M., Pezzoni, V., Hell, R. (2000). Strategies for the allocation of resources under sulfur limitation in the green algae *Dunaliella salina*. *Plant Physiology 124*, 857–864.

Giordano, M., Norici, A., & Hell, R. (2005). Sulfur and phytoplankton : acquisition , metabolism and impact on the environment. *New Phytologist*, *166:* 371–382. https://doi : 10.1111/j.1469-8137.2005.01335.x.

Giordano, M., Chen, Yi-bu., Koblizek, M., Falkowski, P. (2005). Regulation of nitrate reductase in *Chlamydomonas reinhardtii* by the redox state of the plastoquinone pool Regulation of nitrate reductase in *Chlamydomonas reinhardtii* by the redox state of the plastoquinone pool. *European Journal of Phycology, 0262 (40)*, 345-352. https://doi.org/10.1080/09670260500334263.

Giordano, M., Norici, A., Ratti, S., & Raven, J. A. (2008). Role of Sulfur for Algae: Acquisition, Metabolism, Ecology and Evolution. In: Rüdiger Hell, Christiane Dahl, Thomas Leustek. (eds.), *Sulfur Metabolism in Phototrophic Organisms*, p: 397–415. https://doi.org/10.1007/978-1-4020-6863-8_20.

Giordano, M., & Prioretti, L. (2016). Sulphur and Algae: Metabolism, Ecology and Evolution. In: M.A. Borowitzka, J.A Raven, J. Beardall. (eds.), *The Physiology of Microalgae*, *Developments in Applied Phycology 6*, p: 185-200. https://doi.org/10.1007/978-3-319-24945-2.

Govindjee. Chlorophyll a Fluorescence: A Bit of Basics and History. (2004). In: George C. Papageorgiou and Govindjee (eds): Chlorophyll Fluorescence: A Signature of Photosynthesis, *Kluwer Academic Publishers. Printed in The Netherlands,* p: 1–42.

Gorman, J., & Shapiro, L. (2004). Structure of serine acetyltransferase from *Haemophilus influenzae Rd*. *Acta Crystallographica Section D: Biological Crystallography*, *60 (9)*, 1600–1605. https://doi.org/10.1107/S0907444904015240.

Gorman, D. S., Levine, R. P. (1965). Cytochrome f and plastocyanin: their sequence in the photosynthetic electron transport chain of *Chlamydomonas reinhardii. Proc Natl Acad Sci* ,USA 54:1665–1669.

Goujon, M, McWilliam, H., Li, W., Valentin, F., Squizzato, S., Paern, J., & Lopez, R. (2010). A new bioinformatics analysis tools framework at EMBL‐EBI. *Nucleic Acids Research* 38 Suppl: W695–699. https://doi:10.1093/nar/gkq313.

Gray, M. W., & Bore, P. H. (1988). Organization and expression of algal (*Chlamydomonas reinhardtii*) mitochondrial DNA. *Phil. Trans. R. Soc. Land. B*,

319 (B), 135–147.

Gröne, T. & Kirst, G. O. (1992). The effect of nitrogen deficiency, methionine and inhibitors of methionine metabolism on the DMSP contents of T*etraselmis subcordiformis* (Stein). *Marine Biology* 112, 497-503.

Griffiths, L. M., Swartzlander, D., Meadows, K. L., Wilkinson, K. D., Corbett, A. H., & Doetsch, P. W. (2009). Dynamic Compartmentalization of Base Excision Repair Proteins in Response to Nuclear and Mitochondrial Oxidative Stress. *Molecular and Cellular Biology*, *29 (3)*, 794–807. https://doi.org/10.1128/MCB.01357-08.

Grossman, A. (2000). Acclimation of *Chlamydomonas reinhardtii* to its Nutrient Environment. *Protist*, *151 (3)*, 201–224. https://doi.org/10.1078/1434-4610-00020.

Habicht, K. S., Gade, M., Thamdrup, B., & Berg, P. (2002). Calibration of Sulfate Levels in the Archean Ocean. *Science*, *298 (December)*, 2372–2375.

Harris, D. J., Conrad, J. C., & Lewis, J. A. (2009). Evaporative lithographic patterning of binary colloidal films Evaporative lithographic patterning of binary colloidal films. *Phil. Trans. R. Soc. A (2009) 367*, 5157–5165. https://doi.org/10.1098/rsta.2009.0157.

Hatzfeld, Y., Maruyama, A., Schmidt, A., Noji, M., Ishizawa, K., & Saito, K. (2000). β-Cyanoalanine Synthase Is a Mitochondrial Cysteine Synthase-Like Protein in *Spinach* and *Arabidopsi. Plant Physiol. 123: 1163-1171.* https://doi.org/10.1104/pp.123.3.1163.

He, Liyan., Han, Xiaotian., Yu, Zhiming. (2014). A Rare *Phaeodactylum tricornutum Cruciform Morphotype*: Culture Conditions, Transformation and Unique Fatty Acid Characteristics. *PLOS ONE, 9 (4)*, 1-8. https://doi.org/10.1371/journal.pone.0093922

Henikoff, S., & Henikoff, J.G. (1992). Amino acid substitution matrices from protein blocks. *Proc. Natl. Acad. Sci., 89,* 10915-10919.

Heeg, C., Kruse, C., Jost, R., Gutensohn, M., Ruppert, T., & Wirtz, M. (2008). Analysis of the *Arabidopsis* O -Acetylserine (thiol) lyase Gene Family Demonstrates Compartment-Specific Differences in the Regulation of Cysteine Synthesis. *The Plant Cell*, *20 (January)*, 168–185. https://doi.org/10.1105/tpc.107.056747.

Hell R, Jost R, Berkowitz O, & Wirtz M. 2002. Molecular and biochemical analysis of the enzymes of cysteine biosynthesis in the plant *Arabidopsis thaliana*. *Amino Acids 22:* 245–257.

Hell, R., & Wirtz, M. (2008). Metabolism of cysteine in plants and phototrophic bacteria. In: Rüdiger Hell, Christiane Dahl, Thomas Leustek. (eds.), *Sulfur Metabolism in Phototrophic Organisms*, p: 59–91. https://doi.org/10.1007/978-1-4020-6863-8_4.

Hell, R. & Wirtz, M. (2011) Molecular biology, biochemistry and cellular physiology of cysteine metabolism in *Arabidopsis thaliana*. *American Society of Plant Biologist, Arabidopsis* Book 2011, 9, e0154. 1-19, https://doi: 10.1199/tab.0154.

Howarth, J. R., Dom, R., Guti, G., & Wray, J. L. (1997). Cysteine biosynthesis in higher plants: a new member of the *Arabidopsis thaliana* serine acetyltransferase small gene family obtained by functional complementation of an *Escherichia coli* cysteine auxotroph. *Biochim Biophys Acta 1350*, 123–127.

Howarth, J. R., Dom, R., Guti, G., Wray, J. L., Romero, L. C., & Gotor, C. (2003). The serine acetyltransferase gene family in *Arabidopsis thaliana* and the regulation of its expression by cadmium. *Plant Molecular Biology, 51 (4)*, 589–598.

Kah, L. C., Lyons, T. W., & Frank, T. D. (2004). Low Marine Sulphate and Protracted Oxygenation of the Proterozoic Biosphere. *Nature, 431*, 881-884. https://doi.org/10.1038/nature 02974.

Karlin, S., & Altschul, S.F. (1990). Methods for assessing the statistical significance of molecular sequence features by using general scoring schemes, *Proc. Natl. Acad. Sci., 87,* 2264-2268.

Kikutani, S., Tanaka, R., Yamazaki, Y., Hara, S., Hisabori, T., Kroth, P. G., & Matsuda, Y. (2012). Redox Regulation of Carbonic Anhydrases via Thioredoxin in Chloroplast of the Marine Diatom *Phaeodactylum tricornutum. The Journal of Biological Chemistry, 287 (24)*, 20689–20700. https://doi.org/10.1074/jbc.M111.322743.

Kleckner, Nancy., Hanrahan, Michael., Anderson, Greg., & Lawson, Carolyn. (2016). Bioinformatics Tutorial. *Cellular and Mplecular Biology, Bio 242,* 1–28.

Knoll, A. H., Summons, R. E., Waldbauer, J. R., & Zumberge, J. E. (2007). The Geological Succession of Primary Producers in the Oceans. In: (eds.), Falkowski, P. G., Knoll, A. H. Evolution of Primary Producers in the Sea, p: 133–164. https://doi.org/10.1016/B978-0-12-370518-1.X5000-0.

Koonin, E. V., & Galperin, M.Y. (2003). Information Sources for Genomics. In: Koonin EV, Galperin MY. (eds.), *Information Sources for Genomics - Sequence - Evolution - Function*, chapter 3 p: 1–30.

Koonin, E. V., & Galperin, M.Y. (2003). Genome Annotation and Analysis. In: Koonin, E. V., Galperin, M. Y. (eds.), *Information Sources for Genomics - Sequence - Evolution - Function*, chapter 5. p: 1–15.

Kopriva, S. (2006). Regulation of Sulfate Assimilation in *Arabidopsis* and Beyond. *Annals of Botany 97,* 479–495. https://doi.org/10.1093/aob/mcl006.

Kopriva, S., Patron, N. J., Keeling, P., & Leustek, T. (2008). Phylogenetic analysis of sulfate assimilation and cysteine biosynthesis in phototrophic organisms. In: Rüdiger Hell, Christiane Dahl, Thomas Leustek. (eds.), *Sulfur Metabolism in Phototrophic Organisms*, p: 31–58. https://doi.org/10.1007/978-1-4020-6863-8_3.

Kredich, M., & Tomkins, G. M. (1966). The and Enzymic Synthesis of L-Cysteine in *Escherichia coli* and *Salmonella typhimurium*. *The Journal of Biological Chemistry*, *241 (21)*, 4955-4965.

Kredich, M., & Becker, M. A. (1969). [197] Cysteine Biosynthesis : Serine Transacetylase and O-Acetylserine Sulfhydrylase. *Methods of Enzymology, 17 (Part B),* 459–470. https://doi.org/10.1016/0076-6879(71)17082-6.

Kredich, N. M., Becker, M. A., & Tomkins, G. M. (1969). Purification and Characterization of Cysteine Synthetase a Bifunctional Protein Complex, from *Salmonella typhimurium*. *The Journal of Biological Chemistry, 244*. 2428-2439.

Krueger, S., Niehl, A., Martin, M. C. L., Steinhauser, D., Donath, A., Hildebrandt, T., … & Hesse, H. (2009). Analysis of cytosolic and plastidic serine acetyltransferase mutants and subcellular metabolite distributions suggests interplay of the cellular compartments for cysteine biosynthesis in *Arabidopsis*. *Plant, Cell and Environment, 49*, 349–367. https://doi.org/10.1111/j.1365-3040.2009.01928.x.

Kufryk, G. I., Sachet, M., Schmetterer, G., & Vermaas, W. F. J. (2002). Transformation of the cyanobacterium *Synechocystis* sp . PCC 6803 as a tool for genetic mapping : optimization of efficiency. *FEMS Microbiology Letters*, *206*, 215–219.

Kumaran, S., Yi, H., Krishnan, H. B., & Jez, J. M. (2009). Assembly of the Cysteine Synthase Complex and the Regulatory Role of Protein-Protein Interactions *. *The Journal of Biological Chemistry, 284 (15)*, 10268–10275. https://doi.org/10.1074/jbc.M900154200.

Leliaert, F., Smith, D.R., Moreau, H., Herron, M., Verbruggen, H., Delwiche, C.F., & De Clerck O. Phylogeny and molecular evolution of the green algae. *Critical Reviews in Plant Sciences* (in press).

Leliaert, F., Rousseau, F., De Reviers, B. and Coppejans, E. 2003. Phylogeny of the *Cladophorophyceae* (Chlorophyta) inferred from partial LSU rRNA gene sequences: is the recognition of a separate order Siphonocladales justified? *Europen Journal of Phycology, 38 (3),* 233-246. https://doi.org/10.1080/1364253031000136376.

León, J., Romero, L.C., Galván, F. and Vega, J.M. (1987). Purification and physicochemical characterization of O-acetyl-l-serine sulfhydrilase from *Chlamydomonas reinhardtii*. *Plant Science 53,* 93–99.

Leustek, T., Martin, M. N., Bick, J., & Davies, J. P. (2000). PATHWAYS AND REGULATION OF SULFUR METABOLISM REVEALED THROUGHMOLECULAR AND GENETIC STUDIES. *Annu. Rev. Plant Physiol. Plant Molicology. Biology, 51*, 141-165, https://doi.org/1040-2519/00/0601-0141.

Levine, R. P. (1965). Cytochrome F and plastocyanin: their sequence in the photosynthetic electron transport chain of *Chlamydomonas reinhardtii. PROC. N.*

A. S. 54, 1665–1669.

Lewin, B. Y. J. C., Lewin, R. A., & Philpott, D. E. (1958). Observations on *Phaeodactylum tricornutum*. *J. gen. Microbiol. 18: 418–426.*

Lin, X., Kaul, S., Rounsley, S., Shea, T. P., Benito, M., Town, C. D., …& Venter, J. C. (1999). Sequence and analysis of chromosome 2 of the plant *Arabidopsis thaliana*. *Nature, 402 (December)*, 761-768. https://doi.org/10.1038/45471.

Lindberg, P., & Melis, A. (2008). The chloroplast sulfate transport system in the green algae *Chlamydomonas reinhardtii*. *Planta, 228,* 951–961. https://doi.org/10.1007/s00425-008-0795-0.

Liss, P. S., Hatton, A. D., Malin, G., Nightingale, P. D., & Turner, S. M. (1997) Marine sulfur emissions. *Philos T Roy Soc B 352* (1350), 159–168. https://doi.org/10.1098/rstb.1997.0011.

Lowry, O. H., Rosebrough, N. J., Farr, A. L., & Randall, R. J. (1951). Protein measure- ment with the Folin phenol reagent. *J. Biol. Chem. 193,* 265–275.

Mahmood Tahrin and Yang, Ping-Chang. (2012). Western Blot: Technique, Theory, and Trouble Shooting Tahrin. *North American Journal of Medical Science, 4 (9)*, 429-434. https://doi.org/10.4103/1947-2714.100998.

Maqsood, S. A. (1974). DETERMINATION OF ALGAE GROWTH POTENTIAL IN NATURAL ENVIRONMENT. Thesis Graduate Faculty of Texas Tech University in Partial Fulfillment of the Requirements for the Degree of MASTER OF SCIENCE IN CIVIL ENGINEERING.

Maul, J. E., Lilly, J. W., Cui, L., Claude, W., Miller, W., Harris, E. H., & Stern, D. B. (2002). The *Chlamydomonas reinhardtii* Plastid Chromosome : Islands of Genes in a Sea of Repeats. *The Plant Cell 14 (November)*, 2659–2679. https://doi.org/10.1105/tpc.006155.present.

Mayer, K., Schuller, C., Wambutt, R., Murphy, G., Volckaer, G., Pohl, T., …, & McCombie, W. R. (1999). Sequence and analysis of Chromosome 4 of the plant *Arabidopsis thaliana*. *Nature, 402,* 469-477.

McNeil, S. D., Nuccio, M. L., & Hanson, A. D. (1999). Betaines and related osmoprotectants. Targets for metabolic engineering of stress resistance. *Plant Physiol 120*: 945–949

Melis, A., & Chen, H. (2005). Chloroplast sulfate transport in green algae–genes , proteins and effects. *Photosynthesis Research, 86,* 299–307. https://doi.org/10.1007/s11120-005-7382-z.

Merchant, S. S., Prochnik, S. E., Vallon, O., Harris, E. H., Karpowicz, J., Witman, G. B., …& Grossman, A. R. (2010). The *Chlamydomonas* Genome Reveals the Evolution of Key Animal and Plant Functions. *Science*, *318 (5848)*, 245–250. https://doi.org/10.1126/science.1143609.

Mesquita, C., Alexandre, D., Aranda, G., & Couri, S. (2013). Morphological and chemical aspects of Chlorella *galbana* and *Tetraselmis gracilis* microalgae. *Natural Science, 5 (7)*, 783–791. http://dx.doi.org/10.4236/ns.2013.57094.

Miyahara, M., Aoi, M., Inoue-kashino, N., Kashino, Y., Ifuku, K., Electroporation, M., …& Fuku, K. I. (2014). Highly Efficient Transformation of the Diatom *Phaeodactylum tricornutum* by Multi-Pulse Electroporation. *Biosci. Biotechnol. Biochem, 77 (4),* 874-876, https://doi.org/10.1271/bbb.120936.

Murillo, M., Foglia, R., Diller, A., Lee, S., & Leustek, T. (1997). Serine acetyltransferase from *Arabidopsis thaliana* can functionally complement the cysteine requirement of a cysE mutant strain of *Escherichia coli*. *Cell Mol Biol Res 41*, 425–433.

Nakamura, Y., Kaneko, T., Hirosawa, M., Miyajima, N., & Tabata, S. (1998). CyanoBase, a www database containing the complete nucleotide sequence of the genome of *Synechocystis* sp. strain PCC 6803. *Nucleic Acids Research*, *26 (1)*, 63–67. https://doi.org/10.1093/nar/26.1.63.

Nielsen, Henrik., Engelbrecht1, Jacob., & Brunak, Søren. (1997). Identification of prokaryotic and eukaryotic signal peptides and prediction of their cleavage sites. Protein Engineering, 10 (1), 1–6.

Noji, M., Inoue, K., Kimura, N., Gouda, A., & Saito, K. (1998). Isoform-dependent differences in feedback regulation and subcellular localization of serine acetyltransferase involved in cysteine biosynthesis from *Arabidopsis thaliana*. *The Journal of Biological Chemestry. 273 (49)*: 32739-32745. https://doi:10.1074/jbc.273.49.32739.

Norici, A., Hell, R., & Giordano, M. (2005). Sulfur and primary production in aquatic environments : an ecological perspective. *Photosynthesis Research, 86,* 409–417. https://doi.org/10.1007/s11120-005-3250-0.

Notredame, C., Higgins, D, G., & Heringa, J. (2000). T-Coffee : A Novel Method for Fast and Accurate Multiple Sequence Alignment. *Journal Molecular Biology, 302,* 206-217, https://doi.org/10.1006/jmbi.2000.4042.

Olsen, L. R., Huang, B., Vetting, M. W., & Roderick, S. L. (2004). Structure of serine acetyltransferase in complexes with CoA and its cysteine feedback inhibitor. *Biochemistry*, *43 (20)*, 6013–6019. https://doi.org/10.1021/bi0358521.

Oren-shamir, M., Pick, U., & Avron, M. (1990). Plasma Membrane Potential of the Alga *Dunaliella*, and Its Relation to Osmoregulation. *Plant Physiology, 93*, 403–408, https://doi.org/10.0032-0889/90/93/0403/06.

Oren, A. (2005). A hundred years of *Dunaliella* research : 1905–2005. *14*, 1–14. https://doi.org/10.1186/1746-1448-1-2.

Peterson, G. L. (1977). A Simplification of the Protein Assay Method of Lowry et al . Which is More Generally Applicable, *Analytical Biochemistry*, *83*, 346–356.

Prioretti, L. (2014). Sulfur metabolism in microalgae. PhD Thesis. Università Politecnica delle Marche.

Prioretti, L., Gontero, B., Hell, R., & Giordano, M. (2014). Diversity and regulation of ATP sulfurylase in photosynthetic organisms. *Frontiers in Plant Science*, *5 (November)*, 597, 1-12. https://doi.org/10.3389/fpls.2014.00597.

Prioretti, L., & Giordano, M. (2016). Direct and indirect influence of sulfur availability on phytoplankton evolutionary trajectories. *Journal of Phycological 52,* 1094-1102. https://doi.org/10.1111/jpy.12468.

Pye, V. E., Tingey, A. P., Robson, R. L., & Moody, P. C. E. (2004). The structure and mechanism of serine acetyltransferase from *Escherichia coli*. *Journal of Biological Chemistry*, *279 (39)*, 40729–40736. https://doi.org/10.1074/jbc.M403751200.

Rabinowitch, E., Govindjee, 1969. The photosynthetic pigments. In: Rabinowitch, E., Govindjee. (eds.), Photosynthesis. New York, USA: *John Wiley and Sons,* Inc., 102- 123.

Ratti, S., Knoll, A. H., Giordano, M., & Marche, P. (2011). Did sulfate availability facilitate the evolutionary expansion of chlorophyll a + c phytoplankton in the oceans ?. *Geobiology, (2011),* 301–312. https://doi.org/10.1111/j.1472-4669.2011.00284.x.

Roberts, M. A., & Wray, J. L. (1996). Cloning and characterisation of an *Arabidopsis thaliana* cDNA clone encoding an organeilar isoform of serine acetyltransferase. *Plant Molecular Biology, 30,* 1041–1049.

Rochaix, J. D. (1995). *Chlamydomonas reinhardtii* as the Photosynthetic Yeast. *Annual Review of Genetics*, *29*, 209–230. https://doi.org/10.1146/annurev.genet.29.1.209.

Rolland, N., Ruffet, M.-L., Job, D., Douce, R. & Droux, M. (1996). Spinach chloroplast O-acetylserine (thiol) lyase exhibits two cata lytically non-equivalent pyridoxal-5'-phosphate-containing active sites. *Europen Journal of Biochemistry. 236 (1)*, 272–282. https://doi.org/10.1111/j.1432-1033.1996.00272.x.

Saito, K., Yokoyama, H., Noji, M., & Murakoshi, I. (1995) Molecular cloning and characterization of a plant serine acetyltransferase playing a regulatory role in cysteine biosynthesis from watermelon. *Journal Biological. Chemistry*. *270 (27)*, 16321-16326. https://doi: 10.1074/jbc.270.27.16321.

Saitou, N., & Nei, M. (1987). The neighbour-joining method: a new method for reconstructing phylogenetic trees. *Mol Biol Evo*, *4 (4)*, 406–425. https://doi.org/citeulike-article-id:93683.

Salbitani, G., Wirtz, M., Hell, R., & Carfagna, S. (2014). Affinity purification of O-acetylserine(thiol)lyase from *Chlorella sorokiniana* by recombinant proteins from *Arabidopsis thaliana*. *Metabolites, 4*, 629–639. http://dx.doi.org/10.3390/metabo4030629.

Sambrook, J., & Russell, D.W. (2006). The Hanahan Method for Preparation and Transformation of Competent *E. coli*: High-Efficiency Transformation. In: (eds.), Molecular Cloning: A Laboratory Manual, p: 162-167. *Cold Spring Harbor Laboratory Press*, New York, USA.

San Pedro, A., González-López, C. V., Acién, F. G., & Molina-Grima, E. (2013). Marine microalgae selection and culture conditions optimization for biodiesel production. *Bioresource Technology*, *134*, 353–361. https://doi.org/10.1016/j.biortech.2013.02.032.

Sanderson, M. J., & Driskell, A. C. (2003). The challenge of constructing large phylogenetic trees. *Trends in Plant Science, 8 (8)*, 374–379. https://doi.org/10.1016/S1360-1385(03)00165-1.

Salanoubat, M., Lemcke, K., Rieger, M., Ansorge, W., Unseld, M., Fartmann, B., ..., Yasuda, M., & Tabbata, S. (2000). Sequence and analysis of chromosome 3 of the plant *Arabidopsis thaliana*, *Nature*, *408* (December), 820–822.

Schmidt, A. (1979) Photosynthetic assimilation of sulphur compounds. In: Gibbs ML, Latzko E (eds.), *Photosynthesis II. Encyclopedia of plant physiology. Springer,* Berlin, p: 481–496. https://doi.org/10.1007/978-3-642-67242-2_37.

Schmidt, A., & Jager, K. (1992). Open Questions About Sulfur. *Annual Review of Plant Physiology and Plant Molecular Biology*, *43*, 325–49.

Selim, Khaled A., Haase, Florian., Hartmann, Marcus D., Hagemann, Martin., Forchhammer, Karl. (2018). PII-like signaling protein SbtB links cAMP sensing with cyanobacterial inorganic carbon response. *Proc. Natl. Acad. Sci. 115 (21),* E4861-E4869. https://doi/10.1073/pnas.1803790115.

Mayer, K., Schüller, C., Wambutt, R., Murphy, G., Volckaert, G., Pohl. T., …& McCombie, W. R. (1999). Sequence and analysis of chromosome 4 of the plant *Arabidopsis thaliana*. (1999). *Nature, 402,* 769-777.

Sievers, F., Wilm, A., Dineen, D., Gibson, T. J., Karplus, K., Li, W., Lopez, R., McWilliam, H., Remmert, M., Söding, J., Thompson, J. D., & Higgins, D. G. (2011). Fast, scalable generation of high quality protein multiple sequence alignments using Clustal Omega. *Molecular Systems Biology 7* Article number: 539, 1-6. https://doi:10.1038/msb.2011.75

Stanier, R. Y., Kunisawa, R., Mandel, M., & Cohen-Bazire, G. (1971). Purification and properties of unicellular blue-green algae (*Order Chroococcales*). *Bacteriological Reviews*, *35 (2)*, 171–205. https://doi.org/10.1016/j.jbiotec.2013.07.020.

Steinke, M., Malin, G., Archer, S. D., Burkill, P. H., & Liss, P. S. (2002). DMS production in a coccolithophorid bloom : evidence for the importance of dinoflagellate DMSP lyases. *Aquatic Microbial Ecology, 26,* 259–270.

Steinke, M., Malin, G., Gibb, S. W., & Burkill, P. H. (2002). Vertical and temporal variability of DMSP lyase activity in a coccolithophorid bloom in the northern

North Sea. *Deep-Sea Reasarch, 49*, 3001–3016.

Steinke, M., Daniel, C., & Kirst, G.O. (1996). DMSP lyase in marine macro- and microalgae. In: Kienem, R. P., Visscher, P. T., Keller, M. D., & Kirst, G. O., eds. Biology and Environmental Chemistry of DMSP and Related Sulfonium Compounds. *New York, USA: Plenum Press*, 317–324.

Steinke, M., & Kirst, G.O. (1996). Enzymatic cleavage of dimethylsulfoniopropri-onate (DMSP) in cell-free exctracts of the marine macroalgae *Enteromorpha clathrata* (Roth) Grev. (*Ulvales, Chlorophyta*). *Journal of Experimental Marine Biology and Ecology 201 (1-2)*: 73–85. https://doi.org/10.1016/0022-0981(95)00207-3.

Tabata, S., Nakamura, Y., Kotani, H., Kato, T., Asamizu, E.,… Robben, J. (2000). Sequence and analysis of chromosome 5 of the plant Arabidopsis thaliana. *Nature, 408,* 823-826.

Takahashi, H., Kopriva, S., Giordano, M., Saito, K., & Hell, R. (2011). Sulfur Assimilation in Photosynthetic Organisms: Molecular Functions and Regulations of Transporters and Assimilatory Enzymes. *Annual Review of Plant Biology*, *62 (1)*, 157–184. https://doi.org/10.1146/annurev-arplant-042110-103921.

Tamura, K., Peterson, D., Peterson, N., Stecher, G., Nei, M., & Kumar, S. (2011). MEGA5: Molecular evolutionary genetics analysis using maximum likelihood, evolutionary distance, and maximum parsimony methods. *Molecular Biology and Evolution*, *28 (10)*, 2731–2739. https://doi.org/10.1093/molbev/msr121.

Theologis, A., Ecker, J. R., Palm, C. J., Federspiel, N. A., Kaul, S., White, O., …& Davis, R. W. (2000). Sequence and analysis of chromosome 1 of the plant *Arabidopsis thaliana. Nature, 408 (December)*, 816-820.

Tommaso, P. Di, Moretti, S., Xenarios, I., Orobitg, M., & Notredame, C. (2011). T-Coffee : a web server for the multiple sequence alignment of protein and RNA sequences using structural information and homology extension. *Nucleic Acids Research, 39 (May)*, 13–17. https://doi.org/10.1093/nar/gkr245.

Turner, S. M., & Beidel, D. C. (1988). SOME FURTHER COMMENTS ON THE MEASUREMENT OF SOCIAL PHOBIA. *Behavior Research and Therapy, 26 (5)*, 411–413.

Urano, Y., Manabe, T., Noji, M., & Saito, K. (2000). Molecular cloning and functional characterization of cDNAs encoding cysteine synthase and serine acetyltransferase that may be responsible for high cellular cysteine content in *Allium tuberosum. Gene, 257*, 269–277.

Vaara, M. (1992). Eight bacterial proteins, including UDP-N- acetylglucosamine acyltransferase (LpxA) and three other transferases of *Escherichia coli*, consist of a six-residue periodicity theme. *Federation of European Microbiology societies Letters, 76*, 249–254.

Vogel, Christine., Bashton, Matthew., Kerrison, Nicola. D., Chothia, Cyrus., and Teichmann, Sarah. A. (2004). Structure, function and evolution of multidomain

proteins. *Current Opinion in Structural Biology, 14*, 208–216. https://doi.org/10.1016/j.sbi.2004.03.011.

Vuorio, R. (1991). The Ssc protein of enteric bacteria has significant homology to the acyltransferase Lpxa of lipid A biosynthesis, and to three acetyltransferases. *Federation of European Biochemical Societie, 292 (1)*, 90–94.

Vuorio, Riitta., Härkönen, Taina., Tolvanenb, Martti., Vaaraa, Martti. The novel hexapeptide motif found in the acyltransferases LpxA and LpxD of lipid A biosynthesis is conserved in various bacteria. *Federation of European Biochemical Societies Letters, 334,* 289-292.

Weimbs, T., & Santa, C. (2012). Tutorial : How to generate a publication-quality multiple sequence alignment. University of California Santa Barbara, 11/2012.

Wirtz, M., Berkowitz, O., Droux, M., & Hell, R. (2001). The cysteine synthase complex from plants: Mitochondrial serine acetyltransferase from *Arabidopsis thaliana* carries a bifunctional domain for catalysis and protein-protein interaction. *European Journal of Biochemistry*, *268 (3)*, 686–693. https://doi.org/10.1046/j.1432-1327.2001.01920.x.

Wirtz, M., & Droux, M. (2004). O -acetylserine (thiol) lyase : an enigmatic enzyme of plant cysteine biosynthesis revisited in *Arabidopsis thaliana*. *Journal of Experimental Botany, Sulphur Metabolism Special Issue,* 1–14. https://doi.org/10.1093/jxb/erh201.

Wirtz, M., Droux, M., & Hell, R. (2004). O-acetylserine (thiol) lyase: An enigmatic enzyme of plant cysteine biosynthesis revisited in *Arabidopsis thaliana*. *Journal of Experimental Botany*, *55 (404)*, 1785–1798. https://doi.org/10.1093/jxb/erh201.

Wirtz, M., Birke, H., Heeg, C., Müller, C., Hosp, F., Throm, C., …& Hell, R. (2010). Structure and function of the hetero-oligomeric cysteine synthase complex in plants. *Journal of Biological Chemistry*, *285 (43)*, 32810–32817. https://doi.org/10.1074/jbc.M110.157446.

Yao, L., Wei, K., Tan, M., Tan, T. W., & Lee, Y. K. (2017). Exploring the transcriptome of non-model oleaginous microalga *Dunaliella tertiolecta* through high-throughput sequencing and high performance computing. *BMC Bioinformatics,18 (122,)* 1–11. https://doi.org/10.1186/s12859-017-1551-x.

Yeon, J. Y., Yoo, S. J., Takagi, H., & Kang, H. A. (2018). A Novel Mitochondrial Serine O-Acetyltransferase , OpSAT1 , Plays a Critical Role in Sulfur Metabolism in the Thermotolerant Methylotrophic *Yeast Ogataea* parapolymorpha. *Scientific Reports*, (November 2017), 1–12. https://doi.org/10.1038/s41598-018-20630-8.

Yi, H., Dey, S., Kumaran, S., Lee, S. G., Krishnan, H. B., & Jez, J. M. (2013). Structure of soybean serine acetyltransferase and formation of the cysteine regulatory complex as a molecular chaperone. *Journal of Biological Chemistry*, *288 (51)*, 36463–36472. https://doi.org/10.1074/jbc.M113.527143.

Yoch, D. C., Ansede, J. H., & Rabinowitz, K. S. (1997). Evidence for intracellular and extracellular dimethylsulfoniopropionate (DMSP) lyases and DMSP uptake sites in two species of marine bacteria. *Appl Environ Microb* 63 (8), 3182–3188.

Zerulla, K., & Ludt, K. (2016). The ploidy level of *Synechocystis* sp . PCC 6803 is highly variable and is influenced by growth phase and by chemical and physical external parameters. *Microbiology 162:* 730–739. https://doi.org/10.1099/mic.0.000264.

Zuckerkandl, E., & Pauling, L. (1965). Molecules as documents of evolutionary history. *Journal of Theoretical Biology*, *8 (2)*, 357–366. https://doi.org/10.1016/0022-5193(65)90083-4.

7. Supplemental material

7.1. Growth curves

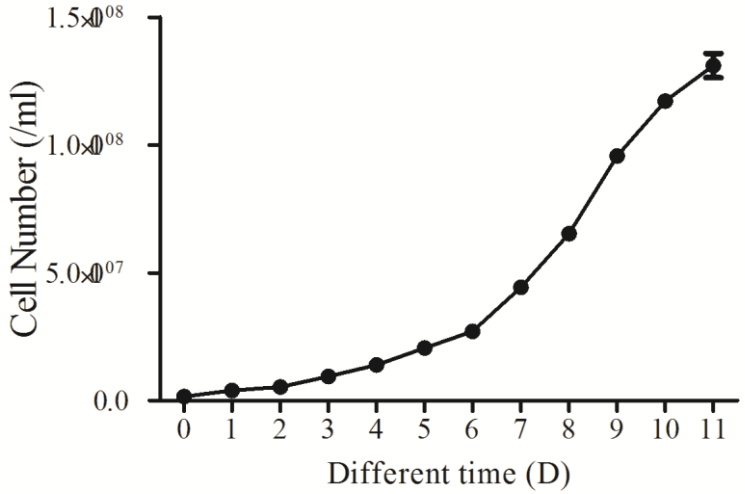

Fig. 7-1. *Synechocystis* sp. PCC6803 growth curve.

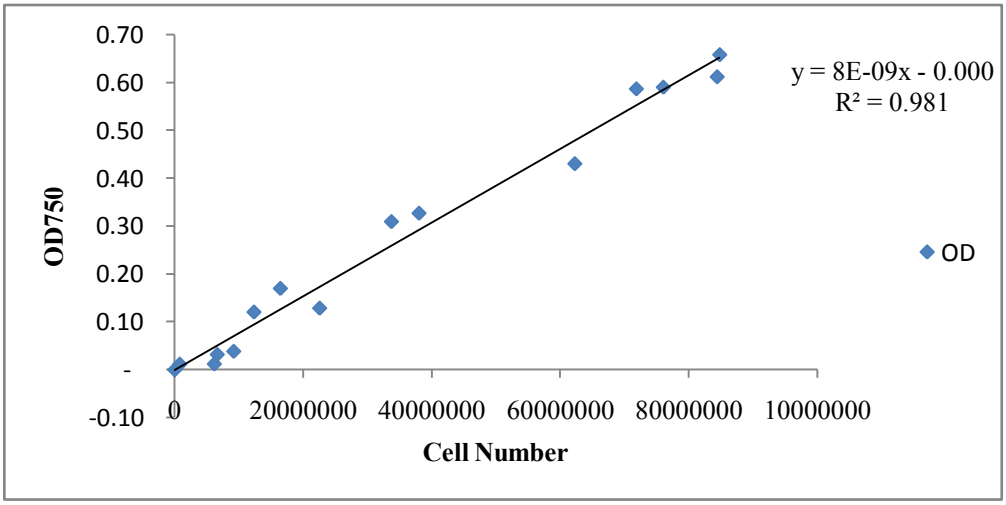

Fig. 7-2. Curve for the conversion of the OD of *Synechocystis* sp. PCC 6803 cultures to cell numbers.

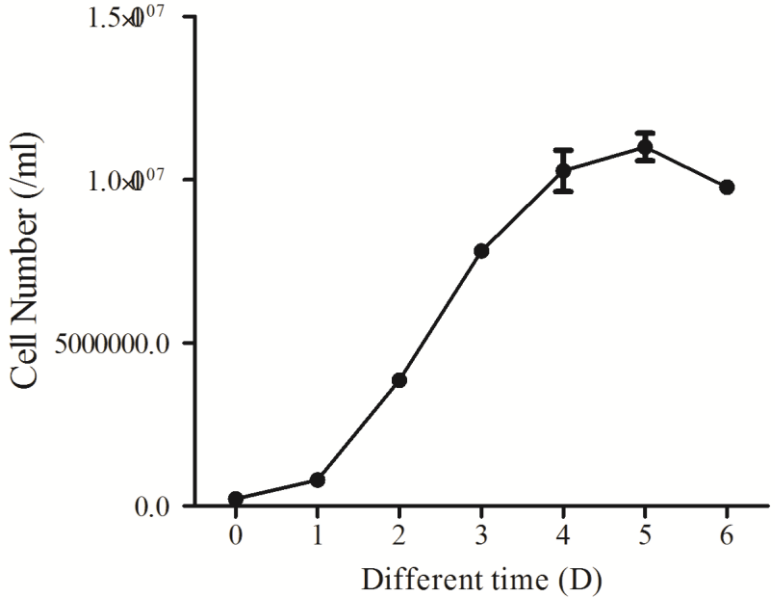

Fig. 7-3. Growth curve of *Chlamydomonas reinhardtii* cultured in TAP medium.

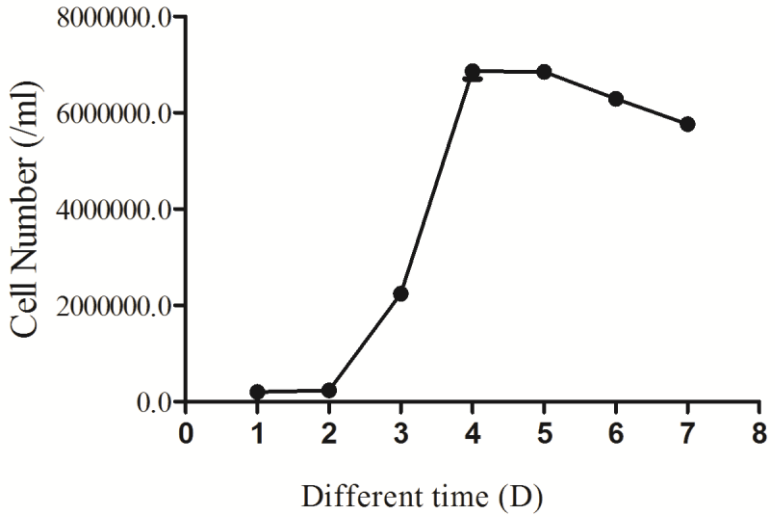

Fig. 7-4. Growth curve of *Chlamydomonas reinhardtii* cultured in TP medium.

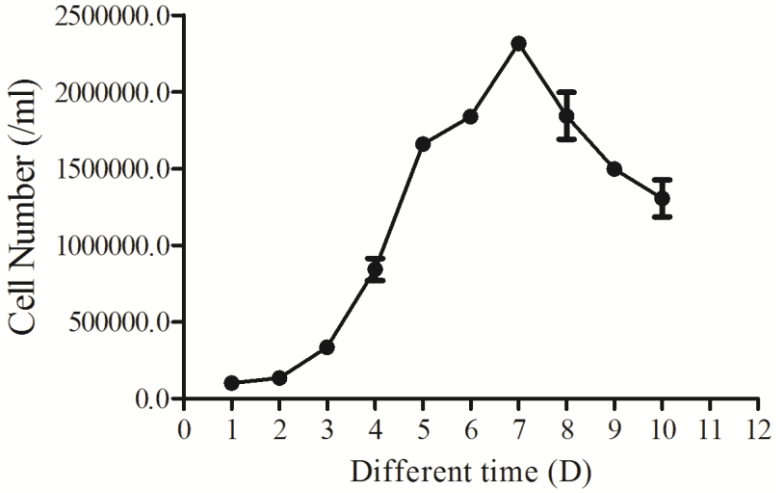

Fig. 7-5. *Dunaliella tertiolecta* growth curve.

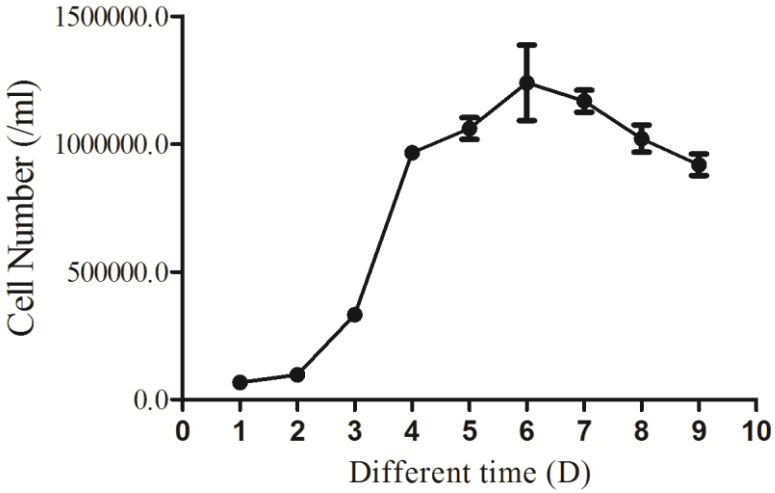

Fig. 7-6. *Tetraselmis suecica* growth curve.

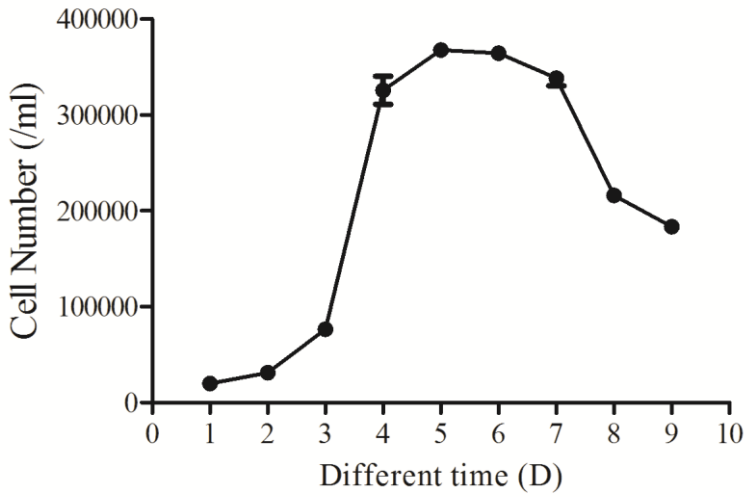

Fig. 7-7. *Thalassiosira pseudonana* growth curve.

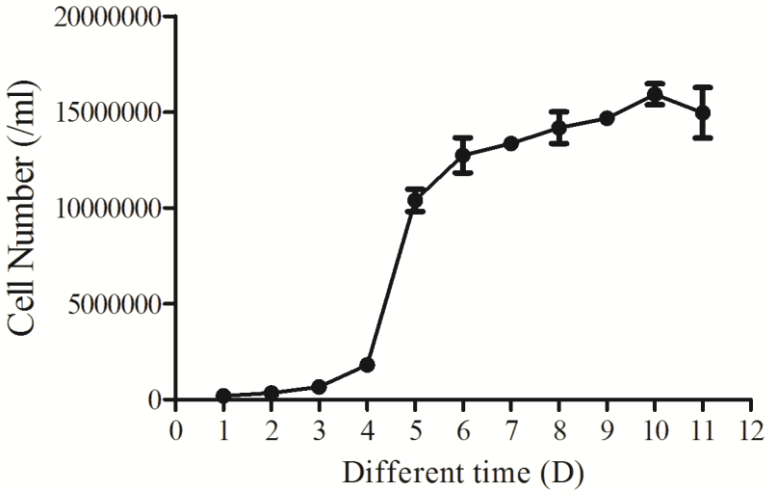

Fig. 7-8. *Phaeodactylum tricornutum* growth curve.

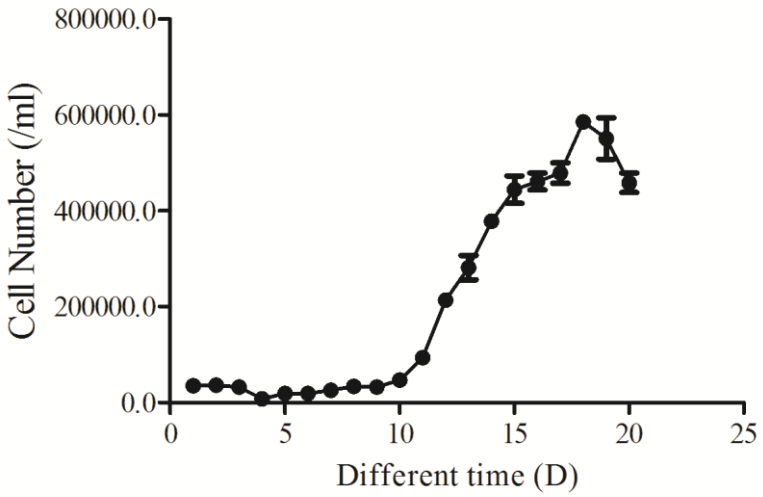

Fig. 7-9. *Amphinidinium klebsii* growth curve.

7.2. Correlation between relative mobility of protein with protein size

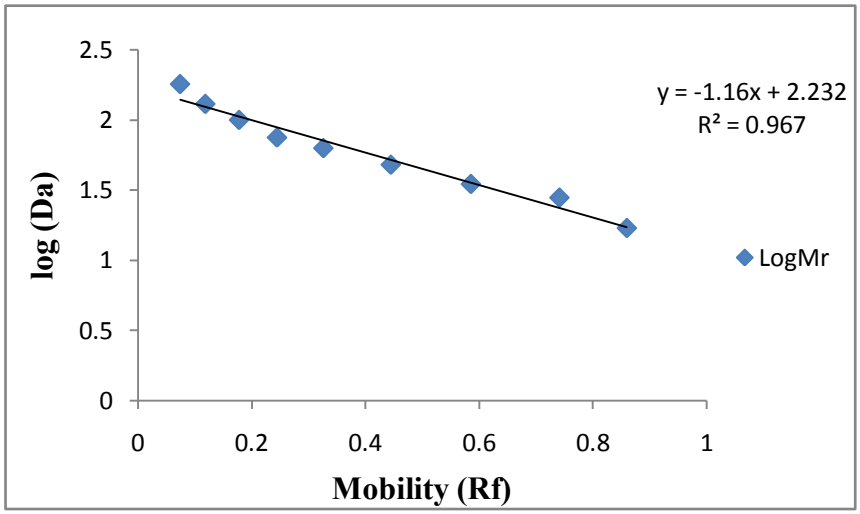

Fig. 7-10. Standard curve for the determination of protein size from the relative protein mobility in binding affinity test chromatography for *Synechocystis* sp. PCC 6803.

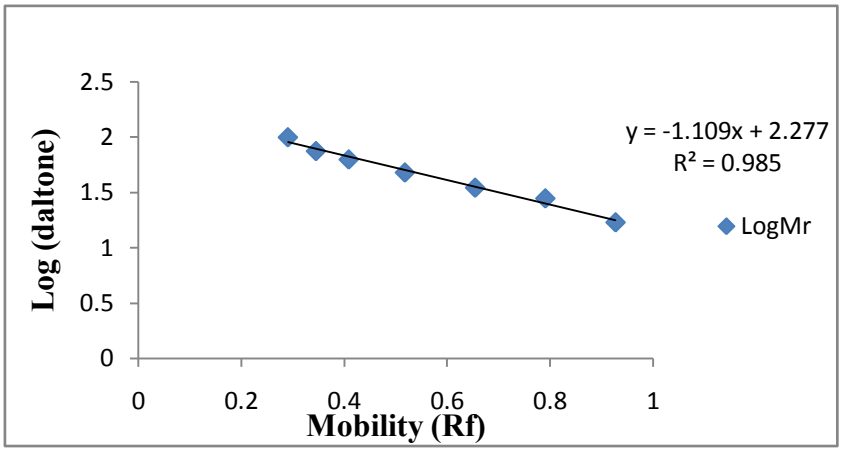

Fig. 7-11. Standard curve for the determination of protein size from relative protein mobility in binding affinity test chromatography for *Chlamydomonas reinhardtii* with TAP medium culture extract.

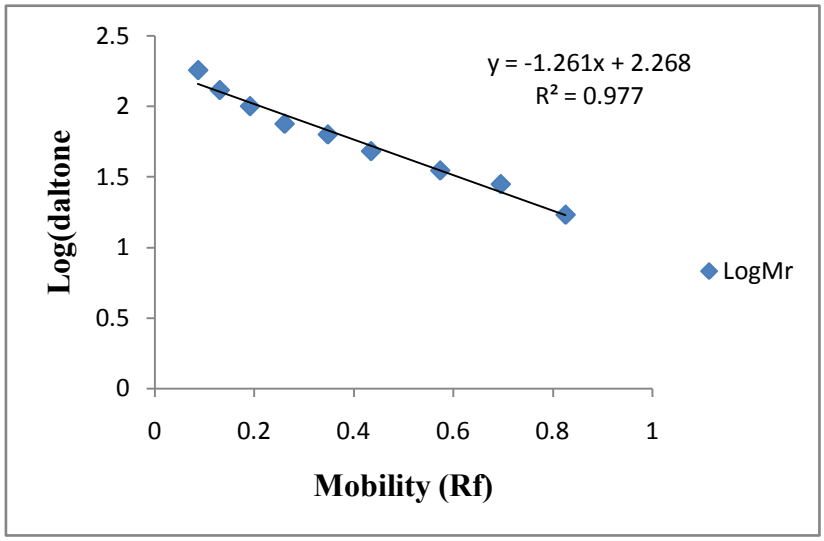

Fig. 7-12. Standard curve for the determination of protein size from the relative protein mobility in binding affinity test chromatography for *Chlamydomonas reinhardtii* with TP medium culture extract.

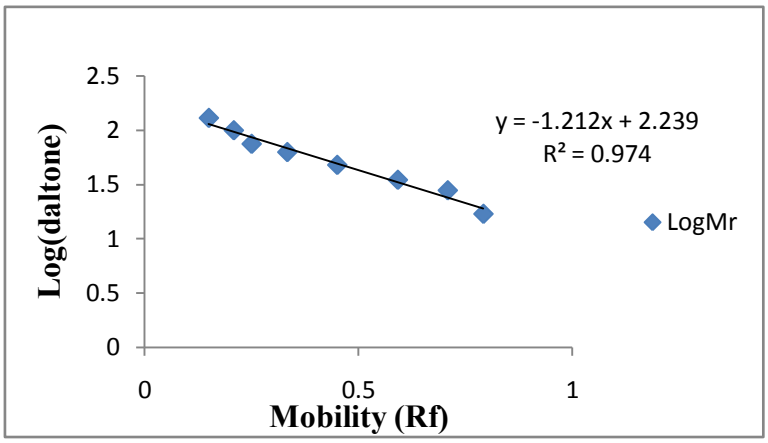

Fig. 7-13. Standard curve for the determination of protein size from the relative protein mobility in binding affinity test chromatography for *Tetraselmis suecica* extract.

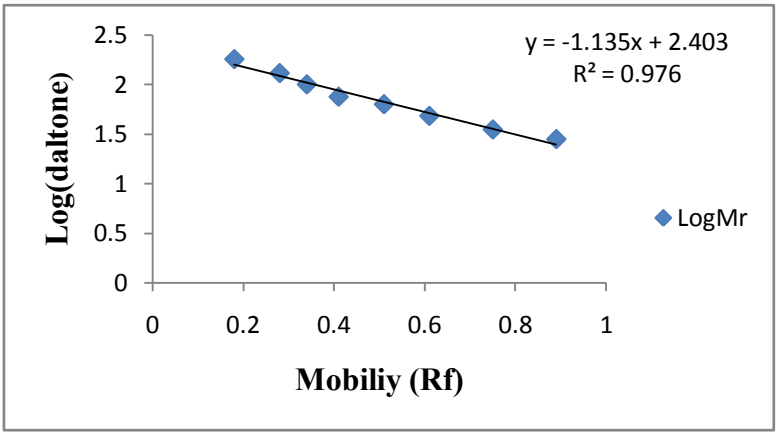

Fig. 7-14. Standard curve for the determination of protein size from the relative protein mobility in binding affinity test chromatography for *Dunaelilla tertiolecta* extract.

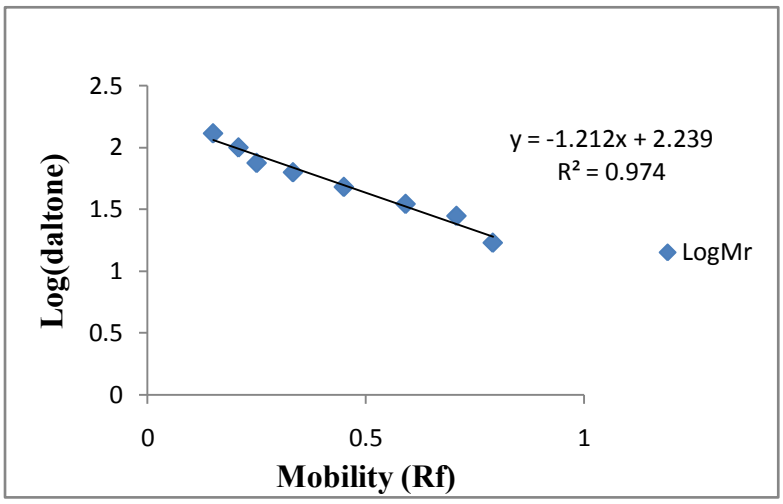

Fig. 7-15. Standard curve for the determination of protein size from the relative protein mobility in binding affinity test chromatography for *Thalassiosira psedonana* extract.

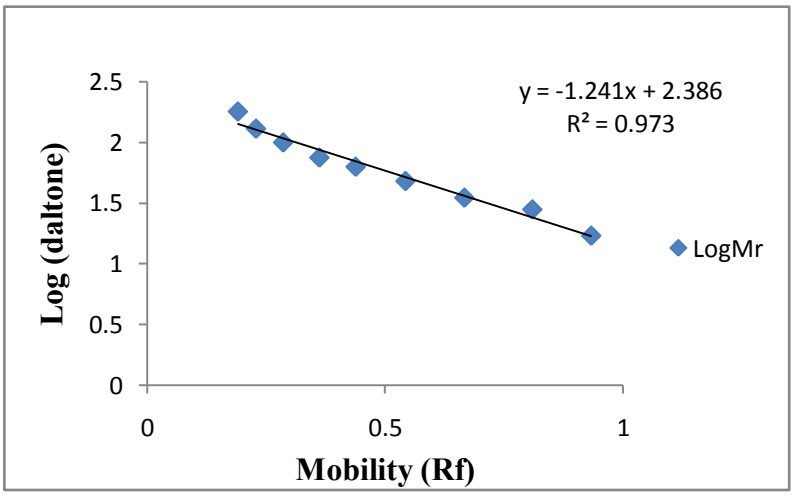

Fig. 7-16. Standard curve for the determination of protein size the relative protein mobility in binding affinity test chromatography for *Phaedactylum tricornum* extract.

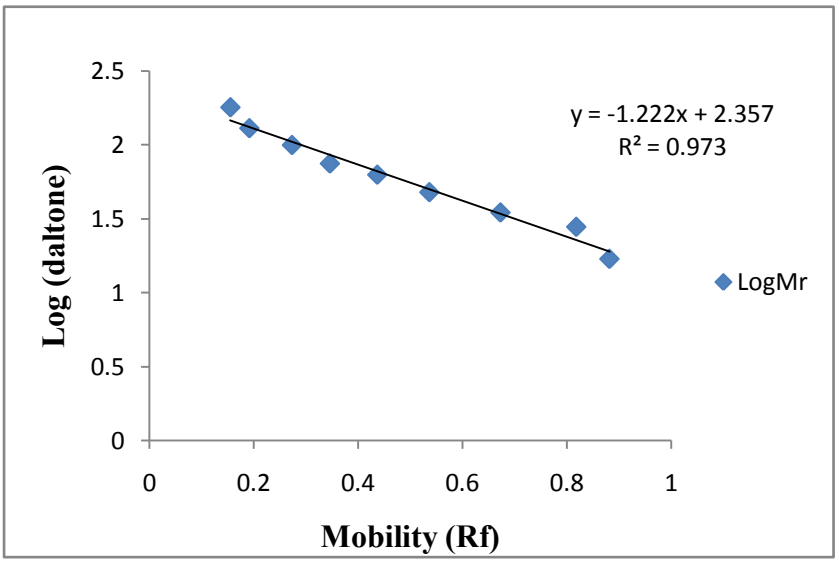

Fig. 7-17. Standard curve for the determination of protein size from the relative protein mobility in binding affinity test chromatography for *Amphidinium klebsii* extract.

7.3. Comparision of algae SAT and OAS-TL with *A. thaliana* sequences

7.3.1. Alignment of the SAT sequences of Cyanobacteria with *A. thaliana* SAT isoforms

Fig. 7-18. Alignment of *Synechocystis* sp. PCC 6803 SAT amino acid sequences with *A. thaliana*.

Fig. 7-19. Alignment of *Synechococcus* sp. WH 7803 SAT amino acid sequences with *A. thaliana*.

7.3.2. Alignment of the SAT sequences of green algae with *A. thaliana* SAT isoforms

Fig. 7-20. Alignment of 1-*C. reinhardtii* SAT amino acid sequence with *A. thaliana* isoforms.

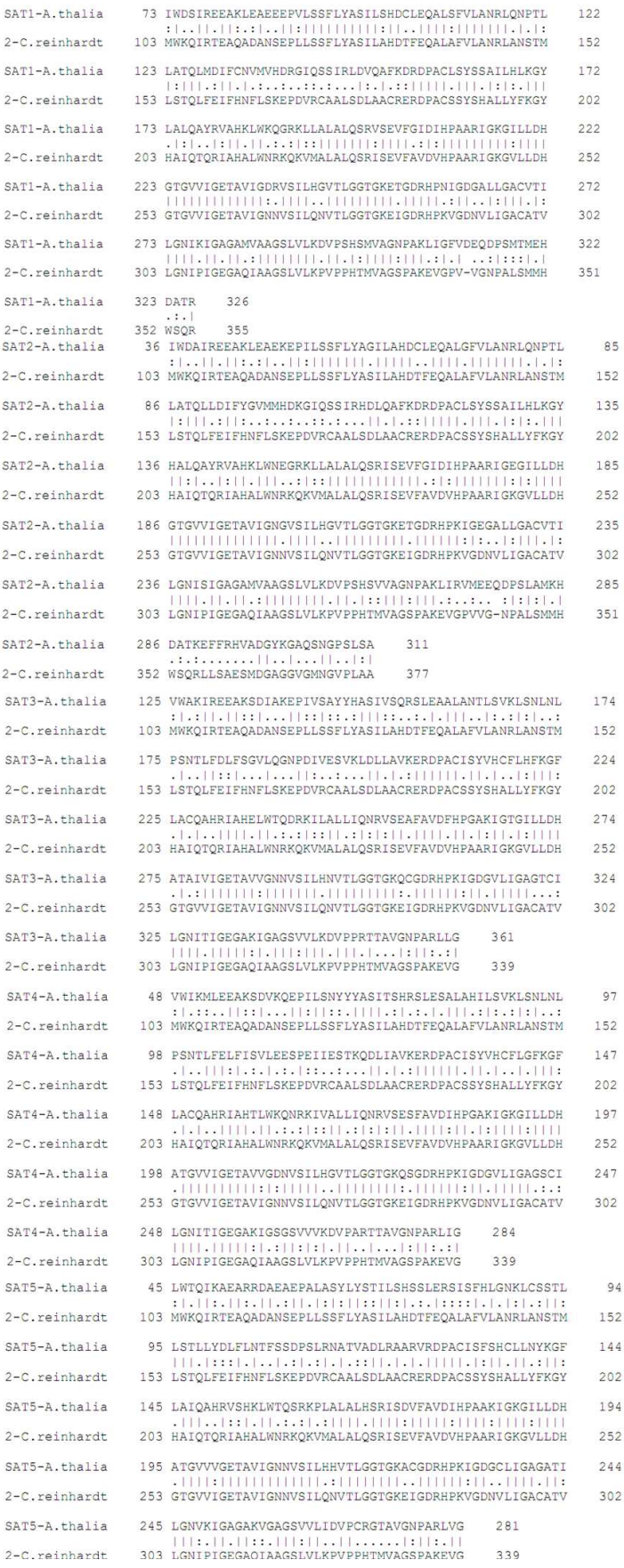

Fig. 7-21. Alignment of 2-*C. reinhardtii* SAT amino acid sequence with *A. thaliana* isoforms.

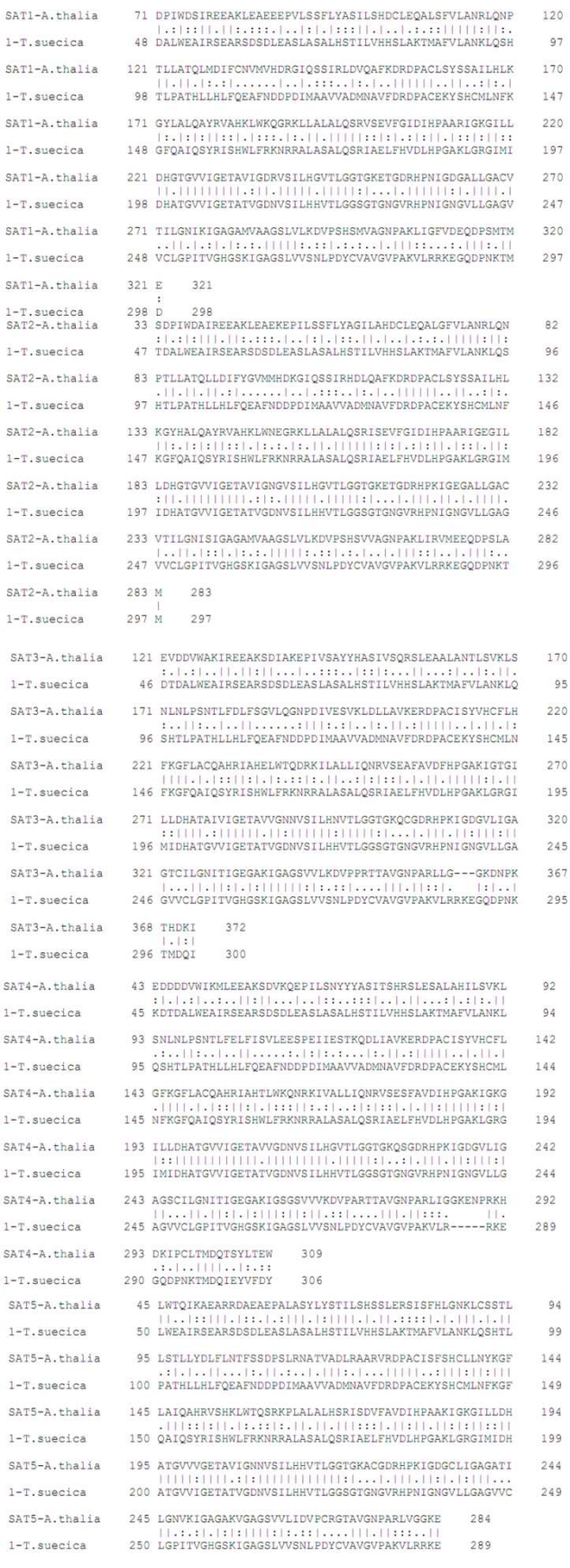

Fig. 7-22. Alignment of 1-*T. suecica* SAT amino acid sequence with *A. thaliana* isoforms.

Fig. 7-23. Alignment of 2-*T. suecica* SAT amino acid sequence with *A. thaliana* isoforms.

Fig. 7-24. Alignment of 3-*T. suecica* SAT amino acid sequence with *A. thaliana* isoforms.

7.3.3. Alignment of the SAT sequences of red algae and red-lineage algae with *A. thaliana* SAT isoforms

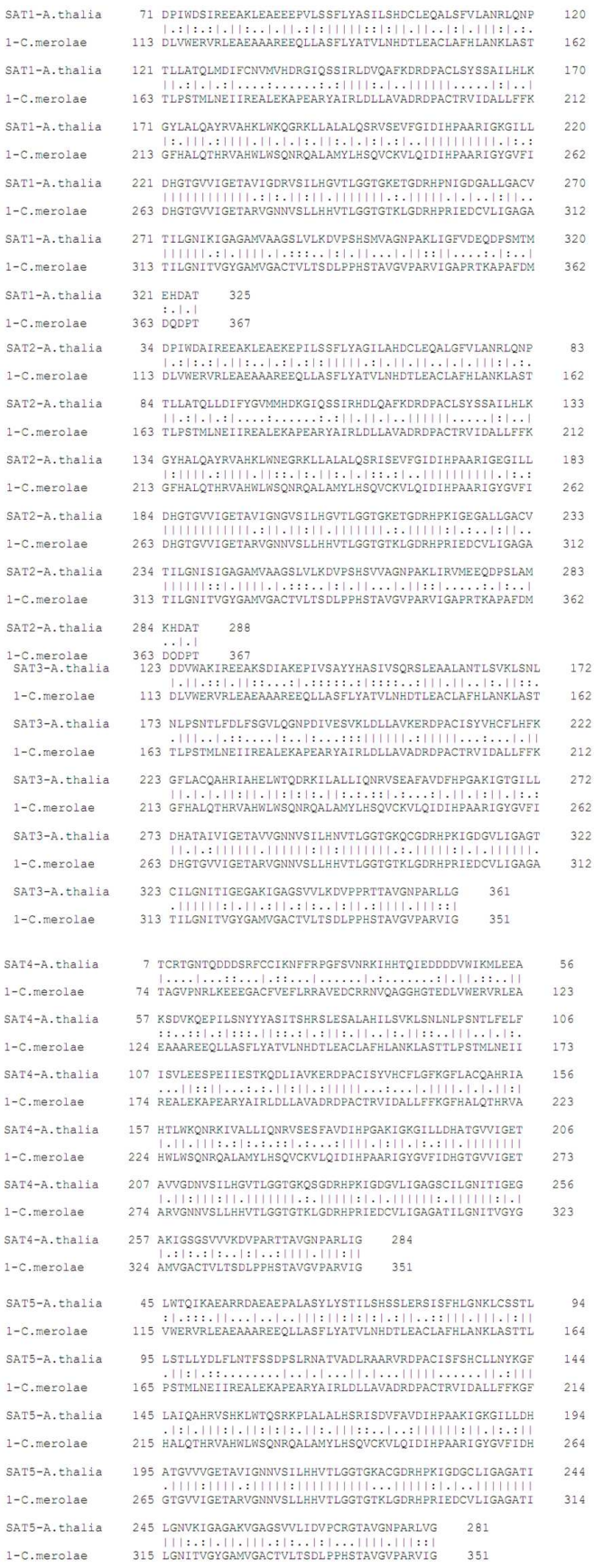

Fig. 7-25. Alignment of 1-*C. merolae* SAT amino acid sequence with *A. thaliana* isoforms.

Fig. 7-26. Alignment of 2-*C. merolae* SAT amino acid sequence with *A. thaliana* isoforms.

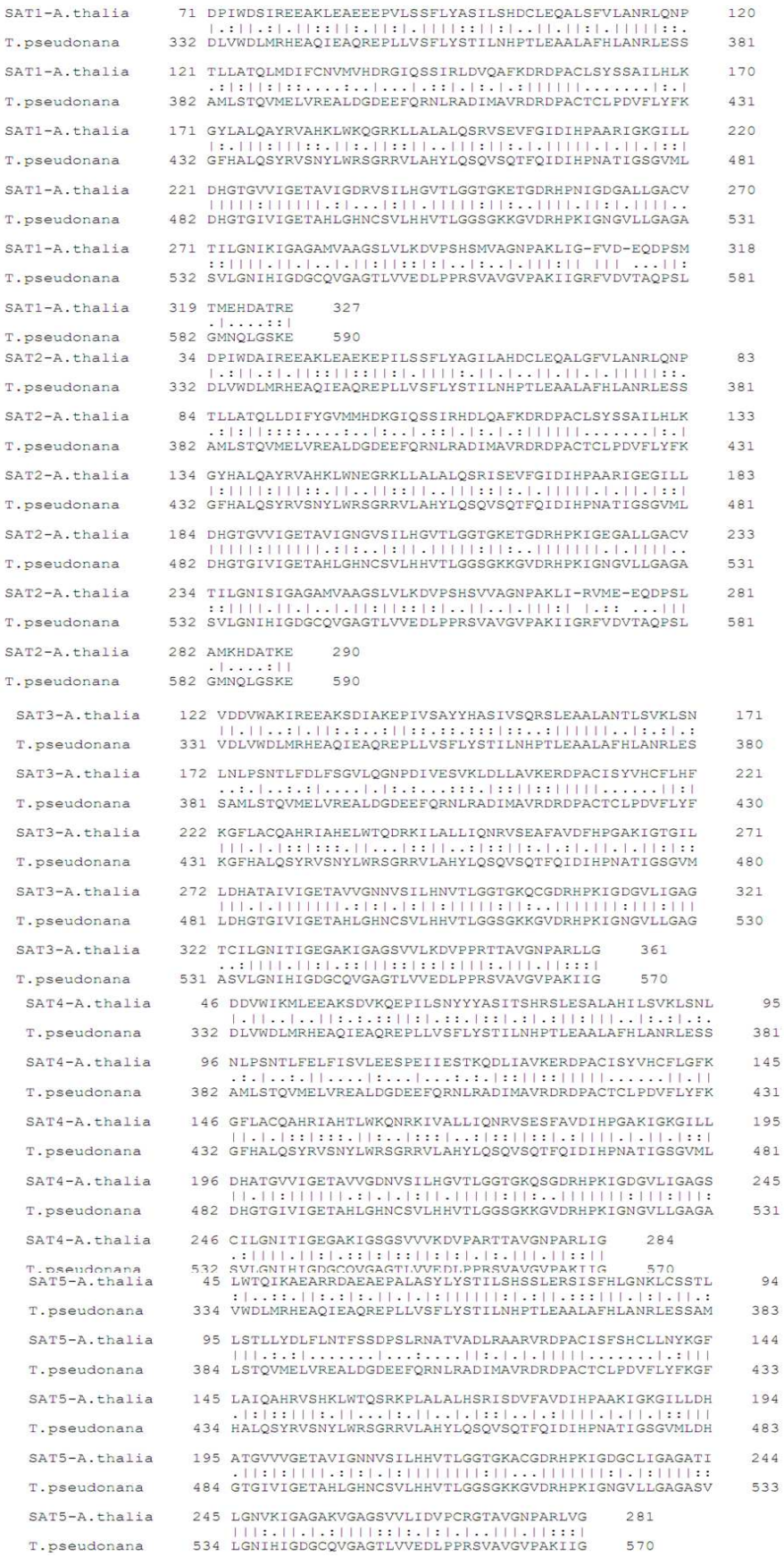

Fig. 7-27. Alignment of *T. pseudonana* SAT amino acid sequence with *A. thaliana* isoforms.

Fig. 7-28. Alignment of *P. tricornutum* SAT amino acid sequence with *A. thaliana* isoforms.

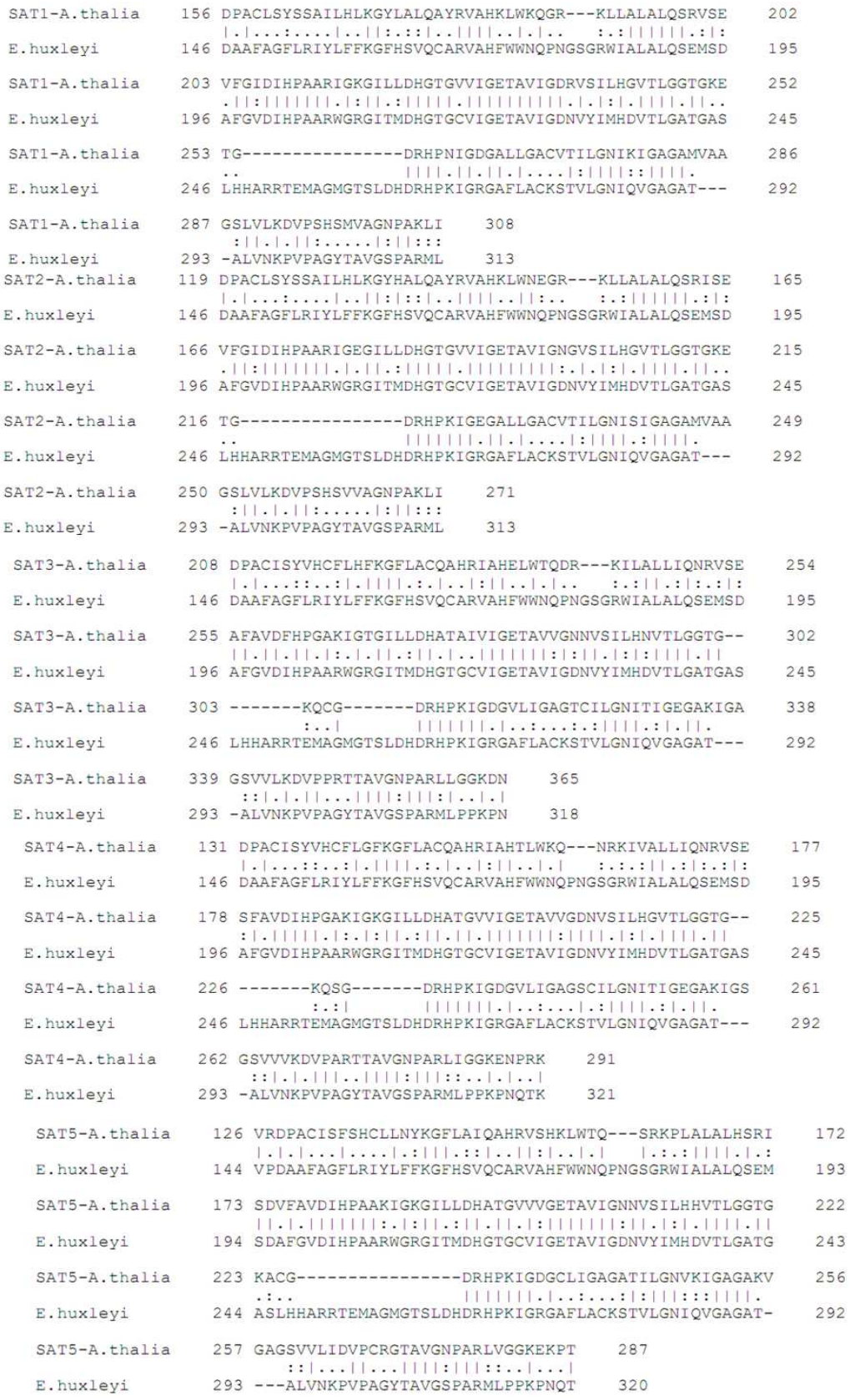

Fig. 7-29. Alignment of *E. huxleyi* SAT amino acid sequence with *A. thaliana* isoforms.

7.3.4. Alignment of the OAS-TL sequence of Cyanobacteria with *A. thaliana* OAS-TL isoforms

Fig. 7-30. Alignment of 1-*Synechocystis* sp. PCC 6803 OAS-TL amino acid with *A. thaliana* isoforms.

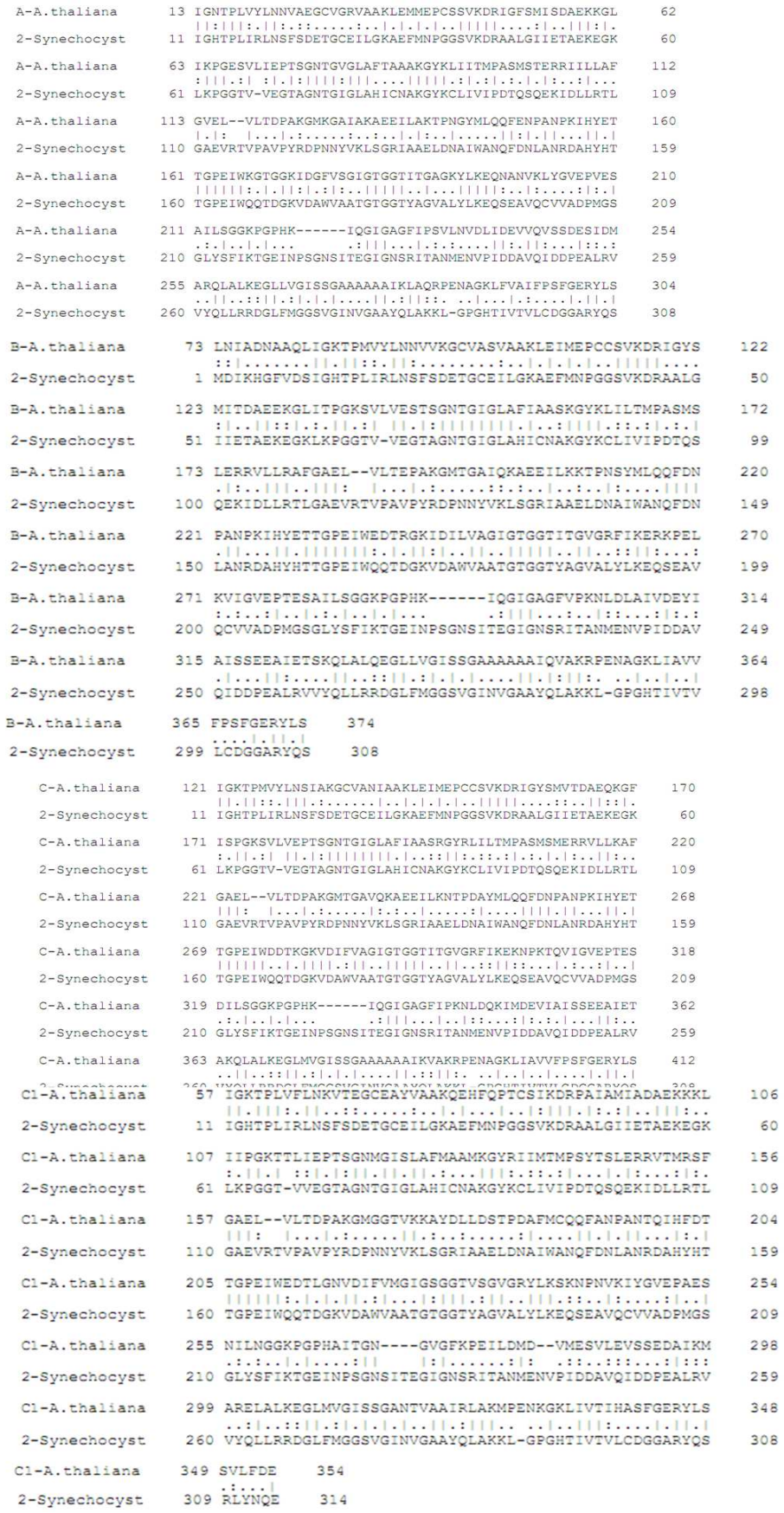

Fig. 7-31. Alignment of 2-*Synechocystis* sp. PCC 6803 OAS-TL amino acid with *A. thaliana* isoforms.

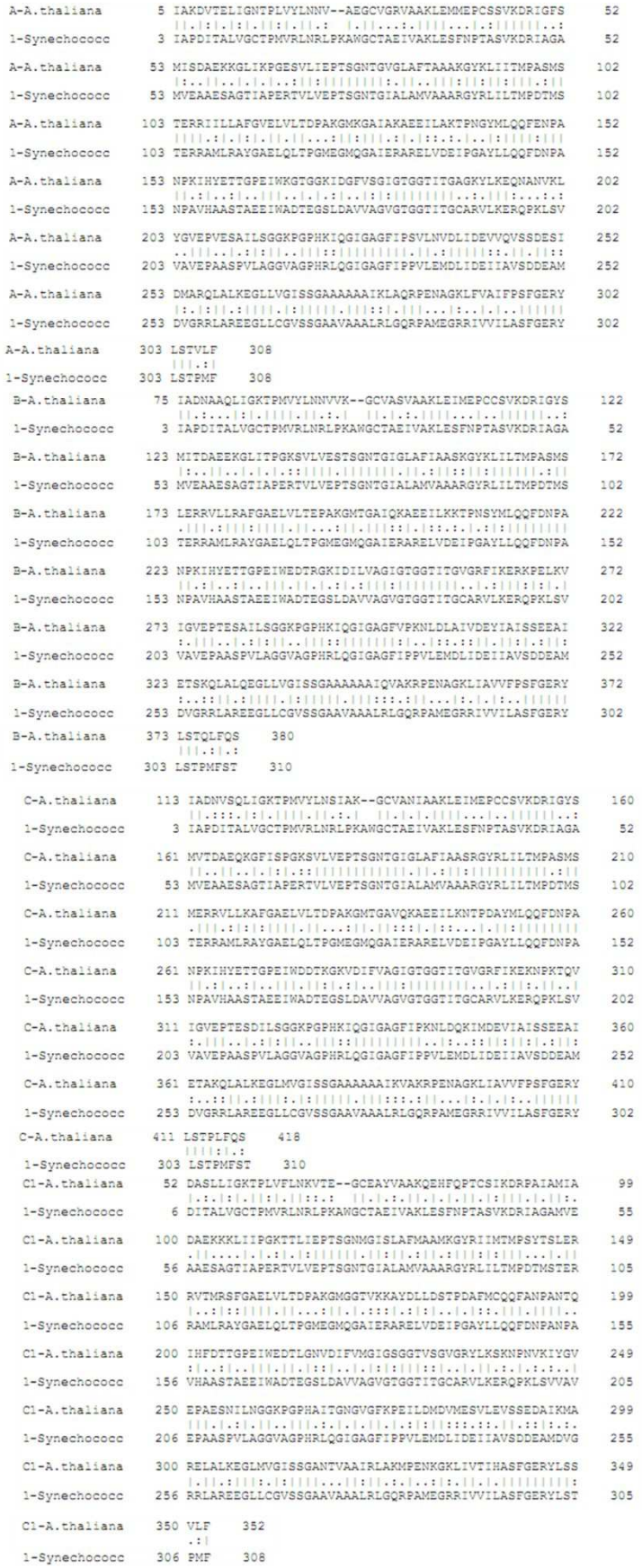

Fig. 7-32. Alignment of 1-*Synechococcus* sp. WH 7803 OAS-TL amino acid with *A. thaliana* isoforms.

Fig. 7-33. Alignment of 2-*Synechococcus* sp. WH 7803 OAS-TL amino acid with *A. thaliana* isoforms.

7.3.5. Alignment of the OAS-TL sequence of green algae with *A. thaliana* OAS-TL isoforms

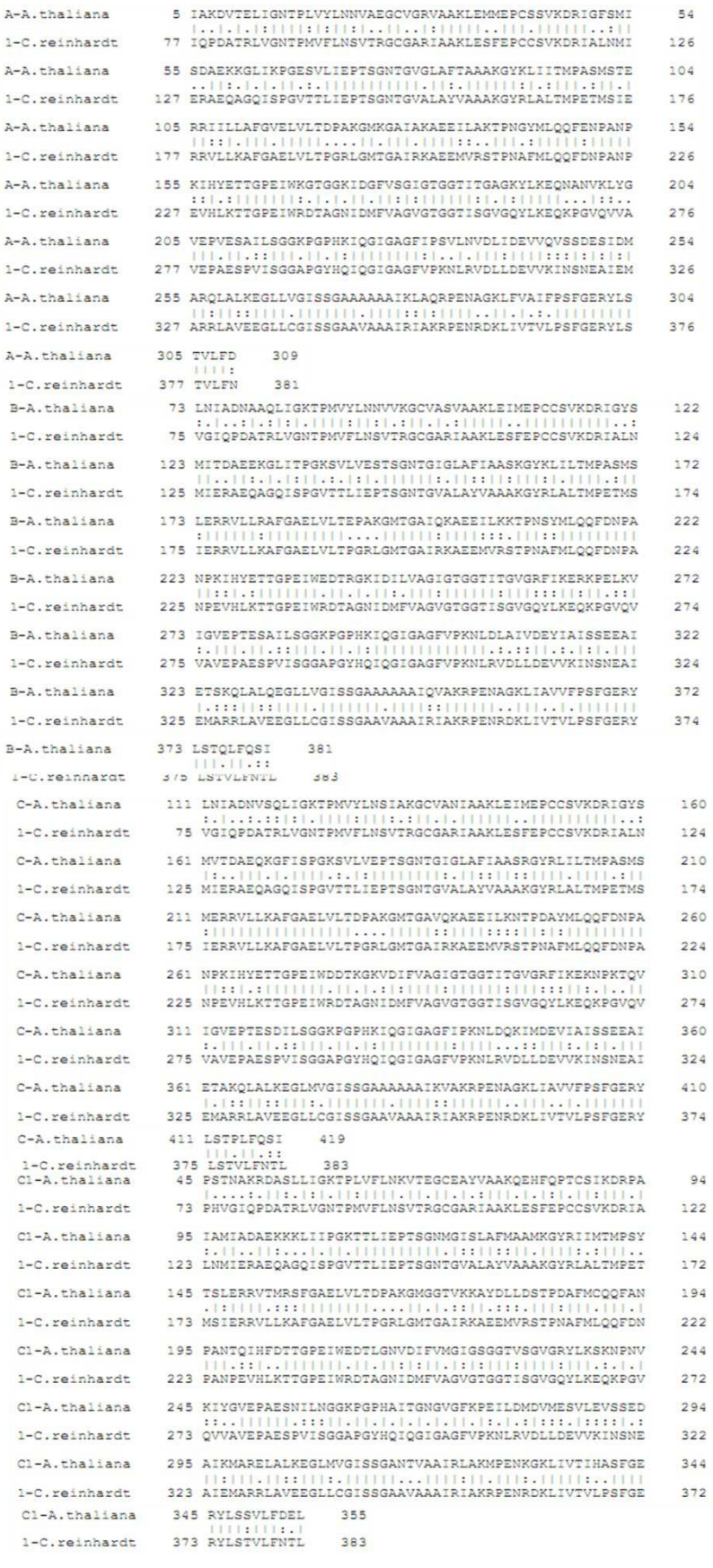

Fig. 7-34. Alignment of 1-*C. reinhardtii* OAS-TL amino acid with *A. thaliana* isoforms.

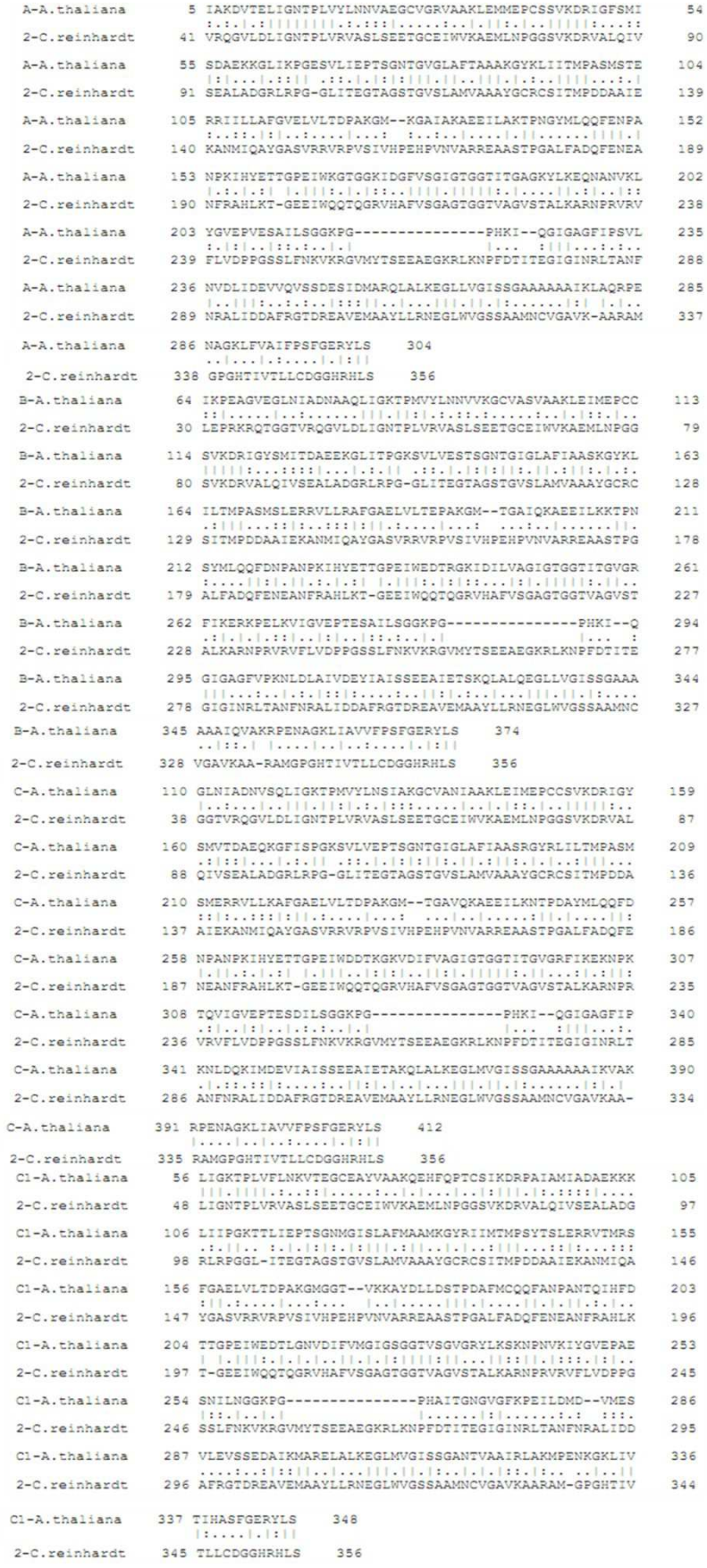

Fig. 7-35. Alignment of 2-*C. reinhardtii* OAS-TL amino acid with *A. thaliana* isoforms.

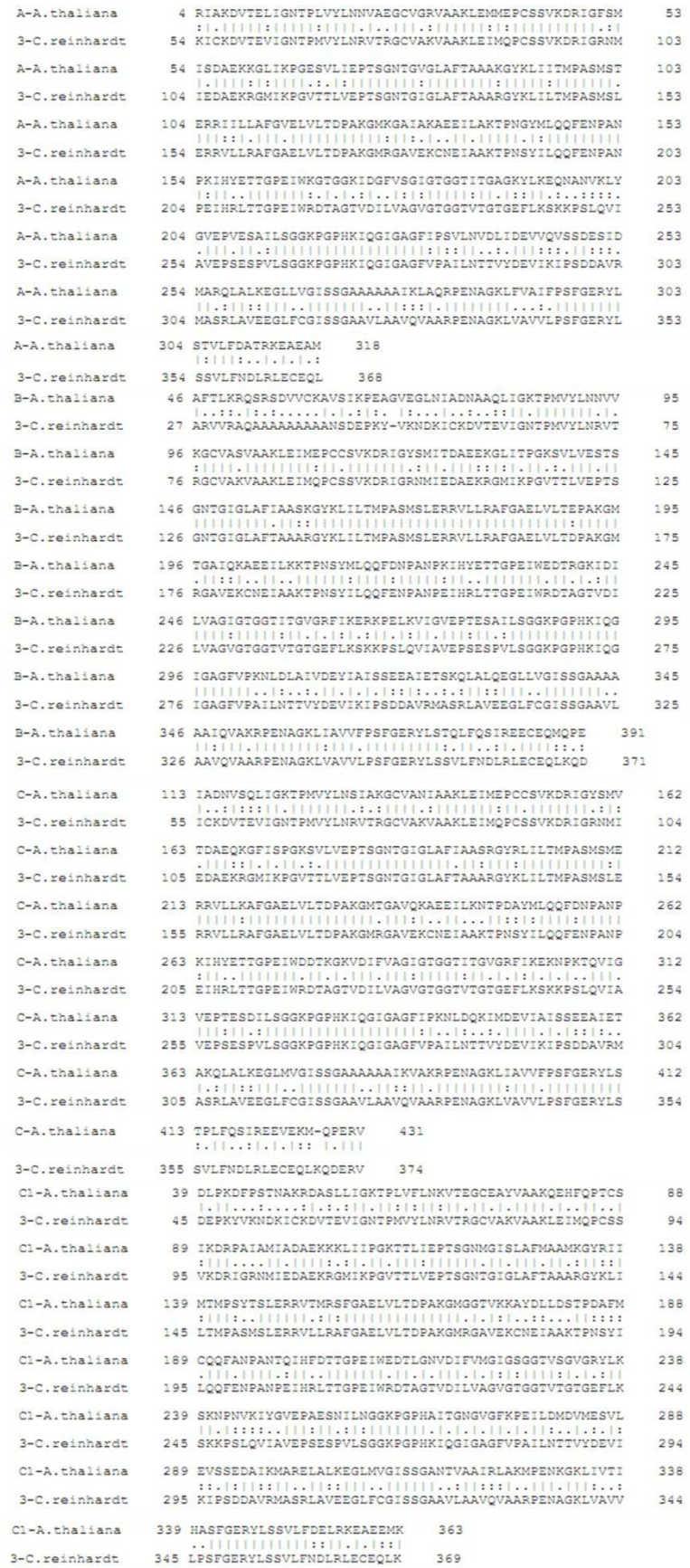

Fig. 7-36. Alignment of 3-*C. reinhardtii* OAS-TL amino acid with *A. thaliana* isoforms.

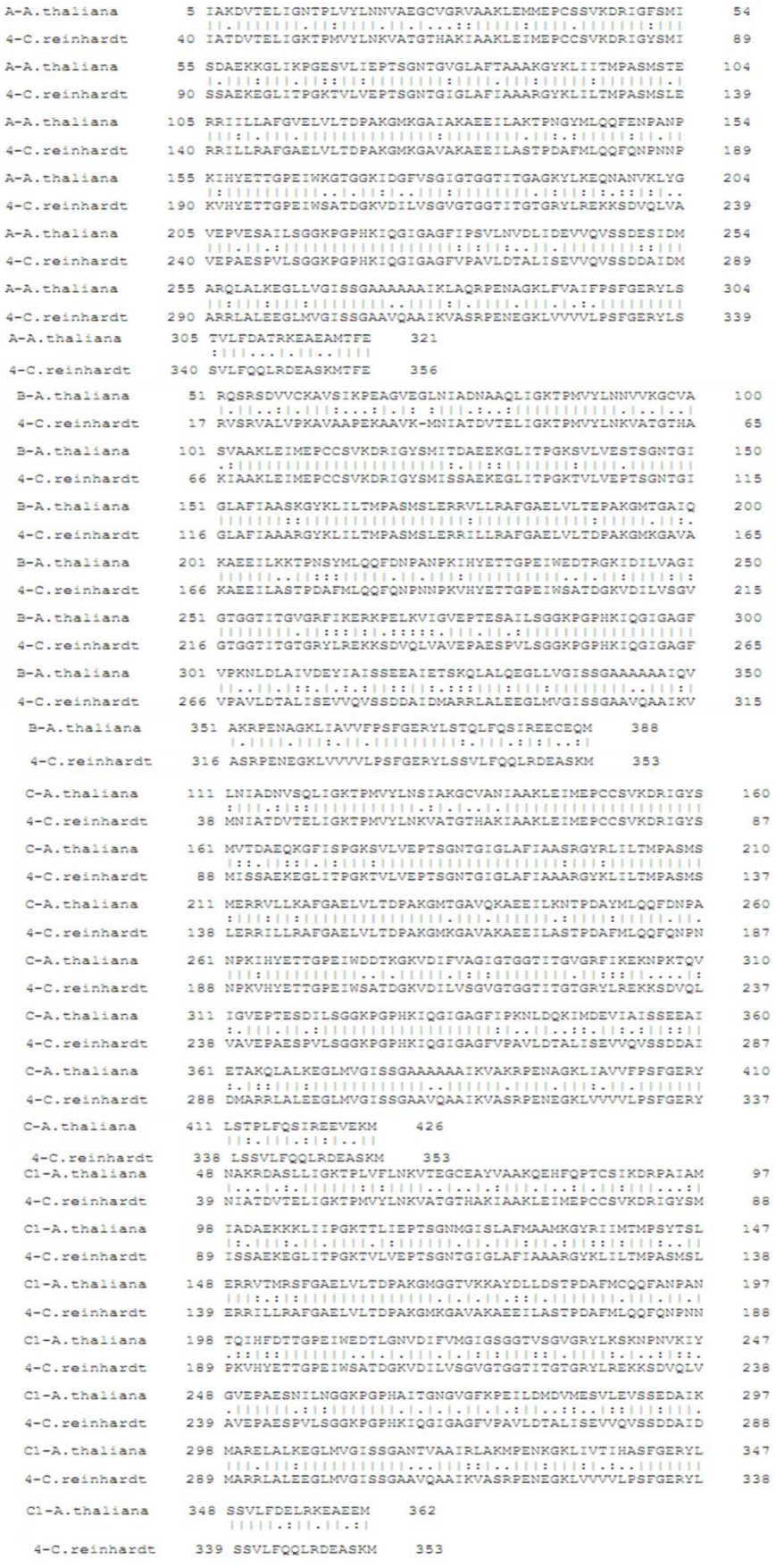

Fig. 7-37. Alignment of 4-*C. reinhardtii* OAS-TL amino acid with *A. thaliana* isoforms.

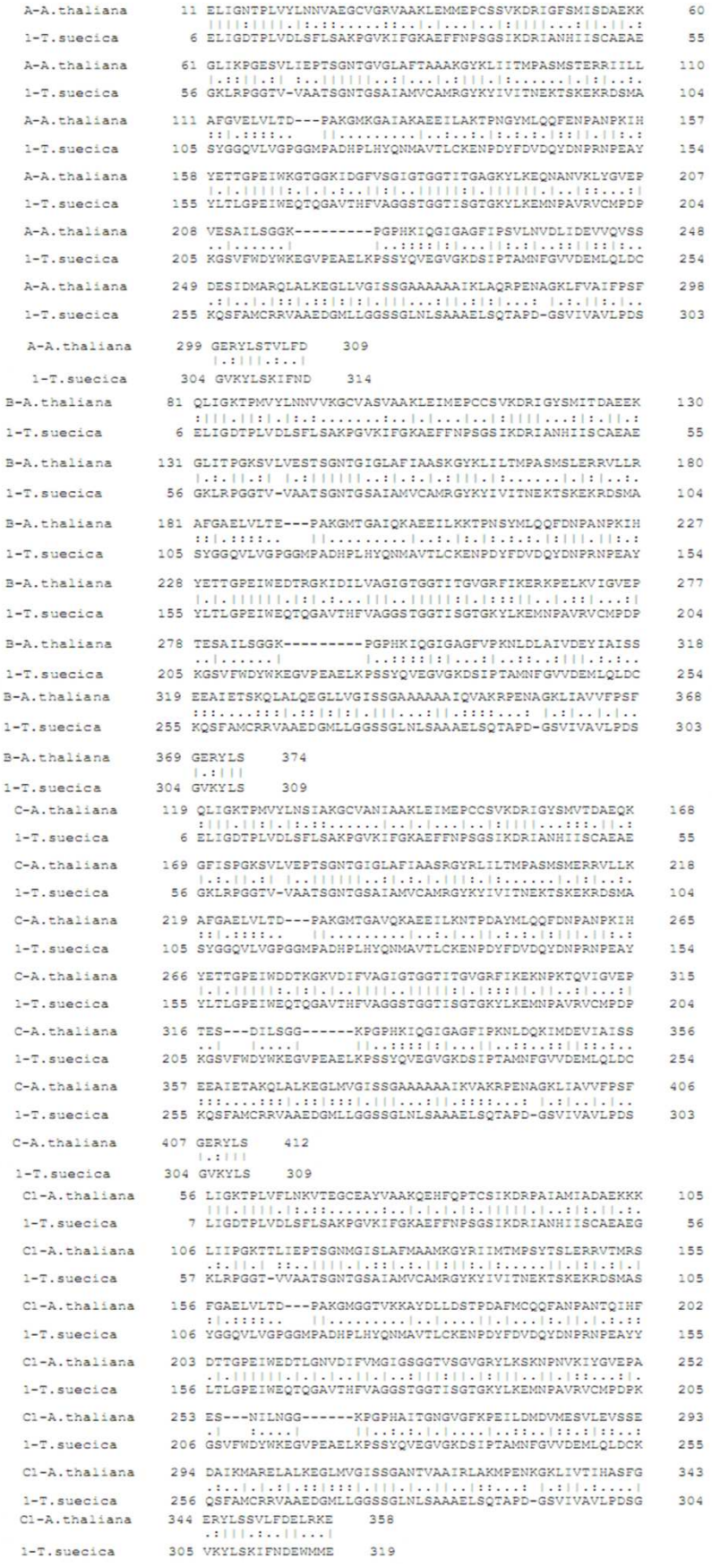

Fig. 7-38. Alignment of 1-*T. suecica* OAS-TL amino acid with *A. thaliana* isoforms.

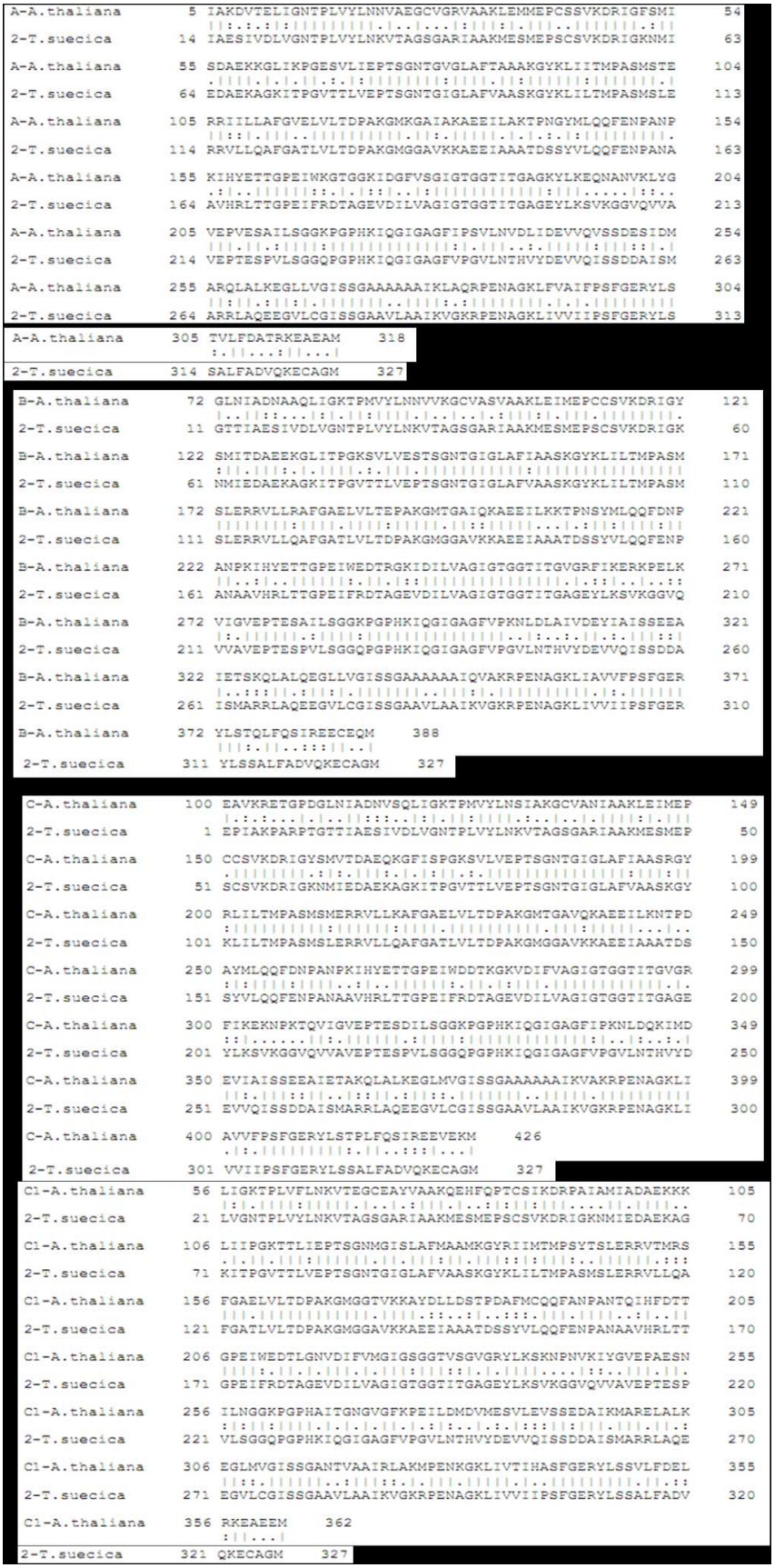

Fig. 7-39. Alignment of 2-*T. suecica* OAS-TL amino acid with *A. thaliana* isoforms.

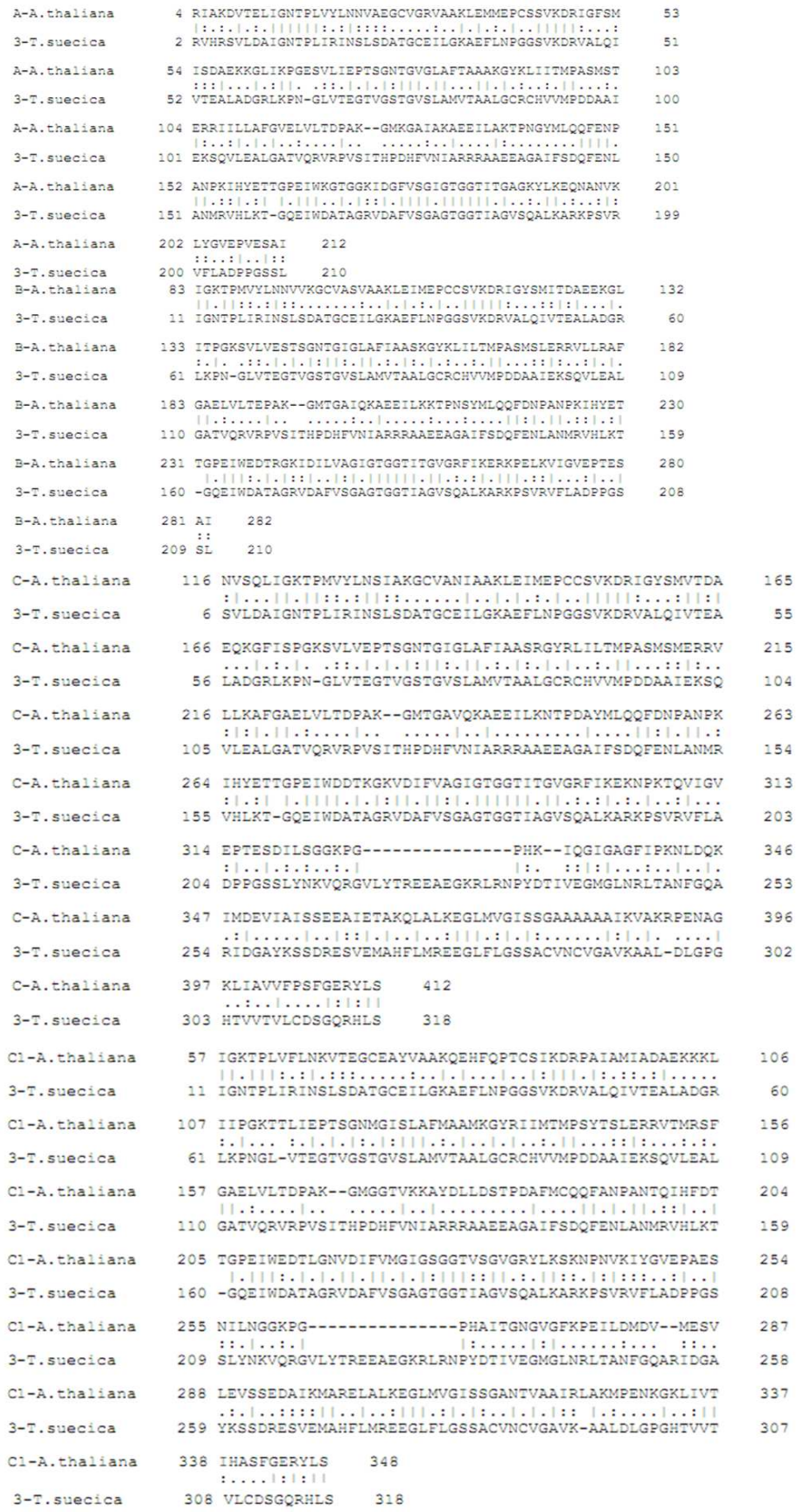

Fig. 7-40. Alignment of 3-*T. suecica* OAS-TL amino acid with *A. thaliana* isoforms.

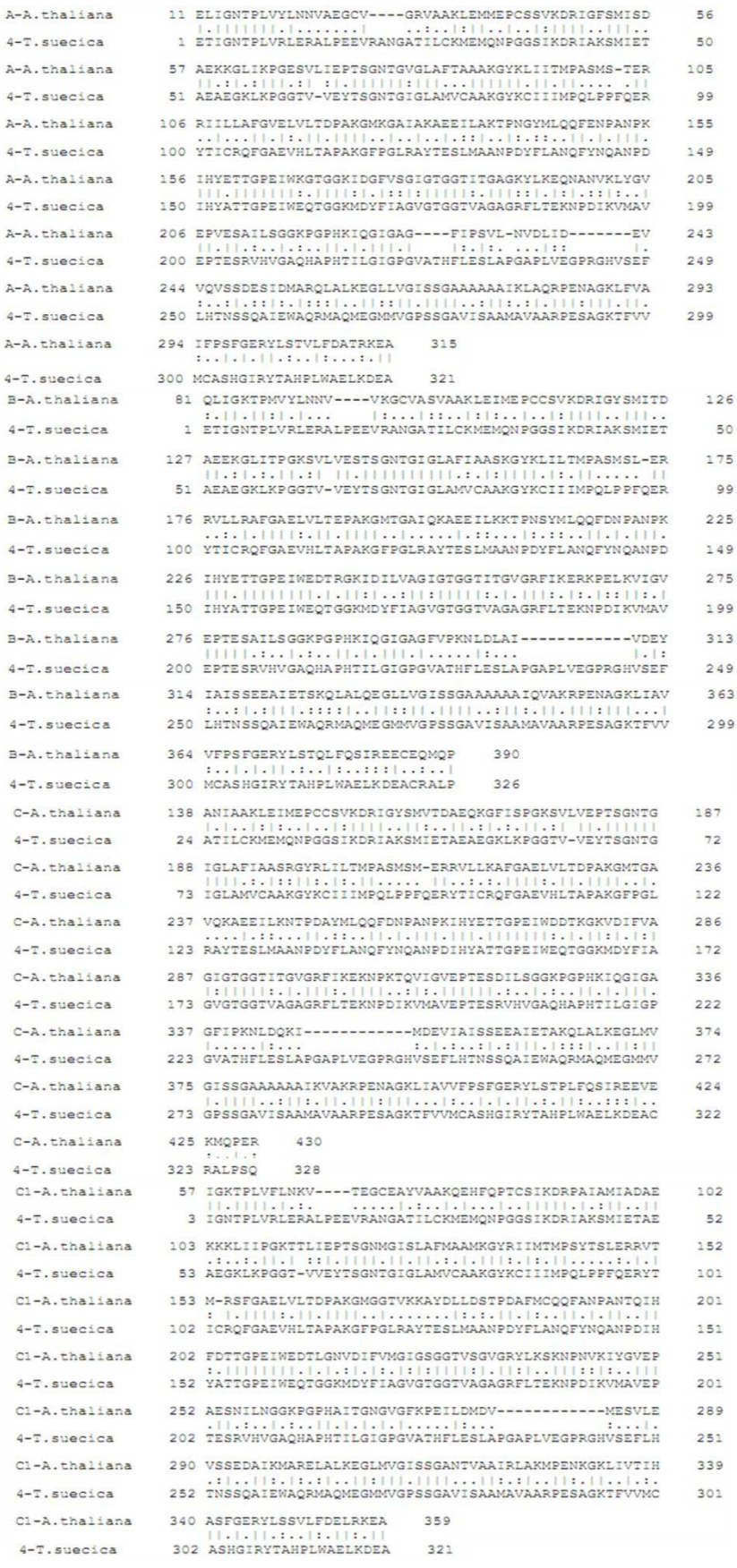

Fig. 7-41. Alignment of 4-*T. suecica* OAS-TL amino acid with *A. thaliana* isoforms.

7.3.6. Alignment of the OAS-TL sequence of red and red-lineage algae with *A. thaliana* OAS-TL isoforms

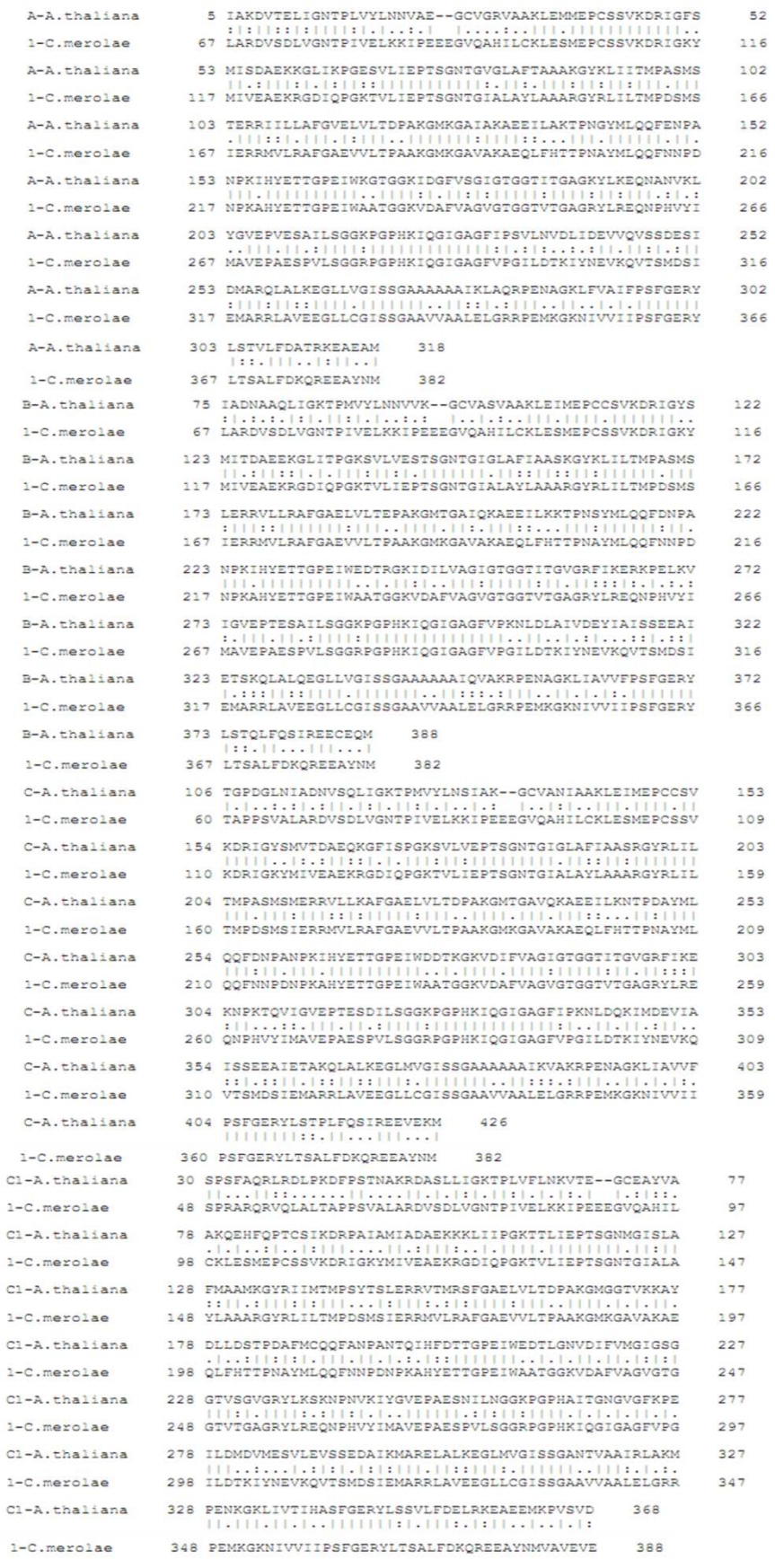

Fig. 7-42. Alignment of 1-*C. merolae* OAS-TL amino acid with *A. thaliana* isoforms.

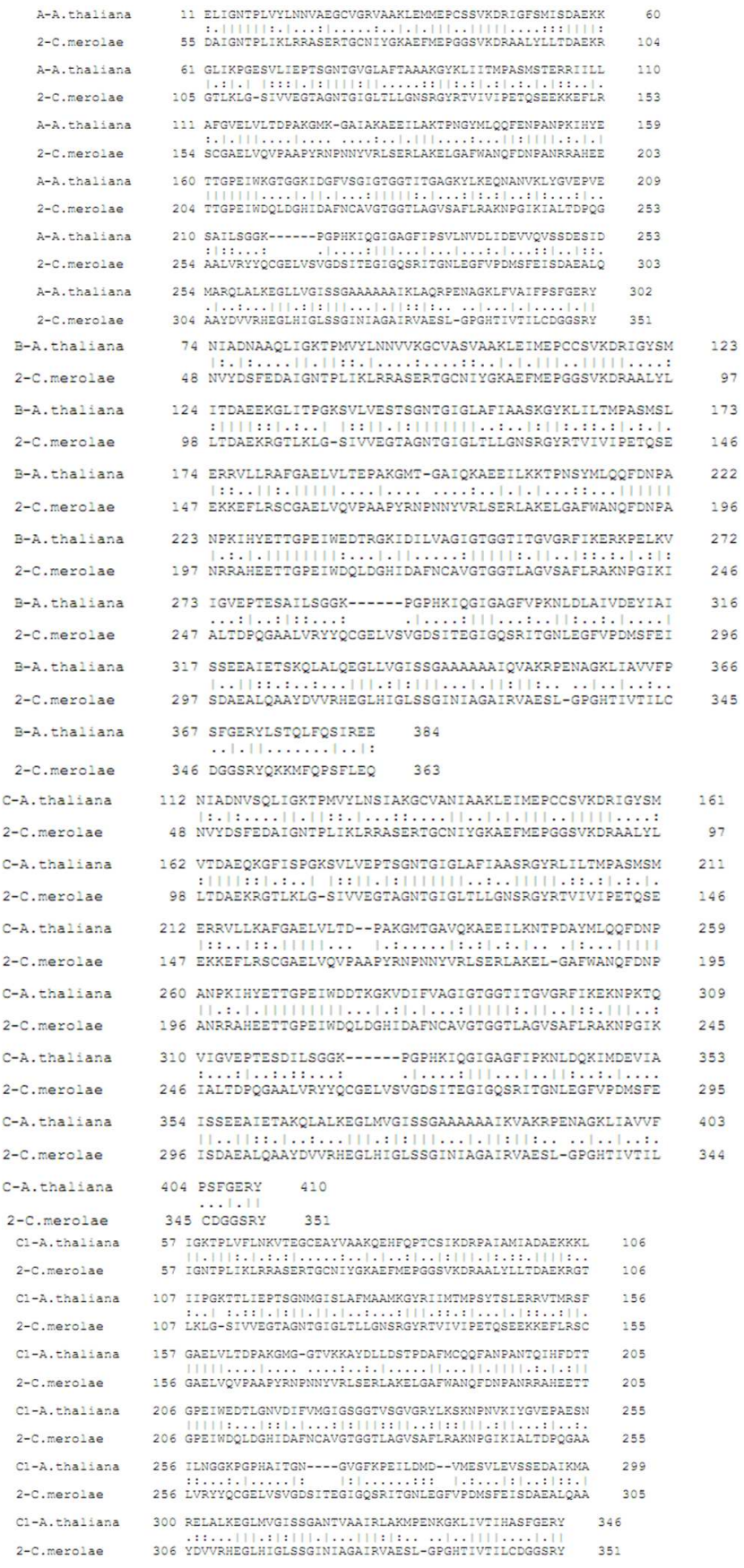

Fig. 7-43. Alignment of 2-*C. merolae* OAS-TL amino acid with *A. thaliana* isoforms.

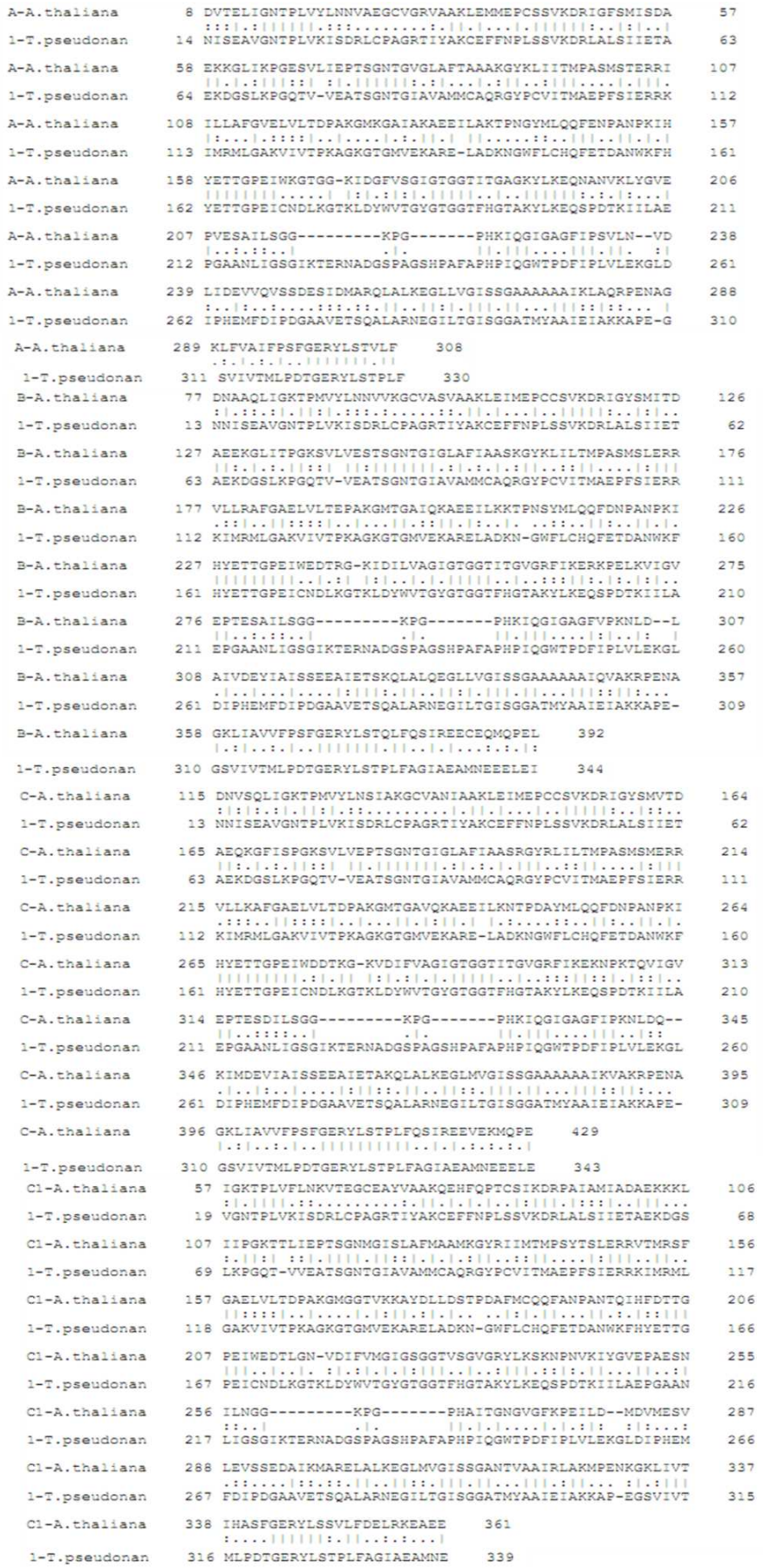

Fig. 7-44. Alignment of 1-*T. pseudonana* OAS-TL amino acid with *A. thaliana* isoforms.

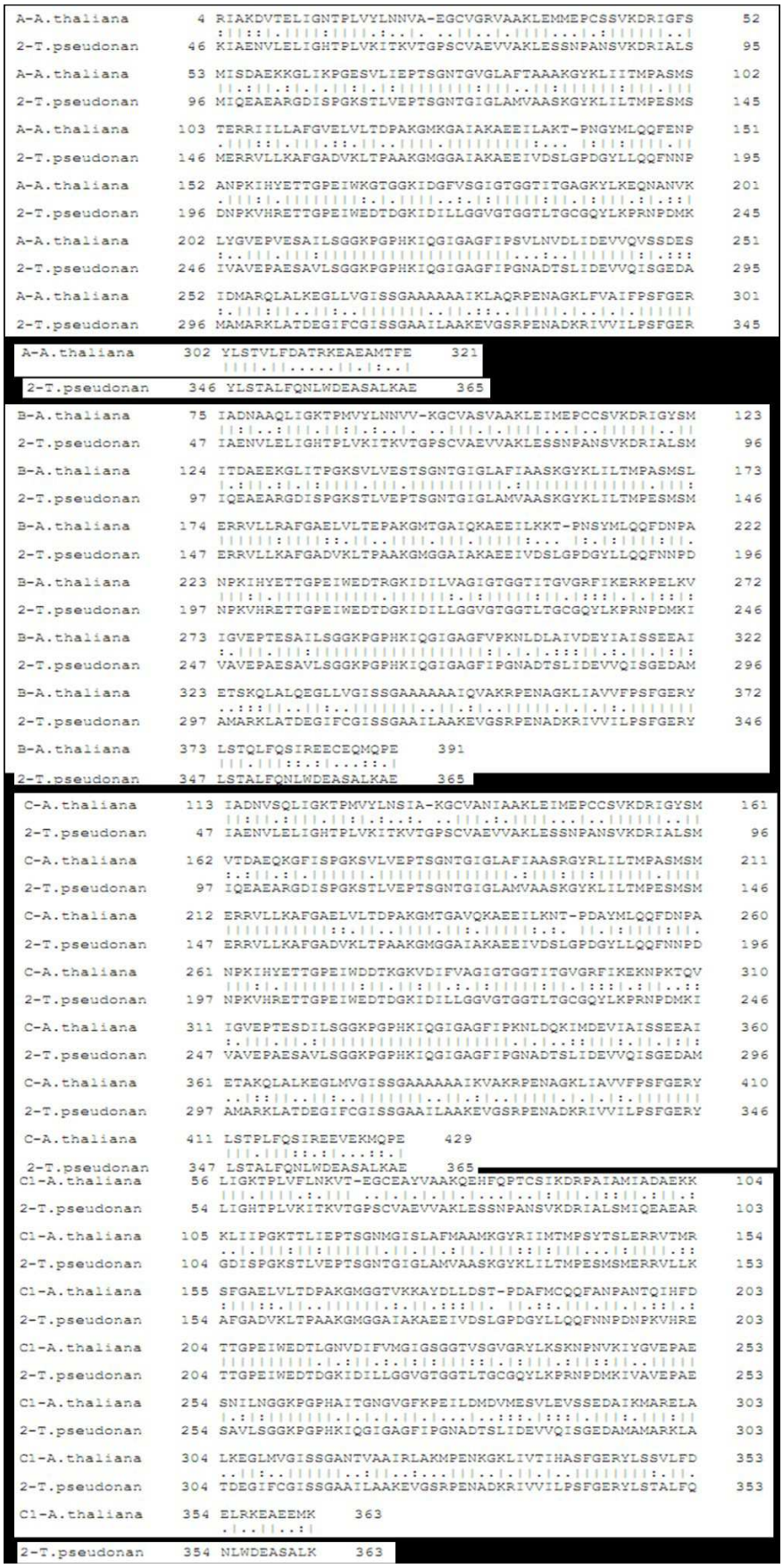

Fig. 7-45. Alignment of 2-*T. pseudonana* OAS-TL amino acid with *A. thaliana* isoforms.

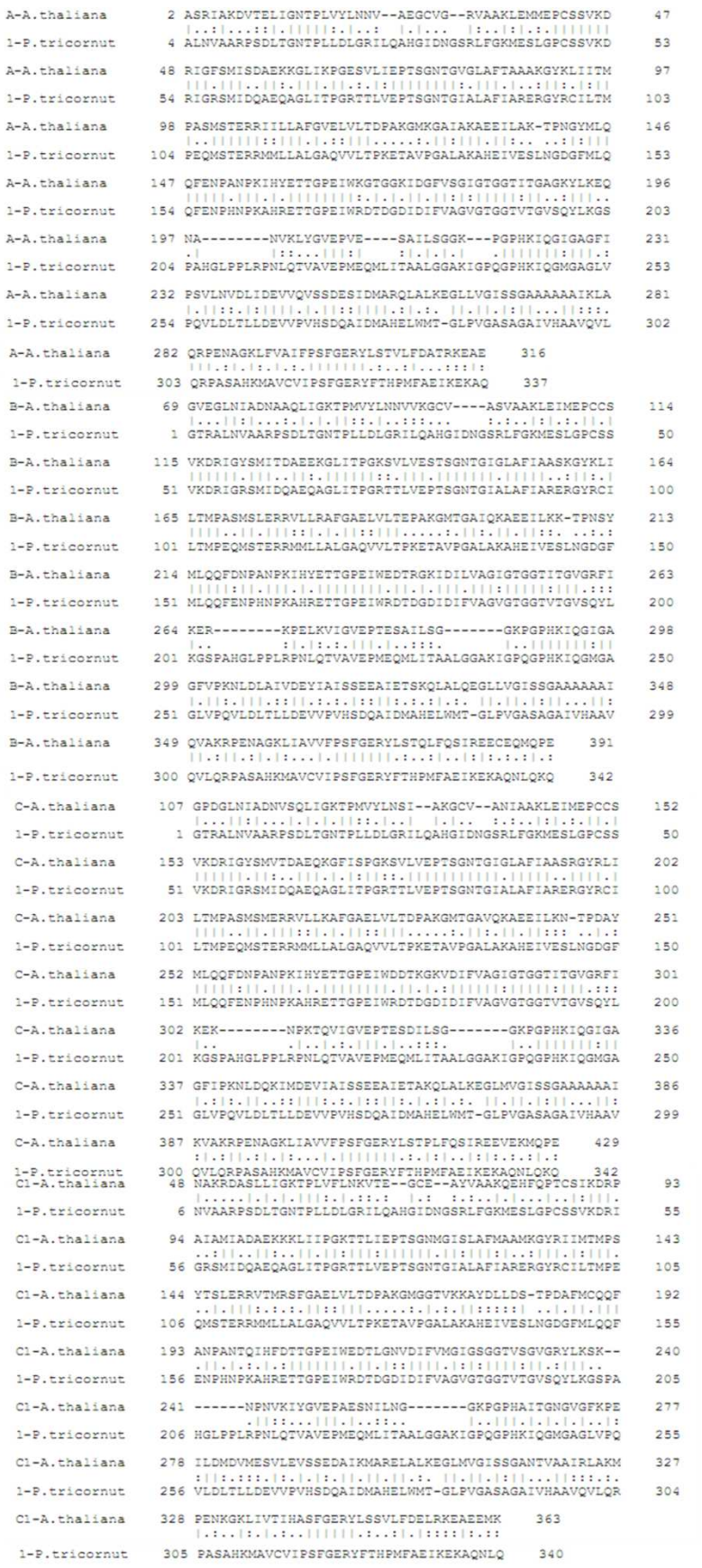

Fig. 7-46. Alignment of 1-*P. tricornutum* OAS-TL amino acid with *A. thaliana* isoforms.

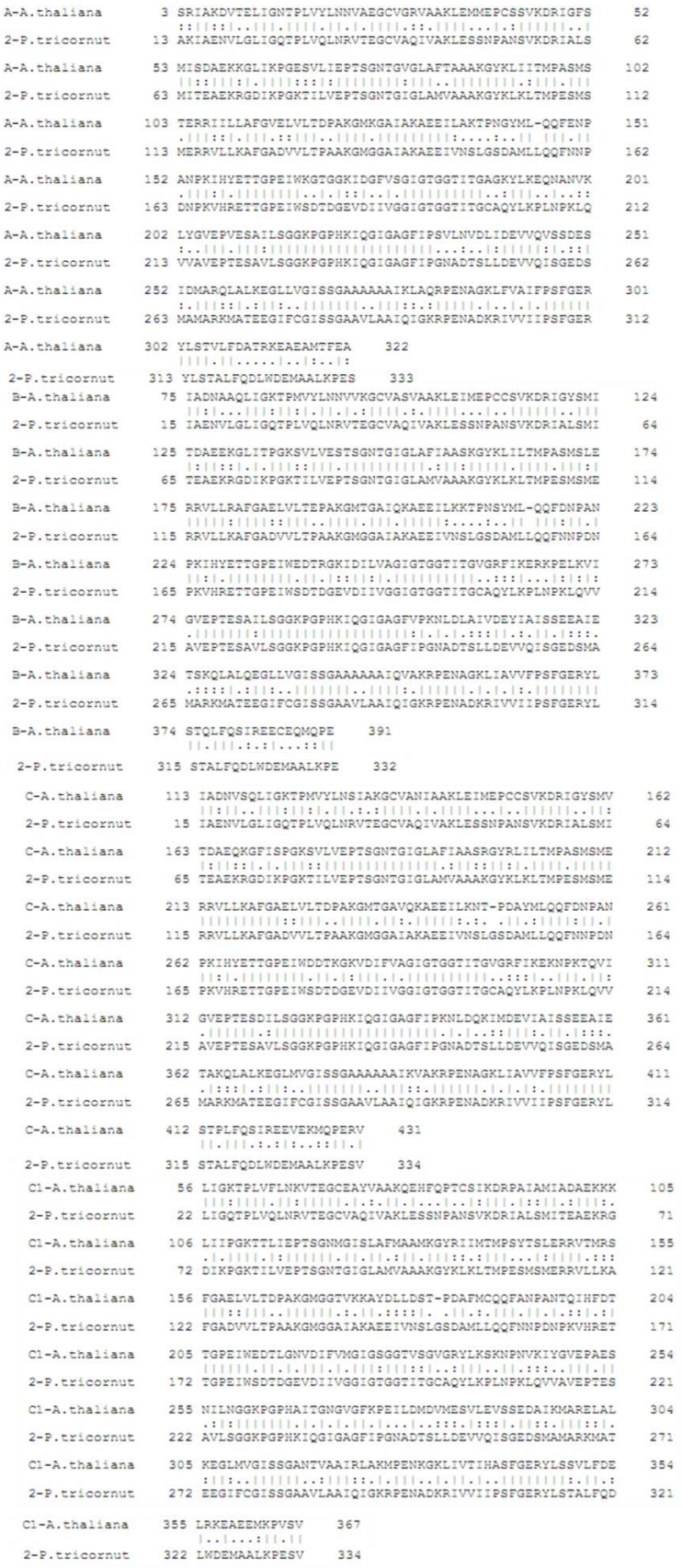

Fig. 7- 47. Alignment of 2-*P. tricornutum* OAS-TL amino acid with *A. thaliana* isoforms.

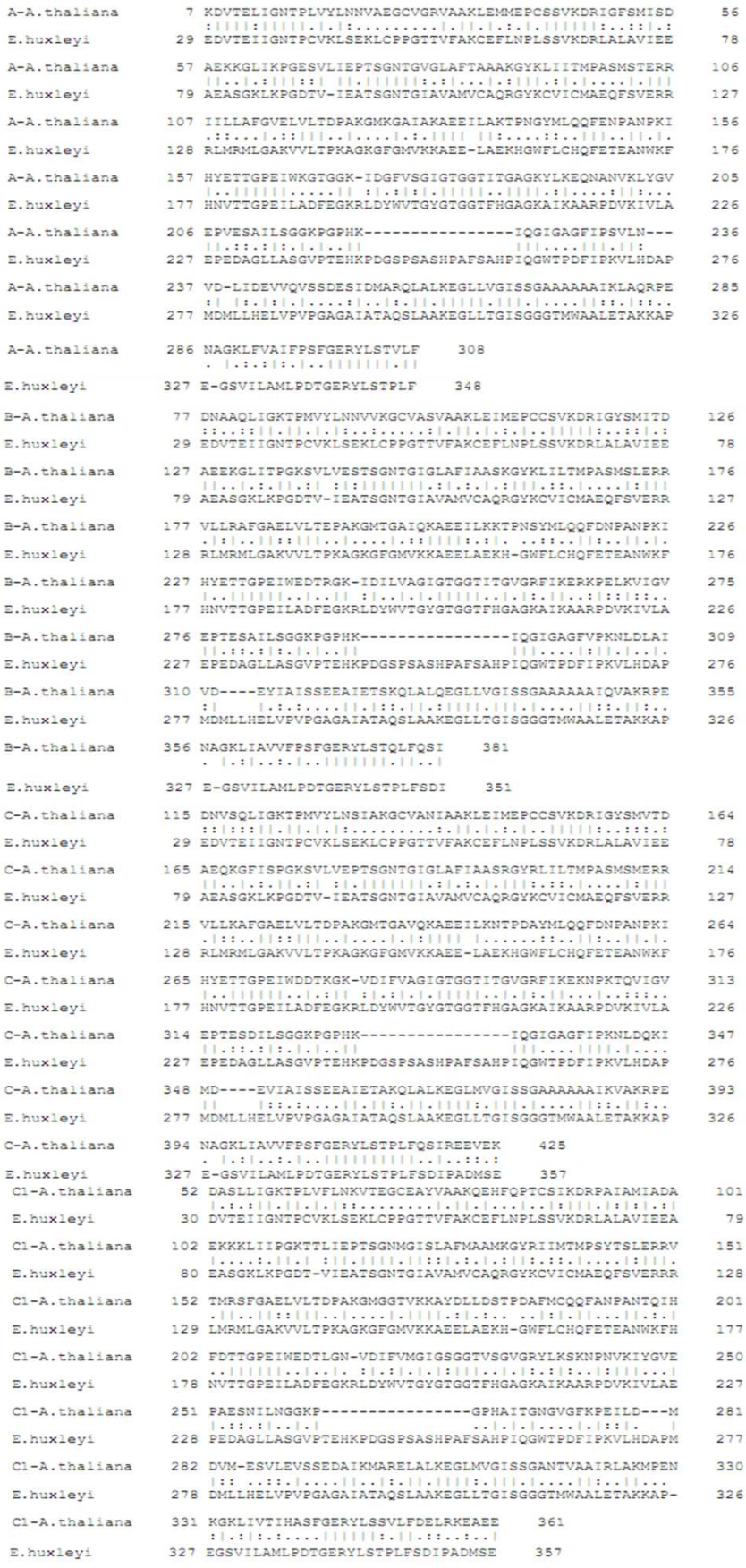

Fig. 7-48. Alignment of *E. huxleyi* OAS-TL amino acid with *A. thaliana* isoforms.

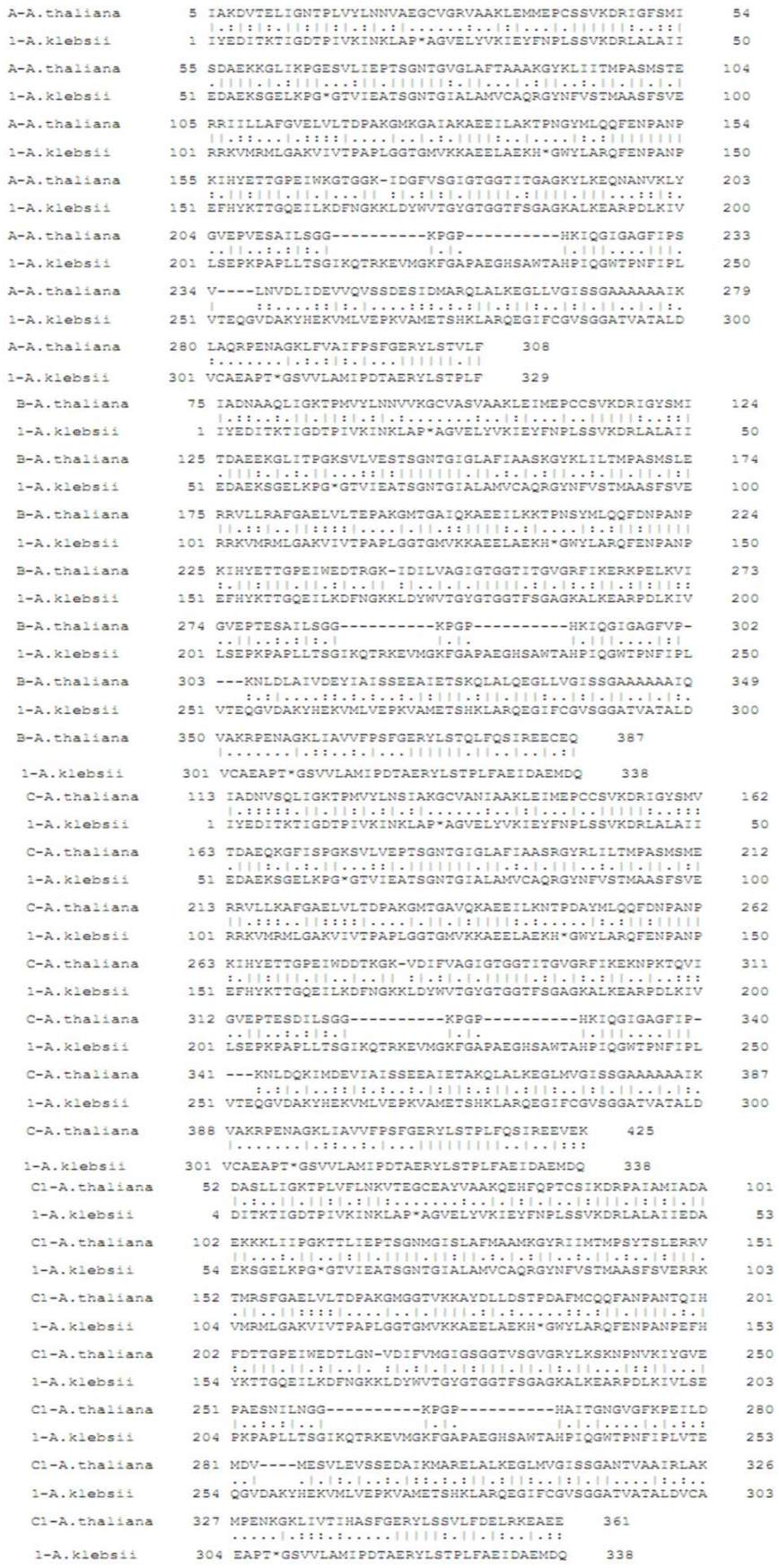

Fig. 7-49. Alignment of 1-*A. klebsii* OAS-TL amino acid with *A. thaliana* isoforms.

```
A-A.thaliana      12 LIGNTPLVYLNNVAEGCVGRVAAKLEMMEPCSSVKDRIGFSMISDAEKKG      61
                     |:|||||:.|..:|:...|||..|.|.:.|....|||:..|::::||..|
2-A.klebsii        5 LVGNTPLIELRALSAATGGRVVGKAEFLSPGGCQKDRVAVSILAEAEATG      54

A-A.thaliana      62 LIKPGESVLIEPTSGNTGVGLAFTAAAKGYKLIITMPASMSTERRIILLA     111
                     .:::|| |.:::|.|||:||:.|...|.::||||::|.||...:.|:..:|..
2-A.klebsii       55 RLQPG-STIVEGTSGSTGISLTLAARSRGYKVLIVMPDDQAEEKVQLLRR     103

A-A.thaliana     112 FGVELVLTDPAKGMKGA----IAKAEEILAKTPNGYMLQQFENPANPKIH     157
                     .|.|:.|..||..:...    :|:..........|....||||.||.|.|
2-A.klebsii      104 LGAEVELVRPASIVSPDHYVNVARRRAHELDATGGLFADQFENLANYKAH     153

A-A.thaliana     158 YETTGPEIWKGTGGKIDGFVSGIGTGGTITGAGKYLKEQNANVKLYGVEP     207
                     :|.||||:|:...::|.||...||||||.|.|.:||:|...:.:|..:.
2-A.klebsii      154 FEGTGPELWEQCDHRLDAFVMSAGTGGTIVGTGSFLKQQAPEIGVYLADV     203

A-A.thaliana     208 VESAIL    213
                     ..|::|
2-A.klebsii      204 PGSSLL    209

B-A.thaliana      80 AQLIGKTPMVYLNNVVKGCVASVAAKLEIMEPCCSVKDRIGYSMITDAEE     129
                     |.|:|.||::.|..:.......|..|.|.:.|....|||:..|::.:||.
2-A.klebsii        3 AGLVGNTPLIELRALSAATGGRVVGKAEFLSPGGCQKDRVAVSILAEAEA      52

B-A.thaliana     130 KGLITPGKSVLVESTSGNTGIGLAFIAASKGYKLILTMPASMSLERRVLL     179
                     .|.:.|| |.:||.|||:|||.|...|.|:|||:::.||...:.|:..||
2-A.klebsii       53 TGRLQPG-STIVEGTSGSTGISLTLAARSRGYKVLIVMPDDQAEEKVQLL     101

B-A.thaliana     180 RAFGAELVLTEPAKGMTGA----IQKAEEILKKTPNSYMLQQFDNPANPK     225
                     |..|||:.|..||..::..    :.:..............||:|.||.|
2-A.klebsii      102 RRLGAEVELVRPASIVSPDHYVNVARRRAHELDATGGLFADQFENLANYK     151

B-A.thaliana     226 IHYETTGPEIWEDTRGKIDILVAGIGTGGTITGVGRFIKERKPELKVIGV     275
                     .|:|.||||:||...::|..|...||||||.|.|.|:||:.||...
2-A.klebsii      152 AHFEGTGPELWEQCDHRLDAFVMSAGTGGTIVGTGSFLKQQAPEIGVYLA     201

B-A.thaliana     276 EPTESAIL    283
                     :...|::|
2-A.klebsii      202 DVPGSSLL    209

C-A.thaliana     120 LIGKTPMVYLNSIAKGCVANIAAKLEIMEPCCSVKDRIGYSMVTDAEQKG     169
                     |:|.||::.|.:::.....:..|.|.:.|....|||:..|::.:||..|
2-A.klebsii        5 LVGNTPLIELRALSAATGGRVVGKAEFLSPGGCQKDRVAVSILAEAEATG      54

C-A.thaliana     170 FISPGKSVLVEPTSGNTGIGLAFIAASRGYRLILTMPASMSMERRVLLKA     219
                     .:.|| |.:||.|||:|||.|...|.||||::::.||...:.|:..||:.
2-A.klebsii       55 RLQPG-STIVEGTSGSTGISLTLAARSRGYKVLIVMPDDQAEEKVQLLRR     103

C-A.thaliana     220 FGAELVLTDPAKGMTGA----VQKAEEILKNTPDAYMLQQFDNPANPKIH     265
                     .|||:.|..||..::..    |.:.....:.....||:|.||.|.|
2-A.klebsii      104 LGAEVELVRPASIVSPDHYVNVARRRAHELDATGGLFADQFENLANYKAH     153

C-A.thaliana     266 YETTGPEIWDDTKGKVDIFVAGIGTGGTITGVGRFIKEKNPKTQVIGVEP     315
                     :|.||||:|:....::|.||...||||||.|.|.|:|::.|:..|...:.
2-A.klebsii      154 FEGTGPELWEQCDHRLDAFVMSAGTGGTIVGTGSFLKQQAPEIGVYLADV     203

C-A.thaliana     316 TESDIL    321
                     ..|.:|
2-A.klebsii      204 PGSSLL    209


C1-A.thaliana     56 LIGKTPLVFLNKVTEGCEAYVAAKQEHFQPTCSIKDRPAIAMIADAEKKK     105
                     |:|.|||:.|..::.....|..|.|...|....|||.|:::::|:||...
2-A.klebsii        5 LVGNTPLIELRALSAATGGRVVGKAEFLSPGGCQKDRVAVSILAEAEATG      54

C1-A.thaliana    106 LIIPGKTTLIEPTSGNMGISLAFMAAMKGYRIIMTMPSYTSLERRVTMRS     155
                     .:.|| :|:::|.|||:.||||...|..:||::::.||...:.|:...:|.
2-A.klebsii       55 RLQPG-STIVEGTSGSTGISLTLAARSRGYKVLIVMPDDQAEEKVQLLRR     103

C1-A.thaliana    156 FGAELVLTDPAKGMG-----GTVKKAYDLLDSTPDAFMCQQFANPANTQI     200
                     .|||:.|..||..:.     ...::....||:|...| ..||.|.||.:.
2-A.klebsii      104 LGAEVELVRPASIVSPDHYVNVARRRAHELDATGGLF-ADQFENLANYKA     152

C1-A.thaliana    201 HFDTTGPEIWEDTLGNVDIFVMGIGSGGTVSGVGRYLKSKNPNVKIYGVE     250
                     ||:.||||:||.....:|.|||..|:|||:.|.|.|.:||.:.|.:.:|..:
2-A.klebsii      153 HFEGTGPELWEQCDHRLDAFVMSAGTGGTIVGTGSFLKQQAPEIGVYLAD     202

C1-A.thaliana    251 PAESNIL    257
                     ...|::|
2-A.klebsii      203 VPGSSLL    209
```

Fig. 7-50. Alignment of 2-*A. klebsii* OAS-TL amino acid with *A. thaliana* isoforms.

Fig. 7-51. Alignment of 3-*A. klebsii* OAS-TL amino acid with *A. thaliana* isoforms.

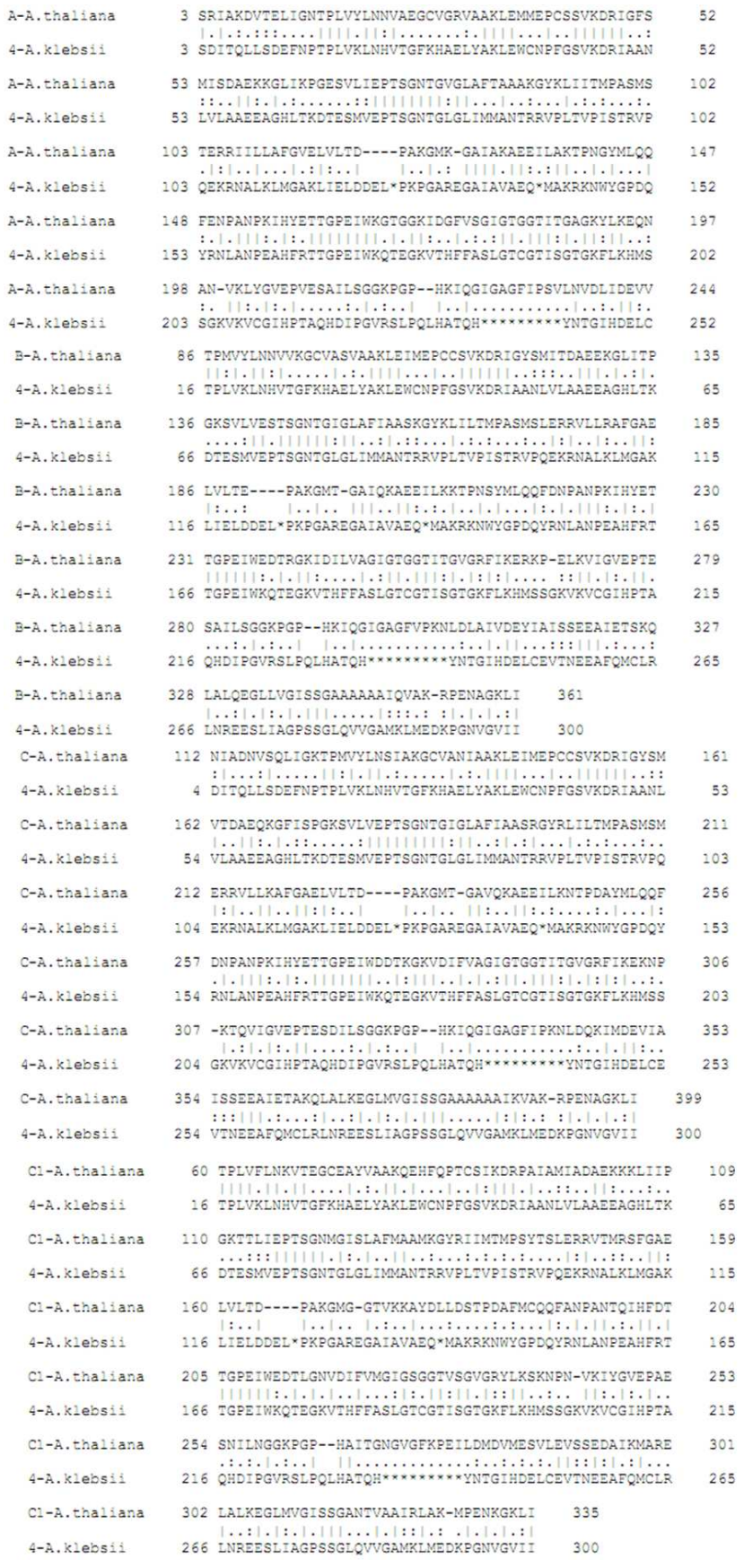

Fig. 7-52. Alignment of 4-*A. klebsii* OAS-TL amino acid with *A. thaliana* isoforms.

7.4. The amino acid code

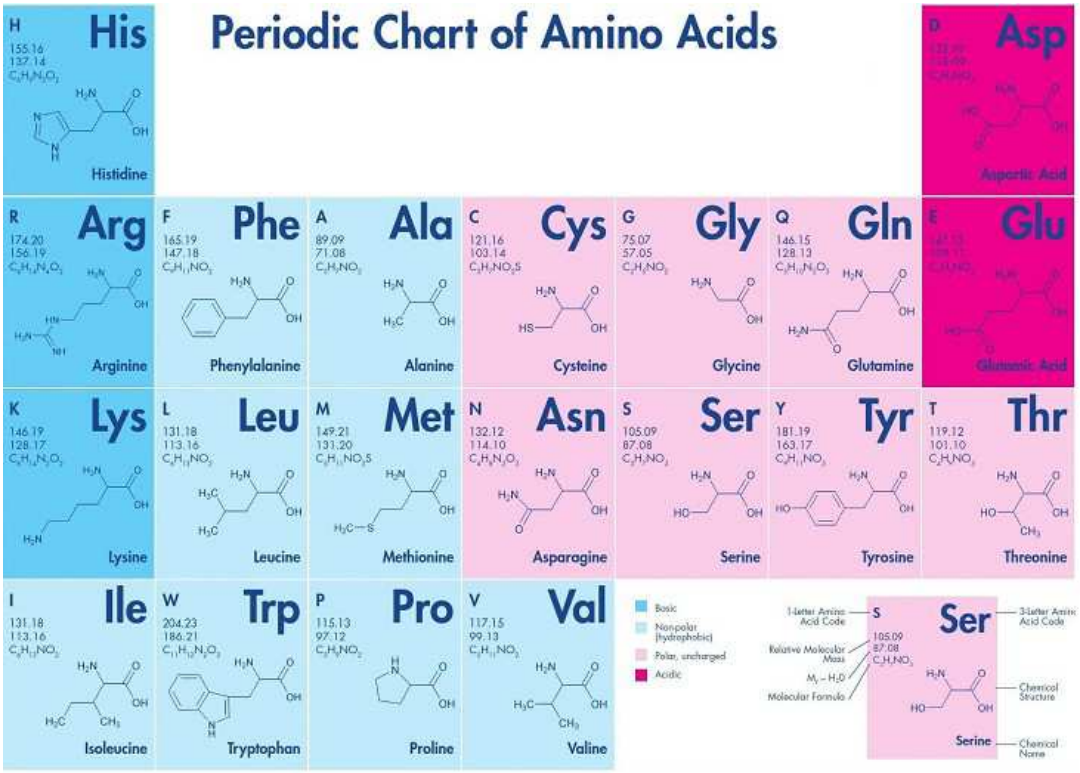

Fig. 7-53. Amino acid code and relative character.

ACKNOWLEDGEMENTS

First of all, I would like to say thanks to my supervisor Mario Giordano for all useful suggestions he gave me during my whole project. Just after, I must express my deeply and sincerely thanks, Alessandra Norici: when I arrived in Italy my life seems linked with her. She trained me in algal culturing techniques and in the comprehension of lab protocols.

I'm particularly grateful to the whole research group of Prof. Rüdiger Hell Centre for Organismal Studies (COS), Heidelberg Plant Molecular Biology, where I spent un unforgettable period. Not only because the cooperation time, but especially for the people I met. Thanks, guys! I'll never forget you. Especially, Shanshan Wang and Eric Linster!

Deeply thanks for the Masbic of Prof Tiziana cacciamani research group. Thanks for your whole group share the time with my long time working schedule. Dr. Valentina Pozzi and Dr. Enrico Junior Baldassarri, two of these young talent researchers are good research cooperator friends.

It's my great honor to meet the following lab mates: Larisa, Marianna Venuleo, Laura, Andrea Pessina, Lucia Gastoldi, Angela Anxhela, Givonna Simonetti. All these guys are very nice :)

Thanks to my neighbor lab research groups: Prof. Carnevali, Prof. Beolchini, Prof. Cecelia, Prof. Totti and Prof. Danovaro. All of these research groups in our department composed a big research family, I was lucky that I could join them.

Luca Lambertucci and Simone Bellagamba you always smile.

Monica Ferraioli thanks for you pay a lot of attention to me. Even you are so busy for dealing with a lot of document, while every time you send the document keeps two languages (English and Italiano) notice.

My big present in Italy I can meet two sisters family Viviana Fonti and Laura Rocchetti. Thanks you bring a lot of unforgettable memory. I will miss you no mater where I will be in the future.

During the past three years study, even far from my homeland, while all of these nice people in my life are all the big surprise from the God. Thanks so much all of you give me the permission I can share these three year with all of you :)

My heart will always be with you mum, dad, and all my family. Thank you always stand on my back. Waiting for my long time hug and big kiss:)

Last but not least, thanks the reviewers.

Anyway, all these nice people I mentioned above rise me up :)